MASARYK UNIVERSITY

Faculty of Medicine

Department of Psychiatry

ELECTROPHYSIOLOGICAL CORRELATES OF BOTH RESTING-STATE MENTAL ACTIVITY AND HIGHER BRAIN FUNCTIONS IN HUMAN

(Methods of scalp and intracerebral electroencephalography)

Habilitation thesis

MUDr. Alena Damborská, Ph.D.

Brno 2022

Preface

This thesis brings together knowledge gained through many years of my work as an electrophysiologist, first in the field of cognitive neuroscience and later in the field of neuropsychiatry, during which I was lucky to have excellent mentors and colleagues. First of all, I would like to mention Miloslav Kukleta, my supervisor during my PhD studies, who greatly inspired me during my initial experiments on the electrophysiology of the human brain. I have been fortunate to have wonderful bosses, Bohumil Fišer and Nataša Honzíková, that supported my research from the position of the Head of the Department of Physiology at the Faculty of Medicine at Masaryk University in Brno. I am also grateful to António Martins da Silva, head of the Neurophysiology Department at Hospital de Santo António in Oporto in Portugal, who was my mentor during my three-month study stay focused on clinical neurophysiology, and thanks to whom I had an inspiring discussion in Aveiro with Fernando Lopes da Silva, one of the most influential neurophysiologists of our time. I would like to acknowledge Ivan Rektor, who supported me from the position of the head of his research group at the Central European Institute of Technology in Brno and whose wide scientific network enabled me to meet later partners in Switzerland. My special thanks go to Christoph Michel, head of the Functional Brain Mapping laboratory at University of Geneva in Switzerland, who excellently advised me during my project DEBRASA that I conducted in his lab within the EU H2020 Marie Skłodowska Curie Action Individual Fellowship. This thesis would not have been possible without support from Tomáš Kašpárek, head of the Department of Psychiatry at University Hospital Brno and the Faculty of Medicine at Masaryk University, who paved my way in the neuropsychiatric research. I wish to thank most sincerely all co-authors, who have contributed to the findings included in this habilitation thesis and to my understanding of the topic. Special thanks go to Robert Roman, Milan Brázdil, Denis Brunet, Maria Rubega, Miralena Ioana Tomescu, Jean-Michel Aubry, Alexandre Dayer, Serge Vulliemoz, Cristina Berchio, Camille Piguet, Jacques Louvel, Martin Lamoš, Radek Mareček, Elis Bartečků, and Jana Hořínková, who were involved most deeply in my research. I also wish to thank my previous and current master‘s and PhD students, who have contributed much to this material. Last but not least, I would like to thank my family for their full support and understanding and to dedicate this thesis to my beloved parents, Jana Pavloušková and Emil Pavloušek.

Summary

The presented set of original and review papers supplemented by commentaries focuses on electrophysiological correlates of both resting-state mental activity and higher brain functions in human. We investigated spatio-temporal characteristics of event-related electrophysiological activity with the aim to contribute to the knowledge on neuronal substrate of non-motor and movement-related cognitive functions. Furthermore, we explored the large-scale brain network dynamics during the resting-state with a special focus on the identification of abnormalities in affective disorders. We also provided reviews on some clinical aspects of event-related potential (ERP) and deep brain stimulation (DBS) techniques. To study the human's mental activity, we employed methods of the scalp and intracerebral electroencephalography during different cognitive tasks and in resting conditions. We used several analytical approaches including ERP investigations, microstate analysis, and functional and effective connectivity estimations.

We extended current knowledge in human neurophysiology by identifying brain regions within the temporal and frontal cortices that are involved in non-motor cognitive functions (Annex 1, page 36). We have also provided evidence that hippocampal activity is related to the evaluation of stimulus meaning rather than to the motor response during a simple sensorimotor task (Annex 2, page 37). Furthermore, we first showed that the primary motor cortex is implicated in the executive control of actions that are not motor in nature (Annex 3, page 38).

One of the most studied ERP components is the P3 waveform that was traditionally viewed as reflecting orientation, attention, update of working memory, decision, and cognitive closure of stimulus identification. Nevertheless, our team brought the first intracerebral evidence that the P3 phenomenon might be related not only to these non-motor cognitive functions but also to the movement-related ones (Annex 4, page 41; Annex 5, page 42).

It is generally accepted that the control of intentional motor action involves brain operations that select, plan, and execute the movement. Our research group extended the knowledge on this topic when we identified large-scale brain networks that might be involved in the process of movement execution (Annex 4, page 41; Annex 5, page

42) and in the process of comparison between the intended and actually performed motor action (Annex 6, page 47; Annex 7, page 48).

The ERP amplitudes are considered to indicate the extent of allocation of neuronal resources to specific cognitive processes required to perform sensorimotor tasks. The ERP latencies are supposed to reflect the speed of such mental processes. Altered ERP patterns might therefore indicate functional brain abnormalities. Attempts to exploit the ERP technique as a possible diagnostic tool for functional brain impairments following a mild traumatic brain injury were summarized in our recent review (Annex 8; page 50).

According to the cross-frequency coupling hypothesis, the communication between two brain regions is established by the phase synchronization of oscillations at lower frequencies (< 25 Hz), which serve as a temporal reference frame for information carried by high-frequency (> 40 Hz) activity. Our team contributed to this topic by providing the first evidence of hierarchical functional linkage in the cross-frequency domain between the resting-state electrophysiological activity of the subthalamic nucleus and cortex in human (Annex 9, page 55).

Our three high-density scalp EEG studies contributed to the understanding of resting-state large-scale brain network activity in affective disorders. We demonstrated interindividual differences in large-scale brain network dynamics related to depressive symptomatology (Annex 10, page 60) and brought the first evidence for disruption of resting-state brain network dynamics in euthymic patients with bipolar disorder (Annex 11, page 61). In the effective (directed functional) connectivity study we focused on cortico-striatal-pallidal-thalamic circuits during the resting state in patients with depression (Annex 12, page 62). We showed a higher-than-normal functional connectivity arising from the right amygdala in depressive patients supporting the view that the amygdala plays an important role in the neurobiology of depression.

DBS has proven effective in the treatment of pharmacoresistant Parkinson's disease, although it can be accompanied by various complications (Annex 13, page 65). Furthermore, there is also preliminary evidence for the efficacy and safety of DBS for treating pharmacoresistant depression. Optimal brain stimulation targets, however, have not been determined yet. In our recent review we provided updated knowledge

substantiating the suitability of each of the current and potential future DBS targets for treating depression (Annex 14, page 66). Despite myriad DBS targets for treating depression tested in human, the amygdala is not among them. From this perspective, our recent finding of higher-than-normal functional connectivity arising from the right amygdala in depressive patients (Annex 12, page 62) contributes to the knowledge that is needed to evaluate deep brain structures as possible candidates for DBS treatment in depression.

Our findings included in this habilitation thesis contributed to a better understanding of the neuronal substrate of both resting-state mental activity and higher brain functions in human. Additionally, the electrophysiological patterns discovered by our team that are associated with depression or related to bipolar disorder might help improve diagnostics and therapy of affective disorders in future.

Souhrn

Prezentovaný soubor originálních a recenzních prací doplněných komentáři se zaměřuje na elektrofyziologické koreláty klidové duševní činnosti a vyšších mozkových funkcí člověka. S cílem přispět k poznání neuronálních substrátů nemotorických a s pohybem souvisejících kognitivních funkcí jsme zkoumali časoprostorové charakteristiky elektrofyziologické aktivity vázané na události. Dále jsme zkoumali dynamiku rozsáhlých mozkových sítí v klidovém stavu se zvláštním zaměřením na identifikaci abnormalit u afektivních poruch. Také jsme shrnuli některé klinické aspekty metod "na událost vázaných neboli kognitivních potenciálů" (ERP) a hluboké mozkové stimulace (DBS). Ke studiu mentální aktivity člověka jsme využili metodu skalpové a intracerebrální elektroencefalografie při různých kognitivních úkolech a v klidových podmínkách. Aplikovali jsme několik analytických přístupů včetně zkoumání ERP, analýzy mikrostavů a výpočtů funkční a efektivní konektivity.

Identifikací mozkových oblastí uvnitř spánkových a čelních laloků podílejících se na nemotorických kognitivních funkcích (příloha 1, strana 36) jsme rozšířili současné poznatky v oblasti neurofyziologie člověka. Poskytli jsme také důkazy o tom, že hipokampální aktivita souvisí spíše s hodnocením významu podnětu než s motorickou reakcí během jednoduchého senzorimotorického úkolu (příloha 2, strana 37). Navíc jsme poprvé ukázali, že primární motorická kůra je zapojena do exekutivní kontroly akcí, které nemají motorický charakter (příloha 3, strana 38).

Jednou z nejstudovanějších ERP komponent je vlna P3, která byla tradičně pokládána za korelát orientace, pozornosti, aktualizace pracovní paměti, rozhodnutí a kognitivního uzavření identifikace podnětu. Náš tým nicméně přinesl první intracerebrální důkaz, že jev P3 může souviset nejen s těmito nemotorickými kognitivními funkcemi, ale také s funkcemi spojenými s pohybem (příloha 4, strana 41; příloha 5, strana 42).

Obecně se má za to, že řízení volní pohybové aktivity zahrnuje mozkové procesy, které jsou podkladem výběru, naplánování a provedení pohybu. Naše výzkumná skupina rozšířila poznatky k tomuto tématu, když jsme identifikovali rozsáhlé mozkové sítě, které by mohly být zapojeny do procesu provádění pohybu (příloha 4, strana 41;

příloha 5, strana 42) a do procesu porovnávání zamýšlené a skutečně provedené motorické akce (příloha 6, strana 47; příloha 7, strana 48).

Má se za to, že amplituda ERP je určena rozsahem neuronální alokace ke specifickým kognitivním procesům potřebným k provádění senzorimotorických úkolů. Předpokládá se, že latence ERP odráží rychlost takových mentálních operací. Změněné vzorce ERP by proto mohly odrážet funkční mozkové abnormity. Pokusy o využití techniky ERP jako možného diagnostického nástroje u funkčních poškození mozku po mírném traumatickém poranění mozku byly shrnuty v našem nedávném přehledu (příloha 8, strana 50).

Podle hypotézy "cross-frequency coupling" je komunikace mezi dvěma mozkovými oblastmi zprostředkována fázovou synchronizací oscilací na nižších frekvencích (< 25 Hz), které slouží jako časový referenční rámec pro informace přenášené vysokofrekvenční (> 40 Hz) aktivitou. Náš výzkumný tým k tomuto tématu přispěl tím, že poskytl první důkaz hierarchické mezifrekvenční funkční vazby mezi klidovou elektrofyziologickou aktivitou subthalamického jádra a kůry mozkové u člověka (příloha 9, strana 55).

Naše tři studie, jež využily skalpové EEG o vysoké hustotě elektrod, přispěly k pochopení aktivity rozsáhlých mozkových sítí v klidovém stavu u afektivních poruch. Prokázali jsme interindividuální rozdíly v dynamice rozsáhlých mozkových sítí v souvislosti s depresivní symptomatologií (příloha 10, strana 60) a přinesli první důkazy o narušení dynamiky mozkových sítí v klidovém stavu u euthymních pacientů s bipolární poruchou (příloha 11, strana 61). Při studii efektivní mozkové konektivity, tj. směru funkčního propojení mozkových oblastí, jsme se zaměřili na kortiko-striatální-pallidální-thalamické okruhy během klidového stavu u pacientů s depresí (příloha 12, strana 62). U depresivních pacientů jsme ukázali abnormálně zvýšenou funkční konektivitu vycházející z pravé amygdaly, což podporuje názor, že amygdala hraje důležitou roli v neurobiologii deprese.

Metoda DBS se osvědčila v léčbě farmakorezistentní Parkinsonovy nemoci, přestože může být provázena různými komplikacemi (příloha 13, strana 65). Dále existují také předběžné důkazy o účinnosti a bezpečnosti DBS při léčbě farmakorezistentní deprese. Optimální cílové mozkové struktury pro stimulaci však zatím nebyly stanoveny. V naší nedávné přehledové práci jsme shrnuli poznatky o současných i možných budoucích

cílových mozkových strukturách využitelných pro DBS léčbu deprese (příloha 14, strana 66). Přestože u lidí byla DBS léčba deprese testována na nesčetném množství cílových struktur, amygdala mezi ně nepatří. Z tohoto pohledu náš nedávný nález abnormálně zvýšené funkční konektivity vycházející z pravé amygdaly u depresivních pacientů (příloha 12, strana 62) přispívá k poznatkům, které jsou potřebné pro posuzování hlubokých mozkových struktur jako možných kandidátů pro DBS léčbu deprese.

Naše nálezy obsažené v této habilitační práci přispěly k lepšímu pochopení neuronálního substrátu klidové duševní činnosti a vyšších mozkových funkcí člověka. Elektrofyziologické vzorce objevené naším týmem, které jsou spojovány s depresí nebo s bipolární poruchou, by navíc mohly v budoucnu pomoci zlepšit diagnostiku a terapii afektivních poruch.

Contents

List of annexes

Annex 6 (page 47)

Damborská, A., Roman, R., Brázdil, M., Rektor, I., & Kukleta, M. (2016). Post-movement processing in visual oddball task - evidence from intracerebral recording. *Clinical Neurophysiology,* 127 (2), 1297 – 1306.
IF(2016) = 3.866, rank Q1
Quantitative contribution: 90%
Content contribution: development of the initial idea, pre-processing, analysis, statistical evaluation, writing the initial draft, table and figure preparation, assistance in corresponding author

Annex 7 (page 48)

Kukleta, M., **Damborská, A.**, Turak, B., & Louvel, J. (2017). Evoked potentials in final epoch of self-initiated hand movement: A study in patients with depth electrodes. *International Journal of Psychophysiology*, 117, 119-125.
IF(2017) = 2.868, rank Q2
Quantitative contribution: 40%
Content contribution: participation in writing the initial draft, participation in table and figure preparation, corresponding author

Annex 8 (page 50)

Gomes, J. & **Damborská, A.** (2017). Event-related potentials as biomarkers of Mild Traumatic Brain Injury. *Activitas Nervosa Superior*,59 (3-4), 87-90.
Quantitative contribution: 50%
Content contribution: development of the initial idea, participation in writing the initial draft, corresponding author

Annex 9 (page 55)

Damborská, A., Lamoš, M., Baláž, M., Deutschová, B., Brunet, D., Vulliemoz, S., Bočková, M., & Rektor, I. (2021) Resting-State Phase-Amplitude Coupling Between the Human Subthalamic Nucleus and Cortical Activity: A Simultaneous Intracranial and Scalp EEG Study, *Brain Topography*, 34(3), 272-282.
IF(2021) = 4.275, rank Q2
Quantitative contribution: 70%
Content contribution: design of the study, participation in data acquisition, pre-processing, table and figure preparation, writing the initial draft, corresponding author

Annex 10 (page 60)

Damborská, A., Tomescu, M.I., Honzírková, E., Barteček, R., Hořínková, J., Fedorová, S., Ondruš Š., Michel C.M. (2019b). EEG resting-state large-scale brain network dynamics are related to depressive symptoms. *Frontiers in Psychiatry*, 548 (10)
IF(2019) = 2.849, rank Q2
Quantitative contribution: 90%
Content contribution: development of the initial idea, design of the study, supervision on data acquisition, pre-processing, analysis, statistical evaluation, writing the initial draft, table and figure preparation, corresponding author

Annex 11 (page 61)

Damborská, A., Piguet, C., Aubry, J-M., Dayer, A.G., Michel C.M., Berchio, C. (2019c). Altered EEG resting-state large-scale brain network dynamics in euthymic bipolar disorder patients. *Frontiers in Psychiatry*, 826 (10)

IF(2019) = 2.849, rank Q2

Quantitative contribution: 80%

Content contribution: development of the initial idea, pre-processing, analysis, statistical evaluation, writing the initial draft, table and figure preparation, corresponding author

Annex 12 (page 62)

Damborská, A., Honzírková, E., Barteček R., Hořínková J., Fedorová, S., Ondruš, Š., Michel, C.M., Rubega, M. (2020). Altered directed functional connectivity of the right amygdala in depression: high-density EEG study. *Scientific Reports*, 4398 (10)

IF(2020) = 4.380, rank Q1

Quantitative contribution: 60%

Content contribution: development of the initial idea, design of the study, supervision on data acquisition, pre-processing, participation in writing the initial draft, participation in table and figure preparation, corresponding author

Annex 13 (page 65)

Ludovico, I.C. & **Damborská, A.** (2017). Deep brain stimulation in Parkinson's disease: Overview and complications. *Activitas Nervosa Superior*, 59(1), 4-11.

Quantitative contribution: 50%

Content contribution: development of the initial idea, participation in writing the initial draft, corresponding author

Annex 14 (page 66)

Drobisz D. & **Damborská A.** (2019). Deep brain stimulation targets for treating depression, *Behavioural Brain Research*, 359 (1), 266-273.

IF(2019) = 2.977, rank Q2

Quantitative contribution: 50%

Content contribution: development of the initial idea, participation in writing the initial draft, figure preparation, corresponding author

List of abbreviations

BD	bipolar disorder
DBS	deep brain stimulation
EEG	electroencephalography
EPSP	excitatory postsynaptic potential
ERP	event-related potential
LMP	late movement potential
iEEG	intracranial electroencephalography
IPSP	inhibitory postsynaptic potential
MDD	major depressive disorder
M1	primary motor cortex
PAC	phase-amplitude coupling
preSMA	the most anterior portion of supplementary motor area
PSP	postsynaptic potential
SR interval	stimulus-response interval; reaction time
STN	subthalamic nucleus

1. Introduction

I started to study the electrophysiology of the human brain at the Department of Physiology at Faculty of Medicine at Masaryk University in Brno under the supervision of Miloslav Kukleta, the leader of the neurophysiology research group, who initiated a new university course on Neuroscience within the General medicine curriculum in early 1990s. Miloslav Kukleta, being a neurophysiologist and board-certified psychiatrist, was a leading actor in the psychosomatic approach to the etiopathogenesis of diseases, especially of mental disorders (Damborská, 2015a, 2015b). I was lucky to come to his lab at the moment, when his studies on intracranially recorded brain activity started, in collaboration with Ivan Rektor and Milan Brázdil from the 1st Department of Neurology at St. Anne's University Hospital in Brno. Using this unique methodological approach, we were disclosing electrophysiological correlates of higher brain functions in human.

In 2015 I welcomed the opportunity to join the team of the Department of Psychiatry at Faculty of Medicine at Masaryk University and University Hospital Brno, where in position of a physician I could exploit my theoretical knowledge in the clinical praxis. With my former experience in electroencephalography (EEG) that was limited to intracranial recording I decided to extend my skills with the method of scalp EEG. In 2016 I gained functional specialization in EEG, which confirmed my expertise in clinical EEG evaluation. Later on, during the years 2017-2019, my long-standing focus on brain electrophysiology, ambition of wider study of EEG methods and rising interest in neuropsychiatry led to collaboration with Christoph Michel on high-density EEG investigations of resting-state large-scale brain network dynamics in affective disorders. In his lab at the University of Geneva in Switzerland I conducted my project DEBRASA funded by the EU (cordis.europa.eu/project/id/739939) (Damborská, 2019a). Within this project, together with the team of Jean-Michel Aubry, head of the Department of Psychiatry at Geneva University Hospital, we investigated resting-state electrophysiological abnormalities in affective disorders identifying promising biomarkers of the disease and providing knowledge perquisite for evaluating deep brain structures as candidates for invasive neurostimulation treatment of depression.

Currently I conduct my research at the Department of Psychiatry at the Faculty of Medicine at Masaryk University and University Hospital Brno, where I focus mainly on large-scale brain neuronal networks in depressive patients, searching for biomarkers of antidepressant treatment response. Some of the specific areas of my actual interests include also study of electrophysiological correlates of responsiveness to dialectical behavioural therapy in borderline personality disorder. Furthermore, at the same time I am involved in studies on the resting-state cortico-subcortical functional coupling of the human brain performed within the research group of Ivan Rektor at the Central European Institute of Technology in Brno.

This thesis is laid out as follows. Following this introductory chapter, the methodology is described in Chapter 2. The unifying aspect of all original studies included in this thesis is the employment of electroencephalography (EEG). The basic principles of EEG signal generation are summarized in Chapter 2.1. For purposes of our studies, we used both intracranial (Chapter 2.2) and scalp (Chapter 2.7) recordings, we even performed simultaneous intracranial-scalp recording (Chapter 2.6), and we used analytical approaches such as event-related potentials (Chapter 2.4), connectivity estimation (Chapter 2.5) and microstates (Chapter 2.8). We are aware of methodological limitations related to intracranial studies and I discuss this issue in Chapter 2.3. The next four chapters provide commentary on my contribution to the field of neuroscience. The reader will be introduced to our findings from three different recording approaches: (1) intracerebral recordings that concern electrophysiological correlates of higher brain functions (Chapter 3); (2) scalp recordings that concern resting-state electrophysiological brain abnormalities in affective disorders (Chapter 5.2), and (3) simultaneous intracranial and scalp recordings that concern resting-state large-scale brain network functional organization in human (Chapter 5.1). In two chapters, commentaries on our critical reviews on clinical applications of electrophysiological findings (Chapter 4) and on deep brain stimulation treatment (Chapter 6) are provided.

Various analytical approaches were used in the processing of EEG data included in this thesis. To investigate electrophysiological correlates of higher brain functions, I evaluated event-related potentials elicited during various cognitive tasks and self-initiated voluntary movement (Chapter 3). To study resting-state brain activity, I

performed microstate analysis and my coauthors calculated phase-amplitude coupling and partial directed coherence (Chapter 5). In all but one study (Roman et al., 2013 - Annex 2, Chapter 3.1) included as annexes to this thesis I am the first and/or corresponding author.

The overarching goal of the studies included in this habilitation thesis is to contribute to the knowledge on neuronal substrate of both resting-state mental activity and higher brain functions in human, which might be exploited to improve diagnostics and treatment in neuropsychiatry in future.

2. Methods

The studies included in this habilitation thesis belong to the field of electrophysiology of the human brain. To study the brain's activity, we employed electroencephalography (EEG) that, having been described by Hans Berger in 1929, now more than 90 years later, is widely used to observe both temporal and spatial characteristics of brain networks in various mental states (Schomer & Da Silva, 2018).

2.1 Genesis of EEG signal

The main principles summarized here are treated in detail in Chapter 2 of Niedermeyer's electroencephalography (Amzica & Da Silva, 2018), to which more interested readers are referred.

The electric activity of brain cells is generated by ionic currents flowing across the neuronal membrane. The neurons are polarized cells with resting membrane potential around -70mV, meaning that intracellular space is negatively charged compared to the extracellular compartment. During the generation of action, postsynaptic, or receptor potentials, ions enter the intracellular space through an active opening of ion channels, thus constituting a so called *primary current* at the synapse region. A potential gradient develops along the membrane in the intra- and extracellular spaces, which causes flow of ions along the membrane. In some distance along the membrane from this current injection, ions passively cross the membrane as a compensatory so-called *ohmic current*.

The main neuronal activity that is reflected in the EEG signal is the postsynaptic potential (PSP), while the contribution of other potentials is considered limited. Two types of PSPs can be generated, i.e., excitatory (EPSPs) or inhibitory (IPSPs). In the case of an EPSP, the primary current is typically carried by the entrance of Na^+ ions into the intracellular space, while in an IPSP, the primary current is typically carried by the entrance of Cl^- ions into the cell or extrusion of K^+ ions from the cell. Thus, in the case of an EPSP (Fig. 1A), the local concentration of positively charged ions in the extracellular space decreases, and therefore it is called an *active sink*. This gives rise to the depolarization of the subsynaptic membrane. In the case of an IPSP (Fig. 1B), the local concentration of positively charged ions in the extracellular space increases, and therefore it is called an *active source*. This gives rise to the hyperpolarization of the subsynaptic membrane. In this way, the primary and ohmic currents across the membrane form sink/source dipoles in the extracellular space. In the case of an EPSP, a negative pole is created in the active sink in the synapse region, while the positive pole occurs in the passive source at a distance along the membrane. In the case of an IPSP, a positive pole is created in the active source in the synapse region, while the negative pole occurs in the passive sink at a distance along the membrane.

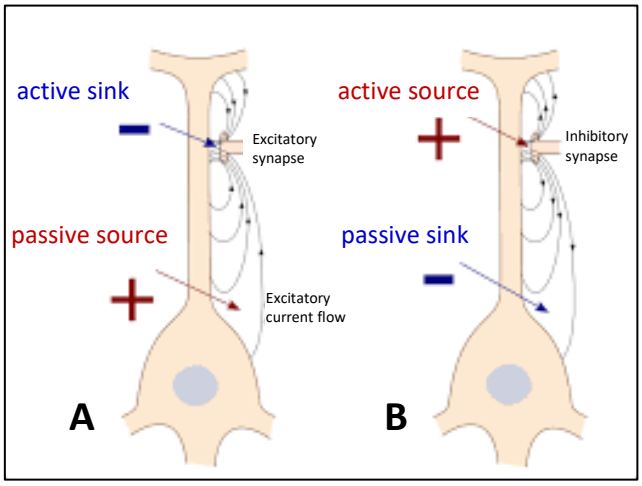

Figure 1 Current flow patterns and formation of extracellular dipole around an idealized neuron due to synaptic activation. **A** Depolarization of the membrane with the sink at the excitatory synapse; **B** Hyperpolarization of the membrane with the source at the inhibitory synapse. (Maksymenko, 2019; adapted from Niedermeyer & Da Silva, 2004)

Resulting from these cellular processes a set of extracellular dipoles distributed within a given brain volume forms electric fields that can be detected, although attenuated, at some distance from their generation. The extracellular potentials that are recorded near their neuronal origin using intracranial electrodes are called *local field potentials*. These potentials further propagate through the brain and surrounding tissue to consequently form the *scalp recorded EEG* signal.

A typical EEG signal in an adult consists of a wide frequency spectrum of oscillations (Krishnan et al., 2018). The range of clinically relevant EEG frequencies lies between 0.1 and 100Hz. Classically, the following frequency bands are distinguished: δ: < 4 Hz, θ: 4 - 7 Hz, α: 8 - 13Hz, β: 14 - 40 Hz, γ: > 40 Hz. Technical advances in EEG recording systems enabled widening the EEG frequency range of interest at both ends of the spectrum. The lower end extends to the so-called ultra-slow activity (< 0.3 Hz) and the upper end extends up to 1000Hz as the so-called high-frequency oscillations, ripples and fast ripples.

2.2 Intracranial electroencephalography

The intracranial approach can be used when non-invasive techniques are not sufficient in diagnostics or therapy of neuropsychiatric disorders. Intracranial electroencephalography was introduced into clinical praxis in the 1940s in basal ganglia disorders treatment (Meyers & Hayne, 1948) and has been further exploited in epilepsy diagnostics since the 1950s (Rasmussen & Jasper, 1958). In Parkinson's disease (PD), intracranially implanted electrodes are used for invasive neurostimulation. In epilepsy, the intracranial electroencephalography (iEEG) is used before surgery to localize the epileptogenic zone, i.e., the area that needs to be resected to abolish seizures.

There are two types of intracranial recording: (1) stereotactic EEG, in which depth electrodes are implanted intracerebrally in cortical and deep brain structures and (2) the subdural recording or electro-corticogram, in which grids or strips of electrodes are placed under the dura mater. Multi-contact depth electrodes penetrating into the cerebral tissue, allowing systematic investigation of deep structures, were introduced in early 1970s (Talairach & Bancaud, 1973). Ten years later, Wyler introduced the subdural electrode (Wyler et al., 1984). Currently, there are no epileptosurgery

guidelines on when, whom, and how to implant with intracranial electrodes, and each centre has different rules based on personal experience and resources. Nevertheless, in all cases before implantation, results of non-invasive examination are considered, and the positions of intracranial electrodes are carefully planned. This is because the implanted electrodes can record from only a limited brain volume. This spatial limitation disadvantage is, however, balanced by the quality of the signal. Compared to the scalp EEG, the iEEG is only minimally affected by muscle and ocular artefacts. Moreover, intracranially recorded signals exhibit a high signal-to-noise ratio because there is no attenuation by the skull. Thus, the intracranial recordings provide a focal but magnified view of the brain.

In order to localize the epileptogenic zone, the electrodes are implanted in the brain for several days. During this period there is a unique opportunity to investigate human brain activity directly when patients agree to participate in a research study. Similarly, during few days between the surgery and definite internalization of the deep brain stimulation electrodes, intracranially recorded activity from subcortical structures can be investigated in PD patients. Furthermore, recent technical advances enable in both epileptic and PD patients to perform simultaneous iEEG and scalp EEG during the short examination period (see Chapter 2.5).

The method of intracranial EEG was introduced in clinical praxis in the Czech Republic in the early 1990s by Ivan Rektor at the 1st Department of Neurology at St. Anne's University Hospital in Brno. Data recorded at this department were used in almost all intracranial studies included in this thesis (Chapter 3).

2.3 Brain physiology studied in patients

The unique advantage of the intracranial technique is the fact that it allows studying brain activity directly. When this approach, however, is used to study the physiology of the human brain, several limits exist due to obvious reasons. First, of course, it cannot be performed in healthy subjects. Second, in patients the brain can be examined only non-systematically. Namely, contrary to animal studies, where almost any region of interest can be examined, the exact position of intracranial electrodes in patients is given strictly by diagnostic and/or therapeutic requirements. Therefore, research interests and hypotheses are restricted to the structures selected by clinical

choice. Third, patients enrolled to neurosurgery program are relatively few in number and consequently they form a less homogenous experimental group in terms of demographic factors. Fourth, the patients' brains investigated are not healthy.

The third limitation can be balanced by a wider span devoted to data collection. In one of our studies (Damborská et al., 2021 – Annex 9, Chapter 5.1), we were collecting data from 11 subjects over eight years. Another possibility is to perform a multicentre study (Frauscher et al., 2018). The last limitation can be mitigated by the selection of available electrodes and by the selection of recording conditions. To mitigate the influence of the disease on our findings, we investigated recordings of epileptic patients that were obtained during interictal state from electrodes placed outside lesional and epileptogenic zones. For the same reason, we explored the brain activity in Parkinson's disease patients under their usual anti-parkinsonian medication. Nevertheless, these precautions are imperfect, since for example epilepsy is viewed as a disease of neuronal networks (Da Silva et al., 2012), and an abnormal functioning of brain regions outside the focus of seizures cannot be excluded. Furthermore, nonspecific abnormalities on EEG in epileptic patients can be detected even during an interictal period (De Stefano et al., 2022). Similarly, suppressing Parkinson's disease symptoms with medication does not necessarily mean the brain networks are normal and their activity physiological.

Taken together, the reader must be aware that in all studies included in Chapter 3 and Chapter 5.1 of this habilitation thesis, the interpretations of our results with regard to the physiological functioning of the brain must be considered with caution.

2.4 Event-related potentials

Electroencephalography (EEG) enables an investigation of human brain functions such as reactions of the brain to various discrete events. Two types of changes in the EEG may occur that are related to particular events: (1) the evoked responses, which are time-locked and phase-locked to a given event; and (2) the induced responses, which are time-locked but not phase-locked to a given event. The former EEG changes are constituted by event-related potentials (ERPs), while the latter include event-related desynchronization and event-related synchronization.

The ERPs are barely apparent on the native EEG record. To visualize them, an averaging of short EEG segments (trials, sweeps) covering both the pre- and post-event periods is used. By averaging, the resulting recording will suppress random background activity (noise) directly unrelated to the event. This is deducted from each other during the computation. On the contrary, regular activity (signal) is raised in the form of ERP. In other words, averaging EEG leads to an increase in the signal-to-noise ratio. The interpretation of ERPs is based on the assumption that in an anatomical region the same neuronal activity occurs in the same time window when the same event is repeated. Depending on the mental processes studied, different events are used as a trigger for averaging procedure, i.e., the stimulus onset or the motor response onset.

The traditional analytical approach using single-channel assessment considers the ERPs as a series of waveforms (components), each characterized with polarity, shape, amplitude, latency, and spatial distribution on the scalp. One subset of the ERPs consists of *early sensory* (visual, auditory, somatosensory) evoked potentials. These include components labelled as C1, P1, N1, P2 that appear up to 250 ms after stimulus onset during a cognitive task. Early ERP components correspond to the sensory processing of the stimulus (Näätänen & Picton, 1987; Crowley & Colrain, 2004; Foxe et al., 2002). These are followed by *late cognitive* potentials. These include components such as N2, P3, N400, P600 that are considered to reflect cognitive processes (Sutton et al, 1965; Donchin et al., 1978; Hillyard et al., 1978; Halgren et al., 1998). The early sensory potentials are particularly influenced by the physical properties of the stimulus. By contrast, it is typical for the late cognitive components that their formation is not influenced by the physical properties of the stimulus, nor is it dependent on the kind of sensory modality. The splitting of components into purely sensory and cognitive is commonly used in literature; nevertheless, this split is to some extent artificial, as the functional base of some components can be multiple and also some waves overlap with each other over time.

For decades, scalp-recorded ERPs elicited during cognitive tasks have been employed as useful tools for studying processes of cognition. Later on, an intracerebral EEG recording enabled to search for the spatiotemporal aspects of these mental operations. The description of spatiotemporal characteristics of intracerebral ERPs provided relevant data for understanding of the organization and functional principles

of cognitive networks (Halgren et al., 1998; Brázdil et al., 2003; Kukleta et al., 2003; Roman et al., 2005; Damborská et al., 2012; 2016; Rektor et al., 2007). The ERP topic covered in Chapters 3 and 4 of this habilitation thesis has been at the centre of our research interests for years. More details on ERP methodology can be found in the doctoral theses (Damborská, 2012; Roman, 2004).

2.5 Spatio-temporal characteristics of neuronal activation

Connectivity studies aim to identify real active relations between brain regions. There are three main connectivity levels that are studied in the brain: (1) the *structural connectivity* describing the existence of white matter tracts physically interconnecting brain regions; (2) the *functional connectivity* defined as a temporal linkage between two signals recorded in two different brain loci, thus reflecting functional interactions between relevant brain regions; (3) the *effective (directed functional) connectivity* describing causal influences that neuronal populations exert over another. Intracranial EEG signals as well as source reconstructed scalp EEG signals are highly suitable for both functional and effective connectivity investigation, since they provide spatio-temporal information about neuronal activation.

Functional connectivity between neuronal groups can be assessed either in the time domain by calculating the *correlation* of the signals or in the frequency domain by calculating the *coherence* of power spectra of the signals. It was shown that intracranial EEG signals recorded in remote brain regions reveal highly significant correlations corresponding to the level of phase synchronization of EEG oscillations that reflect cognitive network interactions (Kukleta et al., 2009; Kukleta et al., 2017 – Annex 7, Chapter 3.3). Furthermore, according to the communication-through-coherence hypothesis, it was proposed that communication between two neuronal groups depends on coherence within specific frequency bands (Fries 2005). Additionally, the authors of the gating-by-inhibition hypothesis suggested that the routing of information flow between brain regions is established by actively inhibiting the pathway not required for the task (Jensen & Mazaheri, 2010). These hypotheses were recently unified via a cross-frequency coupling phenomenon (Bonnefond et al., 2017). It suggests that communication between two regions is established by the phase synchronization of oscillations at lower frequencies (< 25 Hz) which serve as a temporal

reference frame for information carried by high-frequency (> 40 Hz) activity. Specifically, high-frequency oscillations are expected to be nested within low-frequency oscillations, i.e., they would occur only during the excitability phase of the lower-frequency oscillations. One of the best-studied forms of cross-frequency coupling is a *phase-amplitude coupling*, in which the amplitude of a higher frequency oscillation is coupled to the phase of a lower frequency oscillation (Canolty et al. 2006). The phase-amplitude coupling was used in our recent study to assess the spatio-temporal characteristics of coordinated cross-structural subcortico-cortical activity (Damborská et al., 2021 – Annex 9, Chapter 5.1).

To investigate the effective connectivity of brain networks, adaptive estimation algorithms can be used. Particularly, *Granger causality* based on adaptive filtering enables to deal with time-varying multivariate time-series and test direct causal links among multiple brain regions. A signal *x* is said to Granger-cause another signal *y* if the history of *x* contains information that helps to predict *y* above and beyond the information contained in the history of *y* alone (Granger, 1969). A causal relationship between more than two EEG signals can be studied with *directed transfer function* and *partial directed coherence* that is built upon the Granger causality principle (Baccala & Sameshima, 2001). An abnormal increase in directed functional connectivity arising from the right amygdala during resting condition was demonstrated on source reconstructed scalp EEG signal in patients with affective disorders (Damborská et al., 2020 – Annex 12, Chapter 5.2).

2.6 Simultaneous intracranial and scalp electroencephalography

Currently, the simultaneous intracranial electroencephalography (iEEG) and scalp EEG is not applied in clinical practice, although initial attempts have recently been made in seizure onset detection (Abramovici et al., 2018; Antony et al., 2019). Rather, this approach is used in epilepsy research to identify new scalp recorded markers of epileptic activity (De Steffano et al., 2022), develop machine learning models for epileptic seizure prediction from scalp EEG (Li et al., 2021), evaluate the accuracy of interictal (Iachim et al., 2021) and ictal (Barborica et al., 2021) electrical source localization from scalp EEG in epilepsy diagnostics, and assess the localizing value of scalp recorded spikes (Ray et al., 2007). To the best of my knowledge, no sooner than

in our recent study (Damborská et al., 2021 – Annex 9, Chapter 5.1), simultaneous iEEG and scalp EEG (Fig. 2) was performed in Parkinson's disease (PD) patients and exploited to investigate the functional organization of the human brain.

In PD patients the simultaneous iEEG and scalp EEG can be performed by Ag–AgCl electrodes filled with conductive paste and placed on the scalp according to the International 10/10 System. The central scalp region is excluded owing to postoperative bandages around externalized intracranial deep brain stimulation electrodes implanted bilaterally into the subthalamic nucleus (Fig. 2).

Figure 2 Intracranial deep brain stimulation electrode cables (black arrows) and 51 Ag–AgCl scalp electrodes in a Parkinson's disease patient

A more sophisticated scalp electrode acquisition system is currently available for simultaneous recording. An elastic net of 256 plastic cup scalp electrodes is fitted on the patient's head. All electrodes are filled with a conductive paste. The intracranial electrode cables are disconnected prior to the fitting of the scalp net, passed individually through the scalp net and reconnected to the clinical recording system (Fig. 3).

Figure 3 Intracranial electrode cables (white arrows) and 256 plastic cup scalp electrodes (De Stefano et al., 2022)

2.7 Scalp electroencephalography and scalp field potential maps

Electroencephalography (EEG) recording consists of one value for each moment in time and each electrode. The recorded EEG signal is thus represented with two variables, i.e., time and space. The traditional way of EEG signal analysis is based on an assessment of waveform morphology. This approach has been used for years both in the scalp and intracranial recordings and was also employed in all our studies included in Chapter 3. Although the set of only 19 scalp electrodes is still routinely used in clinical praxis, significant technological advances enable to record electrophysiological brain activity simultaneously from up to 256 electrodes distributed over the scalp. In order to capture the spatial information from these simultaneous high-density scalp recordings, a potential map can be constructed for every single moment, reflecting the distribution of the potentials on the scalp. The idea of analyzing these s*calp field potential maps* was formulated decades ago (Lehmann & Skrandies, 1984) and has been called EEG topographical mapping. Methods to analyze the scalp electric field recorded with multichannel EEG are described in detail in Chapter 45 of Niedermeyer's electroencephalography (Michel & He, 2018), to which more interested readers are referred.

Scalp field data can be displayed on a two-dimensional scheme of the electrode positions on the head surface. To this end, the three-dimensional scheme of positions of the electrodes is wrapped on a two-dimensional plane, implying some distortions of electrode distances similar to those encountered at geographic maps representing the earth's surface (Fig. 4).

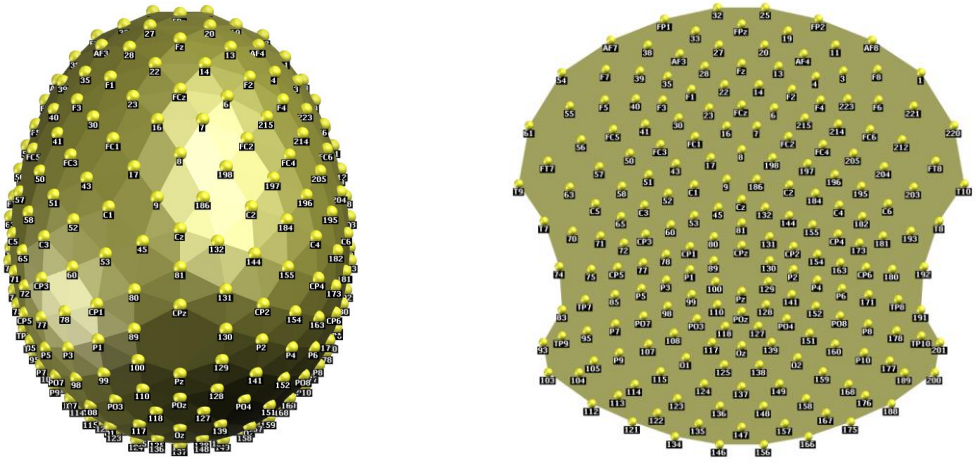

Figure 4 Distribution of 204 electrodes on scalp in three-dimensional (left) and two-dimensional (right) scheme; scalp seen from the top, nose in front, left ear left.

Having constructed the electrode scheme, the voltage values are assigned to their positions. The spatial points between the electrode positions are estimated by interpolation, i.e., values at locations that were not measured are computed. Finally, by adding visual codes for specific values, the visualization of the *scalp field potential map* is made (Fig. 5).

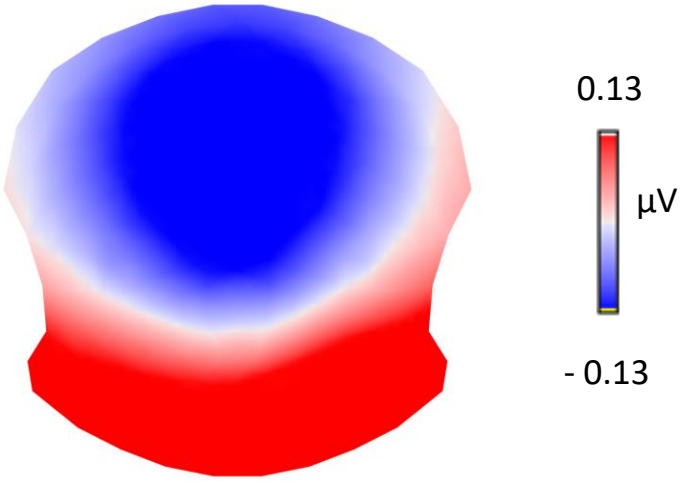

Figure 5 Two-dimensional idealized scalp field map in a time point with a positive (red) and negative (blue) voltage. Colour intensities code different voltages indicated in the colour scale; scalp seen from the top, nose in front, left ear left.

The construction of scalp field potential maps is a basic step in microstate analysis (Fig. 6C, Chapter 2.8) that was employed in our two studies (Damborská et al. 2019 b, c – Annex 10, 11, Chapter 5.2) and a precursor to source imaging that we used in our recent study (Damborská et al., 2020 – Annex 12, Chapter 5.2). By physical laws, different map topographies must have been produced by different source configurations in the brain (Helmholtz, 1853). Thus, the identification of different map topographies over time or between conditions, or subjects, provides important information about whether and when differences in sources of electrical brain activity occur (Michel et al., 2004).

2.8 Microstate analysis

Scalp electroencephalography (EEG) measures the electric potential generated by the neuronal activity in the brain with a temporal resolution in the millisecond range. A sufficient number of electrodes distributed over the scalp, i.e., high-density-EEG (HD-EEG), allows for the reconstruction of a scalp potential map representing the global brain activity (Michel & Murray, 2012). Any change in the map topography reflects a change in the distribution and/or orientation of the active sources in the brain (Lehmann, 1987). Already in 1987, Lehmann et al. observed that in spontaneous resting-state EEG, the topography of the scalp potential map remains stable for a short period of time and then rapidly switches to a new topography in which it remains stable again. Ignoring map polarity, the duration of these stable topographies is around 80–120 ms. Lehmann called these short periods of stability EEG microstates and attributed them to periods of synchronized activity within large-scale brain networks. For a recent review, see ref. (Michel & Koenig, 2018). Assessment of the temporal characteristics of these microstates provides information about the dynamics of large-scale brain networks because this technique simultaneously considers signals recorded from all areas of the cortex. Since the temporal variation in resting-state brain network dynamics may be a significant biomarker of illness and therapeutic outcome (Hutchison et al., 2013; Chang & Glover, 2010; Honey et al., 2007), microstate analysis (Fig 6) is a highly suitable tool for this purpose.

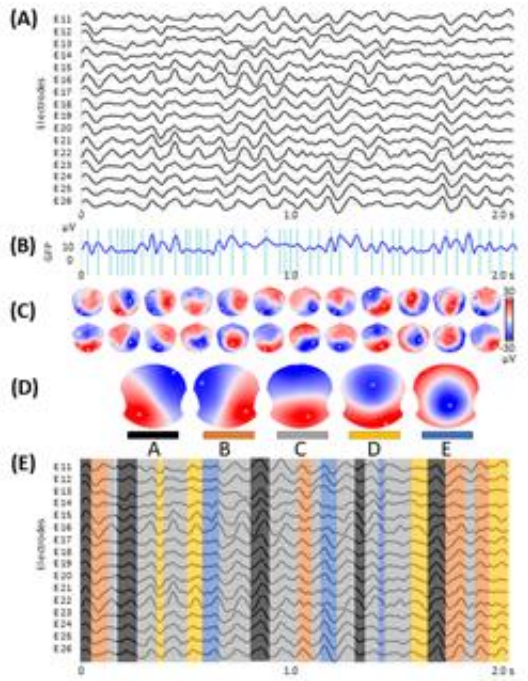

Figure 6 Microstate analysis: (A) resting-state EEG from a subsample of 16 out of 204 electrodes; (B) GFP curve with peaks (vertical lines) in the same EEG period as shown in (A); (C) potential maps at successive GFP peaks, indicated in (B), from the first 1 s period of the recording; (D) set of five cluster maps best explaining the data as revealed by k-means clustering of the maps at the GFP peaks; (E) the original EEG recording shown in (A) with superimposed colour-coded microstate segments. Note that each time point of the EEG recording was labelled with the cluster map, shown in (D), with which the instant map correlated best. The duration of segments, occurrence, and coverage for all microstates is computed on thus labelled EEG recording. (Damborská et al., 2019c - Supplementary Figure 1 - Annex 11, Chapter 5.2); GFP = global field power = standard deviation of values (μV) across all electrodes in a given time point

3. Event-related potentials and higher brain functions

Higher brain functions that are crucial for human behaviour represent the most scientifically challenging functions of human. These complex functions involve cognitive and executive functions. The cognitive functions enable us to attend to, identify and act meaningfully in response to external and internal stimuli. They include detection of the stimulus, decoding its significance, memory involvement, deciding, response selection, planning, response inhibition, response performance, performance and error monitoring. Executive functions are considered to be a part of a control system that adapts cognitive functions to the current environment and state of the organism. The brain regions that carry out such complex functions are the association cortices, which integrate information from different brain regions. The afferent projections come from the primary and secondary sensory and motor cortices, hippocampus, thalamus, and brainstem. The efferent projections reach the hippocampus, basal ganglia, cerebellum, thalamus, as well as other cortical regions (Fig.7)

Fundamental insights into the functional engagement of different brain regions in cognitive and executive processes have already been provided by observations of patients with damage to these areas, non-invasive brain imaging of normal subjects, functional mapping at neurosurgery in patients with e.g., epilepsy or Parkinson´s disease (PD), and invasive animal studies. Evidence from these investigations suggests that the parietal association cortex is important for attending to stimuli, the temporal association cortex for audition and recognizing objects, the frontal association cortex for selecting and planning behavioural responses, and the occipital/parietal association cortex for vision (Purves et al., 2018). Nevertheless, the functional organization of these brain regions into a coordinated activity of large-scale brain networks is not fully understood yet.

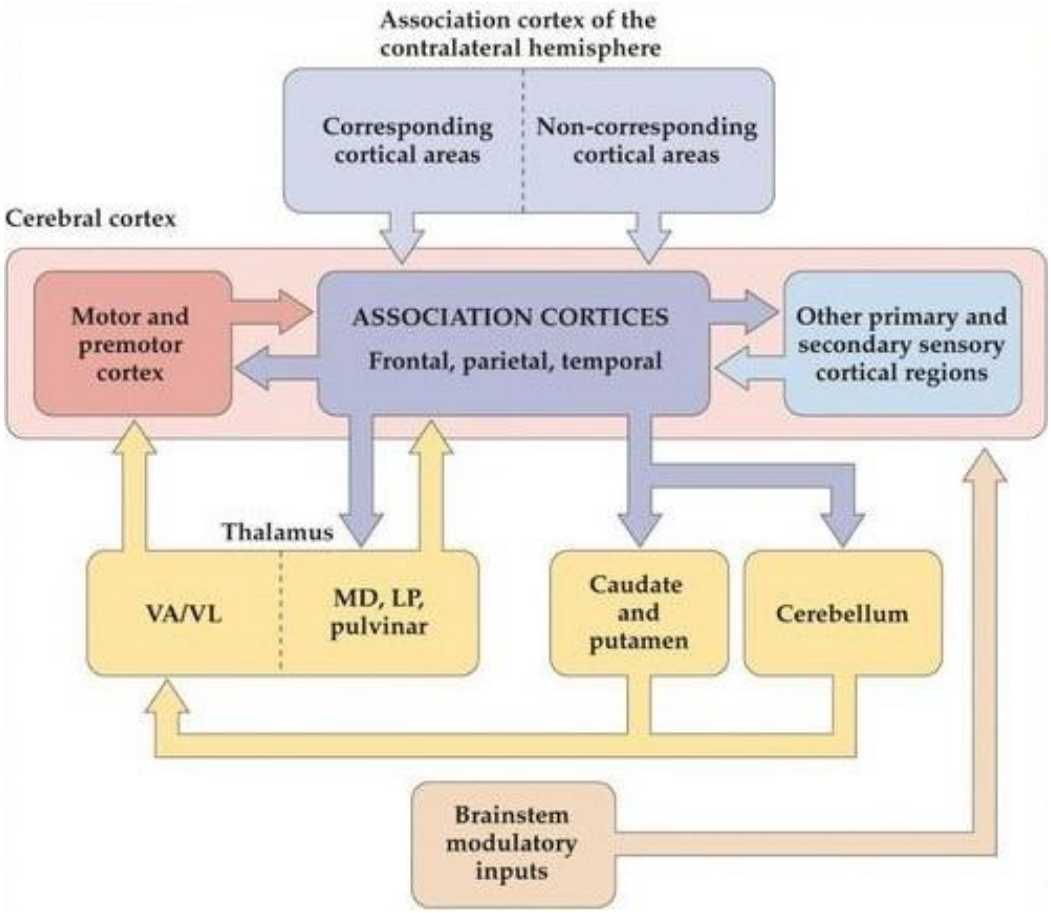

Figure 7 Summary of the overall connectivity of the association cortices. VA ventral anterior nucleus, VL = ventral lateral nucleus, MD = medial dorsal nucleus, LP = lateral posterior nucleus. (From Purves et al., 2018, Figure 27.3)

In studies included in this chapter of the habilitation thesis I focused on the identification and investigation of brain networks engaged in non-motor and movement-related higher brain functions. To this end, together with my colleagues I studied ERP brain activity during non-motor responses to visual stimuli as well as evoked activity before, during and after voluntary movements, either performed as self-paced movements or within different cognitive tasks. All intracerebral studies included in this chapter of the habilitation thesis were conducted at Masaryk University in Brno in collaboration between the Department of Physiology, 1st Department of Neurology, and Central European Institute of Technology. One intracerebral study (Kukleta et al., 2017 – Annex 7, Chapter 3.3) was performed on patients recruited at the Neurosurgery department at Sainte-Anne Hospital Center in Paris. Others were

done on patients that were enrolled into the epileptosurgery program at St. Anne's University Hospital in Brno.

Our intracerebral ERP studies that focused on non-motor cognitive functions in the human brain extended current knowledge on this topic by identifying brain regions within the temporal and frontal cortices involved in these functions (Damborská et al., 2012 - Annex 1, Chapter 3.1). We have also demonstrated that during a simple sensorimotor task, human hippocampi generate a prominent negative ERP that occurs independently of motor execution, thus we provided evidence that hippocampal activity is related to the evaluation of stimulus meaning rather than to the motor response (Roman et al., 2013 - Annex 2, Chapter 3.1). Furthermore, we first showed that the primary motor cortex is implicated in the executive control of actions that are not motor in nature (Kukleta et al., 2016 - Annex 3, Chapter 3.1).

One of the most studied ERP components is the P3 waveform, which was traditionally viewed as reflecting orientation, attention, update of working memory, decision, and cognitive closure of stimulus identification. Nevertheless, a series of studies conducted by our team brought the first intracerebral evidence that the P3 phenomenon might be related not only to these non-motor cognitive functions but also to the movement-related ones (Damborská et al., 2000; 2003; 2004; Damborská et al., 2001 - Annex 4, Chapter 3.2; Damborská et al., 2006 - Annex 5, Chapter 3.2; Damborská, 2012; Roman et al., 2001; 2005).

It is generally accepted that the control of *intentional motor action* involves brain operations that select, plan and execute the movement. The beginning of an action comprises motives for it, evaluation of advantages and disadvantages, and creation of its internal representation. The execution comprises a sequence of specific motor operations, which results in the formation of commands to muscles. The final operation provides confirmation that there is a match between the predicted and the actual state. We extended the knowledge of that time on this topic when we identified large-scale brain networks that might be involved in the process of movement execution (Damborská et al., 2000; 2003; 2004; Damborská et al., 2001 - Annex 4, Chapter 3.2; Damborská et al., 2006 - Annex 5, Chapter 3.2; Roman et al., 2001; 2005) and in the process of comparison between the intended and actually performed motor action (Damborská et al., 2016 - Annex 6, Chapter 3.3; Kukleta et al., 2017 - Annex 7,

Chapter 3.3). Moreover, in our latest work, we provided new findings on inhibition processes that are involved during motor tasks. Using a high-density scalp ERP approach, my PhD student Jiří Kutý has recently identified electrophysiological correlates of inhibition of motor action (Kutý et al., 2021).

3.1 Non-motor cognitive functions

The description of spatiotemporal characteristics of intracerebral ERP components may provide relevant data for understanding of the organization and functional principles of cognitive networks (Brázdil et al., 2003, Rektor et al., 2007). With the aim to search for electrophysiological correlates of non-motor cognitive functions, in our study (Damborska et al., 2012 - Annex 1), we evaluated the spatio-temporal characteristics of intracerebrally recorded ERPs elicited during a visual oddball task. During this task, subjects performed mental counting and motor activity in response to target stimuli, while no overt or covert responses were required after nontarget stimuli. We have demonstrated the existence of the target and nontarget ERPs with courses, initially almost identical and then divergent. We provided evidence that there are sites in the brain that manifest the point of the divergence in the very late phase of the task (more than 420 ms after the stimulus onset) with generators of late post-divergence components in the parahippocampal gyrus, superior, middle and inferior temporal gyri, amygdala, and fronto-orbital cortex. In a paradigm where two different stimuli are presented and two different reactions are required, it is not surprising that the ERPs diverge. Of more interest is the fact that the divergence point in several brain sites was observed so late in the course of the ERP, thus suggesting that the stimuli were being processed equally in these brain sites for a very long time. It seems paradoxical that, during the period in which the stimuli have already been distinguished while the subject must be aware of different demands and the motor response has already been planned and in some cases even executed, some sites in the brain keep responding almost identically. In the light of the previous demonstration of brain sites with task-relevant EEG activity almost identical during the whole oddball task (Kukleta et al., 2003), this finding does not appear so illogical. Evidently, beside the activities specific to each task variant, there exist activities that are common to the target and nontarget task variants. As regards the processes

underlying these non-specific activities, they could include consciousness and sustained attention, since these functions are required for both task variants. On the other hand, the differences between the late post-divergence ERP components described in our study (Damborská et al., 2012 – Annex 1) appear to embody the task-specific activities associated with the different closure of the task including different demands on memory engagement.

Clinical evidence from patients with lesions of the temporal association cortex indicates that the recognition and identification of attended stimuli is one of the major functions of this part of the brain. It is known that damage to either temporal lobe can result in agnosia, i.e., a disorder characterized by difficulty in recognizing, identifying, and naming different categories of objects. Associational connections within the temporal lobe are considered to be hierarchically organized, which enables only highly integrated information to reach the hippocampal formation (Lavenex & Amaral, 2000). ERP recorded in the hippocampus during cognitive motor tasks can be observed around 450 ms after stimulus onset as a large, mostly negative evoked activity (Halgren et al., 1980; Brázdil et al., 2001). This potential was suggested to reflect the arrival of neocortical information into the hippocampus or of recurrent inhibition from hippocampal pyramidal cells (Paller & McCarthy, 2002). As such, this ERP has been used as an index of hippocampal activity during various cognitive tasks. Movement-related increase in theta oscillations was observed in intracerebral recordings from the human hippocampus (Ekstrom et al., 2005). This finding is consistent with the sensorimotor integration theory suggesting that hippocampal theta activity may reflect the processing of sensory information related to the movement preparation and execution (Bland & Oddie, 2001). On the contrary, in our intracerebral EEG study we have demonstrated that the late-latency hippocampal negative ERP occurs independently of motor execution during a simple sensorimotor task (Roman et al., 2013 - Annex 2). We have shown that the hippocampal negative potential was time-locked to the auditory stimulus rather than to the motor response. Its latency did not correlate with reaction time; moreover, it either preceded or followed the motor response. We therefore suggested that this ERP may be related to the stimulus meaning evaluation. The finding of a long hippocampal ERP latency that in some cases exceeded the reaction time could be explained by the existence of a short-cut pathway

from auditory areas to secondary motor areas (Bender et al., 2006). Thus, we also demonstrated that the hippocampal stimulus meaning evaluation is not critical for the movement execution.

The original hypothesis that the primary motor cortex (M1) has an important role in the processing of cognitive information related to motor functions (Georgopoulos et al., 1989) has been supported by both human and monkey studies that have documented the involvement of the M1 in the cognitive – motor processing during e.g. motor imagery (Lotze et al., 1999), serial order coding (Carpenter et al., 1999), and stimulus – response incompatibility (Zhang et al., 1997). Nevertheless, only our human intracerebral study produced the first evidence for the involvement of M1 during situations where no overt or covered motor action is present (Kukleta et al., 2016 - Annex 3). In that study we observed ERP consisting of an isolated late (over 500ms) waveform which was recorded in M1 as a response to the nontarget stimulus of the visual oddball task. The sequence of the main operations underlying the nontarget response ought to comprise detection and cognitive discrimination of the nontarget stimulus, selection and execution of the instructed response (i.e., doing nothing) and control of the accordance between the actual result of the action with its internal representation – in summary a set of predominantly cognitive tasks without direct linkage to the motor functions. Thus, our findings of the late ERP waveform elicited in the M1 during the nontarget task variant clearly suggest functional involvement of the M1 in cognitive processing not related to motor function. Since we observed that the same loci were activated both in correct and incorrect responses, we suggested that this potential does not reflect a process of inhibiting a motor response in the nontarget condition. Our findings rather support the view that these loci are engaged both in the control of correct performance and detection of errors.

The control of accordance between the actual action and its internal representation, together with the processing of other information needed for action valuation and evaluation, is known to be realized by a large network of brain structures including frontal and parietal cortices, basal ganglia, thalamus, and brain stem nuclei (Ullsperger et al., 2014). The involvement of M1 in motor-related actions is not surprising. Its activation in cognitive operations, which are linked to non-motor actions, could be regarded as the manifestation of a relatively low specialization of the

underlying neuronal network. Our study (Kukleta et al., 2016 - Annex 3) thus extends the knowledge about M1 involvement in the executive control of actions by its implication in control of actions, which are not motor in nature.

Annex 1

Damborská, A., Brázdil, M., Rektor, I., & Kukleta, M. (2012). Late divergence of target and nontarget ERPs in a visual oddball task. *Physiological research, 61*(3), 307-318.
IF(2012) = 1.531, rank Q3
Quantitative contribution: 80%
Content contribution: pre-processing, analysis, participation in statistical evaluation, writing the initial draft, table and figure preparation, corresponding author

Annex 2

Roman, R., Brázdil, M., Chládek, J., Rektor, I., Jurák, P., Světlák, M., **Damborská, A.**, Shaw, DJ., Kukleta, M. (2013). Hippocampal negative event-related potential recorded in humans during a simple sensorimotor task occurs independently of motor execution. *Hippocampu*s 23 (12), 1337-1344.
IF(2013) = 4.302; rank Q1
Quantitative contribution: 5%
Content contribution: participation in table and figure preparation, critical commenting

Annex 3

Kukleta, M., **Damborská, A.**, Roman, R., Rektor, I., & Brázdil, M. (2016). The primary motor cortex is involved in the control of a non-motor cognitive action. *Clinical Neurophysiology*, 127 (2), 1547 – 1550.
IF(2016) = 3.866; rank Q1
Quantitative contribution: 40%
Content contribution: participation in writing the initial draft, participation in table and figure preparation, corresponding author

Annex 1

Damborská, A., Brázdil, M., Rektor, I., & Kukleta, M. (2012). Late divergence of target and nontarget ERPs in a visual oddball task. *Physiological research, 61*(3), 307-318.

Physiol. Res. 61: 307-318, 2012

Late Divergence of Target and Nontarget ERPs in a Visual Oddball Task

A. DAMBORSKÁ[1,2], M. BRÁZDIL[1,3], I. REKTOR[1,3], E. JANOUŠOVÁ[4], J. CHLÁDEK[5], M. KUKLETA[1]

[1]CEITEC − Central European Institute of Technology, Masaryk University, Brno, Czech Republic, [2]Department of Physiology, Faculty of Medicine, Masaryk University, Brno, Czech Republic, [3]First Department of Neurology, St. Anne's Faculty Hospital, Masaryk University, Brno, Czech Republic, [4]Institute of Biostatistics and Analyses, Masaryk University, Brno, Czech Republic, [5]Institute of Scientific Instruments, Academy of Sciences of the Czech Republic, Brno, Czech Republic

Received June 24, 2011
Accepted January 26, 2012
On-line April 5, 2012

Summary

Different mental operations were expected in the late phase of intracerebral ERPs obtained in the visual oddball task with mental counting. Therefore we searched for late divergences of target and nontarget ERPs followed by components exceeding the temporal window of the P300 wave. Electrical activity from 152 brain regions of 14 epileptic patients was recorded by means of depth electrodes. Average target and nontarget records from 1800 ms long EEG periods free of epileptic activity were compared. Late divergence preceded by almost identical course of the target and nontarget ERPs was found in 16 brain regions of 6 patients. The mean latency of the divergence point was 570±93 ms after the stimulus onset. The target post-divergence section of the ERP differed from the nontarget one by opposite polarity, different latency of the components, or even different number of the components. Generators of post-divergence ERP components were found in the parahippocampal gyrus, superior, middle and inferior temporal gyri, amygdala, and fronto-orbital cortex. Finding of late divergence indicates that functional differences exist even not sooner than during the final phase of the task.

Key words

Intracerebral recording • Oddball task • Visual evoked potentials • Mental counting • Memory

Corresponding author

Alena Damborská, Department of Physiology, Faculty of Medicine, Masaryk University, Kamenice 5, CZ-625 00 Brno, Czech Republic. E-mail: adambor@med.muni.cz

Introduction

Scalp-recorded event-related potentials (ERPs) elicited during the so-called "oddball" task have been employed for decades as a useful tool for studying the processes of cognition. In the oddball task the subject responds by button pressing and/or mental counting only to the infrequent "target" (T) stimulus, which is presented randomly and repeatedly among frequent "nontarget" (NT) stimuli. The electrophysiological response to the targets is compared with that to the nontargets and the difference is taken as a measure of the differences in underlying brain processes (Sutton *et al*. 1965). As a rule, these ERPs are composed of several components, which differ in amplitude, latency, and/or polarity. The early or exogenous ERP components are thought to express the stimulus identification processes (Jewett *et al.* 1970, Grönfors 1993). On scalp recording these components are referred to as P100, N100, and P200. The later or endogenous ERP components are considered to be associated with cognitive processes. One of the most studied endogenous ERP components is the P300 or P3 wave, the largest positive-going peak occurring after the exogenous components within a time window of 250-500 ms. Subsequent research showed that this component occurs in two main variants, P3a and P3b (Polich 1998, Comerchero and Polich 1999). These variants differ in latency and amplitude distribution.

© 2012 Institute of Physiology v.v.i., Academy of Sciences of the Czech Republic, Prague, Czech Republic

According to recent interpretation (Polich 2007), the P3a originates from stimulus/driven frontal attention mechanisms during task processing, whereas P3b originates from temporal-parietal activity associated with attention and appears related to subsequent memory processing. It has also been suggested that the P300 may be related to updating internal models about context and environment, which is triggered by event-related changes in theta rhythms reflecting self-motion (Shin 2011), thus supporting the view that cognition may be tightly interlocked to motor activity.

The assessment of differences between the target and nontarget ERPs is usually based on the amplitude and latency differences in the components. The differences between the T and NT responses occur in exogenous components if the triggering stimulus situation is complex (Luck and Hillyard 1994). On the other hand, the P300 components always differ in the T and NT responses representing a key differential sign (Hillyard *et al.* 1971, O'Donnell *et al.* 1997). In the nontarget response the P300 component either does not appear at all or exhibits smaller amplitude (Kok 1997).

From the behavioral point of view the oddball task consists of a sequence of brain operations, which include the detection of the stimulus, decoding its significance, decision "what to do", execution of the instructed movement, and/or counting the T stimuli. The difference between the T and NT tasks in principle consists in motor response and counting of stimuli in the target trials and doing nothing in the nontarget ones. Searching for the spatiotemporal relationship between these operations using registration of the ERP is in scalp recording difficult because of large summation of the electrophysiological signals. The intracerebral recording is far more suitable in this respect. For example, in a number of cortical and subcortical brain structures generators of the P3-like wave were found using intracerebral electrodes (McCarthy *et al*. 1989, Baudena *et al.* 1995, Halgren *et al.* 1995a, b, 1998, Brázdil *et al.* 1999, 2003, Rektor *et al.* 2003, 2005, 2007, Sochůrková *et al.* 2006, Damborská *et al.* 2009). Intracerebral recording disclosed also brain sites with different temporal characteristics of the P3-like component in the visual oddball task: one type related to the stimulus, other type related to the movement, and yet another type without any obvious relationship to these events (Roman *et al.* 2005). Another study reports on the modality specific P3-like component elicited in certain brain sites (Halgren *et al.* 1995b). With the help of intracerebral recording, generators of late evoked potentials similar to P3-like component were also found in Contingent Negative Variation paradigm in cortical as well as subcortical sites (Bareš *et al.* 2003). Intracerebral recording methods were also employed in studies using different response conditions in which the existence of task-specific P3-like potential generators (Brázdil *et al*. 2003) and of Contingent Negative Potential generators (Bareš *et al.* 2007) was proved.

The description of spatiotemporal characteristics of intracerebral ERP components may provide relevant data for understanding of organization and functional principles of cognitive networks (Brázdil *et al.* 2003, Kukleta *et al.* 2003, Roman *et al.* 2005, Damborská *et al.* 2006, Rektor *et al.* 2007). The oddball paradigm seems to be very useful in this respect, as it consists of sequence of partial functions both in target and nontarget variants. These functions are believed to be associated with the sequence of ERP components and thus the point of divergence (DP) between the target and nontarget ERPs found in a given brain site can be considered as a demonstration of the beginning of a functional divergence. In accordance with this interpretation the onset of the P3-like component could be considered as one example of such divergences. While there are many intracerebral studies aimed at the P3-like component in the visual oddball task, only two of them concerned also components of longer latency. In lateralized visual oddball intracerebral studies (Clarke *et al.* 1999a, b) patients exhibited late (>600 ms peak latency) ERP components with slow/broad morphology in response to target stimuli that, in turn, were either absent or of smaller amplitude to nontarget stimuli. These components were typically negative-going and followed behavioral motor responses. They were pervasive, and polarity reversals were present in the insula/operculum region. Authors interpreted them as reflecting activity from secondary somatosensory cortex.

In the current study we searched for the divergence points of the target and nontarget ERPs in very late phase of the visual oddball task with mental counting. We supposed that even in the time window exceeding the latency of the P3-like component, differences between the target and nontarget ERPs should appear, thus giving rise to such late divergences, because different mental operations are expected in this phase.

Table 1. Investigated brain structures.

Patient	Electrodes (left/right)	Contacts (left/right)	Structures
1	5/2	28/13	AMY′, PHG′, FG′, STG′, MTG′, ITG′, FOC′, RG′ PHG, ITG, CG, A6
2	5/4	25/16	AMY′, HIP′, PHG′, STG′, MTG′, ITG′, OG′ AMY, HIP, PHG, MTG, OG
3	4/1	27/15	AMY′, PHG′, FG′, MTG′, ITG′, CG′, DLPFC′, WTL′ HIP, BG, WFL
4	1/6	15/26	HIP′, PHG′, BG′, WFL′ AMY, HIP, FG, STG, MTG, ITG, CG, OG, DLPFC, MFG
5	1/1	14/14	AMY′, HIP′, BG′, WTL′, WFL′ AMY, HIP, BG, WTL, WFL
6	6/4	24/17	AMY′, HIP′, STG′, MTG′, OG′, MeFG′ AMY, HIP, MTG, CG, RG, MFG, IFG, WFL
7	1/3	12/29	AMY′, HIP′ HIP, PHG, STG, DLPFC, FOC
8	1/3	13/28	AMY′, PHG′, BG′, STG′, MTG′, WTL′, WFL′ AMY, HIP, BG, STG, MTG, ITG, WTL, WFL
9	0/6	0/41	AMY, HIP, PHG, FG, STG, MTG, ITG, FOC, RG, MeFG, MFG
10	0/4	0/27	AMY, HIP, STG, MTG, WTL
11	0/6	0/36	HIP, FG, STG, MTG, ITG, CG, A4, A5, IPL, MT, WTL, WPL
12	4/5	15/26	HIP′, MTG′, CG′, DLPFC′, A8′, A9′, A10′ HIP, MTG, CG, DLPFC, MFG, A8, WTL, WFL
13	7/0	41/0	AMY′, HIP′, STG′, MTG′, CG′, DLPFC′, FOC′, A9′, WFL′
14	3/0	29/0	AMY′, PHG′, FG′, BG′, MTG′, ITG′, WTL′

Number of the patient; number of electrodes implanted in the left and right hemispheres; number of contacts exploring sites in the left and right hemispheres; anatomical structures investigated: AMY – amygdala, HIP – hippocampus, PHG – parahippocampal gyrus, FG – fusiform gyrus, BG – basal ganglia, STG, MTG, and ITG – superior, middle, and inferior temporal gyri, CG – cingulate gyrus, DLPFC – dorsolateral prefrontal cortex, FOC – fronto-orbital cortex, OG – orbital gyri, RG – rectal gyrus, MeFG, MFG, and IFG – medial, middle, and inferior frontal gyri, A 4, 5, 6, 8, 9, and 10 – Brodmann's areas 4, 5, 6, 8, 9, and 10, IPL – inferior parietal lobule, MT – mesencephalic tegmentum, WTL, WFL, and WPL – white matter of the temporal, frontal, and parietal lobes, symbol (′) indicates structures of the left hemisphere.

Materials and Methods

Subjects

Fourteen patients (3 women) aged from 20 to 45 years were employed in the study. All subjects suffered from medically intractable epilepsy and were candidates for surgical treatment. They all were under antiepileptic drug therapy, which was determined by clinical considerations. During the period of diagnostic examination by intracerebral EEG recording, the doses of medicaments were reduced to allow seizures to develop spontaneously. They had normal or corrected-to-normal vision and all but one (Patient No. 6) were right-handed. The subjects gave us their informed consent to the experimental protocol that had been approved by the Ethical Committee of Masaryk University.

Paradigm

A visual oddball task with mental counting was performed. The patients were sitting comfortably in a moderately lighted room and were focusing the centre of a monitor situated at about 100 cm from their eyes. Yellow capital letters X (target, T) or O (nontarget, NT) appeared repeatedly on white background in random order as experimental stimuli. Each stimulus presentation lasted 200 ms and the interstimulus interval varied randomly between 2 and 5 seconds. The target stimuli were five times less frequent than the nontarget ones. The

subjects were instructed to press a microswitch button with the dominant hand as quickly as possible, whenever a T stimulus appeared, to mentally count the T stimuli, and to ignore the NT stimuli.

Data acquisition

Electrical activity was recorded during the task simultaneously from various brain sites by means of standard Micro Deep semi-flexible multicontact platinum electrodes. Having a diameter of 0.8 mm, each electrode carried 5-15 contacts 2.0 mm long separated by constant intervals of 1.5 mm. Strictly for diagnostic reasons, intracerebral depth electrodes were implanted to the patients; and structures of the frontal, temporal, and parietal lobes were examined (Table 1). Every patient received from 2 to 10 such electrodes exploring either or both hemispheres. Long electrodes examined both lateral and mesial cortical regions. The electrodes were placed using the methodology of Talairach *et al.* (1967) and their position was afterwards verified by magnetic resonance imaging with electrodes in situ. The registration was made with the help of a 64-channel Brain Quick EEG system (Micromed). All the recordings were monopolar with respect to a reference electrode attached to the right processus mastoideus. The impedances used were less than 5 kΩ. The EEG signal was amplified with a bandwidth of 0.1-40 Hz at a sampling rate of 128 Hz. One of the channels recorded the button pressing and yet another channel recorded the presentation of the experimental stimuli. We did not do electrooculography, because in contrast to the scalp recordings artefacts caused by eye movements and blinking are considered to be negligible in depth recordings.

Analysis

The signal analysis was made offline with the help of ScopeWin software providing us 44 channels for simultaneous recordings. The recordings from lesions and epileptogenic zones and the trials with artefacts were rejected offline with visual inspection made by experienced person. Switching the button in response to a nontarget stimulus or its omission in response to a target one were considered as errors. In each subject all artefact-free trials with correct responses were used for calculation of average curves. Excluding of different number of trials explains the interindividual variability in number of trials used (29-58 T trials, 198-331 NT trials). Peristimulus EEG periods (from –300 to +1500 ms from the stimulus onset) were averaged separately for T and NT responses using the stimulus onset as a trigger. The statistical significance of ERP components was computed between the mean amplitude observed during the baseline region (from –600 to –100 ms from the stimulus onset) and the mean value computed as a mean from the neighbourhood of each point (170 ms length) after stimuli using a non-parametric Wilcoxon Rank Sum (Signed Rank) test for paired samples.

Records from one contact of each multicontact intracerebral electrode implanted in a particular anatomical structure were included into the analysis selecting the largest one from ERPs. In such selected contacts the amplitude differences between the target and nontarget records were assessed using a cluster-based permutation test (Maris and Oostenveld 2007). In every contact, clusters of time samples whose absolute t-value was larger than 97.5th quantile of T-distribution were computed in the poststimulus EEG period (from 0 ms to +1500 ms from the stimulus onset). Monte-Carlo estimates of the permutation p-values for each cluster were calculated on 1000 random partitions of the data set and compared with a critical alpha-level of 0.05. We disclosed brain regions with an initially almost identical course of the target and nontarget ERPs followed by a clear-cut divergence. The onset of such divergence was identified as the starting time point of the first statistically significant cluster in the post-stimulus period. To assess the portion of ERPs, attributable to movement-related potentials, we investigated the character of the relationship between the latency of a particular target post-divergence ERP component and the reaction time using the method already applied for classification of P3-like waves (Roman *et al.* 2005).

Results

The performance of subjects during the task was very good not seeming to be substantially influenced by their illness and medication (only 1.3±1.7 % of all responses were incorrect; mean patient's SRI varied between 457±34 ms and 644±78 ms, median 525±63 ms). Total number of explored brain regions was 152; ERPs were found in 102 regions, which make 67 % of explored regions. In assessing the number of ERP components, their polarity, latency and amplitude, various regions generating several types of ERP were identified: 1) regions that generated different ERPs to target and nontarget stimuli (22 brain regions); 2) regions that generated the target and nontarget ERPs exhibiting clear-cut divergence after initially almost identical curves

(41 brain regions); 3) regions that generated target and nontarget ERPs with almost identical course but statistically significantly different amplitudes in some of their components (20 brain regions); 4) regions generating ERP only to target but not to nontarget stimuli (9 brain regions); 5) regions generating almost identical ERPs to target and nontarget stimuli (10 brain regions).

In accordance with the aim of the current study, only ERPs from group 2) were further analyzed. In this group ERPs were arbitrarily divided into two subgroups according to the latency of their divergence. The first subgroup (early divergence) included ERPs diverging sooner than 420 ms after the stimulus onset and the second subgroup (late divergence) included ERPs diverging later than 420 ms after the stimulus onset (see Figure 1 and Table 2).

ERPs exhibiting the early divergence were found in nine patients in 25 brain regions (15 in the frontal lobe, 8 in the temporal lobe, and 2 in the parietal lobe). The mean latency of the point of divergence was 346 ± 35 ms from the stimulus onset. ERPs exhibiting the late divergence were found in six patients in 16 brain regions (13 in the temporal lobe and 3 in the frontal lobe). The mean latency of the point of divergence was 570±93 ms from the stimulus onset. Statistical testing showed significant amplitude differences in post-divergence section of all the early and late diverging ERPs (cluster-based permutation test).

Table 2. Early and late divergences of the target and nontarget ERPs.

EARLY				LATE			
Patient (Contact)	**Struct.**	**Latency**		**Patient (Contact)**	**Struct.**	**Latency**	
		ms	**% RT**			**ms**	**% RT**
1(C´6)	ITG	280	49	*1(A´1)*	AMY	440	77
1(F3)	CG	360	63	*1(B´2)*	PHG	536	93
1(F11)	Area 6	368	64	*1(B2)*	PHG	568	98
1(O´2)	FOC	320	56	*1(C´2)*	PHG	640	111
3(G´2)	CG	312	66	*1(T´3)*	STG	640	111
4(G1)	CG	352	67	*2(B´5)*	ITG	616	96
5(X14)	BG	312	55	*2(C´2)*	PHG	488	76
6(D´4)	STG	344	68	*2(C3)*	FG	552	86
6(G2)	CG	392	78	*3(C´14)*	MTG	448	95
6(O´6)	OG	376	75	*3(B´3)*	PHG	800	169
6(O6)	IFG	416	83	*4(A9)*	MTG	664	126
6(T´1)	STG	368	73	*4(C10)*	ITG	624	119
6(B9)	MTG	328	65	*4(X´1)*	PHG	592	112
6(G10)	MFG	336	67	*5(X´10)*	BG	544	95
11(B4)	HIP	320	67	*9(O11)*	FOC	520	89
11(B9)	MTG	344	72	*9(P1)*	MeFG	440	75
11(G2)	CG	312	65				
11(R5)	Area 5	344	72				
11(B14)	ITG	408	85				
11(G11)	IPL	376	79				
11(T3)	STG	400	84				
12(F´3)	Area 8	360	61				
13(G´1)	CG	288	56				
13(O´8)	DLPFC	312	61				
14(X´15)	BG	328	72				

MFG – middle frontal gyrus, MeFG - medial frontal gyrus, IFG – inferior frontal gyrus, FOC – fronto-orbital cortex, OG – orbital gyri, DLPFC – dorsolateral prefrontal cortex, STG – superior temporal gyrus, MTG – middle temporal gyrus, ITG – inferior temporal gyrus; IPL – inferior parietal lobule, CG – cingulate gyrus; BG – basal ganglia, AMY – amygdala, FG – fusiform gyrus, PHG – parahippocampal gyrus, HIP – hippocampus, Area 5, Area 6, Area 8 – Brodmann's areas; symbol (´) indicates structures of the left hemisphere, the divergence point latency is given in ms and in % of patient's mean reaction time (% RT).

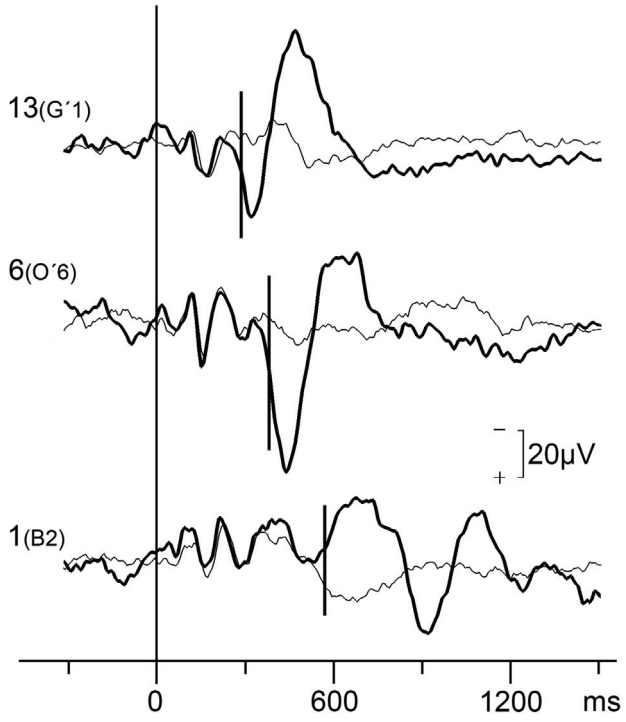

Fig. 1. Selected examples of early (288 ms and 376 ms), and late (568 ms) divergences of ERPs elicited in response to target (thick curve) and nontarget (thin curve) stimuli. Curves are labelled with patient number and recording contact (13G´1 – cingulate gyrus, 6O´6 – orbital gyri, 1B2 – parahippocampal gyrus); vertical line at zero point indicates the stimulus onset; short vertical lines indicate the divergence points of target and nontarget ERPs (i.e. the starting time point of the first statistically significant cluster calculated in the post-stimulus period using the cluster-based permutation test); symbol (´) indicates structures of the left hemisphere.

The relationship between the divergence point latency and the reaction time can be assessed from the values presented in the Table 2. It is evident that the late divergence appeared shortly before, after, or approximately at the moment of the button pressing (in average at 102±23 % of the mean reaction time).

Figure 2 shows all of the late diverging ERPs. Six of them were found in the right and ten of them in the left hemispheres. No clear-cut preponderance of ERPs exhibiting the late divergence was observed in any anatomical structure; however, most of these ERPs exhibited signs of local generation of post-divergence components in structures of temporal lobe. One example of local generation for each type of response is presented in Figure 3. Phase reversals of target post-divergence components were found in the amygdala (1A'1), fronto-orbital cortex (9 O11), and parahippocampal gyrus (1B2); phase reversals of nontarget components were found in the amygdala (1A'1), parahippocampal gyrus (1B2), and middle temporal gyrus (4A9). Relative decrease of amplitude by 36±16 % in adjacent contacts of the same electrode was observed on target post-divergence components in the parahippocampal gyrus (1B'2, 1C'2, 2C'2, 3B´3, and 4X'1), superior (1T'3), middle (3C'14 and 4A9), and inferior (2B'5 and 4C10) temporal gyri. Relative decrease of amplitude by 39±13 % in adjacent contacts of the same electrode was observed on nontarget post-divergence components in the parahippocampal gyrus (1B'2, 1C'2, 2C'2, and 4X'1), middle (3C'14) and inferior (2B'5 and 4C10) temporal gyri. Thus, generators of the target late post-divergence components were found in the amygdala (in 1 out of 16 explored regions), parahippocampal gyrus (in 6 out of 10 explored brain regions), fronto-orbital cortex (in 1 out of 4 explored brain regions), superior temporal gyrus (in 1 out of 11 explored brain regions), middle temporal gyrus (in 2 out of 16 explored brain regions), and inferior temporal gyrus (in 2 out of 9 explored brain regions), generators of the nontarget late post-divergence components were found in the same anatomical structures with the exception of the superior temporal and the fronto-orbital cortex.

From the records presented in Fig. 2 it is evident that clear-cut components were observed in the post-divergence section of not only all target but also of most nontarget late diverging ERPs. The post-divergence section of the target ERP was unequivocally different from the nontarget one exhibiting opposite polarity, different latency, or even different number of the components (see Table 3). The peak latency of the first post-divergence component varied between 516 and 968 ms (mean 695±140 ms) in the T response and between 576 and 1128 ms (mean 725±145 ms) in the NT response. The number of post-divergence ERP components varied between one and three in the T response and was significantly higher than the number of post-divergence ERP components in the NT response, which varied between none and two ($p<0.001$, Student's paired *t*-test). From 32 target post-divergence ERP components (Table 3) only two were time-locked to the button pressing (superior temporal gyrus, fusiform gyrus), seven were time-locked to the stimulus onset (amygdala, parahippocampal gyrus, superior temporal gyrus) and 23 had ambiguous relationship to both these events (amygdala, parahippocampal gyrus, fusiform gyrus, middle and inferior temporal gyri, basal ganglia, fronto-orbital cortex, and medial frontal gyrus).

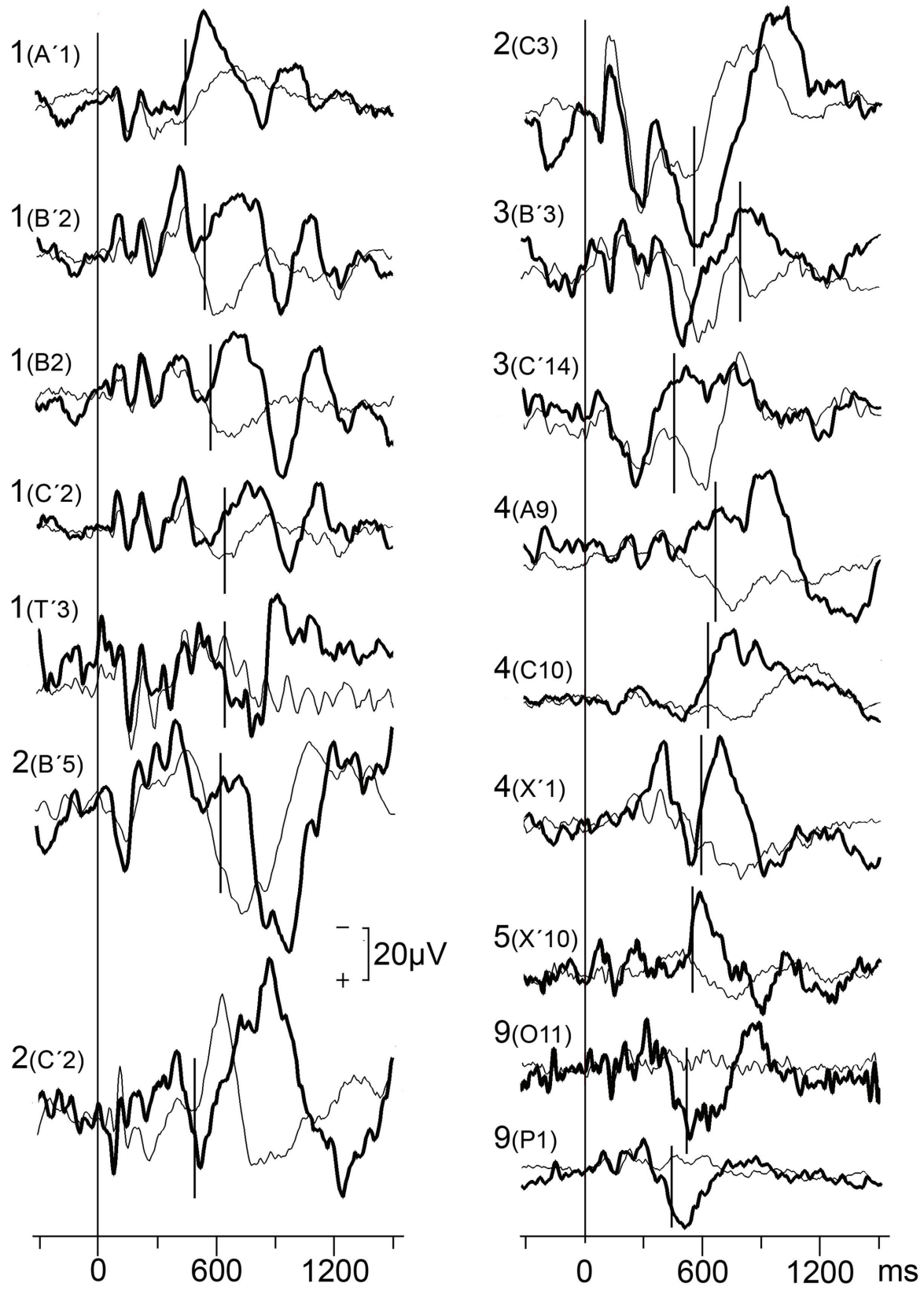

Fig. 2. Late divergence of the ERPs elicited in response to target (thick curve) and nontarget (thin curve) stimuli. Curves are labelled with patient number and recording contact; vertical line at zero point indicates the stimulus onset; short vertical lines indicate the divergence points of target and nontarget ERPs (i.e. the starting time point of the first statistically significant cluster calculated in the post-stimulus period using the cluster-based permutation test); symbol (´) indicates structures of the left hemisphere.

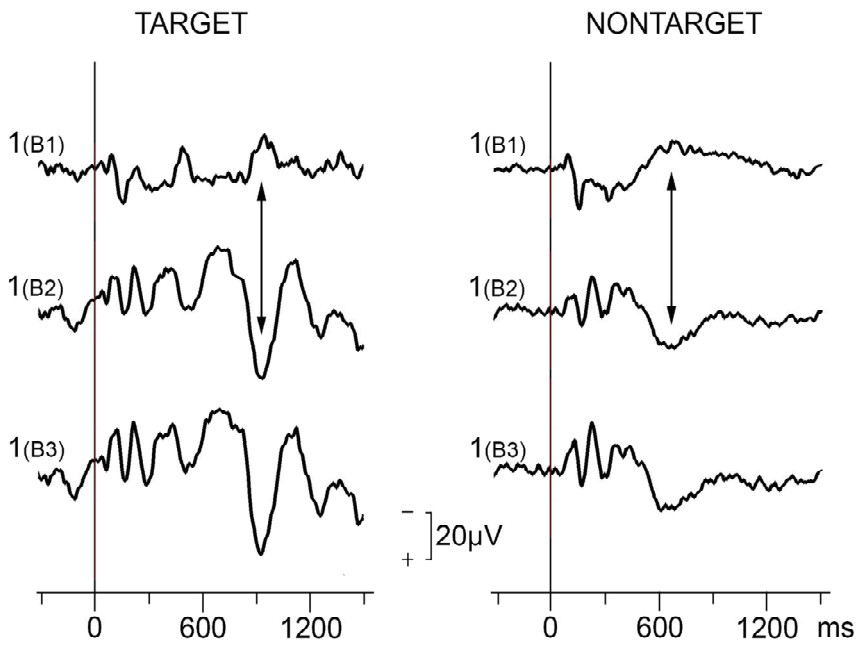

Fig. 3. An example of post-divergence ERP components. **Left section**: records from consecutive contacts of an electrode passing through the right parahippocampal gyrus (phase reversal between B1 and B2) in the target response; **Right section**: records from the same contacts in the nontarget response. Vertical line at zero point indicates the stimulus onset. Records from 1(B2) contact are also presented in Figure 1 and Figure 2.

Table 3. Polarity and latency of the target and nontarget late post-divergence components.

Patient (Contact)	Structure	Target Post-divergence components			Nontarget Post-divergence components	
1(A´1)	AMY	N528[a]	N992		N704	
1(B´2)	PHG	N736	P928[a]	N1088[a]	P576	
1(B2)	PHG	N688	P920	N1112[a]	P656	
1(C´2)	PHG	N752	P952[a]	N1112	P600	N856
1(T´3)	STG	P773[b]	N904[a]			
2(B´5)	ITG	P968			P728	N1072
2(C´2)	PHG	P523	N864	P1240	N600	P776
2(C3)	FG	P568[b]	N944		N824	
3(C´14)	MTG	N752			P600	N776
3(B´3)	PHG	N828	P1211			
4(A9)	MTG	N936	P1360		P744	
4(C10)	ITG	N752			N1128	
4(X´1)	PHG	N680[a]	N1200		P792	
5(X´10)	BG	N584	N882		P744	
9(O11)	FOC	P531	N835			
9(P1)	MeFG	P516				

AMY – amygdala, PHG – parahippocampal gyrus, FOC – fronto-orbital cortex; STG – superior temporal gyrus, MTG – middle temporal gyrus, ITG – inferior temporal gyrus; FG – fusiform gyrus, BG – basal ganglia, MeFG – medial frontal gyrus, N – negativity, upward deflection, P – positivity, downward deflection; symbol (´) indicates structures of the left hemisphere, [a] component time-locked to the stimulus, [b] component time-locked to the button pressing.

Discussion

Our results demonstrated the existence of the target and nontarget event-related potentials initially almost identical in course and then divergent, with the point of divergence manifesting in the very late phase of the visual oddball task. The question arose as to whether these late divergences could be related to the differences

in motor demands between T and NT tasks. Certain factors suggest otherwise. The motor system activities that precede execution of movement include decision-making, action planning, and formation of a motor command. As the results of this study showed, the DP occurred shortly before, after, or at the moment of pressing the button. Thus, all of the pre-movement activities occurred during the period when the two EEG responses were following almost identical courses. Further, post-movement activity cannot be excluded from considerations of factors leading to the divergence. However, such involvement may only be partial because only negligible portion of ERP components was time-locked to the button pressing. The ERPs attributable to movement-related potentials were found in superior temporal and fusiform gyri.

Memory mechanisms are involved in the various steps of the task from beginning to end. They start with cognitive discrimination of the stimuli and continue with selection of the correct response, i.e. the decision as to whether to move or not and whether to count or not, in order to follow the instructions for the experiment. The next important step associated with memory processes involves counting the target stimuli. When counting, one must recall the result of the previous calculation, then do the calculation, which consists of adding "one" to the recalled number, and then store the new result in the memory.

Our results showed that majority of the generators of the late post-divergence ERP components were observed in structures known to participate in memory processes. Due to the fact that recording sites were selected according to diagnostic concerns, and many regions potentially engaged in the task were not explored, the possibility to use this result for functional interpretations is limited. Thus, it still remains in question as to whether the late post-divergence ERP components could represent mental counting processes or other processes, for instance those associated with so-called closure of the whole response (disengagement from the just finished decision, engagement to the consecutive one).

Our results also showed a predominance of targets over nontargets in terms of the number of late post-divergence ERP components. The higher number of late post-divergence ERP components indicated in the T variant suggests higher demands on memory functions in the T response. This interpretation is also in accordance with the results of the visual oddball studies without mental counting (Clarke *et al.* 1999a, b), where only single target components are reported in different brain sites during the very late phase of the task. Unlike in present study no counting process was performed after target stimulus presentation in these studies, which could led there to decreased number of late target ERP components.

In a paradigm where two different stimuli are presented and two different tasks are required it is not surprising that the ERPs diverge (for further details, see Brázdil *et al*. 2003, Rektor *et al.* 2007). Of more interest in the current study is the finding that the divergence point in several brain sites was observed so late in the course of the EEG response. In these responses, the targets and nontargets revealed an almost identical course of ERPs until this very late DP, thus suggesting that the stimuli were being processed equally in these brain sites for a very long time. It seems paradoxical that during the period, in which the stimuli have already been distinguished, while the subject must be aware of different demands and the motor response has already been planned and in some cases even executed, some sites in the brain keep responding almost identically. However, in the light of the previous demonstration of brain sites with task-relevant EEG activity almost identical during the whole oddball task (Kukleta *et al.* 2003); this finding does not appear so illogical. Evidently, as well as the specific electrical activities elicited in the oddball task, there are also activities that are common to the T and NT responses. As regards the processes underlying the non-specific activities, they could include consciousness and sustained attention, since these functions are required for both T and NT responses.

Extensive literature on event-related potentials in target detection tasks shows that the target and nontarget electrophysiological responses may diverge after sensory potentials had been elicited, giving rise to a post-divergence ERP component, well-known as the P300 component (see Polich 2007). This occurs after the initial phase of ERPs in which the stimulus is being detected and discriminated. This component represents the cognitive functions involved in the orientation of attention, contextual updating, response modulation, and response resolution. In scalp recordings it consists mainly of two variants, P3a and P3b (Courchesne *et al.* 1975, Squires *et al.* 1975, Knight 1984, Donchin and Coles 1988, Comerchero and Polich 1999, Polich 2007), which differ in their scalp topography and temporal

characteristics. The P3a exhibits a frontal/central scalp distribution and a relatively short peak latency, while the P3b exhibits a parietal scalp distribution and relatively long peak latency. In this context the early post-divergence components presented in present study could correspond to the P3a-like and P3b-like waveforms.

The differences between EEG responses are generally viewed as reflecting differences between underlying functions engaged in the tasks. By the same logic, differences between the late post-divergence ERP components described in the current study (see Fig. 2 and Table 3) appear to embody different brain processes in the late phase of the target and nontarget task variants. These processes might be associated with the different closure of the task. It is not clear, however, to what extend these differences are associated with different demands on memory engagement in relation to the request for counting the target stimuli. These late post-divergence ERP components generated in the parahippocampal gyrus, superior, middle and inferior temporal gyri, amygdala, and fronto-orbital cortex represent a finding that was previously missing in the whole interpretation of ERP from visual oddball task with mental counting.

Conflict of Interest

There is no conflict of interest.

Acknowledgements

This work was supported by grants Nos. MSM0021622404, MUNI/A/0941/2010 and 1M06039 and the project "CEITEC − Central European Institute of Technology" (CZ.1.05/1.1.00/02.0068) from European Regional Development Fund. The technical part of the study was supported by grant P103/11/0933 of the Grant Agency of the CR. We wish to thank Mgr. Ladislav Červený and Tony Long for language help.

References

BAREŠ M, REKTOR I, KAŇOVSKÝ P, STREITOVÁ H: Cortical and subcortical distribution of middle and long latency auditory and visual evoked potentials in a cognitive (CNV) paradigm. *Clin Neurophysiol* **114**: 2447-2460, 2003.

BAREŠ M, NESTRAŠIL I, REKTOR I: The effect of response type (motor output versus mental counting) on the intracerebral distribution of the slow cortical potentials in an externally cued (CNV) paradigm. *Brain Research Bulletin* **71**: 428-435, 2007.

BAUDENA P, HALGREN E, HEIT G, CLARKE JM: Intracerebral potentials to rare target and distracter auditory and visual stimuli. III. Frontal cortex. *Electroencephalogr Clin Neurophysiol* **94**: 251-264, 1995.

BRÁZDIL M, REKTOR I, DUFEK M, DANIEL P, JURÁK P, KUBA R: The role of frontal and temporal lobes in visual discrimination task − depth ERP studies. *Neurophysiol Clin* **29**: 339-350, 1999.

BRÁZDIL M, ROMAN R, DANIEL P, REKTOR I: Intracerebral somatosensory event-related potentials: effect of response type (button pressing versus mental counting) on P3-like potentials within the human brain. *Clin Neurophysiol* **114**: 1489-1496, 2003.

CLARKE JM, HALGREN E, CHAUVEL P: Intracranial ERPs in humans during a lateralized visual oddball task: I. Occipital and peri-Rolandic recordings. *Clin Neurophysiol* **110**: 1210-1225, 1999a.

CLARKE JM, HALGREN E, CHAUVEL P: Intracranial ERPs in humans during a lateralized visual oddball task: II. Temporal, parietal, and frontal recordings. *Clin Neurophysiol* **110**: 1226-1244, 1999b.

COMERCHERO MD, POLICH J: P3a and P3b from typical auditory and visual stimuli. *Clin Neurophysiol* **110**: 24-30, 1999.

COURCHESNE E, HILLYARD SA, GALAMBOS R: Stimulus novelty, task relevance and the visual evoked potential in man. *Electroencephalogr Clin Neurophysiol* **39**: 131-143, 1975.

DAMBORSKÁ A, BRÁZDIL M, REKTOR I, ROMAN R, KUKLETA M: Correlation between stimulus-response intervals and peak amplitude latencies of visual P3 waves. *Homeostasis Health Dis* **44**: 165-168, 2006.

DAMBORSKÁ A, BRÁZDIL M, REKTOR I, KUKLETA M: Temporal characteristics of intracerebral P3 wave in a visual oddball task. *Physiol Res* **58**: 12P, 2009.

DONCHIN E, COLES MG: Is the P300 component a manifestation of context updating? *Behav Brain Sci* **11**: 357-374, 1988.

GRÖNFORS T: Identification of auditory brainstem responses. *Int J Biomed Comput* **32**: 171-179, 1993.

HALGREN E, BAUDENA P, CLARKE JM, HEIT G, LIEGEOIS C, CHAUVEL P, MUSOLINO A: Intracerebral potentials to rare target and distracter auditory and visual stimuli. I. Superior temporal plane and parietal lobe. *Electroencephalogr Clin Neurophysiol* **94**: 191-220, 1995a.

HALGREN E, BAUDENA P, CLARKE JM, HEIT G, MARINKOVIC K, DEVAUX B, VIGNAL JP, BIRABEN A: Intracerebral potentials to rare target and distracter auditory and visual stimuli. II. Medial, lateral and posterior temporal lobe. *Electroencephalogr Clin Neurophysiol* **94**: 229-250, 1995b.

HALGREN E, MARINKOVIC K, CHAUVEL P: Generators of the late cognitive potentials in auditory and visual oddball tasks. *Electroencephalogr Clin Neurophysiol* **106**: 156-164, 1998.

HILLYARD SA, SQUIRES KC, BAUER JW, LINDSAY PH: Evoked potential correlates of auditory signal detection. *Science* **172**: 1357-1360, 1971.

JEWETT DL, ROMANO MN, WILLISTON JS: Human auditory evoked potentials: possible brain stem components detected on the scalp. *Science* **167**: 1517-1518, 1970.

KNIGHT RT: Decreased response to novel stimuli after prefrontal lesions in man. *Electroencephalogr Clin Neurophysiol* **59**: 9-20, 1984.

KOK A: Event-related-potential (ERP) reflections of mental resources: a review and synthesis. *Biol Psychol* **45**: 19-56, 1997.

KUKLETA M, BRÁZDIL M, ROMAN R, JURÁK P: Identical event-related potentials to target and frequent stimuli of visual oddball task recorded by intracerebral electrodes. *Clin Neurophysiol* **114**: 1292-1297, 2003.

LUCK SJ, HILLYARD SA: Electrophysiological correlates of feature analysis during visual search. *Psychophysiology* **31**: 291-308, 1994.

MARIS E, OOSTENVELD R: Nonparametric statistical testing of EEG- and MEG-data. *J Neurosci Methods* **164**: 177-190, 2007.

McCARTHY G, WOOD CC, WILLIAMSON PD, SPENCER DD: Task-dependent field potentials in human hippocampal formation. *J Neurosci* **9**: 4253-4268, 1989.

O'DONNELL BF, SWEARER JM, SMITH LT, HOKAMA H, McCARLEY RW: A topographic study of ERPs elicited by visual feature discrimination. *Brain Topogr* **10**: 133-143, 1997.

POLICH J: P300 clinical utility and control of variability. *J Clin Neurophysiol* **15**: 14-33, 1998.

POLICH J: Updating P300: an integrative theory of P3a and P3b. *Clin Neurophysiol* **118**: 2128-2148, 2007.

REKTOR I, KAŇOVSKÝ P, BAREŠ M, BRÁZDIL M, STREITOVÁ H, KLAJBLOVÁ H, KUBA R, DANIEL P: A SEEG study of ERP in motor and premotor cortices and in the basal ganglia. *Clin Neurophysiol* **114**: 463-471, 2003.

REKTOR I, BAREŠ M, BRÁZDIL M, KAŇOVSKÝ P, REKTOROVÁ I, SOCHŮRKOVÁ D, KUBOVÁ D, KUBA R, DANIEL P: Cognitive-and movement-related potentials recorded in the human basal ganglia. *Mov Disord* **20**: 562-568, 2005.

REKTOR I, BRÁZDIL M, NESTRAŠIL I, BAREŠ M, DANIEL P: Modifications of cognitive and motor tasks affect the occurrence of event-related potentials in the human cortex. *Eur J Neurosci* **26**: 1371-1380, 2007.

ROMAN R, BRÁZDIL M, JURÁK P, REKTOR I, KUKLETA M: Intracerebral P3-like waveforms and the length of the stimulus-response interval in a visual oddball paradigm. *Clin Neurophysiol* **116**: 160-171, 2005.

SHIN J: The interrelationship between movement and cognition: theta rhythm and the P300 event-related potential. *Hippocampus* **21**: 744-752, 2011.

SOCHŮRKOVÁ D, BRÁZDIL M, JURÁK P, REKTOR I: P3 and ERD/ERS in a visual oddball paradigm: a depth EEG study from the mesial temporal structures. *J Psychophysiol* **20**: 32-39, 2006.

SQUIRES NK, SQUIRES KC, HILLYARD SA: Two varieties of long-latency positive waves evoked by unpredictable auditory stimuli in man. *Electroencephalogr Clin Neurophysiol* **38**: 387-401, 1975.

SUTTON S, BAREN M, ZUBIN J, JOHN ER: Evoked-potential correlates of stimulus uncertainty. *Science* **150**: 1187-1188, 1965.

TALAIRACH J, SZIKLA G, TOURNOUX P, PROSALENTIS A, BORDAS-FERRER M, COVELLO J, JACOB M, MEMPEL H, SUSER P, BANCAUD J: *Atlas d'Anatomie Stéréotaxique du Télencéphale.* Masson & Cie, Paris, 1967.

Annex 2

Roman, R., Brázdil, M., Chládek, J., Rektor, I., Jurák, P., Světlák, M., **Damborská, A.**, Shaw, DJ., Kukleta, M. (2013). Hippocampal negative event-related potential recorded in humans during a simple sensorimotor task occurs independently of motor execution. *Hippocampu*s 23 (12), 1337-1344.

HIPPOCAMPUS 23:1337–1344 (2013)

Hippocampal Negative Event-Related Potential Recorded in Humans During a Simple Sensorimotor Task Occurs Independently of Motor Execution

Robert Roman,[1,2]* Milan Brázdil,[2,3] Jan Chládek,[2,4] Ivan Rektor,[2,3] Pavel Jurák,[4] Miroslav Světlák,[1] Alena Damborská,[1,2] Daniel J. Shaw,[2] and Miloslav Kukleta[2]

ABSTRACT: A hippocampal-prominent event-related potential (ERP) with a peak latency at around 450 ms is consistently observed as a correlate of hippocampal activity during various cognitive tasks. Some intracranial EEG studies demonstrated that the amplitude of this hippocampal potential was greater in response to stimuli requiring an overt motor response, in comparison with stimuli for which no motor response is required. These findings could indicate that hippocampal-evoked activity is related to movement execution as well as stimulus evaluation and associated memory processes. The aim of the present study was to investigate the temporal relationship between the hippocampal negative potential latency and motor responses. We analyzed ERPs recorded with 22 depth electrodes implanted into the hippocampi of 11 epileptic patients. Subjects were instructed to press a button after the presentation of a tone. All investigated hippocampi generated a prominent negative ERP peaking at ~420 ms. In 16 from 22 cases, we found that the ERP latency did not correlate with the reaction time; in different subjects, this potential could either precede or follow the motor response. Our results indicate that the hippocampal negative ERP occurs independently of motor execution. We suggest that hippocampal-evoked activity, recorded in a simple sensorimotor task, is related to the evaluation of stimulus meaning within the context of situation. © 2013 Wiley Periodicals, Inc.

KEY WORDS: intracranial recordings; auditory task; hippocampus; ERP latency; motor response

INTRODUCTION

Electrophysiological recordings from the hippocampus in humans (e.g., Halgren et al., 1980; Stapleton and Halgren, 1987; Grunwald et al., 1995; Brázdil et al., 2001; Fell et al., 2005; Boutros et al., 2008; Axmacher et al., 2010) and in animals (e.g., Paller et al., 1992; Shinba et al., 1996; Shin, 2011) reveal a large, mostly negative, event-related potential (ERP) with a peak latency of around 450 ms. There is no consensus on the terminology used to refer to this cognitive potential. Some authors regard it as one of the putative generators of the scalp recorded P300 and label this ERP accordingly; Grunwald et al. (1999) and Fell et al. (2004), for example, used the term MTL-P300, while Halgren et al. (1995) labeled it the depth P3b. Likewise, similar ERPs recorded from the hippocampus and various other brain structures have been referred to as P3-like waveforms (Brázdil et al., 2003; Roman et al., 2005; Damborská et al., 2012). Hippocampal activity is not related to some functions associated with scalp P300, however, and it can be observed also after frequent stimuli in oddball task (Kukleta et al., 2003). We believe that the descriptive term "large negative ERP" used by Paller and McCarthy (2002) seems to be the most accurate so far, and hereafter, we refer to this potential as the hippocampal negative ERP, or simply the negative potential, rather than the MTL-P300 or the P3-like waveform.

McCarthy et al. (1989) have speculated that this hippocampal ERP is generated by the synchronous activation of spatially aligned hippocampal pyramidal cells. Later, these same authors suggested that this potential may reflect the arrival into the hippocampus of neocortical information, of modulatory inputs from diffusely projecting brain systems, or of recurrent inhibition from hippocampal pyramidal cells (Paller and McCarthy, 2002). As such, this ERP has been used as an index of hippocampal activity during various cognitive tasks.

One view on the medial temporal lobe functional arrangement is the hierarchically organized set of associational networks. Associational connections within the perirhinal, parahippocampal, and entorhinal cortices enable a significant amount of integration of unimodal and polymodal inputs, so that only highly integrated information reaches the remainder of the hippocampal formation (Lavenex and Amaral, 2000). Sensory inputs to the long axis of the hippocampus are organized topographically, as are its efferent connections. Studies report an anterior–posterior

[1] **Department of Physiology, Medical Faculty, Masaryk University, Brno, Czech Republic;** [2] **CEITEC, Central European Institute of Technology, Masaryk University, Brno, Czech Republic;** [3] **Department of Neurology, St. Anne Hospital, Masaryk University, Brno, Czech Republic;** [4] **Institute of Scientific Instruments, Academy of Sciences of the Czech Republic, Brno, Czech Republic**

Grant sponsor: European Regional Development Fund and MŠMT ČR; Grant numbers: CZ.1.05/1.1.00/02.0068, MSM0021622404; CZ.1.05/2.1.00/01.0017; Grant sponsor: GACR Czech Science Foundation; Grant number: GAP103/11/0933.

*Correspondence to: Robert Roman, Department of Physiology, Masaryk University, Kamenice 5, Brno 625 00, Czech Republic. E-mail: roman@med.muni.cz

Accepted for publication 17 July 2013.
DOI 10.1002/hipo.22173
Published online 9 September 2013 in Wiley Online Library (wileyonlinelibrary.com).

© *2013 WILEY PERIODICALS, INC.*

differentiation of hippocampal activation during various tasks (Paller and McCarthy, 2002; Crottaz-Herbette et al., 2005; Ludowig et al., 2010). Such functional organization is likely based on interconnections between transverse circuits within the longitudinal axis of hippocampus (Small, 2002; Aggleton, 2010; Aggleton et al., 2012).

The hippocampus is involved in novelty detection (Grunwald et al., 1998; Cohen et al., 1999; Strange and Dolan, 2001), salience detection (Rosburg et al., 2007), spatial memory and navigation (e.g., Watrous et al., 2011), and in encoding and recollection of episodic memory (e.g., Fernández el al., 2002; Eichenbaum, 2004; Amaral and Lavenex, 2007; Ranganath, 2010; Lega et al., 2012; Eichenbaum et al., 2012). In a recently published review, Olsen et al. (2012) suggest that the hippocampus supports multiple cognitive processes through relational binding and comparison, with or without conscious awareness for the relational representations that are formed, retrieved, and/or compared.

Despite the fact that most evidence points to cognition variables, some animal studies showed hippocampal theta activity associated with motor behavior (Vanderwolf, 1969; Wyble et al., 2004; Bland et al., 2006; Shin, 2011). Intracranial recordings from human hippocampi have also demonstrated movement-related increase in theta oscillatory activity (Ekstrom et al., 2005). These findings are consistent with sensorimotor integration theory, according to which hippocampal theta activity may reflect both the processing of sensory information related to the preparation for movement and the execution of movement (Bland and Oddie, 2001).

Besides theta oscillatory power changes, additional evidence for the role of the hippocampus in motor execution comes from studies demonstrating a modulation of hippocampal-evoked activity during motor responses. In studies employing the oddball task, for example, the amplitude of the hippocampal ERP is consistently reported to be higher after target stimuli requiring a motor response, relative to frequent stimuli for which no motor response is required (e.g., Brázdil et al., 1999; Fell et al., 2005; Ludowig et al., 2010). The amplitude of this potential was also found to be significantly greater after button pressing compared to mental counting (Brázdil et al., 2003). Furthermore, in our previous study (Roman et al., 2005) we observed that hippocampal P3-like waveforms to target stimuli could be time-locked to the onset of the stimulus or the motor response. These findings could indicate that this potential partially reflects processes also related to the motor response and not just to stimulus evaluation and associated memory functions. To explore this possibility, we investigated the temporal relationship between the hippocampal negative potential latency and the onset of a stimulus-cued movement. To do so, we employed a simple stimulus-response task, during which subjects were required to press a single button in response to a single, unchanging auditory stimulus. The subjects were instructed to respond at their own pace—that is, not to respond as fast as possible. The latency parameter of the examined hippocampal ERPs was then analyzed in subgroups of EEG trials with slower and faster responses.

MATERIAL AND METHODS

Subjects

Eleven patients (nine females and two males; one male subject was left-handed; mean age 35 ± 11 yrs) with medically intractable epilepsy participated in the study. All subjects had normal or corrected-to-normal vision. Informed consent was obtained from each subject before the experiment, and the study received the approval of the Ethical Committee of Masaryk University.

Intracranial Recordings

For clinical purposes a total of 91 depth multicontact electrodes were implanted orthogonally to the frontal, parietal, and temporal lobes to localize seizure origin before surgical treatment. In this study, we investigated ERP data from 22 electrodes that were positioned at the anterior (electrodes B mostly in hippocampal head, occasionally in the anterior part of hippocampal body) or posterior part of the hippocampi (electrodes C mostly in hippocampal body or its posterior part) in both right (nine electrodes) and left hemispheres (13 electrodes). The number of contacts located in hippocampal tissue ranged from two to four per electrode. The number of electrodes implanted into the hippocampi per patient varied from one to four (see Table 1); no electrodes recorded from epileptic foci.

ERPs were recorded with standard semiflexible multilead electrodes (ALCIS), each with a diameter of 0.8 mm. Recording contacts were 2.0 mm in length, and successive contacts were separated by 1.5 mm. The exact position of the electrodes and their contacts in the brain were verified using postplacement MRI with electrodes in situ.

The EEG was recorded with a sampling rate of 1,024 Hz during seizure-free periods using the 128-channel TrueScan EEG system (Deymed Diagnostic). All recordings were monopolar, with a linked earlobe reference. All impedances were less than 5 kΩ. Eye movements were recorded from a cathode placed 1 cm lateral and 1 cm above the canthus of the left eye, and from an anode 1 cm lateral and 1 cm below the canthus of the right eye.

Behavioral Task

A single-stimulus auditory task was performed, consisting of five sessions of 30 trials (i.e., 150 trials). On a given trial, we presented a single 1-kHz tone. The duration of auditory stimuli was constant at 200 ms. The interstimulus interval varied randomly between 4,000 and 6,000 ms. The intersession interval was 1 min. Subjects were instructed to press a button with their dominant hand after presentation of the tone. They were also instructed not to respond as fast as possible.

Data Analysis

ScopeWin and Physioplore software were used for offline analysis. EEG data were digitally filtered with pass band from 0.1 to

TABLE 1.

Reaction Time and Hippocampal Negative ERP Parameters Measured in All Investigated Contacts, for All Subjects

Subject	Reaction time mean ± SD (ms)	Reaction time median (ms)	Contact	Onset latency (ms)	50% area latency (ms)	Peak latency (ms)	Peak amplitude (μV)
1	387 ± 58	371	B4	300	468	512	−125
			C3	324	552	528	−94
			B′1	214	423	462	−37
			C′2	300	503	522	−92
2	660 ± 61	654	B′1	270	389	385	−136
3	260 ± 31	259	B3	296	453	427	−205
			C′3	321	478	465	−239
4	384 ± 64	387	C′2	268	426	445	−80
5	608 ± 144	566	B2	227	369	330	−133
			B′2	226	358	339	−77
			C′2	283	430	437	−61
6	649 ± 134	636	B′2	239	420	361	−40
7	668 ± 160	652	B4	240	355	341	−94
			C4	226	388	407	−145
8	440 ± 64	444	B3	272	430	386	−188
			C3	274	442	384	−202
			B′3	295	464	494	−59
9	1,113 ± 269	1,117	B′1	265	366	351	−65
			C′2	279	401	383	−51
10	693 ± 93	688	C′3	260	405	353	−78
11	552 ± 45	552	B3	267	372	370	−300
			B′4	290	434	396	−338

B = anterior hippocampus, C = posterior hippocampus, ′ = left hemisphere.

5.5 Hz. This filter was chosen because the most informative aspect of the signal we were analyzing resides within frequencies below 5 Hz (Jacobs et al., 2007; Lega et al., 2012; Watrous et al., 2011, 2013). Furthermore, we wanted to exclude possible influence of higher frequency components on the shape of the ERPs obtained from subgroups with a low number of trials. The filtered signal was then segmented according to the stimulation trigger onset, and segment lengths were 2,000 ms with a 600-ms prestimulus period used as baseline (−700 to −100 ms before stimulus onset). In Figures 2–4, only a short prestimulus period (∼500 ms) is depicted, resulting in a shorter time axis. Segments containing artefacts were rejected manually on the basis of visual inspection. In each subject, the reaction time (RT) was measured in artifact-free EEG segments. Outliers, i.e., 5% of segments with extremely long or short RT, were excluded from subsequent averaging. For further analysis, we selected in each electrode the one contact with the highest peak amplitude of negative ERP.

We evaluated ERP parameters derived from fractional area measures (Luck, 2005). We used a measurement window delimited by a line intersecting the waveform at the 50% peak amplitude level. The time point at which the waveform reached 50% of its peak amplitude represented the "onset latency." The 50% "area latency" was obtained by computing the area under the ERP waveform above the aforementioned measurement window and then identifying the time point that bisected that area. We used this latter parameter as a measure of the latency of a given potential, and it is this particular measure that is the focus of our analyses; for the sake of brevity, we refer to this parameter as "ERP latency." We also expressed ERP latency as a relative value—i.e., the percentage fraction of RT. This gave us a measure of "relative latency." We measured also the "peak latency," allowing the comparison of our results with the majority of other studies. Figure 1 illustrates all parameters measured in the present study.

To investigate whether or not any temporal relationship existed between the hippocampal negative potential and the motor response (i.e., the moment of button pressing) we performed the following procedure. In each subject, the artifact-free EEG segments were sorted according to the respective RT from the fastest to the slowest responses. Subsequently, the segments were divided into five subgroups and averaged separately (sorted averages). In creating the subgroups, we attempted to fulfill the following criteria: a sufficient number of segments for averaging in each subgroup; an identical number of segments in all subgroups; and similar variability of the RT across subgroups. Finally, the ERP latency and relative latency, obtained from all five sorted averages, were correlated with the median RT for each subgroup.

Nonparametric statistics—Spearman correlation and Wilcoxon pair test—were performed using the routines included in the Statistica program (StatSoft).

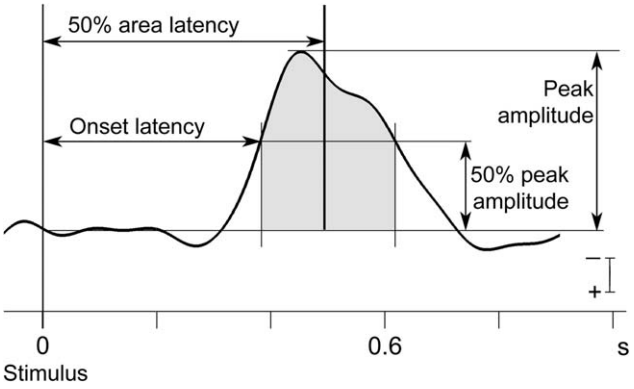

FIGURE 1. Schematic representation of event-related potential (ERP) parameters derived from fractional area measurements. The 50% area latency was used as the primary measure of ERP latency. The time point at which the waveform reached 50% of the peak amplitude represented the onset latency.

RESULTS

All the subjects responded to all presented stimuli. RT in a group of 11 subjects measured only from artifact-free EEG segments was 583 ± 227 ms (mean ± SD) and individual RT values are listed in Table 1. The average number of artifact-free segments across all subjects was 92 ± 21, ranging from 61 to 126. The shortest responses were measured in subject 3 (260 ± 31 ms), while subject 9 responded very slowly with the highest variability of responses (1,113 ± 269 ms). For the rest of the subjects, mean RTs and standard deviations ranged, respectively, 384–693 and 45–160 ms.

We found prominent hippocampal negative potentials characterized by a local origin, indicated by a steep voltage gradient change, in all investigated electrodes. Two examples of locally generated ERPs are demonstrated in Figure 2. The values of our selected ERP parameter measurements (mean ± SD) across 22 cases were as follows: 50% area latency = 424 ± 49 ms; peak latency = 413 ± 62 ms; onset latency = 270 ± 31 ms; peak amplitude = −129 ± 84 μV. Parameter values from each individual subject are presented in Table 1.

In all investigated contacts, averages created from sorted subgroups of segments revealed waveforms comparable to the waveform averaged from all artifact-free segments (compare one example in Figs. 3A,B). The number of segments included in each subgroup varied from 14 ± 1 to 25 ± 4.

To test the temporal relationship between the negative potential latency and motor responses, in each subject, we performed correlation analyses between two measures of ERP latency—both absolute (50% area latency) and relative latency—with median RT obtained from sorted subgroup averages (Table 2). First, we observed nonsignificant correlations between ERP latency and median RT in all but two cases; specifically, C′2 in subject 1 and C′3 in subject 3. These findings reflect relatively constant hippocampal negative potential latency that is independent of RT. Second, we found significant negative correlations between ERP relative latency and median RT in 16 of 22 cases. These results demonstrate that with longer RT the hippocampal negative potential latency, expressed as a relative value of corresponding RT, became correspondingly lower. Although many of the correlations observed are far more robust than those reported typically in the literature, yet they failed to reach statistical significance. This is unsurprising given the low degrees of freedom. Nevertheless, we performed resampled procedures and we obtained very similar results: for the coefficient of −0.8 (i.e., subject 1, C′2), $P > 0.067$; and for the coefficient −0.7 (i.e., subject 1, B′1), $P = 0.119$.

In the light of the previous results, we also correlated median RT and ERP latency parameters but measured from

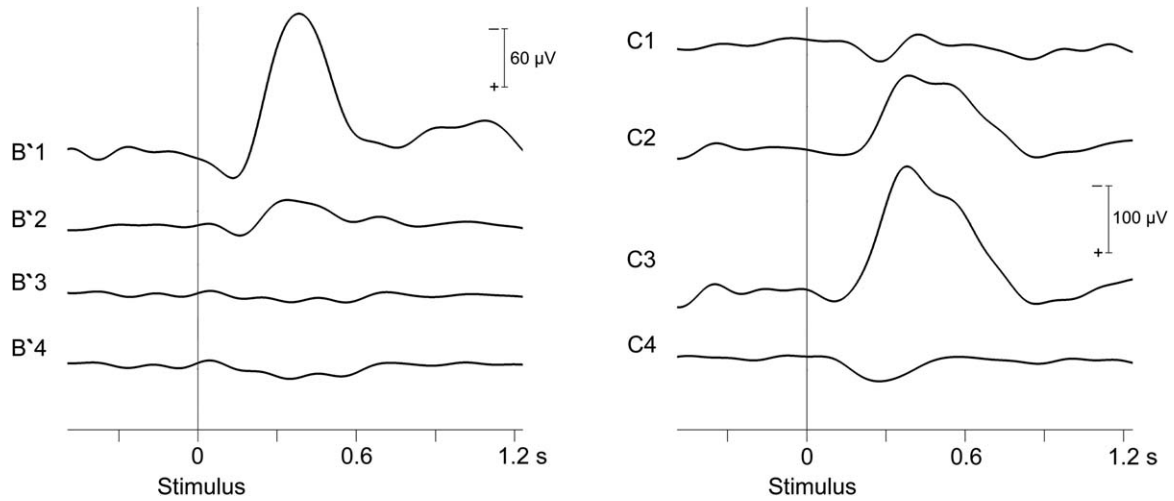

FIGURE 2. Two examples of locally generated hippocampal negative ERP revealed by steep voltage gradient changes. In subject 2 (left), contact B′1 was located in the left hippocampal head, while contacts B′2–4 were located outside this structure; In subject 8 (right), contacts C1–3 penetrate right hippocampal body, while contact C4 lay outside this structure.

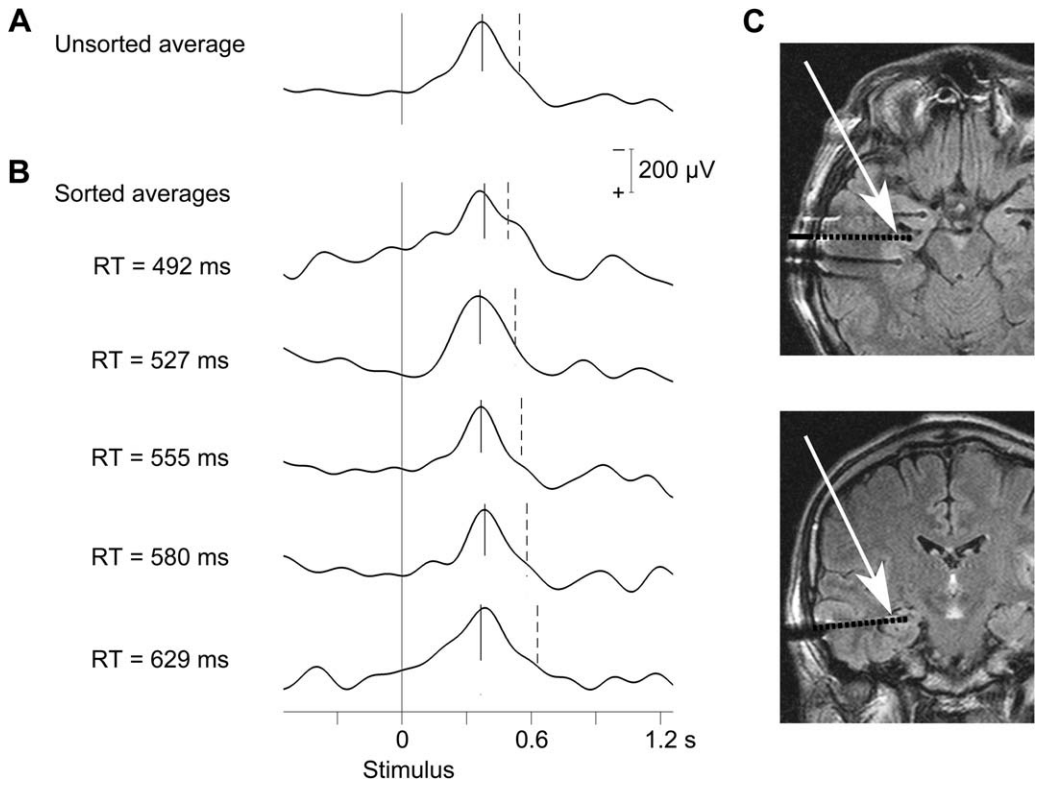

FIGURE 3. Hippocampal negative ERP recorded from the right hippocampal head in subject 11, contact B3. A: ERP averaged from 88 artifact-free EEG segments (unsorted average). B: ERPs recorded from the same contact and patient, averaged from five subgroups of EEG segments defined according to median RT (sorted averages), ordered from the shortest (upper) to the longest (lower). ERP latency is indicated by short vertical solid lines crossing the waveforms. The vertical dashed lines depict median RT expressed numerically on the left. C: Transversal and coronal MR images demonstrate the location of electrode B, with the B3 contact position indicated by a white arrow.

unsorted averages across subjects. For this analysis, if the studied ERP is related to the motor response one would expect high positive correlations. On the contrary, however, we observed significant negative correlations between median RT and ERP latency ($r = -0.77$, $P < 0.001$) and between median RT and onset latency ($r = -0.55$, $P < 0.01$). This finding supports the proposal that the studied ERP is unrelated to the motor response.

In all investigated sites, the hippocampal ERP latency—our primary measure—varied along the time axis in relation to the motor response (see Table 1). In 14 cases, it was shorter than the median RT and preceded the motor response—in two cases in subject 9, it was shorter by 751 and 716 ms; in 12 cases, it varied from 297 to 2 ms (mean value 182 ± 98 ms) before the average motor response. In eight cases, the hippocampal ERP latency was longer than the median RT; this is true especially for subject 3, who provided the fastest responses, whereby ERP latency was longer by 219 ms in C′3 and 194 ms in B3. In the six other remaining cases, it varied from 20 to 181 ms (mean value 87 ± 62 ms) after the motor response (see examples in Fig. 4). In contrast, our other measure of ERP latency—onset latency—preceded the motor response in all interrogated contacts except two in subject 3. It also demonstrates that there is no fixed relationship between the studied ERP and the motor response.

Differences in the measured parameters between anterior and posterior parts of the hippocampus were assessed in six pairs of contacts for subjects 1, 5, 7, 8, and 9 (Wilcoxon pair test). A significant anterior—posterior difference ($P < 0.05$) revealed that ERP latency was shorter in the anterior compared with posterior hippocampi—i.e., 400 ± 47 and 452 ± 63 ms, respectively. No significant differences were found between right and left hippocampi in any of the measured parameters in five investigated pairs of contacts (subjects 1, 5, 8, and 11).

DISCUSSION

In the present study, we found that the human hippocampi consistently generate a large negative ERP during simple auditory stimulus-response task. Analyses focusing on the latency of this hippocampal ERP suggested that it is not time-locked to the motor response (i.e., to movement execution). First, the

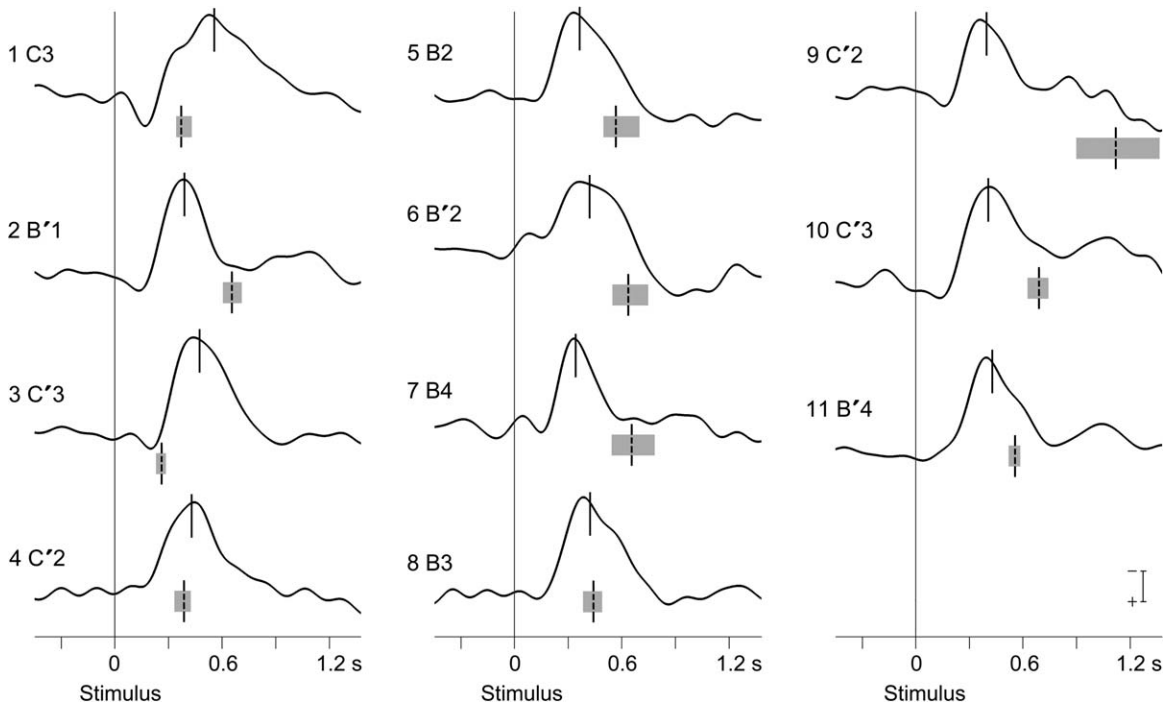

FIGURE 4. Examples of hippocampal negative ERPs from each subject. Contacts B are located in hippocampal head or in the anterior part of the hippocampal body, and contacts C are positioned within the posterior part of hippocampal body; apostrophes indicate left-hemisphere locations. ERP latency is indicated by vertical solid lines crossing the waveforms. Shadow rectangles below each waveform represent reaction times quartile ranges and vertical dashed lines, crossing the rectangles, signify median RT. Scaling was adjusted separately for each waveform so as to optimize amplitude.

hippocampal negative ERP latency measured in five sorted subgroups of segments did not correlate with median RT. When the same latency parameter was expressed as a relative value of RT, however, it correlated highly with median RT in most of the cases. Second, there is no fixed temporal relationship between the hippocampal negative ERP and the motor response expressed as median RT. In some cases, the ERP latency was shorter and, in other cases, it was longer than median RT, i.e., negative potential preceded or followed the motor response, respectively. Third, across the entire group of subjects, the variability of the ERP latency and the onset latency was at least four times lower than the variability of RTs.

Our conclusion is based on a simplified conceptualization of sensorimotor tasks; specifically, we assume that the hippocampal ERP reflects activity related either to the stimulus presentation *or* to the execution of the response. The results of our correlation analyses between RT and the latency (absolute and relative) of the hippocampal negative potential should then reveal the temporal relationship between this ERP and the stimulus or the response. In the first case, the latency of the ERP should be independent of RT. The opposite would be expected if the studied ERP reflects processes linked to the execution of the response; the ERP latency should depend entirely on RT. By averaging subgroups of EEG segments sorted according to RT in each subject, we measured an almost constant potential latency in all sorted averages. Moreover, when this potential latency was expressed as a relative value of RT, it was lower for longer RTs. In other words, we revealed that the hippocampal ERP is linked to the auditory stimulus rather than the motor response.

One of the suggested hippocampal functions is its support in multiple cognitive processes through relational binding and comparison. The comparison occurs when recently processed perceptual information is evaluated with respect to associated relevant information that is maintained in the memory (Vinogradova, 2001). In our study, the auditory stimulus was given a task-relevant meaning by verbal instruction. After each presentation of the stimulus, its identification and comparison with memorized representation had to be accomplished. We believe that the hippocampal negative potential could represent an electrophysiological correlate of such evaluation processing.

In our study, several subjects performed the task so quickly that the latency of hippocampal waveform followed the execution of instructed movement. This could be explained by the existence of a short-cut pathway from auditory areas to secondary motor areas involved in movement programming (Bender et al., 2006). This is in line with the finding of early processing of auditory stimuli in the frontal cortex as well (Kukleta et al., 2010). It demonstrates that aforementioned hippocampal evaluation is not critical for movement execution.

TABLE 2.

Spearman Correlation Coefficients (df = 4) for the Relationship Between Median RT and ERP Latency, and Between Median RT and ERP Relative Latency (the Percentage Fraction of Reaction Time

Subject	Contact	Latency	Relative latency
1	B4	0.7	−0.9*
	C3	0.5	−0.8
	B′1	0.1	−0.7
	C′2	0.9*	−0.8
2	B′1	0.7	−0.1
3	B3	0.2	−1.0*
	C′3	0.9*	−1.0*
4	C′2	0.6	−0.9*
5	B2	0.5	−0.9*
	B′2	0.5	−0.9*
	C′2	−0.2	−1.0*
6	B′2	0.6	−0.9*
7	B4	−0.3	−1.0*
	C4	−0.3	−0.9*
8	B3	−0.4	−0.9*
	C3	−0.3	−0.9*
	B′3	0.1	−0.6
9	B′1	0.3	−0.9*
	C′2	0.3	−0.9*
10	C′3	−0.6	−1.0*
11	B3	−0.3	−0.9*
	B′4	0.5	−0.7

B = anterior hippocampus, C = posterior hippocampus, ′ = left hemisphere.
*$P < 0.05$.

Low variability of RTs in some subjects represented a certain limitation for our analysis. In such cases, we obtained very small differences of median RT between the subgroups we created. Since the ERP latency varied minimally in the sorted averages also, this may have influenced the correlation coefficients we obtained in subjects 1 and 3.

Another finding from the present study is the primarily shorter ERP latencies recorded from anterior relative to posterior orthogonal electrodes; i.e., 400 ± 47 and 452 ± 63 ms, respectively. The small number of cases did not allow deeper statistical evaluation, however. Very similar but nonsignificant anterior–posterior differences in peak latencies were also observed in axial electrodes penetrating the hippocampal head 429 ± 96 ms and hippocampal body 486 ± 69 ms (Ludowig et al., 2010). These findings seem to be in accordance with a model of memory recall that assumes a spreading of hippocampal activation from anterior to posterior during information retrieval (Small, 2002). The recent finding of traveling theta waves with the same direction of propagation observed in hippocampi of freely behaving rats is not in contradiction with this model (Lubenov and Siapas, 2009).

The hippocampal negative ERP was found to be uniform in shape and polarity across all subjects and investigated sites. It is for this reason that we chose to employ parameters derived from fractional area measures for the description of this potential. The 50% area latency parameter is obtained by computing the area under the ERP waveform over a delimited measurement window, and then identifying the time point that bisects that area. Thus, it can be related to RT more directly because this is similar to the median RT, which is the point separating the fastest and slowest halves of RTs. It also has several other advantages over peak latency that is used in the majority of ERP studies; the same value is expected irrespective of the noise level of the data, for example, rendering it less sensitive to noise (Luck, 2005). That is why we use the 50% area latency parameter as a measure of the latency of the investigated negative potential instead of the peak latency. Concerning RT, we use the mean RT for description of group behavioral performance and median RT to compare the size of the latency effect to the size of the RT effect.

The primary finding of the present study is that during a simple sensorimotor task, human hippocampi generate a prominent negative ERP that occurs independently of motor execution. We suggest that this electrophysiological phenomenon is related to evaluation of stimulus meaning within the context of the current situation.

Acknowledgments

The authors thank Josef Halámek for his helpful comments during the preparation of this manuscript.

REFERENCES

Aggleton JP. 2012. Multiple anatomical systems embedded within the primate medial temporal lobe: Implications for hippocampal function. Neurosci Biobehav Rev 36:1579–1596.

Aggleton JP, Wright NF, Vann SD, Saunders RC. 2012. Medial temporal lobe projections to the retrosplenial cortex of the macaque monkey. Hippocampus 22:1883–1900.

Amaral DG, Lavenex P. 2007. Hippocampal neuroanatomy. In: Andersen P, Morris R, Amaral DG, Bliss T, O'Keefe J, editors. The Hippocampus Book. Oxford: Oxford University Press. pp 37–114.

Axmacher N, Cohen MX, Fell J, Haupt S, Dümpelmann M, Elger CE, Schlaepfer TE, Lenartz D, Sturm V, Ranganath CH. 2010. Intracranial EEG correlates of expectancy and memory formation in the human hippocampus and nucleus accumbens. Neuron 65: 541–549.

Bender S, Oelkers-AX R, Resch F, Weisbrod M. 2006. Frontal lobe involvement in the processing of meaningful auditory stimuli develops during childhood and adolescence. Neuroimage 33: 759–773.

Bland BH, Oddie SD. 2001. Theta band oscillation and synchrony in the hippocampal formation and associated structures: The case for its role in sensorimotor integration. Behav Brain Res 127:119–136.

Bland BH, Jackson J, Derrie-Gillespie D, Azad T, Rickhi A, Abriam J. 2006. Amplitude, frequency, and phase analysis of hippocampal theta during sensorimotor processing in a jump avoidance task. Hippocampus 16:673–681.

Boutros NN, Mears R, Pflieger ME, Moxon KA, Ludowig E, Rosburg T. 2008. Sensory gating in the human hippocampal and rhinal regions: Regional differences. Hippocampus 18:310–316.

Brázdil M, Roman R, Daniel P, Rektor I. 2003. Intracerebral somatosensory event-related potentials: Effect of response type (button pressing versus mental counting) on P3-like potentials within the human brain. Clin Neurophysiol 114:1489–1496.

Brázdil M, Roman R, Daniel P, Rektor I. 2005. Intracerebral error-related negativity in a simple Go/NoGo task. J Psychophysiol 19: 244–255.

Brázdil M, Rektor I, Dufek M, Daniel P, Jurák P, Kuba R. 1999. The Role of Frontal and Temporal Lobes in Visual Discrimination Task—Depth ERP Studies. Neurophysiol Clin 29: 339–350.

Brázdil M, Rektor I, Daniel P, Dufek M, Jurák P. 2001. Intracerebral event-related potentials to subthreshold target stimuli. Clin Neurophysiol 112:650–661.

Cohen NJ, Ryan J, Hunt C, Romine L, Wszalek T, Nash C. 1999. Hippocampal system and declarative (relational) memory: Summarizing the data from functional neuroimaging studies. Hippocampus 9:83–98.

Crottaz-Herbette S, Lau KM, Glover GH, Menon V. 2005. Hippocampal involvement in detection of deviant auditory and visual stimuli. Hippocampus 15:132–139.

Damborská A, Brázdil M, Rektor I, Janoušová E, Chládek J, Kukleta M. 2012. Late divergence of target and nontarget ERPs in a visual oddball task. Physiol Res 61:307–318.

Eichenbaum H. 2004. Hippocampus: Cognitive processes and neural representations that underlie declarative memory. Neuron 44:109–120.

Eichenbaum H, Sauvage M, Fortin N, Komorowski R, Lipton P. 2012. Towards a functional organization of episodic memory in the medial temporal lobe. Neurosci Biobehav Rev 36:1597–1608.

Ekstrom AD, Caplan JB, Ho E, Shattuck K, Fried I, Kahana MJ. 2005. Human hippocampal theta activity during virtual navigation. Hippocampus 15:881–889.

Fell J, Dietl T, Grunwald T, Kurthen M, Klaver P, Trautner P Schaller C, Elger CE, Fernández G. 2004. Neural bases of cognitive ERPs: More than phase reset. J Cogn Neurosci 16:1595–1604.

Fell J, Köhling R, Grunwald T, Klaver P, Dietl T, Schaller C, Becker A, Elger CE, Fernández G. 2005. Phase-locking characteristics of limbic P3 responses in hippocampal sclerosis. Neuroimage 24:980–989.

Fernández G, Klaver P, Fell J, Grunwald T, Elger CE. 2002. Human declarative memory formation: Segregating rhinal and hippocampal contributions. Hippocampus 12:514–519.

Grunwald T, Elger CE, Lehnertz K, Van Roost D, Heinze HJ. 1995. Alterations of intrahippocampal cognitive potentials in temporal lobe epilepsy. Electroencephalogr Clin Neurophysiol 95:53–62.

Grunwald T, Lehnertz K, Heinze HJ, Helmstaedter C, Elger CE. 1998. Verbal novelty detection within the human hippocampus proper. Proc Natl Acad Sci USA 95:3193–3197.

Grunwald T, Beck H, Lehnertz K, Blümcke I, Pezer N, Kutas M, Kurthen M, Karakas HM, Van Roost D, Wiestler OD, Elger CE. 1999. Limbic P300s in temporal lobe epilepsy with and without ammon's horn sclerosis. Eur J Neurosci 11:1899–1906.

Halgren E, Squires NK, Wilson CL, Rohrbaugh JW, Babb TL, Crandall PH. 1980. Endogenous potentials generated in the human hippocampal formation and amygdala by infrequent events. Science 210:803–805.

Halgren E, Baudena P, Clarke JM, Heit G, Marinkovic K, Devaux B, Vignal JP, Biraben A. 1995. Intracerebral potentials to rare target and distracter auditory and visual stimuli. II. medial, lateral and posterior temporal lobe. Electroencephalogr Clin Neurophysiol 94:229–250.

Jacobs J, Kahana MJ, Ekstrom AD, Fried I. 2007. Brain oscillations control timing of single-neuron activity in humans. J Neurosci 27: 3839–3844.

Kukleta M, Brázdil M, Roman R, Jurák P. 2003. Identical event-related potentials to target and frequent stimuli of visual oddball task recorded by intracerebral electrodes. Clin Neurophysiol 114: 1292–1297.

Kukleta M, Turak B, Louvel J. 2010. Very early EEG responses to a meaningful auditory stimulus in the frontal lobes: An intracerebral study in humans. Physiol Res 59:1019–1027.

Lavenex P, Amaral DG. 2000. Hippocampal-neocortical interaction: A hierarchy of associativity. Hippocampus 10:420–430.

Lega BC, Jacobs J, Kahana M. 2012. Human hippocampal theta oscillations and the formation of episodic memories. Hippocampus 22: 748–761.

Lubenov EV, Siapas AG. 2009. Hippocampal theta oscillations are travelling waves. Nature 459:534–539.

Luck SJ. 2005. Measuring ERP latencies. In: Luck SJ, editor. An Introduction to the Event-Related Potential Technique. Cambridge: MIT Press. pp 237–249.

Ludowig E, Bien CG, Elger CE, Rosburg T. 2010. Two P300 generators in the hippocampal formation. Hippocampus 20:186–195.

McCarthy G, Wood CC, Williamson PD, Spencer DD. 1989. Task-dependent field potentials in human hippocampal formation. J Neurosci 9:4253–4268.

Olsen RK, Moses SN, Riggs L, Ryan JD. 2012. The hippocampus supports multiple cognitive processes through relational binding and comparison. Front Hum Neurosci 6:1–13.

Paller KA, McCarthy G. 2002. Field potentials in the human hippocampus during the encoding and recognition of visual stimuli. Hippocampus 12:415–420.

Paller KA, McCarthy G, Roessler E, Allison T, Wood CC. 1992. Potentials evoked in human and monkey medial temporal lobe during auditory and visual oddball paradigms. Electroencephalogr Clin Neurophysiol 84:269–279.

Ranganath C. 2010. A unified framework for the functional organization of the medial temporal lobes and the phenomenology of episodic memory. Hippocampus 20:1263–1290.

Roman R, Brázdil M, Jurák P, Rektor I, Kukleta M. 2005. Intracerebral P3-like waveforms and the length of the stimulus-response interval in a visual oddball paradigm. Clin Neurophysiol 116:160–171.

Rosburg T, Trautner P, Ludowig E, Schaller C, Kurthen M, Elger CE, Boutros NN. 2007. Hippocampal event-related potentials to tone duration deviance in a passive oddball paradigm in humans. NeuroImage 37: 274–281.

Shin J. 2011. The interrelationship between movement and cognition: Theta rhythm and the P300 event-related potential. Hippocampus 21:744–752.

Shinba T, Andow Y, Shinozaki T, Ozawa N, Yamamoto K. 1996. Event-related potentials in the dorsal hippocampus of rats during an auditory discrimination paradigm. Electroencephalogr Clin Neurophysiol 100:563–568.

Small SA. 2002. The longitudinal axis of the hippocampal formation: Its anatomy, circuitry, and role in cognitive function. Rev Neurosci 13:183–194.

Stapleton JM, Halgren E. 1987. Endogenous potentials evoked in simple cognitive tasks: Depth components and task correlates. Electroencephalogr Clin Neurophysiol 67:44–52.

Strange BA, Dolan RJ. 2001. Adaptive anterior hippocampal responses to oddball stimuli. Hippocampus 11:690–698.

Vanderwolf CH. 1969. Hippocampal electrical activity and voluntary movement in the rat. Electronceph Clin Neurophysiol 26:407–418.

Watrous AJ, Fried I, Ekstrom AD. 2011. Behavioral correlates of human hippocampal delta and theta oscillations during navigation. J Neurophysiol 105:1747–1755.

Watrous AJ, Tandon N, Conner CR, Pieters T, Ekstrom AD. 2013. Frequency-specific network connectivity increases underlie accurate spatiotemporal memory retrieval. Nat Neurosci 16:349–356.

Wyble BP, Hyman JM, Rossi CA, Hasselmo ME. 2004. Analysis of theta power in hippocampal EEG during bar pressing and running behavior in rats during distinct behavioral contexts. Hippocampus 14:662–674.

Annex 3

Kukleta, M., **Damborská, A.**, Roman, R., Rektor, I., & Brázdil, M. (2016). The primary motor cortex is involved in the control of a non-motor cognitive action. *Clinical Neurophysiology*, 127 (2), 1547 – 1550.

Clinical Neurophysiology 127 (2016) 1547–1550

Contents lists available at ScienceDirect

Clinical Neurophysiology

journal homepage: www.elsevier.com/locate/clinph

The primary motor cortex is involved in the control of a non-motor cognitive action

Miloslav Kukleta [a], Alena Damborská [a,b,*], Robert Roman [a,b], Ivan Rektor [a,c], Milan Brázdil [a,c]

[a] CEITEC – Central European Institute of Technology, Masaryk University, Brno, Czech Republic
[b] Department of Physiology, Faculty of Medicine, Masaryk University, Brno, Czech Republic
[c] 1st Department of Neurology, St. Anne's Faculty Hospital, Masaryk University, Brno, Czech Republic

ARTICLE INFO

Article history:
Accepted 29 November 2015
Available online 11 December 2015

Keywords:
Intracerebral EEG
Primary motor cortex
Cognition
Oddball task

HIGHLIGHTS

- Late component of event related potentials can be evoked by non-target visual oddball stimuli in prefrontal areas and primary motor cortex.
- Primary motor cortex involvement concerns also situations where no overt or covered motor action is present.
- Low specialized neuronal network is suggested to be activated during cognitive operations linked to non-motor actions.

ABSTRACT

Objective: Adaptive interactions with the outer world necessitate effective connections between cognitive and executive functions. The primary motor cortex (M1) with its control of the spinal cord motor apparatus and its involvement in the processing of cognitive information related to motor functions is one of the best suited structures of this cognition-action connection. The question arose whether M1 might be involved also in situations where no overt or covered motor action is present.
Methods: The EEG data analyzed were recorded during an oddball task in one epileptic patient (19 years) with depth multilead electrodes implanted for diagnostic reasons into the M1 and several prefrontal areas.
Results: The main result was the finding of an evoked response to non-target stimuli with a pronounced late component in all frontal areas explored, including three loci of the M1. The late component was implicated in the evaluation of predicted and actual action and was synchronized in all three precentral loci and in the majority of prefrontal loci.
Conclusion: The finding is considered as direct evidence of functional involvement of the M1 in cognitive activity not related to motor function.
Significance: Our results contribute to better understanding of neural mechanisms underlying cognition.
© 2015 International Federation of Clinical Neurophysiology. Published by Elsevier Ireland Ltd. All rights reserved.

1. Introduction

The classical view of the primary motor cortex (M1), which was based principally on direct cortical stimulation and which attributed to this structure a role in selecting the muscles and force for executing an intended movement, was, over the last two decades, substantially revised. This revision was imposed firstly by new findings demonstrating that the somatotopic organization of the M1 can be modified by peripheral changes in neuromuscular connections or motor training (Classen et al., 1998; Giraux et al., 2001; Karni et al., 1998; Pons et al., 1991; Wise et al., 1998). A second research stream brought the evidence of involvement of the M1 in cognitive functions. The original hypothesis that the M1 has an important role in the processing of cognitive information related to motor functions (Georgopoulos et al., 1989) has been supported by numerous studies which have documented the involvement of the M1 in the cognitive – motor processing during

* Corresponding author at: CEITEC – Central European Institute of Technology, Brain and Mind Research Program, Masaryk University, Kamenice 735/5, CZ-625 00 Brno, Czech Republic. Tel.: +420 549 497 454.
E-mail address: adambor@med.muni.cz (A. Damborská).

http://dx.doi.org/10.1016/j.clinph.2015.11.049
1388-2457/© 2015 International Federation of Clinical Neurophysiology. Published by Elsevier Ireland Ltd. All rights reserved.

spatial transformations (Georgopoulos and Massey, 1987), serial order coding (Carpenter et al., 1999; Pellizzer et al., 1995), stimulus–response incompatibility (Riehle et al., 1997; Zhang et al., 1997), and in motor imagery (Lotze et al., 1999). Based on these studies we hypothesized that M1 might even be also involved during situations, where no overt or covered motor action is present. With the aim to demonstrate the suggested M1 involvement in the non-motor cognitive processing we searched for event-related potentials (ERPs) recorded in the M1 during non-target variant of visual oddball task. We chose this electrophysiological method, since it is well established in cognitive neuroscience research having also promising applications in clinical practice (Holeckova et al., 2014; Landa et al., 2014). The sequence of the main operations underlying the non-target response ought to comprise detection and cognitive discrimination of the non-target stimulus, selection and execution of the instructed response (i.e. doing nothing), and control of the accordance between the actual result of the action with its internal representation – in summary a set of predominantly cognitive tasks without direct linkage to the motor functions. To suggest the answer to the question whether the M1 loci are an integral part of the neuronal network engaged in executive control of non-motor actions, we focused on identification and comparison of ERP components elicited in different cortical regions at the end of the non-target task. To assess the linkage of the electrophysiological event and a function supposed to be running at this period of the task we decided to analyze ERPs both of correct and incorrect responses.

The salient characteristics of one subject (i.e. recording electrodes in motor and prefrontal cortices, performance difficulties of the patient manifested in a high number of incorrect responses) provided necessary data with respect to the aims of the current study.

2. Methods

2.1. Subject

The male candidate for the surgical treatment of epilepsy (19 years) was selected from a group of 18 patients employed in another intracerebral study as subject No. 9 (Damborská et al., 2016) for his unique localization of electrodes, which included the primary motor cortex in both hemispheres. His antiepileptic drug therapy was reduced during the intracerebral EEG recording to allow seizures to develop spontaneously. Standard MicroDeep semi-flexible multilead electrodes (DIXI) with a diameter of 0.8 mm, length of each recording contact 2 mm, and inter-contact intervals of 1.5 mm were used for EEG monitoring. The exact position of the electrodes in the brain was verified using post-placement magnetic resonance imaging and indicated in relation to the axes defined by the Talairach system (Talairach et al., 1967). Cortical stimulation of right precentral gyrus and left and right supplementary motor areas repeatedly elicited contractions confirming engagement of these regions in motor functions. Informed consent was obtained from the patient prior to his participation in the experiment, and the study received an approval from the Ethical Committee of Masaryk University.

2.2. Procedure

A visual oddball task with mental counting was performed in one session. Yellow capital letters X (target stimuli, T) or O (non-target stimuli) appeared repeatedly on white background in random order for 200 ms and the interstimulus interval varied randomly between 2 and 5 s. The target stimuli were five times less frequent than the non-target ones. The microswitch button pressing and mental counting was the instructed response to the T stimuli and doing nothing was the response to the non-target stimuli.

2.3. Data acquisition and processing

The EEG activity was recorded using a 64-channel Brain Quick EEG system (Micromed). The recordings were monopolar with the reference electrode placed on the right processus mastoideus. EEGs were amplified with a bandwidth of 0.1–40 Hz at a sampling rate of 128 Hz. The EEG signal was analyzed offline with the help of Scope-Win software. The artefact rejection was performed, based on visual inspection made by two experienced persons. ERPs elicited in response to non-target stimuli were analyzed on averaged artefact-free recordings with the non-target stimulus used as a trigger. Number of trials used for each average curve were as follows: 14 false alarms and 343 correct rejections. The statistical significance of ERP waves was computed between the mean amplitude observed during the baseline period (from −600 to −100 ms from the stimulus onset) and the mean value computed as a mean from the neighborhood of each point (170 ms length) after stimuli using a nonparametric Wilcoxon Rank Sum (Signed Rank) test for paired samples. One record selected from responses obtained in a cortical region from the neighboring electrode contacts was analyzed choosing the one with the largest amplitude of ERP. In our previous study (Damborská et al., 2016) the data of 18 subjects were analyzed to investigate the neuronal network engaged in processes occurring in post-movement period in visual oddball task. Contrary to that and in accordance with the current aim we searched in the present study for sites in primary motor cortex activated during non-target task variant of visual oddball task in one subject (patient No. 9 of Damborská et al., 2016 data set).

3. Results

The study was based on the analysis of event-related potentials obtained from 12 cortical regions of one subject as a response to the non-target stimulus of the visual oddball task. As is evident from Fig. 1, which presents one selected response from each region explored, the evoked responses consisted of early (up to 500 ms) and late (over 500 ms) components. The interest of the study was focused on the late component, which was present in all the explored regions, and in the majority of cases was located in a relatively stable segment of the time axis (the peak latency from 690 to 740 ms in eleven precentral and prefrontal loci, see Table 1). In half of the regions including all investigated regions of M1 cortex this component was observed as an isolated late ERP waveform. Table 1 presents the exact position of recording contacts from which the presented ERPs were derived. The calculation of the correlation coefficient in the time window from 508 to 939 ms in record pairs, which were created from all records presented in Fig. 1, showed significant r-value over 0.80 in 70% of the pairs. All of the three pairs within precentral loci reached r-values over 0.97. The mean distance between paired loci was 34.4 ± 10.8 mm, which allowed considering the analyzed waveforms as phenomena generated independently in each locus (Lachaux et al., 2003; Menon et al., 1996). The record pairs, which compared records obtained from loci in the gyrus praecentralis (area 4) on the one hand and records from the supplementary motor area (area 6), the gyrus cinguli anterior (areas 32 and 24), and the dorsolateral prefrontal cortex (areas 9 and 44) on the other hand, yielded in the time window 508–939 ms correlation coefficients ranging from 0.83 to 0.94 in nine pairs in the right hemisphere, and from 0.89 to 0.98 in three pairs in the left hemisphere. These values could be considered as evidence of transitory high-level activity

synchronization of loci situated in the primary motor cortex with the premotor and prefrontal loci investigated.

In an attempt to assess a possible relation of the late ERP component and the mental operation(s) expected to be running in this period of the task, the trials with incorrect responses (button pressing instead of doing nothing) were compared with correct responses. In spite of the small number of incorrect responses (14 responses) and the eventually less effective averaging procedure, clear-cut differences in the configuration and latency of the late component were found in five of the regions explored (see Fig. 2). The main difference concerned the marked delay (259 ± 81 ms) of the peak latency of the late ERP component in all incorrect (994 ± 78 ms) with respect to correct (734 ± 7 ms) responses.

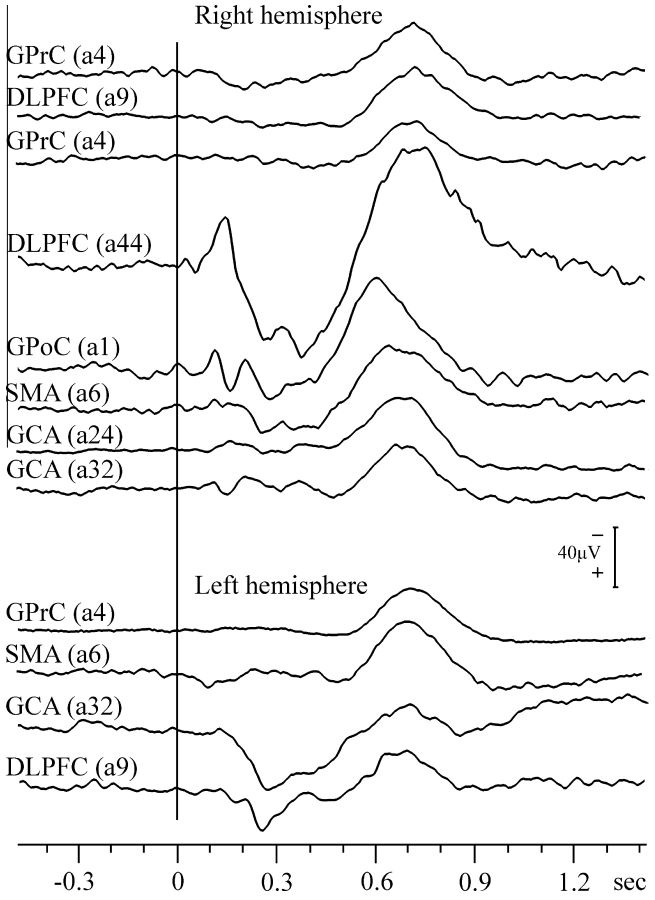

Fig. 1. The event-related potentials elicited by non-target stimuli. The abbreviations designate anatomical locations from which the records were derived; their explanations together with Talairach's coordinates of the loci and the amplitude and latency values of late waveforms are given in Table 1. The vertical line shows the onset of stimulus presentation.

4. Discussion

The ERP consisting of an isolated late waveform, which was recorded in three M1 loci as a response to the non-target oddball stimulus, is the main finding of the study. Almost identical late ERP components were found in several prefrontal sites, which suggested implication of all these sites in an identical operation. The changes in timing of these late waveforms in trials with incorrect responses suggested the association of this electrophysiological phenomenon with the control of accordance between the internal representation of the instructed action and its actual state. In sum, the finding of late ERP waveforms elicited in M1 loci by non-target stimuli demonstrated the implication of the primary motor cortex in cognitive processing not related directly to a motor function. Our finding is consistent with very recent discovery that the precentral gyrus is involved in cognitive or sensory function not requiring motor action (Potes et al., 2014).

Another interesting result is the fact that the same loci were activated both in correct and incorrect responses. This finding is relevant to the current discussion about the origin of response-related negativities on scalp EEG records following correct and incorrect responses (Endrass et al., 2012; Hoffmann and Falkenstein, 2010, 2012). Based on our results we suggest that some loci engaged in the control of correct performance and detection of errors are identical. Our observation of the late ERP waveform both in correct and incorrect responses also suggests that this potential does not reflect a process of inhibiting a motor response in the non-target condition.

The control of accordance between the actual action and its internal representation, together with the processing of other information needed for action valuation and evaluation is known to be realized by a large network of brain structures including frontal and parietal cortices, basal ganglia, thalamus, and brain stem nuclei (Ullsperger et al., 2014). The involvement of the primary motor cortex with its connections to the spinal cord motor apparatus in performance monitoring is not surprising in situations which comprise grasping, manipulating an object, motor imagery, and

Table 1
The location of electrode contacts from which the event-related potentials elicited by non-target stimuli were derived together with selected characteristics of late waveforms of these potentials.

Location of recording contact	Abbreviation	Contact	Talairach coordinates			Late waveform amplitude (μV)	Late waveform latency (ms)
			x	*y*	*z*		
Right hemisphere							
Gyrus praecentralis (a4)	GPrC	M12	61	−13	35	34	734
Dorsolateral prefrontal cortex (a9)	DLPFC	F14	48	27	40	34	742
Gyrus praecentralis (a4)	GPrC	R4	49	−7	50	26	727
Dorsolateral prefrontal cortex (a44)	DLPFC	G14	46	11	37	79	742
Gyrus postcentralis (a1)	GPoC	S2	61	−17	35	59	617
Supplementary motor area (a6)	SMA	M2	10	−7	55	45	690
Gyrus cinguli anterior (a24)	GCA	G2	6	8	32	34	695
Gyrus cinguli anterior (a32)	GCA	F2	8	24	35	30	693
Left hemisphere							
Gyrus praecentralis (a4)	GPrC	M′11	−47	−10	55	28	727
Supplementary motor area (a6)	SMA	M′1	−30	−8	60	34	720
Gyrus cinguli anterior (a32)	GCA	F′2	−8	21	40	16	720
Dorsolateral prefrontal cortex (a9)	DLPFC	F′6	−47	21	45	29	720

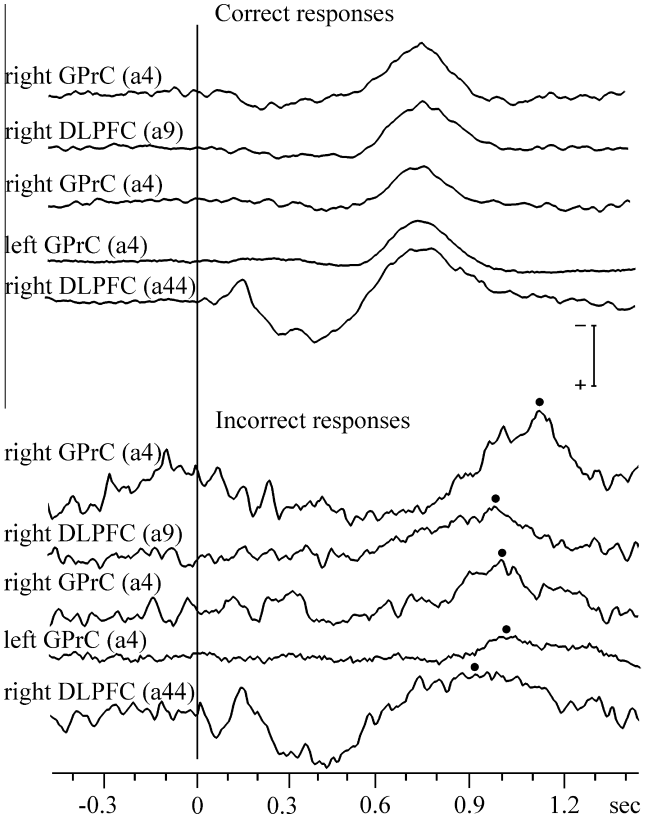

Fig. 2. The event-related potentials in trials with correct and incorrect responses to non-target stimuli. The abbreviations designate anatomical locations from which the records were derived; their explanations together with Talairach's coordinates are given in Table 1. The vertical line shows the onset of stimulus presentation. The black points over curves designate the peak of late ERP component in the incorrect responses. Seeing from top to bottom, the latencies of these peaks were 1117 ms, 968 ms, 1000 ms, 1009 ms, and 875 ms. The amplitude scaling is equal to 80 μV in the records from right DLPFC (a44) and to 40 μV in all remaining records.

other motor related actions. Its activation in cognitive operations, which are linked to more abstract, non-motor actions, could be regarded as the manifestation of a relatively low specialization of the underlying neuronal network.

Although our study was limited by the experimental paradigm, case-report design, nonsystematic electrode coverage, and clinical history of the subject, the results presented here are encouraging and could not be readily derived with other neuroimaging or processing techniques in healthy humans. Despite these notable issues our findings clearly suggest functional involvement of the M1 in cognitive activity not related to motor function.

In the light of early and recent knowledge (Potes et al., 2014; Scott et al., 2015; Stippich et al., 2007), the role of the primary motor cortex in brain functioning can, thus, be seen in the following domains: (i) the M1 transforms voluntary motor plans into appropriate movements, which consists mainly in selecting the proper muscles and encoding the force for executing the intended motor action; (ii) using the sensory feedback from somatic receptors the M1 contributes to a smooth accomplishment of the intended action; (iii) the M1 is implicated in the executive control of actions, including those which are not motor in nature.

Acknowledgements

Supported by the project "CEITEC – Central European Institute of Technology" (CZ.1.05/1.1.00/02.0068) from the European Regional Development Fund.

The funder had no role in study design, data collection and analysis, decision to publish, or preparation of the manuscript.

Conflict of interest: None of the authors have potential conflicts of interest to be disclosed.

References

Carpenter AF, Georgopoulos AP, Pellizzer G. Motor cortical encoding of serial order in a context-recall task. Science 1999;283:1752–7.

Classen J, Liepert J, Wise SP, Hallett M, Cohen LG. Rapid plasticity of human cortical movement representation induced by practice. J Neurophysiol 1998;79:1117–23.

Damborská A, Roman R, Brázdil M, Rektor I, Kukleta M. Post-movement processing in visual oddball task – evidence from intracerebral recording. Clin Neurophysiol 2016;127:1297–306. http://dx.doi.org/10.1016/j.clinph.2015.08.014.

Endrass T, Klawohn J, Gruetzmann R, Ischebeck M, Kathmann N. Response-related negativities following correct and incorrect responses: evidence from temporospatial principal component analysis. Psychophysiology 2012;49:733–43.

Georgopoulos AP, Lurito JT, Petrides M, Schwartz AB, Massey JT. Mental rotation of the neuronal population vector. Science 1989;243:234–6.

Georgopoulos AP, Massey JT. Cognitive spatial-motor processes – 1. The making of movements at various angles from a stimulus direction. Exp Brain Res 1987;65:361–70.

Giraux P, Sirigu A, Schneider F, Dubernard JM. Cortical reorganization in motor cortex after graft of both hands. Nat Neurosci 2001;4:691–2.

Hoffmann S, Falkenstein M. Independent component analysis of erroneous and correct responses suggests online response control. Hum Brain Mapp 2010;31:1305–15.

Hoffmann S, Falkenstein M. Predictive information processing in the brain: errors and response monitoring. Int J Psychophysiol 2012;83:208–12.

Holeckova I, Cepicka L, Mautner P, Stepanek D, Moucek R. Auditory ERPs in children with developmental coordination disorder. Act Nerv Super 2014;56:37–44.

Karni A, Meyer G, Jezzard P, Turner R, Ungerleider LG. The acquisition of skilled motor performance: fast and slow experience-driven changes in primary motor cortex. Proc Natl Acad Sci USA 1998;95:861–8.

Landa L, Krpoun Z, Kolarova M, Kasparek T. Event-related potentials and their applications. Act Nerv Super 2014;56:17–23.

Lachaux JPh, Rudrauf D, Kahane P. Intracranial EEG and human brain mapping. J Physiol Paris 2003;97:613–28.

Lotze M, Montoya P, Erb M, Hulsmann E, Flor H, Klose U, et al. Activation of cortical and cerebellar motor areas during executed and imagined hand movement: an fMRI study. J Cogn Neurosci 1999;11:491–501.

Menon V, Freeman WJ, Cutillo BA, Desmond JE, Ward MF, Bressler SL, et al. Spatio-temporal correlations in human gamma band electrocorticograms. Electroencephalogr Clin Neurophysiol 1996;98:89–102.

Pellizzer G, Sargent P, Georgopoulos AP. Motor cortical activity in a context-recall task. Science 1995;269:702–5.

Pons T, Garraghty PE, Ommaya AK, Kass JH, Taub E, Mishkin M. Massive cortical reorganization after sensory deafferentation in adult macaques. Science 1991;252:1857–60.

Potes C, Brunner P, Gunduz A, Knight RT, Schalk G. Spatial and temporal relationships of electrocorticographic alpha and gamma activity during auditory processing. NeuroImage 2014;97:188–95.

Riehle A, Kornblum S, Requin J. Neuronal correlates of sensorimotor association in stimulus-response compatibility. J Exp Psychol Hum Percept Perform 1997;23:1708–26.

Scott SH, Cluff T, Lowrey CR, Takei T. Feedback control during voluntary motor actions. Curr Opin Neurobiol 2015;33:85–94.

Stippich C, Blatow M, Durst A, Dreyhaupt J, Sartor K. Global activation of primary motor cortex during voluntary movements in man. NeuroImage 2007;34:1227–37.

Talairach J, Szikla G, Tournoux P, Prossalentis A, Bordas-Ferrer M, Covello L, et al. Atlas d'Anatomie Stéréotaxique du Télencéphale. Paris: Masson; 1967.

Ullsperger M, Danielmeier C, Jocham G. Neurophysiology of performance monitoring and adaptive behavior. Physiol Rev 2014;94:35–79.

Wise SP, Moody SL, Blomstrom KJ, Mitz AR. Changes in motor cortical activity during visuomotor adaptation. Exp Brain Res 1998;121:285–99.

Zhang J, Rielhe A, Requin J, Kornblum S. Dynamics of single neuron activity in monkey primary motor cortex related to sensorimotor transformation. J Neurosci 1997;15:2227–46.

3.2 P3-like waveform and movement execution

An extensive literature on event-related potentials (ERPs) in target detection tasks shows that the target and nontarget electrophysiological brain activity may diverge after sensory potentials have been elicited, giving rise to a post-divergence ERP component with latency 250 to 600 ms after the stimulus onset, well-known as the P3 component (Sutton et al., 1965; for review see Polich 2007). This component was traditionally viewed as representing cognitive functions involved in the decision making, orientation of attention, contextual updating, and cognitive closure of the stimulus identification (Paller et al., 1987; Squires et al., 1975). The association of P3 waveform to non-motor cognitive functions started to be used in clinical practice to evaluate cognitive ability in different neuropsychiatric conditions. No sooner than two decades later, intracerebral generators of the P3 component were found in different brain structures (Halgren et al., 1995 a, b; Brázdil et al., 1999). The intracerebrally recorded potentials were labelled as the P3-like potentials due to their temporal coincidence and similar configuration with the scalp-recorded P3 wave. Using the depth electrodes, spatio-temporal characteristics of these potentials could be explored and underlying mental processes could be investigated. Our team stayed at the very beginning of this research direction and brought evidence for heterogeneity of the P3-like waveform in a series of studies (Roman et al., 2001; 2005; Damborská et al., 2000; 2003; 2004; Damborská et al., 2001 – Annex 4; Damborská et al., 2006 – Annex 5; Damborská, 2012). We showed that the P3-like waveform probably reflects different mental processes including those related to motor execution. In the time window of the P3 wave we observed an intracerebrally recorded U-shaped potential preceding the movement that, in the majority of the explored brain sites, exhibited the same amplitude (Damborská et al., 2001 - Annex 4; Damborská et al., 2003) and the same width (Damborská et al., 2001 - Annex 4) when movement or stimulus onsets were used as triggers for averaging. Nevertheless, in around a quarter of explored brain sites in the frontal and temporal lobes, this potential showed larger amplitude (Damborská et al., 2001 - Annex 4; Damborská et al., 2003) and/or smaller width (Damborská et al., 2001 - Annex 4) in averaging triggered by movement. Thus, we suggested that the latter, less frequent, type of potential might represent movement-related cognitive processes. We further developed this idea in our pilot (Damborská et al., 2004) and

subsequent (Damborská et al., 2006 – Annex 5) studies using another analytical procedure on the intracerebrally recorded potential occurring in the time window of the visual P3 wave. After creating subgroups of EEG sweeps (trials) with equal stimulus-response (SR) intervals, we correlated the potential latency with the length of the SR interval across these subgroups. Almost in a quarter of explored brain sites in two thirds of examined subjects the peak of the waveform closely preceded the movement onset and showed a significant correlation between the waveform latency and the SR interval (Damborská et al., 2006 – Annex 5). Thereby, we showed that in some brain sites in the time window of the P3 wave, a potential occurs that is temporally linked to the movement onset. This finding confirmed our previously provided evidence that there exist P3-like waveforms time-locked to the motor response (Roman et al., 2001). Thus, for the first time only in our intracerebral studies, it was suggested that some neuronal processes represented with P3-like waves might be somehow engaged in movement execution.

Annex 4

Damborská, A., Brázdil, M., Jurák, P., Roman, R., & Kukleta, M. (2001). Steep U-shaped EEG potentials preceding the movement in oddball paradigm: Their role in movement triggering. *Homeostasis in Health and Disease, 41*(1-2), 60-63.
Quantitative contribution: 70%
Content contribution: pre-processing, analysis, writing the initial draft, table and figure preparation

Annex 5

Damborská, A., Brázdil, M., Rektor, I., Roman, R., & Kukleta, M. (2006). Correlation between stimulus-response intervals and peak amplitude latencies of visual P3 waves. *Homeostasis in Health and Disease*, 44*(4), 165*-168.
Quantitative contribution: 70%
Content contribution: pre-processing, analysis, writing the initial draft, table and figure preparation

Annex 4

Damborská, A., Brázdil, M., Jurák, P., Roman, R., & Kukleta, M. (2001). Steep U-shaped EEG potentials preceding the movement in oddball paradigm: Their role in movement triggering. *Homeostasis in Health and Disease, 41*(1-2), 60-63.

Steep U-shaped EEG potentials preceding the movement in oddball paradigm: Their role in movement triggering

A. Damborská[1], M. Brázdil[2], P.Jurák[3], R. Roman[1], M. Kukleta[1]

Department of Physiology, Medical Faculty, Masaryk University, Brno, Czech Republic[1]
Department of Neurology, St. Anne Hospital, Masaryk University, Brno, Czech Republic[2]
Laboratory of MRI electronics, Institute of Scientific Instruments, Academy of Sciences, Brno, Czech Republic[3]

EEG potentials of U shape that closely precede the execution of movement performed during a visual oddball paradigm were analysed with the aim to obtain the data relevant to mechanisms of the movement triggering. For this purpose, only waves registered in response to target stimuli were included in the analysis. The starting idea of our study was the fact that the efficacy of averaging procedure is determined by the degree of synchronisation of single electrical events with the trigger used for averaging. In oddball paradigm two triggers can be used: stimulus or movement. By comparing amplitudes and widths of the resulting averaged potentials created in these two

different ways, i.e., by comparing the efficacies of averaging, it is possible to assess whether the analysed potential is temporally more linked to the stimulus or to the movement. Finding the evident temporal association between the wave and movement can be used as an argument for the interpretation that this wave is directly engaged in the mechanism of movement triggering.

One left-handed and seventeen right-handed patients (four women and fourteen men), age ranging from 19 to 45 years (median 28.5), all suffering from medically intractable epilepsies, were investigated. The patients were implanted with depth multilead electrodes to localize the seizure origin prior to surgical treatment. A total of 637 sites in the temporal, frontal and parietal lobes of the right (354) and left (283) hemispheres were examined by means of 102 multilead depth electrodes. Lesional anatomical structures and epileptogenic zone structures were not included in the analysis. The exact positions of the electrodes in the brain were verified using post placement MRI with electrodes in situ.

The standard visual oddball paradigm was performed in each patient. Two different stimuli were displayed in the centre of the screen in a random order. Clearly visible yellow capital letters X (target) and O (frequent) on a white background were used as experimental stimuli. The ratio of target to frequent stimuli was 1:5. The interstimulus interval varied randomly between 2 and 5 s. Each subject was instructed to press a microswitch button with the dominant hand as quickly as possible as a response to every target stimulus. At the same time mental counting of the target stimuli was required.

Fig 1. Three types of steep U-shaped potential shift preceding the movement: A - potential more synchronised with the movement, B - potential more synchronised with the target stimulus, C - potential with the same degrees of synchronisation. Zero point on time axis marks the pressing of the microswitch button (movement as a trigger of averaging - thick curves). The curves calculated with target stimulus as a trigger (thin lines) have been manually superimposed over the thick curves. The stimulus-response intervals are 471ms (A), 657ms (B), and 497ms (C); the peak latencies are 415ms, 523ms, and 433ms, respectively. Curves from three subjects are presented.

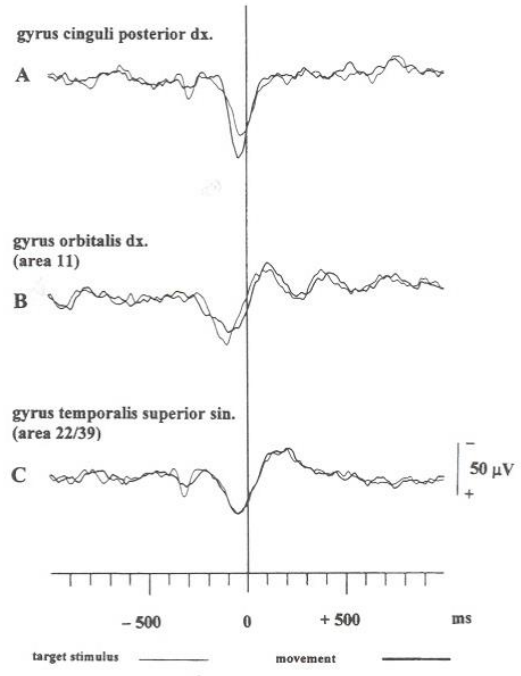

The EEG signal was recorded simultaneously from various intracerebral structures using 64 channel Brain Quick EEG system. All recordings were monopolar with respect to a reference electrode on the processus mastoideus. EEG signal was amplified with the bandwidth of 0.1 - 40 Hz at the sampling rate of 128 Hz.

The signal analysis was made with help of Scope Win software. Two-second EEG periods were averaged off-line using firstly the movement onset, secondly the target stimulus, and thirdly the frequent stimulus as triggers. The visual inspection of averaged records has been made, and each potential that fitted all the

following descriptions has been chosen: i) it appears in response to the target stimulus only, ii) it reaches its maximal amplitude during 200 ms period before the movement, iii) it falls or rises from the baseline with a slope above ±100 μV/sec, iiii) it is of U shape. Thus selected potential was further analysed. The averaged record triggered by movement was compared with that triggered by target stimulus. The amplitude and width differences of an averaged potential were evaluated. The larger the amplitude and/or the smaller the width, the greater is the synchronisation of the wave with the trigger. Amplitudes were measured from the baseline to the peak; widths were measured at the level of 5 μV below or above the baseline. The baseline was defined in the first 200 ms of analysis window.

The mean stimulus-response interval of subjects ranged from 446 to 657 ms (mean 534.7±55.5). The averaging and later selection revealed mostly positive potentials, which could be sorted into three groups. Figure 1 shows all the three types. The potential of A type reaches larger amplitude and/or smaller width in the averaging calculated from the movement than in the averaging triggered by target stimulus. Therefore, it is more synchronised with the movement. Its peak latency from the stimulus varies between 353 and 570 ms (median 433). The potential of B type reaches larger amplitude and/or smaller width in the averaging calculated from the target

Table 1: Localisations and occurrences of potentials

Potential more synchronised with the movement		
Localisation	Left	Right
Hippocampus	**2**	**0**
g. parahippocampalis	**0**	**1**
Ganglia basalia	**7**	**3**
g. cinguli	**4**	**7**
g. rectus	**0**	**1**
Cortex frontoorbitalis	**0**	**3**
area 9	**1**	**0**
g. frontalis medius	**0**	**1**
g. frontalis inf.	**0**	**1**
g. temporalis sup.	**0**	**3**
g. temporalis med.	**0**	**2**
g. temporalis inf.	**2**	**2**
White matter	**3**	**1**
Total of 44(19 left, 25 right) sites		

Potential more synchronised with the stimulus		
Localisation	Left	Right
Amygdala	**0**	**1**
Hippocampus	**2**	**0**
Ganglia basalia	**2**	**0**
g. orbitalis	**0**	**2**
Cortex praefrontalis dorsolateralis	**3**	**1**
Total of 11 (7 left, 4 right) sites		

Potential with the same degrees of synchronisation		
Localisation	Left	Right
Amygdala	**5**	**3**
Hippocampus	**5**	**3**
Ganglia basalia	**2**	**5**
g. cinguli	**2**	**5**
g. rectus	**0**	**3**
g. orbitalis	**6**	**0**
Cortex frontoorbitalis	**6**	**2**
Cortex praefrontalis dorsolateralis	**4**	**4**
area 9	**10**	**0**
g. frontalis medius	**0**	**1**
g. frontalis medialis	**2**	**2**
Praemotoric cortex	**0**	**1**
g. temporalis sup.	**3**	**0**
g. temporalis med.	**4**	**4**
g. temporalis inf.	**2**	**0**
g. fusiformis	**1**	**1**
White matter	**5**	**7**
Total of 98 (57 left, 41 right) sites		

stimulus than in the averaging triggered by movement. Therefore, it is more synchronised with the target stimulus. Its peak latency from the stimulus varies between 325 and 528 ms (median 426). The potential of C type reaches the same amplitude and the same width in both ways of averaging. Therefore, it has the same degree of synchronisation with both triggers. Its peak latency from the stimulus varies between 269 and 634 ms (median 441). In comparing we have adopted the difference equal to 20% of the larger value to be the minimal difference necessary for including the potential in the group of A or B type. Smaller differences have not been taken into consideration, and such potentials were included in the group of C type. Table 1 shows localisations and occurrences of the three types of potentials.

In conclusion, steep potential shift of U shape shortly preceding the movement appears in the electric brain response to target stimulus. This potential when averaged synchronises more with the movement or with the stimulus or equally with both of them. These three different results indicate that the potential is in some cases temporally more closely linked to the movement, in other cases to the stimulus, and in other cases to none of them or equally loosely to both of them. Most of these potentials fit the description of the P3 component of event-related potentials (ERPs). This long-latency mostly positive waveform is generally viewed as a target detection response and as reflecting cognitive processes. On the basis of our results we suggest that the P3 component of ERPs in some cases can reflect the processes, which are more temporally linked to the movement than to the target stimulus, and which can play some role in movement triggering.

REFERENCES

Brázdil, M., Rektor, I., Dufek, M., Daniel, P., Jurák, P., Kuba, R. : The role of frontal and temporal lobes in visual discrimination task - depth ERP studies. Neurophysiol. Clin. 29: 339-350, 1999

Guillem, F., N' Kaoua, B, Rougier A., Claverie, B. : Intracranial topography of event-related potentials (N400/P600) elicited during a continuous recognition memory task. Psychophysiology 32:382-92, 1995

Smith, ME. , Halgren, E., Sokolik, M., Baudena, P., Mussolino, A., Liéteois-Chauvel, C., et al.: The intracranial topography of the P3 event-related potential elicited during auditory oddball. Electroencephalography and Clinical Neurophysiology 76: 235-48, 1990

37th Conf. on Higher Nervous Functions
Olomouc, September 2001

A.D.,Dept. of Physiol., Med. Fac.
Komenského nám. 2, 662 43 Brno, CR

Annex 5

Damborská, A., Brázdil, M., Rektor, I., Roman, R., & Kukleta, M. (2006). Correlation between stimulus-response intervals and peak amplitude latencies of visual P3 waves. *Homeostasis in Health and Disease,* 44(4), 165-168.

Correlation between stimulus-response intervals and peak amplitude latencies of visual P3 Waves

A. Damborská[1], M. Brázdil[2], I. Rektor[2], R. Roman[1], M. Kukleta[1]

Department of Physiology, Medical Faculty, Masaryk University, Brno, Czech Republic[1]
Department of Neurology, St. Anne's Hospital, Masaryk University, Brno, Czech Republic[2]

Mechanisms of the movement triggering are in the centre of our attention. An oddball paradigm testing includes the act of moving and is therefore suitable for this purpose. Some visual P3 waves prove to differ in the amplitude, width, and/or waveform dependently on the trigger used for averaging. Few potentials appear to be temporally more closely linked to the movement than to the target stimulus (Damborská et al. 2001; Damborská et al. 2003; Roman et al. 2005). In the study presented we have carried out a detailed analysis of visual P3 waves in order to assess the temporal association between the wave and the movement. We have made use of analytical potency of correlating P3 peak latencies with stimulus-response intervals. Thus, P3 wave was tested as a possible reflection of the movement triggering processes.

METHODS AND MATERIALS

Fourteen epileptic patients participated in the standard visual oddball paradigm testing. Two different visual stimuli (target and non-target) were presented in random order with the ratio of 1: 5. The interstimulus interval varied between 2 and 5 seconds. The task was to press a microswitch button with the dominant hand as quickly as possible in response to each target stimulus. The EEG signal was recorded simultaneously from various intracerebral structures by means of depth electrodes implanted before the surgical treatment of epilepsy. The frontal, temporal, and parietal lobes of both hemispheres were examined. All recordings were monopolar with respect to a reference electrode on the processus mastoideus. EEG signal was amplified with the bandwidth of 0.1–40 Hz at the sampling rate of 128 Hz. The signal analysis was made with help of Scope Win software. Epileptogenic zone structures were not included in the analysis.

The stimulus – response (SR) interval of every single trial was measured. In each patient the trials with nearly the same SR intervals (at most 10 ms difference) were put together in subgroups. In each patient we have averaged two-second EEG periods firstly from all trials, secondly within each subgroup. P3 waves were identified by visual inspection, and their peak latencies were measured. Pearson correlations between P3 peak latencies and SR intervals were calculated across subgroups for each recorded site.

RESULTS

The total of 29–58 trials was distributed into 5–9 subgroups according to the SR intervals (Table 1). Each subgroup included 2–13 single trials. For example, in patient number 8 the following six subgroups were created (SR interval and the number of trials are used as subgroup labels): 425 ms (3 trials), 456 ms (8 trials), 472 ms (5 trials), 482 ms (5 trials), 507 ms (3 trials), and 537 (4 trials). In patient number 11 the following seven subgroups were created: 388 ms (3 trials), 424 ms (3 trials), 441 ms (4 trials), 462 ms (5 trials), 479 ms (9 trials), 492 ms (6 trials), and 542 ms (3 trials).

Table1. Patients' characteristics, number of sites with detectable P3 waves (130 in total), their location in the cerebral lobes, mean stimulus – response (SR) interval, total of trials and their distribution into subgroups. All patients except for No. 10 were right-handed.

Pt. No*	Age	Sex	Number of sites	Cerebral lobes**	SR interval mean ≤ SD	Total of trials	Number of subgroups
1	20	M	4	r F, l T	516 ± 58	42	8
2	28	M	4	r T, l T	604 ± 82	31	5
3	37	M	16	r FT, l FT	525 ± 63	50	8
4	45	M	7	r FT, l FT	644 ± 78	29	6
5	30	M	13	r F, l FT	575 ± 150	50	8
6	31	F	11	r FT	585 ± 111	49	8
7	32	M	3	r FT	573 ± 58	43	6
8	30	M	10	r FT, l T	472 ± 43	36	6
9	27	F	8	r T	572 ± 61	51	9
10	25	M	17	r FT, l FT	503 ± 46	55	8
11	34	M	8	r FPT	477 ± 51	42	7
12	23	M	15	r FT, l F	594 ± 92	58	8
13	28	F	12	l FT	521 ± 67	50	7
14	27	M	2	l T	457 ± 34	42	6

* Pt. No = patient's number, ** F = frontal, P = parietal, T = temporal, r = right, l = left

Table 2. Location of recording contacts, their position in the cerebral lobes, and occurrence of B type among P3 waves analysed.

Anatomical site	Cerebral lobe	No. of B type/ no. of P3 waves
Cortex frontoorbitalis	F	3/11
Gyrus frontalis medius	F	3/ 5
Gyrus frontalis medialis	F	6/11
Gyrus frontalis inferior	F	1/ 1
Gyrus rectus	F	0/ 6
Cortex praemotoricus	F	0/ 1
Cortex dorsolateralis praefrontalis	F	2/12
Gyrus cinguli	F	5/11
Lobus parietalis	P	0/ 2
Amygdala	T	1/ 5
Hippocampus	T	2/13
Gyrus parahippocampalis	T	1/ 6
Gyrus temporalis superior	T	2/ 4
Gyrus temporalis medius	T	3/16
Gyrus temporalis inferior	T	0/ 7
Gyrus fusiformis	T	0/ 2
Ganglia basalia	T	1/ 9
White matter	F, T	0/ 8
Total	**F, T, P**	**30/130**

Fig. 1. Two main types of P3 waves. Long vertical lines mark the stimulus presentation; short vertical lines show the movement onset. Upper curves in both sections represent EEG averages calculated from all trials. The other curves are subgroup averages. The number above each curve designates the number of trials. Curves under A belong to patient No 8 – recording contact in the gyrus temporalis inferior dexter; curves under B belong to patient No 11 – recording contact in the gyrus temporalis medius dexter.

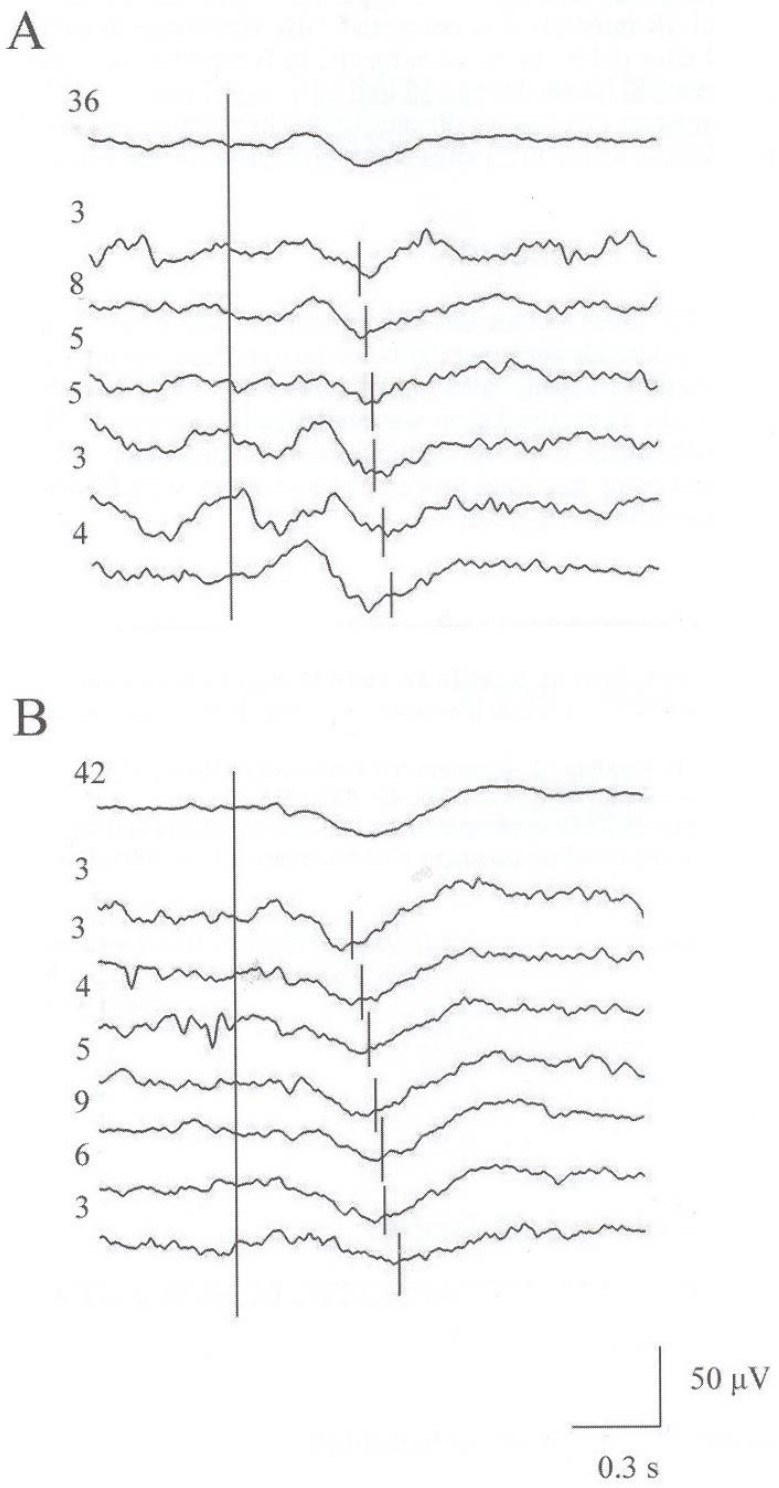

P3 waves were identified in 150 sites, when averaging EEG periods from all trials. P3 waves detectable as well in subgroups were found in 130 of them (2–17 sites in each patient). Further analysis was performed on the subgroup P3 waves and revealed two main types of P3 waves (Figure 1). Notice the position of P3 peaks, which vary independently on the point of the movement initiation in A type but closely precede the movement onset across all subgroup averages in B type. In A type the correlation between P3 peak latencies and SR intervals was not statistically significant at $p<0.05$, ($r = 0.30$). It was found in 79 sites (61%) in all 14 subjects. In B type the correlation between P3 peak latencies and SR intervals was statistically significant at $p<0.01$, ($r = 1$). Such considerable correlation occurred in 30 sites (23%) in 9 subjects (Table 2). The rest of P3 waves, which were detected in 21 sites (16%) in 8 subjects, have no clear degree of correlation.

CONCLUSION

We have confirmed that visual P3 waves include different potentials, which vary in their temporal characteristics. These potentials are generally believed to reflect cognitive processes /3/. In our study, on the contrary, peak latencies of several P3 waves correlated with stimulus – response intervals. This correlation was statistically significant. Thus, they have shown to be temporally linked to the movement onset. In agreement with our previous studies we suggest that some neuronal processes represented with P3 waves are somehow engaged in the movement triggering.

REFERENCES

Damborská A., Brázdil M., Jurák P., Roman R., Kukleta M. Steep U-shaped EEG potentials preceding the movement in oddball paradigm: Their role in movement triggering. Homeostasis, 41, 2001, 60–63.

Damborská A., Brázdil M., Rektor I., Kukleta M. Temporal characteristics of U-shaped P–3 waves registered with intracerebral electrodes in humans. Homeostasis, 42, 2003, 213–215.

Roman R., Brázdil M., Jurák P., Rektor I., Kukleta M. Intracerebral P3–like waveforms and the length of the stimulus – response interval in a visual oddball paradigm. Clin Neurophysiol, 16, 2005, 160–171.

41st Conf. on Higher Nervous Functions
Brno, August 2006

A.D., Dept. of Physiol., Med. Fac. Masaryk Univ., Komenského nám. 2, 662 43 Brno, Czech Republic

3.3 Movement-related cognitive functions

The basic information about the organization of operations in an intention–action functional coupling during voluntary movements has emerged from psychophysiological experiments and from analyses of relevant neurological and psychiatric case studies (for review see Jeannerod, 2009). According to their results, the operations underlying an intentional motor action could be dissociated into three relatively independent functional wholes. The first one is responsible for the creation of an internal *representation* of the future action, the second one is responsible for its *execution*, and the third one assures the *comparison* of the predicted and the actual result of the action. The first whole is by definition a pre-movement event, therefore can be associated with electrophysiological cortical activity preceding the electromyogram activation onset. Similarly, the second whole could be associated with electrophysiological correlates elicited in the brain during electromyogram activation. Although one could suppose the third whole to occur only after the movement has been finished, the results of previous observations suggest otherwise. Movements unfold through time, and it is thought that a comparison between the motor intention and sensory feedback occurs continuously throughout the duration of a movement (Shadmehr et al., 2010).

Scalp-recorded ERPs elicited during the oddball task have been employed for decades as a useful tool for studying cognition processes including the movement-related ones. In the oddball task the subject responds by button pressing only to the infrequent ‘‘target” stimulus, which is presented randomly and repeatedly among frequent ‘‘nontarget” stimuli. Two types of correct performance are observed – motor response in the target variant (correct hit) and refraining from movement in the nontarget variant (correct rejection). The oddball paradigm can also induce two types of errors – response omission in the target variant (incorrect rejection) and erroneous motor response (false alarm) in the nontarget variant. As such, the analysis of intracerebrally recorded ERPs after movement onset within this simple cognitive task seems to be very useful for studying mechanisms of performance monitoring by exploring spatiotemporal characteristics of these late ERP components.

Previous intracerebral studies employing motor tasks to search for electrophysiological correlates of movement-related cognitive functions focused on

middle latency ERPs, such as P3-like potentials (Roman et al., 2005; Rektor et al., 2007) or ERPs appearing before and during a simple acral limb movement (Rektor et al., 1998; Rektor, 2000). Multiple generators of P3-like potential were discovered (Rektor et al., 2007) and heterogeneity of the P3-like phenomenon with respect to stimulus evaluation and movement-related processes was shown in a series of studies mentioned in Chapter 3.2 of this habilitation thesis. Furthermore, generators of potential occurring during voluntary limb movement were discovered, i.e., the movement-accompanying slow potential, MASP (Rektor et al., 1998). In that study, generators of the MASP were identified in motor and supplementary motor, premotor and prefrontal, midtemporal, somatosensory, superior parietal and cingular cortices. Although with no ambition to study MASP in detail, authors interpreted this evidently heterogenic phenomenon to be associated with "readiness to subsequent act" and "attention to action".

With the arrival of a new millennial, the research community employing intracerebral EEG recording focused on the investigation of performance monitoring as a critical executive function of the human brain (Ullsperger et al., 2014). ERPs elicited in the post-performance period, i.e., exceeding the reaction time were explored. In a search for the sources of post-performance ERPs in incorrect responses, the key role of frontomedian wall structures, in particular the ventral and dorsal anterior cingulate cortex and the preSMA, in error processing was suggested (Brázdil et al., 2002; 2005). Nevertheless, no intracerebral study aimed at identifying sources of post-performance ERPs in correct responses. One decade later, our team filled this gap by providing first intracerebral evidence for the existence of multiple cortical sources of late ERP components elicited after the correct response (Damborská et al., 2016 – Annex 6). These large-scale brain networks include mesiotemporal structures, anterior midcingulate, prefrontal, and temporal cortices. Thus, besides anterior cingulate cortex, whose involvement in correct response-related ERP generation was previously documented by a source localization study (Roger et al., 2010), our findings suggested the recruitment of several other brain structures following correct motor responses. In this study, we also demonstrated equivalent involvement of these structures in task-variant nonspecific and target-specific processes. The mere existence of these two types of post-movement ERP favours the view that after correct

movement execution, parallel processing in at least two distinct systems takes place sharing at least partially the same anatomical substrate. Parallel activation of two different systems, i.e., performance-monitoring and movement-monitoring, was also suggested in error processing (Yordanova et al., 2004). Moreover, our study (Damborská et al., 2016 – Annex 6) also showed that large-scale brain networks generating correct and incorrect performance-related potentials probably share some common nodes. Thus, we contributed to a better understanding of neuronal mechanisms underlying goal-directed behaviour.

In further search for electrophysiological correlates of the comparison of the internal model of the action with its actual result, we examined the final epoch of a voluntary self-initiated hand movement (Kukleta et al., 2017 – Annex 7). We aimed to identify brain structures activated during that period. To prevent any contamination by electrophysiological manifestations of the preceding operations such as planning and movement initiation, we searched for brain sites, which generated exclusively late potentials, i.e., following the peak of electromyogram activity of investigated hand. We identified late movement potential (LMP) in multiple loci of both hemispheres, mostly in both mesial and lateral localizations, including remote regions of mesiotemporal structures, cingulate, frontal, temporal, parietal, and occipital cortices. Moreover, we observed synchronization of neuronal activity in remote brain loci of this large-scale network that reflected probably a temporarily restricted functional linkage of thus far independent loci. We suggested that the brain sites generating the LMP could be involved in the late online movement and the post-movement comparisons of intended and actually performed actions. A series of experimental psychophysiological studies demonstrated the crucial role of the accordance between an intention and its result for the creation of agentive experience (Ullsperger et al., 2014). This experience that we are in control of our own actions is one of the key components of human consciousness. Our description of a large-scale network generating the LMPs could thus be considered a step toward structural delineation of this significant component of human consciousness.

Annex 6

Damborská, A., Roman, R., Brázdil, M., Rektor, I., & Kukleta, M. (2016). Post-movement processing in visual oddball task - evidence from intracerebral recording. *Clinical Neurophysiology,* 127 (2), 1297 – 1306.

IF(2016) = 3.866, rank Q1
Quantitative contribution: 90%
Content contribution: development of the initial idea, pre-processing, analysis, statistical evaluation, writing the initial draft, table and figure preparation, assistance in corresponding

Annex 7

Kukleta, M., **Damborská, A.**, Turak, B., & Louvel, J. (2017). Evoked potentials in final epoch of self-initiated hand movement: A study in patients with depth electrodes. *International Journal of Psychophysiology*, 117, 119-125.
IF(2017) = 2.868, rank Q2
Quantitative contribution: 40%
Content contribution: participation in writing the initial draft, participation in table and figure preparation, corresponding author

Annex 6

Damborská, A., Roman, R., Brázdil, M., Rektor, I., & Kukleta, M. (2016). Post-movement processing in visual oddball task - evidence from intracerebral recording. *Clinical Neurophysiology,* 127 (2), 1297 – 1306.

Clinical Neurophysiology 127 (2016) 1297–1306

Contents lists available at ScienceDirect

Clinical Neurophysiology

journal homepage: www.elsevier.com/locate/clinph

Post-movement processing in visual oddball task – Evidence from intracerebral recording

Alena Damborská [a,b], Robert Roman [a,b,*], Milan Brázdil [a,c], Ivan Rektor [a,c], Miloslav Kukleta [a]

[a] CEITEC – Central European Institute of Technology, Masaryk University, Brno, Czech Republic
[b] Department of Physiology, Faculty of Medicine, Masaryk University, Brno, Czech Republic
[c] 1st Department of Neurology, St. Anne's Faculty Hospital, Masaryk University, Brno, Czech Republic

ARTICLE INFO

Article history:
Accepted 25 August 2015
Available online 4 September 2015

Keywords:
Intracerebral EEG
ERP
Movement
Monitoring
Correct performance
Error

HIGHLIGHTS

- Multiple cortical structures are activated after correct motor performance including mesiotemporal structures, anterior midcingulate, prefrontal, and temporal cortices.
- Equivalent involvement of these structures in task-variant nonspecific and target specific processes is suggested.
- Networks generating correct and incorrect performance-related potentials probably share some common nodes.

ABSTRACT

Objective: To identify intracerebral sites activated after correct motor response during cognitive task and to assess associations of this activity with mental processes.
Methods: Intracerebral EEG was recorded from 205 sites of frontal, temporal and parietal lobes in 18 epileptic patients, who responded by button pressing together with mental counting to target stimuli in visual oddball task.
Results: Post-movement event-related potentials (ERPs) with mean latency 295 ± 184 ms after movement were found in all subjects in 64% of sites investigated. Generators were consistently observed in mesiotemporal structures, anterior midcingulate, prefrontal, and temporal cortices. Task-variant nonspecific and target specific post-movement ERPs were identified, displaying no significant differences in distribution among generating structures. Both after correct and incorrect performances the post-performance ERPs were observed in frontal and temporal cortices with latency sensitive to error commission in several frontal regions.
Conclusion: Mesiotemporal structures and regions in anterior midcingulate, prefrontal and temporal cortices seem to represent integral parts of network activated after correct motor response in visual oddball task with mental counting. Our results imply equivalent involvement of these structures in task-variant nonspecific and target specific processes, and suggest existence of common nodes for correct and incorrect responses.
Significance: Our results contribute to better understanding of neural mechanisms underlying goal-directed behavior.
© 2015 International Federation of Clinical Neurophysiology. Published by Elsevier Ireland Ltd. All rights reserved.

1. Introduction

It is widely accepted that successive components of event-related potentials (ERPs) elicited during a cognitive task are related to successive stages in processing. Therefore, electrophysiological recording can be used to monitor the probable location, timing and intensity of brain activation during the task (Halgren et al., 1998). Recently, an increased interest in the neural sources of ERPs elicited in the post-performance period has been observed with the aim to identify anatomical structures engaged in performance monitoring. A well-known event-related potential provoked by errors, error-related negativity (Ne/ERN) typically peaking

* Corresponding author at: Department of Physiology, Faculty of Medicine, Masaryk University, Kamenice 5, 625 00 Brno, Czech Republic. Tel.: +420 549 496 818.
E-mail address: roman@med.muni.cz (R. Roman).

http://dx.doi.org/10.1016/j.clinph.2015.08.014
1388-2457/© 2015 International Federation of Clinical Neurophysiology. Published by Elsevier Ireland Ltd. All rights reserved.

100–150 ms after an erroneous response (Falkenstein et al., 1990; Gehring et al., 1993) was proved by intracerebral studies to stem from activation of multiple sources, with the most consistent involvement being that of frontomedian wall and mesiotemporal lobe structures (Brázdil et al., 2002, 2005; Pourtois et al., 2010). A positive deflection occurring 200–500 ms after an incorrect response and following the Ne/ERN referred to as error positivity (Pe; Falkenstein et al., 1991, 1995, 2000) was suggested to be generated in the anterior cingulate cortex (ACC; Herrmann et al., 2004) and to have a common origin with the Ne/ERN (Brázdil et al., 2002). In patients and also in healthy subjects the so-called "correct response-related negativity" (Nc/CRN) is often seen as negative deflection following correct responses in surface electrophysiological recordings (Bonnefond et al., 2011; Coles et al., 2001; Ford, 1999; Gehring and Knight 2000; Scheffers and Coles, 2000; Vidal et al., 2000, 2003). Surprisingly, few studies carefully investigated neural sources of Nc/CRN. This ERP was observed at frontal (Mathalon et al., 2002; Meckler et al., 2011) and frontocentral electrodes (Falkenstein et al. 2000; Hajcak et al., 2005), and, therefore, generators in the rostral cingulate zone were suggested (Carter et al., 1998; Roger et al., 2010). Similarly to erroneous responses a small positivity can also be found for correct responses called the correct response positivity (Pc), but it has generally been used only as a baseline comparison for the Pe and little has been written about it (Bates et al., 2004; Mathalon et al., 2002). We believe, however, that studies focused on correct response processing could contribute to better understanding of neural mechanisms underlying successful goal-directed behavior. In addition to these theoretical implications, studying the functional significance of post-performance ERPs might also help to understand deficits in action control and behavior adaptation observed in psychopathological and neurological conditions (Taylor et al., 2007).

Scalp-recorded event-related potentials (ERPs) elicited during the so-called "oddball" task have been employed for decades as a useful tool for studying cognition processes. In the oddball task the subject responds by button pressing and/or mental counting only to the infrequent "target" stimulus, which is presented randomly and repeatedly among frequent "nontarget" stimuli. Two types of correct performance are observed – motor response in the target variant (correct hit) and refraining from movement in the nontarget variant (correct rejection). The oddball paradigm can also induce two types of errors – response omission in the target variant (incorrect rejection) and erroneous motor response (false alarm) in the nontarget variant. As such, the analysis of ERPs recorded in the post-performance period of this simple cognitive task seems to be very useful for studying mechanisms of performance monitoring. Previous intracerebral studies employing motor tasks, however, focused rather on P3-like potentials (Rektor et al. 2007) or ERPs appearing before and during a simple acral limb movement (Rektor et al. 1998; Rektor, 2000) and did not investigate ERP components that might appear later. To our knowledge, the activity following correct responses in motor tasks has not been systematically examined by any intracerebral study yet.

While multiple sources were proved for event-related activity in the post-performance period provoked by errors (Brázdil et al., 2002, 2005; Pourtois et al., 2010) we have hypothesized whether also in correct reactions to target stimuli of visual oddball task multiple brain regions might be involved in processes that take place there. If so, ERP activity in the post-movement period of correctly performed task might be observed within a large-scale neuronal network rather than limited to a single brain structure. To this end, the present intracerebral ERP study was designed to identify the cerebral sites consistently activated after correct motor reactions in a visual oddball task. Therefore we assessed across examined brain structures the occurrence frequency of post-movement ERP evoked during the target task variant. In an attempt to associate these ERPs with underlying mental processes, we decided to evaluate these potentials in relation to ERPs elicited after correct performance of nontarget task variant and after both types of errors induced during the task. If the post-movement ERP reflects different mental processes then in sites where this ERP was detected, differences in post-performance activity in the nontarget task variant should be observed. If the brain network related to incorrect responses shares some common nodes with that related to correct responses, then sites active in both conditions should be identified. To explore the character of mental processes underlying the post-movement ERPs we evaluated their latency and distribution among brain structures.

2. Methods and materials

2.1. Subjects

Eighteen patients (14 men) aged from 23 to 45 years (median 30) were employed in the study (Table 1). All subjects suffered from medically intractable epilepsy and were candidates for surgical treatment. They all were under antiepileptic drug therapy, which was determined by clinical considerations. During the period of diagnostic examination by intracerebral EEG recording, the doses of medicaments were reduced to allow seizures to develop spontaneously. All patients had normal or corrected-to-normal vision. The subjects gave us their informed consent to the experimental protocol that had been approved by the Ethical Committee of Masaryk University.

2.2. Experimental task

A visual oddball task was performed. The patients were sitting comfortably in a moderately lighted room and were focusing on the center of a monitor situated at about 100 cm from their eyes. Yellow capital letters X (target) or O (nontarget) appeared repeatedly on white background in random order as experimental stimuli. Each stimulus presentation lasted 200 ms and the interstimulus interval varied randomly between 2 and 5 s. The target stimuli were five times less frequent than the nontarget ones. The subjects were instructed to press a microswitch button with

Table 1
Patient characteristics and lobes investigated.

Patient	Sex*	Age	Lobes investigated *	Number of sites investigated
1	M	20	RFT, LFT	11
2	M	28	RFT, LT	7
3	M	37	RFT, LFT	13
4	M	45	RFT, LFT	15
5	M	30	RFT, LFT	14
6	F	31	RFT	12
7	M	32	RFT, LTF	4
8	M	30	RFT, LFT	10
9	M	19	RF, LF	12
10	F	31	RFT, LFT	14
11	F	27	RT	6
12	M	19	RT, LT	14
13	M	41	RF, LF	8
14	M	25	RFT, LFT	17
15	M	34	RFTP	14
16	M	23	RFT, LFT	16
17	F	28	LFT	10
18	M	27	LT	8

* M = male; F = female; R = right, L = left; F = frontal, T = temporal, P = parietal.

the dominant hand as quickly as possible, whenever a target stimulus appeared, to mentally count the target stimuli, and to ignore the nontarget stimuli.

2.3. Data acquisition

Electrical activity was recorded during the task simultaneously from various brain sites by means of standard Micro Deep semiflexible multicontact platinum electrodes. Having a diameter of 0.8 mm, each electrode carried 5–15 contacts 2.0 mm long separated by constant intervals of 1.5 mm. Strictly for diagnostic reasons 113 intracerebral depth electrodes were implanted into the structures of the frontal, temporal, and parietal lobes (Table 1). Every patient received 2–10 such electrodes exploring either or both hemispheres. Long electrodes examined both lateral and mesial cortical regions. The electrodes were placed using the methodology of Talairach et al. (1967) and their position was afterwards verified by magnetic resonance imaging with electrodes in situ. The registration was made with the help of a 64-channel Brain Quick EEG system (Micromed). All the recordings were monopolar with respect to a reference electrode attached to the right processus mastoideus. The impedances used were less than 5 kΩ. The EEG signal was amplified with a bandwidth of 0.1–40 Hz at a sampling rate of 128 Hz.

2.4. Analysis

The EEG signal was analyzed offline with the help of ScopeWin software. The recordings from lesions and epileptogenic zones and the trials with artefacts were rejected offline with visual inspection made by two experienced persons. Switching the button in response to a nontarget stimulus or its omission in response to a target stimulus was considered as error. In each subject all artefact-free trials with correct and at least 10 incorrect performances were used for calculation of average curves. Exclusion of a different number of trials and commission of a different number of errors explains the interindividual variability in the number of trials used for each average curve (target variant: 41–80 trials with correct hits, 14 and 25 trials with incorrect refraining from movement; nontarget variant: 191–342 trials with correct refraining from movement, and 13, 14 and 18 trials with false alarms). Post-movement ERP waves in the latency range of 0–900 ms from movement were analyzed. Periresponse EEG periods (from −900 to +900 ms from the movement onset) were averaged for target correct responses using movement onset as a trigger. Peristimulus EEG periods (from −300 to +1500 ms from the stimulus onset) were averaged separately for target and nontarget correct and incorrect performances using the stimulus onset as a trigger. The statistical significance of ERP waves was computed between the mean amplitude observed during the baseline period (from −600 to −100 ms from the stimulus onset) and the mean value computed as a mean from the neighborhood of each point (170 ms length) after stimuli or responses using a nonparametric Wilcoxon Rank Sum (Signed Rank) test for paired samples. Records from one contact of each multicontact intracerebral electrode implanted in a particular anatomical structure were included in the analysis selecting the one with the largest amplitude of ERP. The intracerebral findings of steep voltage gradients uniquely proved the focal origin of the waveform (Fig. 1).

The statistical analysis of recorded potentials was performed by comparing the presence with the absence of the post-movement ERP in correct reactions to target stimuli. The frequency differences between brain structures were examined using the binomial test. Involvement of these structures after correct performance in nontarget task variant was compared using Fischer's exact test. To test the statistical significance of differences in latency of ERPs the *t*-test for independent samples was used. In all tests the threshold for statistical significance was set to $P < 0.05$.

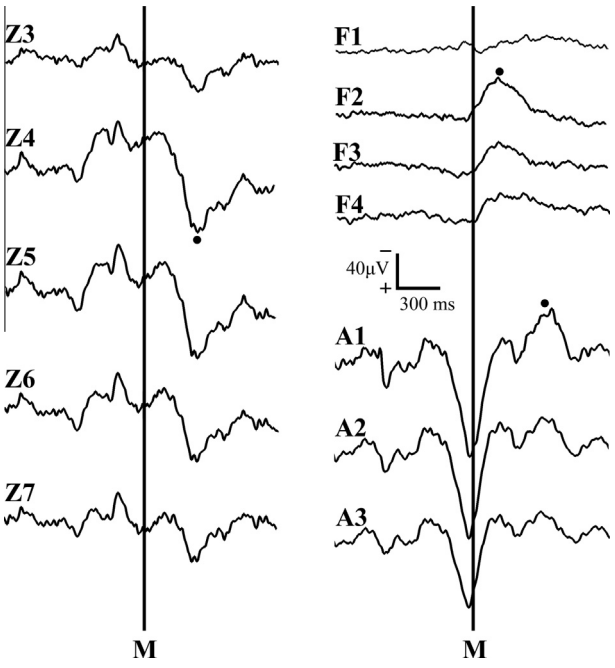

Fig. 1. The response-triggered averaged ERPs for correct target trials recorded from neighboring electrode contacts exhibiting steep voltage gradients in post-movement period in right hippocampus in patient No. 2 (Z3–Z7), right anterior midcingulate cortex in patient No. 9 (F1–F4), and right amygdala in patient No. 4 (A1–A3). Note the voltage variations across contacts with maximal peak amplitude marked with black point (M = movement).

3. Results

The performance of the subjects during the task was very accurate; only three subjects (Nos. 5, 9, and 12) committed higher number of errors (Table 2). The mean reaction time in correct responses ranged from 457 ± 34 ms to 644 ± 78 ms (median 522 ms). In the response-triggered averages (RTAs) of correct reactions to target stimulus a prominent event-related potential in the post-performance period (see Fig. 2) was detected in all subjects in 131 sites, i.e. 64% of sites investigated, with no significant difference in localization within well examined frontal and temporal lobes. These sites were distributed among multiple brain structures (see Table 3); involving mesiotemporal structures, lateral temporal, prefrontal, cingulate, frontal and parietal cortices, and basal ganglia. The occurrence of the post-movement ERP in enough examined (at least 5 investigated sites) brain structures ranged from 43% to 100% (mean 67 ± 15%) of investigated sites. The binomial test revealed no significant differences in frequency of findings of post-movement ERP among these eleven structures. The only exception were basal ganglia where finding of post-movement ERP was significantly more frequent than in several, mostly temporal, sufficiently examined brain structures (Table 4), and anterior midcingulate cortex with borderline significantly higher post-movement ERP occurrence than in inferior temporal gyrus ($P = 0.0485$). When we restrict our results to observation of generators, however, the list of presumably consistently involved structures is shorter (see Table 5). The data in Fig. 1 demonstrate three regions exhibiting signs of a local generator. Most frequently (53% of sites investigated) the post-movement ERP was generated in amygdala. Quite frequently, with occurrence not significantly different from amygdala, generators were also observed in

Table 2
Number of artefact-free trials.

Patient	Target		Nontarget	
	Correct hit	Incorrect rejection	Correct rejection	False alarm
1	49	0	281	3
2	45	0	236	1
3	62	6	266	1
4	41	5	221	1
5	65	1	332	18
6	57	3	328	2
7	49	0	261	0
8	52	0	247	0
9	77	25	343	14
10	46	3	267	0
11	59	1	243	2
12	80	14	282	13
13	53	3	201	0
14	61	1	316	4
15	63	1	242	0
16	66	3	305	3
17	57	0	222	0
18	57	2	270	1

Correct hit = motor response to target stimulus; Incorrect rejection = movement omission after target stimulus; Correct rejection = refraining from movement in nontarget task variant; False alarm = erroneous motor response in nontarget task variant.

hippocampus, parahippocampal and middle temporal gyri, anterior midcingulate cortex, medial frontal, orbitofrontal, and dorsolateral prefrontal gyri. On the other hand, despite sufficient examination, the post-movement ERP was generated significantly less frequently than in amygdala in superior and inferior temporal gyri and no generator was found in basal ganglia. The comparison between brain lobes revealed no significant differences in post-movement ERP generator occurrence. In post-movement ERPs generated in temporal and frontal lobes the mean peak latency relative to motor response was 288.9 ± 171.6 ms and 248.7 ± 176.4 ms, respectively. This difference, however, did not reach the statistical significance.

The observed post-movement ERPs were mostly (80% sites) monophasic, less frequently complex biphasic (14% sites) with waveforms of opposite polarities, only occasionally (6% sites) two separate waves of the same polarity were detected. In total, 157 ERP waves were observed in the post-movement period in the target task variant. Their peak latency ranged from 14 to 726 ms (mean 295 ± 184 ms, median 258 ms) with approximately half of them (48%) appearing between 100 and 300 ms after movement onset. Less than one third of post-movement ERPs (27%) were observed in sites where no ERP component was detected during the stimulus–response interval. This was revealed by the analysis of stimulus-triggered averages (STAs) of correct reactions to target stimulus. In these cases the post-movement ERP was observed as a very late isolated ERP with a latency exceeding the mean reaction time (e.g. in contact X′8 in patient 3, see Fig. 3A); in the majority of brain sites, however, this potential appeared only after components elicited within the stimulus–response interval (e.g. in contact D′2 in patient 14, see Fig. 3A).

Approximately in 50% of the sites where post-movement ERP was detected in the RTA of correct reactions to target stimuli, no very late ERP was observed in the STA of correctly ignored nontarget stimuli (e.g. examples in Fig. 3A). In the other half of the sites, however, one (61 sites) or two (6 sites) potential waves with a latency exceeding the subject's mean reaction time were observed (e.g. examples in Fig. 3B–D). The latency of all these 73 nontarget post-performance ERP waves ranged from 500 to 1162 ms (mean 757 ± 168 ms) after the stimulus onset. A comparison of the first nontarget with the first target post-performance ERP wave in the STAs revealed that the latency of the nontarget ERP was shorter

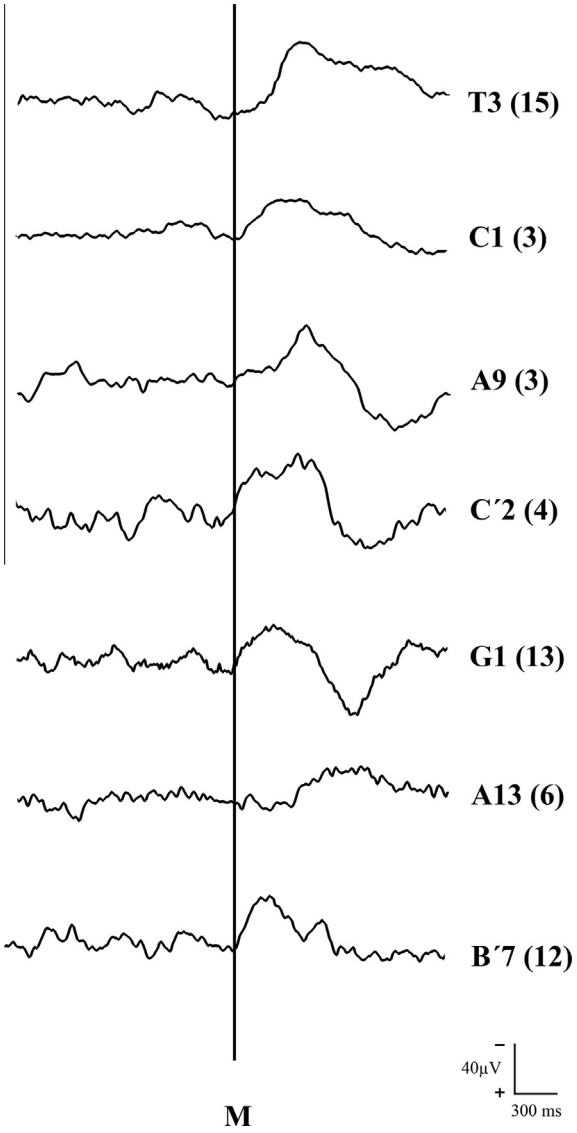

Fig. 2. Response-triggered averaged post-movement ERPs for correct target trials (M = movement). Contact (subject), anatomical structure: T3 (15), right superior temporal gyrus; C1 (3), right fusiform gyrus; A9 (3), right middle temporal gyrus; C′2 (4), left parahippocampal gyrus; G1 (13), right anterior cingulate cortex; A13 (6), right middle temporal gyrus; B′7 (12), left superior temporal gyrus.

by 174 ± 118 ms in 34 sites (Fig. 3B) and longer by 166 ± 88 ms in 26 sites (Fig. 3C). In the remaining 7 sites the latencies were almost identical differing by less than 20 ms (Fig. 3D).

In most anatomical structures examined both task-variant nonspecific and target specific post-movement ERPs were observed (Table 3). In the former case an ERP was detected both in target post-movement and nontarget post-performance periods while in the latter case the potential was found only in target task variant. Mean latency of task-variant nonspecific (244.6 ± 142.1 ms) and target specific (251.3 ± 164.5 ms) post-movement ERPs differed only slightly and the differences did not reach a statistical significance. Both the task-variant nonspecific and target specific post-movement ERPs were observed in all but two patients. Only the former or latter types of ERP were observed in subject No. 9 and 11, respectively. The occurrence frequency of task-variant nonspecific and target specific ERP types did not significantly differ between frontal and temporal lobes neither among individual brain structures investigated. The only exception were the basal

Table 3
Distribution of ERPs across brain regions in correct reactions to target stimulus.

Anatomical structure	Post-movement ERP[a]	Sites examined/subjects	Target specific ERP/subjects[b]	Task-variant nonspecific ERP/subjects[c]
Anterior midcingulate cortex	9(82)	11/7	3/3	6/5
Pregenual anterior cingulate cortex	2(67)	3/2	2/1	0/0
Rostro- and dorsomedial prefrontal cortices	6(75)	8/5	2/2	4/2
Orbitofrontal cortex	8(57)	14/8	6/5	2/2
Dorsolateral prefrontal cortex	15(71)	21/10	8/5	7/3
Supplementary motor area	0(0)	2/1	0/0	0/0
Premotor cortex	1(100)	1/1	1/1	0/0
Primary motor cortex	3(75)	4/2	0/0	3/2
Basal ganglia	7(100)	7/5	7/5	0/0
Amygdala	10(67)	15/12	5/5	5/5
Hippocampus	17(65)	26/15	10/8	7/6
Parahippocampal gyrus	6(55)	11/8	1/1	5/3
Fusiform gyrus	4(100)	4/5	1/1	3/3
Superior temporal gyrus	13(57)	23/11	5/5	8/4
Middle temporal gyrus	19(61)	31/15	9/6	10/7
Inferior temporal gyrus	6(43)	14/8	1/1	5/4
Lingual gyrus	1(50)	2/1	0/0	1/1
Posterior cingulate cortex	0(0)	2/1	0/0	0/0
Inferior parietal lobule	2(67)	3/1	1/1	1/1
Somatosensory cortex	2(67)	3/2	1/1	1/1
Frontal lobe	51(72)	71/14	29/13	22/7
Temporal lobe	76(60)	126/17	32/14	44/14
Parietal lobe	4(50)	8/2	2/1	2/1
Total	131(64)	205/18	63/17	68/17

[a] Number of sites (% of sites examined) with positive observations of post-movement ERP in response-triggered averages of correct reactions to target stimulus.
[b] Number of sites/subjects with observed target post-movement ERP but with negative finding in post-performance period of nontarget task variant.
[c] Number of sites where ERP was observed both in target post-movement and nontarget post-performance periods.

Table 4
Comparison between basal ganglia and other brain structures (*P*-values).

Anatomical structure	Binominal test	Fisher's exact test
Anterior midcingulate cortex	0.2341	0.0114*
Rostro- and dorsomedial prefrontal cortices	0.1553	0.0210*
Orbitofrontal cortex	0.0400*	0.4667
Dorsolateral prefrontal cortex	0.1073	0.0513
Amygdala	0.0843	0.0441*
Hippocampus	0.0663	0.0648
Parahippocampal gyrus	0.0037*	0.0047*
Superior temporal gyrus	0.0341*	0.0147*
Middle temporal gyrus	0.0454*	0.0227*
Inferior temporal gyrus	0.0112*	0.0047*

* $P < 0.05$, significant difference in numbers of post-movement ERPs (binominal test) or in frequency of target specific and task-variant nonspecific ERPs (Fisher's exact test) between basal ganglia and other sufficiently examined brain structures.

ganglia in which only target specific ERPs were found (e.g. Fig. 3A) and thus this result was significantly different from several brain structures (see the last column in Table 4). No significant differences in ERP type distribution, however, were found among generating brain structures (see Table 5).

Errors, i.e. erroneously omitted (incorrect rejection) or erroneously performed (false alarm) motor responses, were committed quite frequently in three of the patients (Nos. 5, 9, and 12; see Table 2). The subject's mean reaction time was longer for false alarms (RTf) compared to correct hits (RTc) by 56 ms, 23 ms, and 138 ms in patients Nos. 5, 9, and 12, respectively. In patient No. 5 no ERP was found after false alarms in sites where post-movement ERP was recorded in correct reactions to target stimuli. In both remaining patients, however, a very late ERP with latency exceeding both RTc and RTf was observed in stimulus-triggered

Table 5
Distribution of generators across brain regions in correct reactions to target stimulus.

Anatomical structure	Generators[a]	Target specific ERP[b]	Task-variant nonspecific ERP[c]
Anterior midcingulate cortex	5(42)	1	4
Pregenual anterior cingulate cortex	1(50)	1	0
Rostro- and dorsomedial prefrontal cortices	2(25)	1	1
Orbito-frontal cortex	3(21)	2	1
Dorsolateral prefrontal cortex	8(38)	3	5
Supplementary motor area	0(0)	0	0
Premotor cortex	1(100)	1	0
Primary motor cortex	1(25)	0	1
Basal ganglia	0(0)	0	0
Amygdala	8(53)	4	4
Hippocampus	8(31)	4	4
Parahippocampal gyrus	5(45)	1	4
Fusiform gyrus	1(25)	1	0
Superior temporal gyrus	5(22)	3	2
Middle temporal gyrus	10(32)	5	5
Inferior temporal gyrus	2(14)	0	2
Lingual gyrus	0(0)	0	0
Posterior cingulate cortex	0(0)	0	0
Inferior parietal lobule	0(0)	0	0
Somatosensory cortex	1(33)	0	1
Frontal lobe	21	9	12
Temporal lobe	39	18	21
Parietal lobe	1	0	1
Total	61	27	34

Sufficiently examined brain structures (at least 5 sites investigated) with high occurrence of generators are in bold format.
[a] Number of sites (% of sites examined) displaying signs of proximity to structure generating the target post-movement ERP either.
[b] With negative finding in nontarget post-performance period,
[c] With ERP observed in nontarget post-performance period.

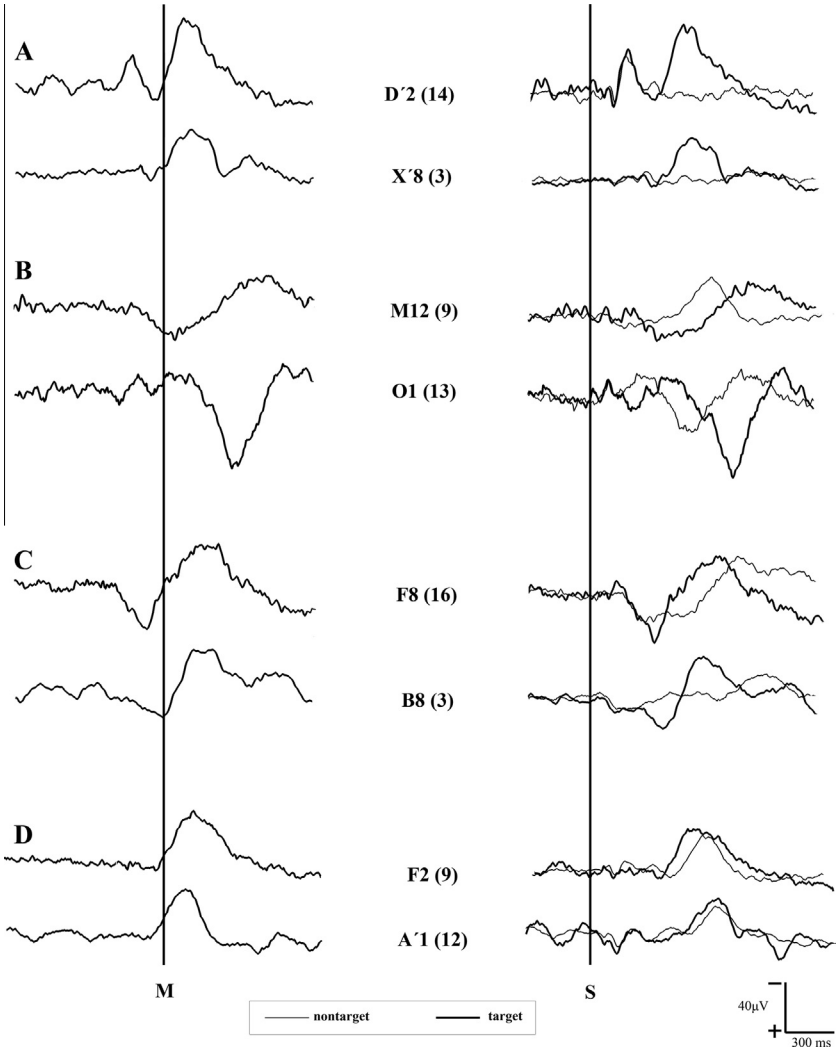

Fig. 3. Post-performance ERP: (A) prominent in target but absent in nontarget trials; (B) with shorter latency in nontarget than in target trials; (C) with longer latency in nontarget than in target trials; (D) with almost identical latency in target and nontarget trials. On the left side, response-triggered (M = movement) averaged ERPs for correct target trials; on the right side, stimulus-triggered (S = stimulus) averaged ERPs for correct target (thick lines) and correct nontarget (thin lines) trials in the same contact. Note that post-performance target ERP is either preceded by clear-cut earlier components or not, e.g. in D′2(14) or X′8(3) in section A, respectively. Contact (subject), anatomical structure: D′2(14), left superior temporal gyrus; X′8(3), left putamen; M12(9), right primary motor cortex; O1(13), right orbitofrontal cortex; F8(16), right dorsolateral prefrontal cortex; B8(3), right middle temporal gyrus; F2(9), right anterior cingulate cortex; A′1(12), left superior temporal gyrus.

averages of erroneous responses. Tables 6 and 7 show distribution of these ERPs across brain regions. Latencies of stimulus-triggered averaged ERPs detected after correct and incorrect performances are displayed in Table 8. In patient No. 9 the latency after incorrect rejection or false alarm was either longer, with a delay of up to 469 ms (Fig. 4A), or almost identical, with a difference no greater than 20 ms (Fig. 4B), compared to the latency observed after correct hit or correct rejection, respectively. In patient No. 12 the latencies after correct and incorrect performances differed less than by 20 ms (Fig. 4B).

In an attempt to associate the post-movement ERP observed in the target variant of a visual oddball task with underlying mental processes the following competent characteristics of post-performance ERPs were identified: (1) a waveform prominent to target but absent to nontarget stimuli; (2) a waveform prominent both to target and nontarget stimuli; (3) a longer latency of ERP when motor response was erroneously omitted in reaction to target stimulus; (4) a longer latency of ERP when motor response was erroneously performed in reaction to nontarget stimulus.

4. Discussion

This study examined the electrophysiological indicators of post-performance brain activity. By using depth EEG recording during a visual oddball task we have demonstrated that: (1) post-movement ERPs in correct target trials were observed in multiple cortical structures; (2) ERPs recorded after correct performance were either specific for the target task variant or were observed in both variants of the visual oddball task; (3) in several brain sites both after correct and incorrect performances clear-cut ERP components were observed; (4) in brain sites sensitive to error commission the latency of the post-performance ERP was longer in incorrect compared to correct performance.

4.1. Generators of post-performance ERPs in correctly performed target trials are distributed in multiple brain regions

Two recent source localization studies on performance monitoring focused on identifying ICA components reflecting the post-performance ERPs for correct and incorrect responses (Hoffmann

Table 6
Distribution of ERPs across brain regions in correct reactions to target and erroneous reactions to nontarget stimuli.

Anatomical structure	Post-movement ERPs[a]	Sites examined/ subjects	False alarm/ subjects[b]
Anterior cingulate cortex	3	4/2	0/0
Orbitofrontal cortex	0	2/1	–
Dorsolateral prefrontal cortex	3	3/1	3/1
Supplementary motor area	0	2/1	–
Premotor cortex	1	1/1	0/0
Primary motor cortex	2	3/1	2/1
Amygdala	1	1/1	0/0
Hippocampus	1	2/1	0/0
Parahippocampal gyrus	3	3/1	0/0
Superior temporal gyrus	7	9/2	1/1
Middle temporal gyrus	2	3/2	1/1
Inferior temporal gyrus	0	4/1	–
Lingual gyrus	1	2/1	0/0
Somatosensory cortex	0	1/1	–
Frontal lobe	9	15/2	5/1
Temporal lobe	15	24/2	2/1
Parietal lobe	0	1/1	–
Total	24	40/3	7/2

[a] Number of sites with positive observations of post-movement ERP in response-triggered averages of correct reactions to target stimulus.
[b] Number of sites/subjects with positive observation of ERP elicited both after correct reactions to target and erroneous reactions to nontarget stimuli.

Table 7
Distribution of ERPs across brain regions in correct and erroneous reactions to target stimuli.

Anatomical structure	Post-movement ERPs[a]	Sites examined/ subjects	Incorrect rejection/ subjects[b]
Anterior cingulate cortex	2	3/1	2/1
Dorsolateral prefrontal cortex	3	3/1	3/1
Supplementary motor area	0	2/1	–
Primary motor cortex	2	3/1	2/1
Hippocampus	1	2/1	0/0
Superior temporal gyrus	6	8/1	2/1
Middle temporal gyrus	2	2/1	1/1
Lingual gyrus	1	2/1	0/0
Somatosensory cortex	0	1/1	–
Frontal lobe	7	11/1	7/1
Temporal lobe	10	14/1	3/1
Parietal lobe	0	1/1	–
Total	17	26/2	10/2

[a] Number of sites with positive observations of post-movement ERP in response-triggered averages of correct reactions to target stimulus.
[b] Number of sites/subjects with positive observation of ERP elicited both after correct and erroneous reactions to target stimuli.

Table 8
Latency (ms) of post-performance ERP measured from stimulus onset in two patients.

Anatomical structure/contact	Target			Nontarget		
	Correct hit	Incorrect rejection	Delay	Correct rejection	False alarm	Delay
Patient No 9 (RTc = 474 ms, RTf = 497 ms)						
aMCC/*G1*	617	1086	469	703	–	–
aMCC/F2	601	1062	461	693	–	–
DLPFC/G14	804	1062	258	742	875	133
DLPFC/F14	688	1070	382	742	968	226
DLPFC/F9	601	1055	454	727	723	−4
PMC/M12	1046	1125	79	734	1117	383
PMC/M′11	950	966	16	727	1009	282
Patient No 12 (RTc = 594 ms, RTf = 732 ms)						
STG/T4	1018	999	−19	–	–	–
STG/T′5	836	827	−9	774	789	15
MTG/D′12	824	827	3	768	762	−6

Correct hit = motor response to target stimulus; Incorrect rejection = movement omission after target stimulus; Correct rejection = refraining from movement in nontarget task variant; False alarm = erroneous motor response in nontarget task variant; Delay = the ERP latency difference between incorrect and correct performances; RTc = mean reaction time for correct hit condition; RTf = mean reaction time for false alarm condition; aMCC = anterior midcingulate cortex; DLPFC = dorsolateral prefrontal cortex; PMC = primary motor cortex; STG = superior temporal gyrus; MTG = middle temporal gyrus; ′ = left side; regions generating post-movement ERP are written in *italics* format.

and Falkenstein, 2010; Roger et al., 2010). Both studies, however, aimed to identify ICA components related to the ERN/Ne, and the component selection was based on error trials (Roger et al., 2010) or on differences between error and correct trials (Hoffmann and Falkenstein, 2010). To the best of our knowledge, no source localization or even intracerebral study primarily aimed at identifying sources of post-performance ERPs for correct responses. Similarly, several EEG/fMRI studies identified correlations between the hemodynamic response in the rostral cingulate zone and scalp recorded ERN (for review see Ullsperger et al., 2014) but none of them was focused on correct response-related activity. From this point of view, the current study provides unique intracerebral data suggesting the existence of multiple sources of ERPs elicited after correct performance. We observed clear-cut correct response-related activation in many different brain regions (Table 3). Since converging observations seem to indicate that the field created by neurons more than one centimeter away from the recording site account for only a negligible portion of the intracranially recorded EEG signal (Lachaux et al., 2003), these ERPs might be considered to emerge from the brain structure in which they were observed. Most convincingly, our results suggest engagement of mesiotemporal structures, anterior midcingulate, prefrontal and lateral temporal cortices, in which steep voltage gradient across neighbouring contacts was observed as an unequivocal evidence of a potential generation. Thus, besides ACC whose involvement was previously documented by source localization study (Roger et al., 2010) in correct response-related negativity generation; our results suggest recruitment of several other brain structures following correct motor responses. Our results support the view, that the post-movement brain processes in correct responses of visual oddball task are realized through activation of large-scale neuronal networks. In the present study most brain structures that form these networks were active in discrete sites while in other sites no evoked electrophysiological activity was recorded. No difference in occurrence frequency was found among involved brain structures except for basal ganglia where post-movement ERP was found in all examined sites. Due to the fact that recording sites were selected according to diagnostic concerns, and most regions were not explored, the possibility to use this result for quantitative comparison of activation of different brain structures is limited. Thus, it still remains in question as to whether some structures generate the post-movement ERP in a greater portion of its volume than other structures.

4.2. Parallel systems of correct performance processing

In all well examined structures except for basal ganglia, i.e. in mesiotemporal structures, anterior midcingulate, prefrontal and lateral temporal cortices, we observed task-variant nonspecific post-movement ERP type. This suggests that the studied post-movement ERP might reflect some processes that are supposed to take place in both variants of the task, such as stimulus evaluation

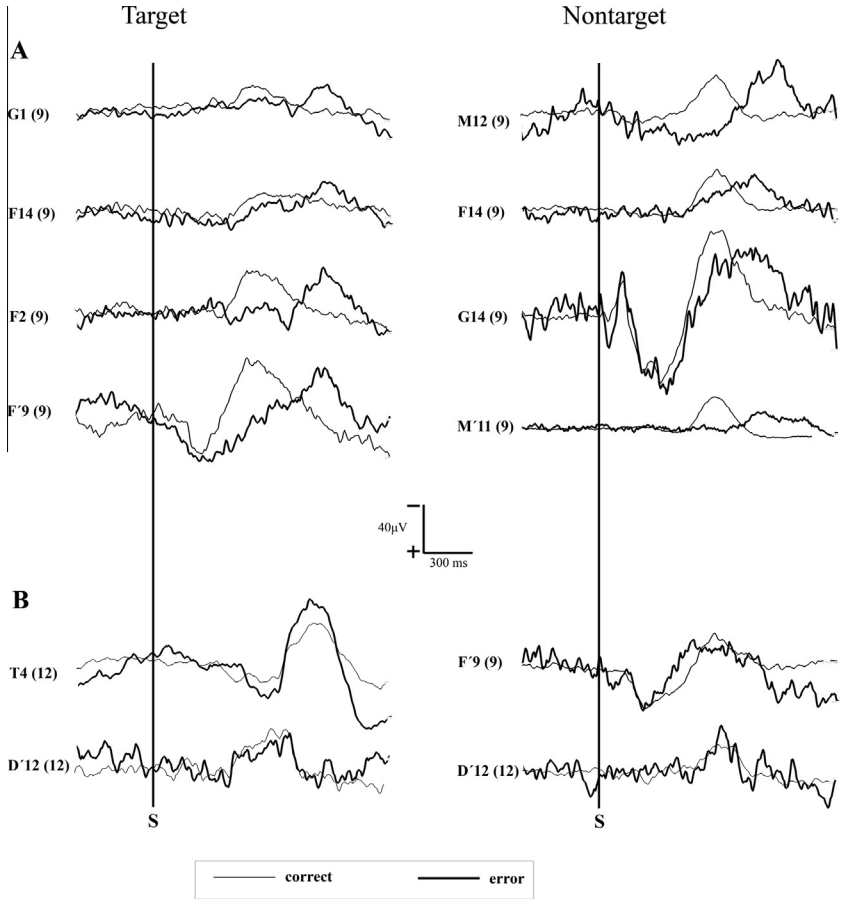

Fig. 4. Stimulus-triggered (S = stimulus) averaged ERPs for correct (thin line) and incorrect (thick line) trials. (A) Longer latency of post-performance ERP when motor response was erroneously omitted in reaction to target stimulus (left section) or erroneously performed in reaction to nontarget stimulus (right section). (B) Almost identical latency of post-performance ERP after correct and incorrect performance of target (left section) or nontarget (right section) task variant. Contact (subject), anatomical structure: G1(9), right anterior cingulate cortex; F14(9), right dorsolateral prefrontal cortex; F2(9), right anterior cingulate cortex; F′9(9), left dorsolateral prefrontal cortex; T4(12), right superior temporal gyrus; D′12(12), left middle temporal gyrus; M12(9), right primary motor cortex; G14(9), right dorsolateral prefrontal cortex; M′11(9), left primary motor cortex.

processing, attentional processes or performance monitoring. This interpretation is in line for instance with our previous study where we provided evidence that hippocampal ERPs, either preceding or following correct motor responses, could represent some stimulus evaluation processing (Roman et al., 2013) or with widely accepted role of frontal lobe for monitoring the effect of actions on the external environment (Stuss and Benson, 1986; Stuss, 2011). Such a monitoring process could just follow each correctly performed task, irrespective of whether the required behavior was movement execution and mental counting or movement inhibition and ignoring of the stimuli.

The finding of target specific ERPs in all well examined brain structures of frontal and temporal lobes may indicate their involvement in counting related brain processes. Previous observations of counting related brain activity in the lateral temporal neocortex and ACC (Brázdil et al., 2003) support this view. Since higher demands on memory functions in the target task variant with mental counting are expected, participation of these structures in memory processes might be suggested. Nevertheless, this type of ERP could as well only reflect more attention or higher cognitive load related to arithmetic without any specific relation to maintenance of episodic information in short term memory. Some processes underlying target specific activity may also be related to previous movement execution. In case of basal ganglia, in which we have found only target specific ERPs, this interpretation would perfectly fit with their prominent role in motor functions. According to another interpretation, this ERP could simply reflect passive re-entrance of somatosensory signals or a post-performance resetting of brain circuits without any elaboration or use of the performance features.

Both the task variant nonspecific and target specific ERP types were consistently generated in the same structures (see Table 5). The mere existence of these two types of post-movement ERP favors the view that after correct movement execution parallel processing in at least two distinct systems takes place sharing at least partially the same anatomical substrate. Parallel activation of two different systems, i.e. performance-monitoring and movement-monitoring, was also identified to be responsible for Ne/ERN generation (Yordanova et al., 2004).

4.3. Common nodes of correct and incorrect behavior processing

In the present study we demonstrated that there are brain sites in which both correct and incorrect performances may elicit a prominent potential in the post-performance period. We found sites in which ERPs were recorded both after correct motor response and its erroneous omission in the target variant of the task. In some of these sites we even recorded ERPs both after correct refraining from movement and erroneous movement execution in the nontarget task variant. Our findings suggest that

cortical networks engaged in the generation of correct and incorrect performance-related potentials could have some common nodes. The fact that in several sites post-performance ERPs were observed both in correct hit and false alarm conditions seems to further support findings of recent studies using independent component analysis, which strongly suggest that Ne/ERN and Nc/CRN stem from largely overlapping generators (Roger et al., 2010; Wessel et al., 2012). The demonstration of post-performance ERPs in false alarms stands in line with a large body of literature on error processing and supports the existence of an already known and well-described Ne/ERN and Pe complex (Wessel, 2012). On the other hand, our finding of post-performance ERPs after erroneous movement omission is rather unique. Our finding suggests that some kind of error processing might take place also after incorrect movement inhibition. Actually, it should not be surprising that also after this type of error some monitoring process might take place that compares the predicted behavior with the actual one.

Another interesting finding of the present study is that there are sites in anterior midcingulate, dorsolateral prefrontal and primary motor cortices, where the error commission has an influence on the latency of post-performance ERP with higher values for incorrect performance (Fig. 4A). Erroneous refraining from movement in the target variant of the task revealed a longer latency of the ERP than the correct hit condition. Similarly, erroneously performed movement in the nontarget variant of the task revealed a longer latency than correct inhibition of motor response. If the observed latency differences indicated that the preceding processes are prolonged or higher in number in case of error commission, then both correct and incorrect post-performance ERP components might represent some final evaluation processes related to finished action. Our findings of latency differences are analogous with those reported in a recent intracerebral study (Pourtois et al., 2010). In a go/nogo task the authors demonstrated local field potentials in the amygdala with evident temporal unfolding. A monophasic ERP around motor execution for correct hits was delayed by ~300 ms for false alarms, even though the actual reaction times were almost identical in these two conditions. Our findings not only confirmed typical involvement of ACC in action monitoring and cognitive control (Ridderinkhof et al., 2004) but also suggested recruitment of the dorsolateral prefrontal cortex and the primary motor cortex in error detection mechanisms.

A striking result of our current study was activation of the primary motor cortex in nonmotor task conditions, both after erroneous and correct movement inhibition (Table 8 and Fig. 4). This result extends the recent hypothesis of rostral premotor-subcortical networks serving as a gateway between the cognitive and motor networks (Hanakawa, 2011) suggesting that the primary motor cortex might be also involved in processes not directly associated with motor action.

5. Conclusions

Although the present study was limited by non-systematic examination of the brain due to strictly diagnostic purposes of electrode implantation, the results clearly suggest that besides the anterior cingulate cortex, also the mesiotemporal structures, and lateral temporal and prefrontal cortices are activated following correct responses. The spatiotemporal characteristics, task-variant specificity, and sensitivity to errors demonstrated that the observed post-movement activity might code various pieces of information needed for cognitive control, movement- and performance monitoring, and evaluation processes. It appears, however, that a one-to-one matching of post-movement ERP type and type of information is beyond the limitations of our study.

Acknowledgments

Supported by the project "CEITEC – Central European Institute of Technology" (CZ.1.05/1.1.00/02.0068) from the European Regional Development Fund.

The funder had no role in study design, data collection and analysis, decision to publish, or preparation of the manuscript.

Conflict of interest: None of the authors have potential conflicts of interest to be disclosed.

References

Bates AT, Liddle PF, Kiehl KA, Ngan ETC. State dependent changes in error monitoring in schizophrenia. J Psychiatr Res 2004;38:347–56.
Bonnefond A, Doignon-Camus N, Hoeft A, Dufour A. Impact of motivation on cognitive control in the context of vigilance lowering: an ERP study. Brain Cogn 2011;77:464–71.
Brázdil M, Roman R, Falkenstein M, Daniel P, Jurák P, Rektor I. Error processing – evidence from intracerebral ERP recordings. Exp Brain Res 2002;146:460–6.
Brázdil M, Roman R, Daniel P, Rektor I. Intracerebral somatosensory event-related potentials: Effect of response type (button pressing versus mental counting) on P3-like potentials within the human brain. Clin Neurophysiol 2003;114:1489–96.
Brázdil M, Roman R, Daniel P, Rektor I. Intracerebral error-related negativity in a simple Go/NoGo task. J Psychophysiol 2005;19:244–55.
Carter CS, Braver TS, Barch DM, Botvinick MM, Noll D, Cohen JD. Anterior cingulate cortex, error detection, and the online monitoring of performance. Science 1998;280:747–9.
Coles MGH, Scheffers MK, Holroyd CB. Why is there an ERN/Ne on correct trials? Response representations, stimulus-related components, and the theory of error-processing. Biol Psychol 2001;56:173–89.
Falkenstein M, Hohnsbein J, Hoormann J, Blanke L. Effects of errors in choice reaction tasks on the ERP under focused and divided attention. In: Brunia CHM, Gaillard AWK, Kok A, editors. Psychophysiological brain research. Tilburg: Tilburg University Press; 1990. p. 192–5.
Falkenstein M, Hohnsbein J, Hoormann J, Blanke L. Effects of crossmodal divided attention on late ERP components. II. Error processing in choice reaction tasks. Electroencephalogr Clin Neurophysiol 1991;78:447–55.
Falkenstein M, Koshlykova NA, Kiroj VN, Hoormann J, Hohnsbein J. Late ERP components in visual and auditory Go/Nogo tasks. Electroencephalogr Clin Neurophysiol 1995;96:36–43.
Falkenstein M, Hoormann J, Christ S, Hohnsbein J. ERP components on reaction errors and their functional significance: a tutorial. Biol Psychol 2000;51:87–107.
Ford JM. Schizophrenia: the broken P300 and beyond. Psychophysiology 1999;36:667–82.
Gehring WJ, Knight RT. Prefrontal-cingulate interactions in action monitoring. Nat Neurosci 2000;3:516–20.
Gehring WJ, Goss B, Coles MGH, Meyer DE, Donchin E. A neural system for error detection and compensation. Psychol Sci 1993;4:385–90.
Hajcak G, Moser JS, Yeung N, Simons RF. On the ERN and the significance of errors. Psychophysiology 2005;42:151–60.
Halgren E, Marinkovic K, Chauvel P. Generators of the late cognitive potentials in auditory and visual oddball tasks. Electroencephalogr Clin Neurophysiol 1998;106:156–64.
Hanakawa T. Rostral premotor cortex as a gateway between motor and cognitive networks. Neurosci Res 2011;70:144–54.
Herrmann MJ, Römmler J, Ehlis AC, Heidrich A, Fallgatter AJ. Source localization (LORETA) of the error-related-negativity (ERN/Ne) and positivity (Pe). Cogn Brain Res 2004;20:294–9.
Hoffmann S, Falkenstein M. Independent component analysis of erroneous and correct responses suggests online response control. Hum Brain Mapp 2010;31:1305–15.
Lachaux JP, Rudrauf D, Kahane P. Intracranial EEG and human brain mapping. J Physiol Paris 2003;97:613–28.
Mathalon DH, Fedor M, Faustman WO, Gray M, Askari N, Ford JM. Response-monitoring dysfunction in schizophrenia: an event-related brain potential study. J Abnorm Psychol 2002;111:22–41.
Meckler C, Allain S, Carbonnell L, Hasbroucq T, Burle B, Vidal F. Executive control and response expectancy: a laplacian ERP study. Psychophysiology 2011;48:303–11.
Pourtois G, Vocat R, N'Diaye K, Spinelli L, Seeck M, Vuilleumier P. Errors recruit both cognitive and emotional monitoring systems: simultaneous intracranial recordings in the dorsal anterior cingulate gyrus and amygdala combined with fMRI. Neuropsychologia 2010;48:1144–59.
Rektor I. Cortical activation in self-paced versus externally cued movements: a hypothesis. Parkinsonism Relat D 2000;6:181–4.
Rektor I, Louvel J, Lamarche M. Intracerebral recording of potentials accompanying simple limb movements: a SEEG study in epileptic patients. Electroencephalogr Clin Neurophysiol 1998;107:277–86.

Rektor I, Brázdil M, Nestrašil I, Bareš M, Daniel P. Modifications of cognitive and motor tasks affect the occurrence of event-related potentials in the human cortex. Eur J Neurosci 2007;26:1371–80.

Ridderinkhof KR, Ullsperger M, Crone EA, Nieuwenhuis S. The role of the medial frontal cortex in cognitive control. Science 2004;306:443–7. http://dx.doi.org/10.1126/science.1100301.

Roger C, Bénar CG, Vidal F, Hasbroucq T, Burle B. Rostral cingulate zone and correct response monitoring: ICA and source localization evidences for the unicity of correct- and error-negativities. NeuroImage 2010;51:391–403.

Roman R, Brázdil M, Chládek J, Rektor I, Jurák P, Světlák M, Damborská A, Shaw DJ, Kukleta M. Hippocampal negative event-related potential recorded in humans during a simple sensorimotor task occurs independently of motor execution. Hippocampus 2013;23:1337–44.

Scheffers MK, Coles MGH. Performance monitoring in a confusing world: Error-related brain activity, judgments of response accuracy, and types of errors. J Exp Psychol Human 2000;26:141–51.

Stuss DT. Functions of the frontal lobes: relation to executive functions. J Int Neuropsychol Soc 2011;17:759–65.

Stuss DT, Benson DF. Personality and emotions. The frontal lobes. New York: Raven Press; 1986. pp 121–138.

Talairach J, Szikla G, Tournoux P, Prosalentis A, Bordas-Ferrer M, Covello J. Atlas d'anatomie stéréotaxique du télencéphale. Paris: Masson; 1967.

Taylor SF, Stern ER, Gehring WJ. Neural systems for error monitoring: recent findings and theoretical perspectives. Neuroscientist 2007;13:160–72.

Ullsperger M, Danielmeier C, Jocham G. Neurophysiology of performance monitoring and adaptive behavior. Physiol Rev 2014;94:35–79.

Vidal F, Hasbroucq T, Grapperon J, Bonnet M. Is the 'error negativity' specific to errors? Biol Psychol 2000;51:109–28.

Vidal F, Burle B, Bonnet M, Grapperon J, Hasbroucq T. Error negativity on correct trials: a reexamination of available data. Biol Psychol 2003;64:265–82.

Wessel JR. Error awareness and the error-related negativity: evaluating the first decade of evidence. Front Hum Neurosci 2012;6:88.

Wessel JR, Danielmeier C, Morton JB, Ullsperger M. Surprise and error: common neuronal architecture for the processing of errors and novelty. J Neurosci 2012;32:7528–37.

Yordanova J, Falkenstein M, Hohnsbein J, Kolev V. Parallel systems of error processing in the brain. NeuroImage 2004;22:590–602.

Annex 7

Kukleta, M., **Damborská, A.**, Turak, B., & Louvel, J. (2017). Evoked potentials in final epoch of self-initiated hand movement: A study in patients with depth electrodes. *International Journal of Psychophysiology*, 117, 119-125.

International Journal of Psychophysiology 117 (2017) 119–125

Contents lists available at ScienceDirect

International Journal of Psychophysiology

journal homepage: www.elsevier.com/locate/ijpsycho

Evoked potentials in final epoch of self-initiated hand movement: A study in patients with depth electrodes

Miloslav Kukleta[a], Alena Damborská[a,b,*], Baris Turak[c], Jacques Louvel[c]

[a] Central European Institute of Technology (CEITEC), Masaryk University, Brno, Czech Republic
[b] Department of Psychiatry, Medical Faculty, Masaryk University, Brno, Czech Republic
[c] Service de Neurochirurgie Stéréotaxique, Hôpital Ste Anne, Paris, France

ARTICLE INFO

Keywords:
Intracerebral EEG recordings
Evoked potentials
Voluntary movement
Motor intention
Motor action

ABSTRACT

Comparison between the intended and performed motor action can be expected to occur in the final epoch of a voluntary movement. In search for electrophysiological correlates of this mental process the purpose of the current study was to identify intracerebral sites activated in final epoch of self-paced voluntary movement. Intracerebral EEG was recorded from 235 brain regions of 42 epileptic patients who performed self-paced voluntary movement task. Evoked potentials starting at 0 to 243 ms after the peak of averaged, rectified electromyogram were identified in 21 regions of 13 subjects. The mean amplitude value of these late movement potentials (LMP) was 56.4 ± 27.5 μV. LMPs were observed in remote regions of mesiotemporal structures, cingulate, frontal, temporal, parietal, and occipital cortices. Closely before the LMP onset, a significant increase of phase synchronization was observed in all EEG record pairs in 9 of 10 examined subjects; $p < 0.001$, Mann-Whitney *U* test. In conclusion, mesiotemporal structures, cingulate, frontal, temporal, parietal, and occipital cortices seem to represent integral functionally linked parts of network activated in final epoch of self-paced voluntary movement. Activation of this large-scale neuronal network was suggested to reflect a comparison process between the intended and actually performed motor action. Our results contribute to better understanding of neural mechanisms underlying goal-directed behavior crucial for creation of agentive experience.

1. Introduction

The current study was focused on investigation of the functional neuronal network engaged in the final epoch of a voluntary movement. It is generally accepted that the control of intentional motor action involves brain operations that select, plan, and execute the movement. The beginning of an action comprises motives for it, evaluation of advantages and disadvantages, and creation of its internal representation, i.e. a series of operations which are mostly connected loosely with the execution and may occur in a time preceding largely the action itself. The execution comprises a sequence of specific motor operations, which results in the formation of commands to muscles. The final operation provides confirmation that there is a match between the predicted and the actual state. The extent of brain areas engaged in this complex function can be illustrated by measurements of regional cerebral blood flow during the generation and execution of self-initiated finger movements (Jahanshahi et al., 1995; Jenkins et al., 2000). In these experiments, a significant increase of metabolic demands suggesting an increased neuronal activity was observed in fifteen distinct brain areas localized in both associative and primary cortices and other brain structures. The increased activity was found in the contralateral primary sensorimotor cortex, the thalamus and rostral cingulate motor areas, the ipsilateral dorsolateral prefrontal cortex, the supplementary motor area, the premotor cortex, the insula, and parietal area 40 on both sides. The results obtained in other neuroimaging studies were in general agreement with the idea that the control of a voluntary movement results from the interactions of numerous brain loci operating in a large-scale network (Ball et al., 1999; Deiber et al., 1991, 1996, 1999; MacKinnon et al., 1996; Toro et al., 1994).

The electrophysiological manifestations of self-initiated movements enabled investigation of temporospatial relations of components of evoked potentials and allowed to propose their association with the underlying brain operations. The majority of relevant studies used scalp-recorded evoked responses (Libet et al., 1982; Kukleta et al., 1996; Shibasaki and Hallett, 2006; Shibasaki, 2012); several studies were done using evoked responses from intracerebral electrodes (Paradiso et al., 2004; Rektor et al., 1994, 1998, 2001; Rektor, 2000, 2003). Research of scalp EEG responses brought results allowing to

* Corresponding author at: CEITEC - Central European Institute of Technology, Brain and Mind Research Program, Masaryk University, Kamenice 753/5, CZ-625 00 Brno, Czech Republic.
E-mail address: adambor@med.muni.cz (A. Damborská).

http://dx.doi.org/10.1016/j.ijpsycho.2017.05.004
Received 20 February 2017; Received in revised form 15 April 2017; Accepted 8 May 2017
Available online 10 May 2017
0167-8760/ © 2017 Elsevier B.V. All rights reserved.

propose the sequence of neuronal activations in the period preceding closely the movement onset. The available findings suggest that the activation begins in the presupplementary motor area with no site specificity and in the supplementary motor area proper according to the somatotopic organization, and shortly thereafter in the lateral premotor cortex bilaterally with relative clear somatotopy. The next step is the activation in the contralateral primary motor cortex and lateral premotor cortex with precise somatotopy. A recent finding from intracerebral EEG recording suggested that the estimation of time elapsed from the previous movement could play a role in the formation of the initial part of the electrophysiological response and, consequently, in the decision to start the next movement (Kukleta et al., 2012, 2015). The specific baseline shifts supposedly associated with this decision were found in the brain sites engaged, according to neuroimaging studies, in volitional processes. The evaluation of phase synchronization of neuronal activity in pairs of such sites revealed transient increases associated with these shifts. This finding suggested a temporarily restricted functional linkage of the sites in which the baseline shifts were found.

The current study focuses on cortical potentials elicited in the final epoch of a voluntary movement. The aim of the study was to analyze their temporospatial characteristics and associations with closing mental operations of self-initiated hand movements. The potentials were at first analyzed from the point of view of their morphology. In the case of hand movements, such approach applied in previous studies identified several consequential peaks immediately following movement onset (N + 50, P + 90, N + 160, P + 300) with characteristic scalp distributions (Bötzel et al., 1997; Hallett, 1991; Kornhuber and Deecke, 1965; Kristeva-Feige et al., 1996; Shibasaki et al., 1980a, 1980b). The component N + 50 was demonstrated to be prominent over the frontal region, the component P + 90 was predominant over the parietal region, being larger over the contralateral hemisphere. The component N + 160 was found to be localized in the contralateral parietal area, thus forming a positive-negative complex with P + 90 (Shibasaki and Hallett, 2006). The onset of passive movement is also followed with evoked potentials (Seiss et al., 2002). These electrophysiological brain activations are largely dependent on muscle spindle input, co-vary with the duration of the movement, and have their source in the precentral cortex. The evident difference between the intended and the passive movement potentials in their distribution and localization of generators suggested their different functional connotation. There is a largely accepted view postulating that an intended motor action proceeds from an internal model of the action which anticipates and controls its course. The last step in this control is believed to be the confirmation that there is a match between the predicted and the actual state. The leading hypothesis of the current study was that electrophysiological correlates of the comparison of the internal model of the action with its actual result can be detected in the final epoch of the self-initiated movement task. To prevent any contamination by electrophysiological manifestations of the preceding operations such as planning and movement initiation we searched for brain sites which generated exclusively late potentials, i.e. following the peak of electromyogram (EMG) activity of investigated hand. We hoped that this feature would enable us to bring some new information related to the organization of the underlying functional network.

2. Methods and materials

2.1. Subjects

Intracerebral EEG records obtained from 13 epilepsy surgery candidates (9 men, 4 women, aged 18–38 years) during repeated self-paced hand movements were analyzed in the study. The patients were selected from a data pool of 42 patients who were implanted unilaterally with chronic depth multilead electrodes for diagnostic reasons (Hôpital Sainte-Anne, Service de Neurochirurgie; INSERM, U 97). List of explored brain structures with number of regions investigated is given in Table 1. The criterion for the selection of the patient into the further analyzed dataset was the finding of at least one evoked EEG response consisting of one and only waveform immediately following the peak of averaged, rectified EMG. All the patients were informed that the experiment had no relevance to their clinical examination, and all agreed to participate. Clinical findings other than epilepsy were normal. None of the patients had any major cognitive deficit. All of them were under standard antiepileptic therapy which was determined by clinical considerations. During the period of diagnostic examination by intracerebral EEG recording, the doses of medicaments were reduced to allow seizures to develop spontaneously or in response to a focal repetitive electrical stimulation. A summary of the characteristics of the patients participating in the study and of the evoked responses investigated is given in Table 2.

Table 1
Isolated late movement potentials found in anatomical structures explored.

Anatomical structure	Number of investigations	Number of positive findings	Percentage of positive findings
Gyrus frontalis superior	1	1	100
Gyrus frontalis medius	18	4	22
Gyrus frontalis medialis	17	1	6
Gyrus frontalis inferior	32	1	3
Gyrus precentralis	14	2	14
Lobulus paracentralis	3	0	0
Gyrus cinguli anterior	24	2	8
Gyrus cinguli	23	0	0
Gyrus cinguli posterior	4	1	25
Gyrus parahippocampalis	15	1	7
Hippocampus	2	0	0
Amygdala	3	0	0
Gyrus postcentralis	8	2	25
Lobulus parietalis inferior	14	1	7
Gyrus supramarginalis	4	0	0
Precuneus	8	1	13
Gyrus temporalis superior	13	0	0
Gyrus temporalis medius	9	1	11
Gyrus temporalis inferior	4	0	0
Gyrus fusiformis	1	0	0
Gyrus occipitalis medius	1	0	0
Gyrus occipitalis inferior	1	0	0
Gyrus lingualis	6	1	17
Cuneus	4	2	50
Claustrum	1	0	0
Nucleus caudatus	2	0	0
Putamen	1	0	0
Thalamus	2	0	0
Total	235	21	9

2.2. Recording procedures

Microdeep (DIXI Besançon) intracerebral stainless steel or platinum electrodes were orthogonally implanted according to the clinical and EEG characteristics of the disease. In one patient, an additional diagonal electrode was inserted into the mesial parietal cortex. Each 0.8 mm diameter electrode had a series of 2 mm long recording contacts (5–15), with a distance of 1.5 mm between the contacts. The positions of the electrodes were indicated in relation to the axes defined by the Talairach system using the ‘x, y, z’ format where ‘x’ is lateral, millimeters to midline, positive right hemisphere, ‘y’ is anteroposterior, millimeters to the AC (anterior commissure) line, positive anterior, and ‘z’ is vertical, millimeters to the AC/PC (posterior commissure) line, positive upward (Talairach et al., 1967). All electrode positions were verified radiologically in anteroposterior and lateral views. Surface electromyograms were recorded with a pair of cup electrodes placed on the skin over the flexor digitorum communis. During the experiment, the patients laid comfortably on the bed and watched a point on the

Table 2
Characteristics of patients, recording sites, and evoked responses. The EMG-LMP latency difference was measured between the peak of the averaged, rectified EMG and the onset of the LMP.

Patient (sex)	Age	Location of recording contact	Talairach coordinates			Type of the response	LMP amplitude and polarity		EMG – LMP difference
			x	y	z				
B (m)	34	R lobulus parietalis inferior (LPI)	47	− 32	30	LMP	68.3 μV	Negative	60 msec
		R gyrus frontalis inferior (GFI)	57	23	14	LMP + late BP	24.5 μV	Positive	0 msec
D (m)	18	L gyrus cinguli posterior (GCP)	− 14	− 39	27	LMP	50.2 μV	Negative	0 msec
		L cuneus 1, area 30 (CU)	− 23	− 70	10	LMP	105.9 μV	Negative	0 msec
		L cuneus 2, area18 (CU)	− 9	− 78	29	LMP	102.8 μV	Negative	0 msec
		L precuneus (PRC)	− 20	− 59	50	LMP + late BP	40.0 μV	Negative	0 msec
La (f)	28	L gyrus frontalis inferior (GFI)	− 59	9	22	LMP	60.3 μV	Negative	67 msec
		L gyrus precentralis, area 4 (GPRC)	− 22	− 23	55	LMP	87.5 μV	Negative	23 msec
		L gyrus postcentralis, area 3 (GPOC)	− 19	− 30	53	LMP	77.1 μV	Negative	50 msec
		L gyrus supramarginalis (GSM)	− 48	− 38	32	LMP + EBS	19.2 μV	Negative	75 msec
Lb (m)	20	L gyrus frontalis medius 1 (GFMu)	− 30	9	49	LMP	17.6 μV	Positive	106 msec
		L gyrus frontalis medius 2 (GFMu)	− 37	13	41	LMP + EBS	55.4 μV	Positive	100 msec
M (m)	38	R gyrus cinguli anterior, area 32 (GCA)	16	39	13	LMP	13.8 μV	Positive	135 msec
		R gyrus frontalis superior (GFS)	10	33	45	LMP	30.9 μV	Positive	135 msec
N (f)	24	L precuneus (PRC)	− 8	− 54	38	LMP	62.9 μV	Negative	183 msec
		L gyrus lingualis (GL)	− 14	− 55	5	LMP	125.4 μV	Positive	183 msec
O (m)	27	L gyrus parahippocampi (GH)	− 21	− 5	− 12	LMP	41.1 μV	Negative	71 msec
		L gyrus temporalis medius (GTM)	− 61	− 5	− 3	LMP + EBS	80.9 μV	Positive	75 msec
Pa (m)	29	L gyrus frontalis medius 1 (GFMu)	− 30	− 7	58	LMP	66.1 μV	Negative	0 msec
		L gyrus cinguli anterior, area 32 (GCA)	− 11	25	24	LMP	71.3 μV	Positive	0 msec
		L gyrus frontalis medius 2, (GFMu)	− 40	46	28	LMP	57.3 μV	Positive	0 msec
Pb (m)	30	L gyrus postcentralis (GPOC)	− 50	− 17	25	LMP	55.7 μV	Negative	70 msec
Sa (f)	30	R gyrus precentralis, area 6 (GPRC)	58	− 4	31	LMP	38.5 μV	Negative	82 msec
Sb (f)	22	R gyrus frontalis medius (GFMu)	15	− 13	58	LMP	40.6 μV	Negative	112 msec
		R gyrus precentralis, area 44 (GPRC)	58	8	11	LMP + EBS	59.9 μV	Negative	137 msec
V (m)	35	R gyrus temporalis medius (GTM)	58	− 70	13	LMP	57.9 μV	Negative	0 msec
		R lobulus parietalis inferior, area 40 (LPI)	55	− 55	40	LMP + EBS	30.7 μV	Negative	0 msec
W (m)	19	R gyrus frontalis medialis, area 6 (GFM)	8	− 22	50	LMP	36.2 μV	Negative	243 msec

Note: EBS – early baseline shift; late BP – late component of the Bereitschaftspotential; LMP – late movement potential; EMG – electromyogram; R – right; L – left; m – male; f – female.

video screen positioned approximately 150 cm in front of their eyes.

2.3. Protocols

In the experimental session each patient was instructed to repeatedly clench a joystick at will ("self-pacing") and was asked to maintain intervals of at least 10 s between the successive movements, without counting or otherwise estimating the time. The hand opposite to the hemisphere explored was used. Approximately 35 movements were performed in the session.

2.4. Data acquisition and processing

The intracerebral EEG activity was recorded and averaged using a 32-channel amplifier device (Nihon-Kohden, bandpass between 0.016 and 100 Hz) fed into a Cambridge electronic device (CED) 1401 + interface with SIGNAL 2 software. Each data frame had a duration of 5 s (4 s before movement onset and 1 s after it) and was digitized at a frequency of 100 Hz. All the records were taken with binaural reference. The data processing was performed offline using artifact-free EEG records only (the selection was based on visual inspection of the records by two experienced persons). Lesional and epileptic zone sites were not included in the study. None of the explored sites showed any epileptiform activity. It was possible, however, that some sites got involved in a more widespread generalized episode out of the recording period. All available trials were used for the averaging so that the number of the trials averaged slightly varied across the patients (minimal number was 28). The averaging was triggered by the EMG onset. The records with the EEG-evoked responses starting at or after the peak of averaged, rectified EMG were analyzed in the current study (see Fig. 1); we use the designation late movement potentials (LMP) for them. The selection of one record from usually quasi-identical responses obtained from the neighboring contacts of an electrode was based on evaluation of the LMP amplitude selecting the one with the highest value. In order to disclose a possible functional relationship between the brain sites which yielded the LMPs, we arranged, where possible, the records collected into pairs and, in each of them, we assessed the level of phase synchronization of EEG oscillations. We used the technique of running correlation in this assessment, consisting in the successive computation of the correlation coefficient in a window which moves by steps along the time axis (see Fig. 1, B). The empirically chosen length of the sliding window was 400 msec, the length of the steps was 20 msec (160 *r*-values in the early pre-movement period from − 4.0 to − 0.8 s). The mean *r*-value in this pre-movement period was then used as a baseline synchronization of the record pair. The determination of LMP onsets in pairs was based on visual assessment (consensus of two experienced persons was required). The Boltzmann sigmoid function was used for the determination of early baseline shifts in several cases in which the recording site exhibited, besides the LMP, also a pre-movement evoked activity (see Fig. 1, A). It was calculated in the pre-movement period from − 4.0 to − 0.8 s using the procedure from the analysis menu of Signal 5 program. The arbitrary choice of the − 0.8 s time point as the proximate limit of the analyzed pre-movement period was determined by the intention to exclude every possible contamination by processes associated with the late Bereitschaftspotential component. Statistical evaluation of the results was performed by the routines included in the program package Statistica'99 (StatSoft Inc., Tulsa, U.S.A.).

3. Results

The total number of explored brain regions in 42 subjects was 235; the intracranial record with one and only late movement potential was observed sometimes repeatedly in different anatomical brain structures (Table 1). In 13 subjects (i.e. 31% of subjects examined) we observed 21 records of one and only LMP (i.e. 9% of explored brain regions), which

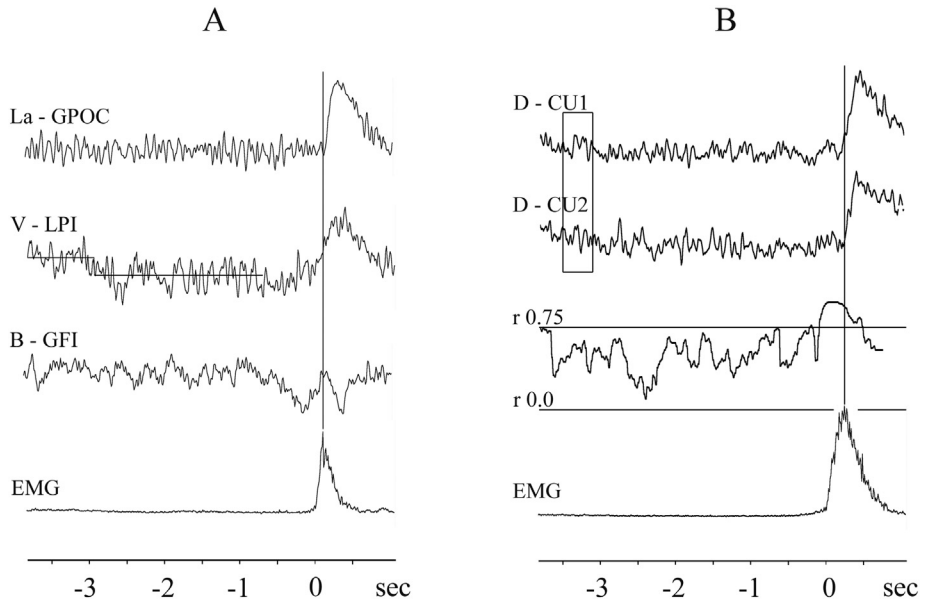

Fig. 1. (A) Three variants of EEG records with late movement potential (LMP) analyzed – a record with one and only LMP of patient La from the gyrus postcentralis, a record with LMP and the early baseline shift of patient V from the lobulus parietalis inferior, and a record with LMP and late BP of patient B from the gyrus frontalis inferior. Horizontal lines on the record of patient V represent the Boltzmann sigmoid function. (B) A selected pair of records with one and only LMP of patient D from two sites of the cuneus. The third curve was created from correlation coefficients calculated successively every 20 msec from upper records in time windows of 400 msec (the window presented yielded the *r*-value at − 3.5 s). Horizontal lines on the correlation curve represent 0.0 and 0.75 *r*-values. Vertical lines represent the peak of averaged, rectified EMG.

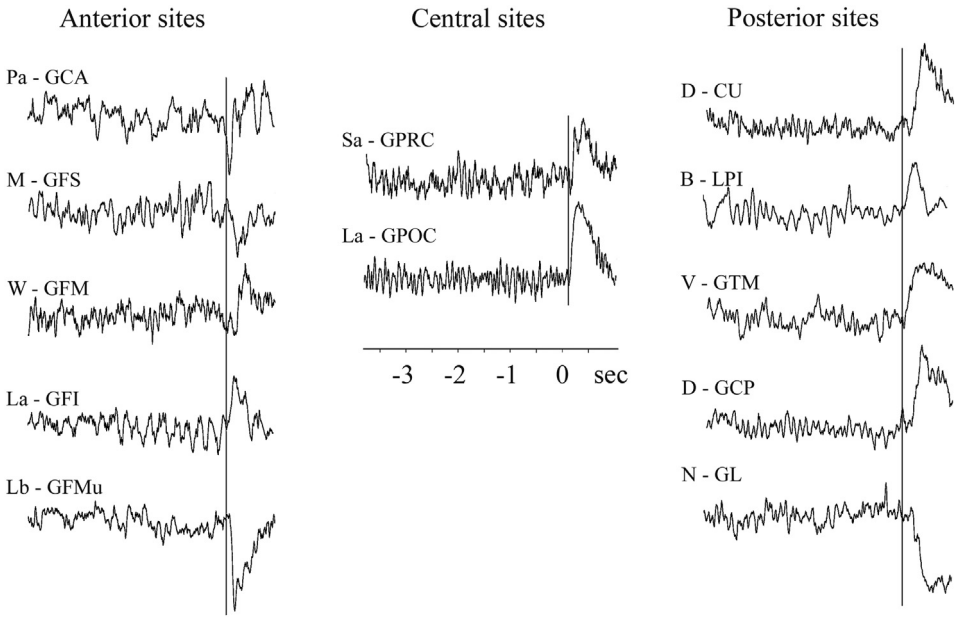

Fig. 2. Twelve selected EEG records with one and only late movement potential. The labels on each record designate the patient and anatomical structure from which the record was derived (for abbreviations meaning see Table 2).Vertical lines represent the peak of averaged, rectified EMG.

together with 7 other cases with the additional early (5 cases) or late pre-movement waveforms (2 cases), were analyzed in the study. Fig. 2 presents twelve records with the isolated LMP, which were selected to illustrate their forms in the anterior, central, and posterior brain regions. Table 2 summarizes data concerning location of brain sites from which the LMPs were derived, the amplitude values of these potentials, their polarity and temporal relation to the EMG record. The solitary LMPs were recorded in the following anatomically delineated brain structures: the left gyrus cinguli anterior, the right gyrus cinguli anterior, the right gyrus frontalis superior, the right gyrus frontalis medialis, the right and left gyrus frontalis medius, the left gyrus frontalis inferior, the right gyrus precentralis, the left gyrus postcentralis, the right lobulus parietalis inferior, the left gyrus cinguli posterior, the left precuneus, the left cuneus, the left gyrus lingualis, the left gyrus parahippocampalis, the right gyrus temporalis medius. The polarity of LMP, assessed in all the records analyzed, was either negative (19 cases) or positive (9 cases). In one and the same person with more than one region generating LMP its polarity change was either identical (in 6 subjects) or opposite (in 4 subjects). The mean amplitude value of LMP was 56.4 ± 27.5 μV. Approximately one third of these evoked potentials started at the peak of the averaged rectified EMG, the other two thirds started later (23–243 msec after the EMG peak).

Ten subjects who yielded more than one LMP allowed us to create 22 record pairs and to analyze temporospatial relations of these potentials in individual brains. The mean distance between the loci,

Table 3
Characteristics of record pairs – location of recording contacts from which the late movement potentials (LPMs) were obtained, distance between them, differences of LMP onsets, LMPs polarity, and selected data from correlation curves. The value of indicator "Onset of high *r*-values" shows the interval on the correlation curve between the time point at which the *r*-value becomes > 0.75 (− 0.75) and the onset of the LMP.

Patient	Pair no.	Paired records from	Contact distance	Differences of LMP onsets	Polarity of LMP in the pair	Mean *r*-value (from − 4.0 to − 0.8 s)	Onset of high *r*-values
Pairs with LMP and LMP							
D	1	L GCP vs L CU 1	42 mm	0 msec	Identical	0.05 ± 0.26	347 msec
	2	L GCP vs L CU 2	40 mm	0 msec	Identical	0.07 ± 0.31	319 msec
	3	L CU 1 vs L CU 2	26 mm	0 msec	Identical	0.51 ± 0.13	340 msec
La	4	L GPRC vs L GFI	54 mm	30 msec	Identical	0.07 ± 0.17	280 msec
	5	L GPOC vs L GFI	59 mm	0 msec	Identical	0.07 ± 0.15	291 msec
	6	L GPRC vs L GPOC	9 mm	20 msec	Identical	0.20 ± 0.19	347 msec
M	7	R GCA vs R GFS	33 mm	50 msec	Identical	0.32 ± 0.29	322 msec
N	8	L PRC vs L GL	35 mm	0 msec	Opposite	− 0.07 ± 0.30	242 msec
Pa	9	L GCA vs L GFMu 1	56 mm	120 msec	Opposite	0.54 ± 0.16	–
	10	L GFMu 1 vs L GFMu 2	64 mm	120 msec	Opposite	0.50 ± 0.16	–
	11	L GCA vs L GFMu 2	34 mm	0 msec	Identical	0.95 ± 0.05	–
Pairs with LMP and LMP + EBS							
La	12	L GFI vs L GSM	48 mm	0 msec	Identical	0.10 ± 0.24	252 msec
	13	L GPRC vs L GSM	32 mm	50 msec	Identical	− 0.22 ± 0.24	291 msec
	14	L GPOC vs L GSM	25 mm	30 msec	Identical	0.40 ± 0.23	291 msec
Lb	15	L GFMu 1 vs L GFMu 2	17 mm	0 msec	Identical	0.33 ± 0.28	350 msec
O	16	L GH vs L GTM	44 mm	0 msec	Opposite	0.25 ± 0.35	328 msec
Sb	17	R GFMu vs R GPRC	62 mm	0 msec	Identical	0.52 ± 0.16	265 msec
V	18	R GTM vs R LPI	31 mm	0 msec	Identical	0.01 ± 0.24	297 msec
Pairs with LMP and LMP + late BP							
B	19	R LPI vs R GFI	48 mm	0 msec	Opposite	0.05 ± 0.32	270 msec
D	20	L GCP vs L PRC	32 mm	0 msec	Identical	0.53 ± 0.18	627 msec
	21	L CU 1 vs L PRC	41 mm	90 msec	Identical	0.22 ± 0.22	335 msec
	22	L CU 2 vs L PRC	28 mm	36 msec	Identical	0.19 ± 0.27	352 msec

Note: abbreviations are explained in Table 1.

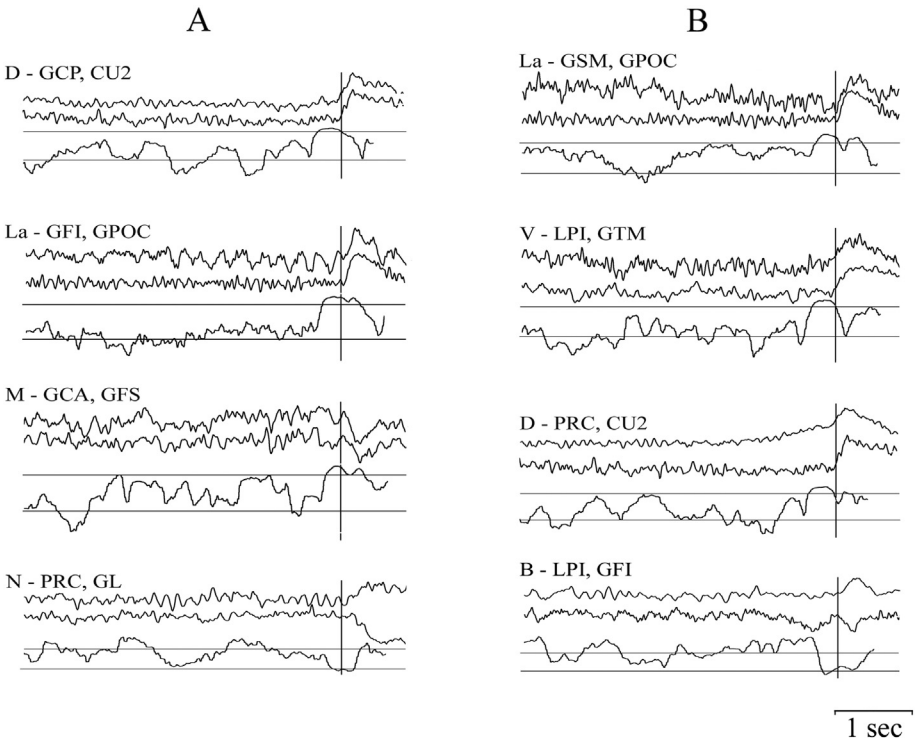

Fig. 3. Eight selected pairs of records. Each segment consists of two EEG records and the correlation curve calculated from these records. The labels on each record pair designate the patient and anatomical structures from which the records were derived (for abbreviations meaning see Table 2). Vertical lines represent the peak of averaged, rectified EMG. Horizontal lines on the correlation curves represent 0.0 and 0.75 *r*-values (− 0.75 in patients N and B).

which generated LMP, was 39.6 ± 14.4 mm. The onset of LMP was identical in 13 pairs and different in 9 pairs. There was no correlation between inter-loci distances and onset differences (Spearman r 0.13; $p > 0.05$). With the exception of data from subject Pa, the records paired exhibited, closely before the LMP onset, a significant increase of phase synchronization (see data presented in Table 3). The mean r-value calculated from the correlation curves was 0.17 ± 0.23 in the "baseline" period from 4.0 to 0.8 s prior to the movement and 0.84 ± 0.13 (− 0.72 ± 0.04 in three negative correlations) in the 300 msec period preceding closely the LMP onset (difference significant in all cases; $p < 0.001$, Mann-Whitney U test). Fig. 3 illustrates this finding on eight selected record pairs.

4. Discussion

The results of the current study demonstrated that, during self-paced movements, some brain loci generated an evoked potential consisting of one and only waveform occurring in the final epoch of the task. These loci were distributed across brain areas from prefrontal to occipital poles of both hemispheres. The significant decrease of electric signals with distance in brain tissue (inversely proportional to the square of the distance separating the source from the recording contact) and physical characteristics of the depth macroelectrodes used enable us to suppose that the LMPs collected represent an integrated activity of neurons spatially distributed within approximately a centimeter radius (Lachaux et al., 2003; Menon et al., 1996). This estimate allowed to consider the loci, from which the LMPs were obtained, as nodes of a specific neuronal network engaged in the final periods of the task with self-initiated hand movement. These loci represented 9% from all the brain regions explored and made only minor portion of investigations within a few sufficiently explored anatomical structures. The fact that there were both positive and negative findings for the same kind of exploration might be explained by rather restricted size and/or low number of these loci within a given anatomical structure. Thus, our results could be considered as a rather scarce incidence. On the other hand, the spatial distribution of these loci was impressive – they were found in frontal, parietal, temporal, and occipital lobes, mostly in both mesial and lateral localizations. Their onset times differed both inter- and intraindividually, which seems to point out a heterogeneous character of the putative underlying processes. The finding of LPM-locked increases of r-values on the correlation curves in pairs pointed out another particular feature of this network, namely its transitory character. The synchronization of neuronal activity in remote brain loci, which was followed by a generation of quasi-identical evoked potentials, reflected very probably a temporarily restricted functional linkage of thus far independent loci. Alternative interpretation of this synchronization could be the existence of a third common driver that modulates both sites of an investigated pair.

Another question to be discussed is the polarity of the LMPs recorded. In approximately two thirds of the cases the potential change was electrically negative; in the remaining cases it was positive. In general, the polarity of the potential changes in intracerebral recordings depends on the structure and orientation of generators with regard to the reference electrodes. At present, we have no detailed answer to the question why the potential change recorded in comparable brain structures against the same references was positive in some subjects and negative in others.

Another result deserving interest is the finding of brain loci which generated the LMPs together with pre-movement evoked components (early baseline shifts in five cases, late Bereitschaftspotential in two cases). The fact that one site generates one and only EEG component and another site can generate two distinct components or even a complete evoked response (Damborská et al., 2012; Kukleta et al., 2012) suggests differences of integrative potency of sites forming the large-scale functional network engaged in the motor task.

As far as the relation of intracerebral and scalp late movement potentials is concerned, our data were not representative enough for such analysis.

The key question of the study concerns the relation between the LMPs and the cognitive operation occurring at the final period of the motor task. The basic information about the organization of operations in an intention–action functional coupling has emerged from psychophysiological experiments and from analyses of relevant neurological and psychiatric case studies (the most important of them are presented in the monograph of Jeannerod, 2009). According to their results, the operations underlying an intentional action could be dissociated into three relatively independent functional wholes. The first one is responsible for the creation of internal representation of the future action, the second one is responsible for its execution, and the third one assures the comparison of the predicted and the actual result of the action. The first whole is by definition a pre-movement event, therefore can be associated with electrophysiological cortical activity preceding the EMG activation onset. Similarly the second whole could be associated with electrophysiological correlates elicited in the brain during EMG activation. Although one could suppose the third whole to be a pure post hoc event, i.e. occurring only after movement has been finished, results of recent studies suggest otherwise. Movements unfold through time, and it is thought that a comparison between the motor intention and sensory feedback occurs continuously throughout the duration of a movement (Shadmehr et al., 2010). In present study LMP were identified as a result of search for electrophysiological correlates of comparison between the intended and performed motor action. This mental operation was namely in the logic of understanding the problem expected to occur in the final epoch of a voluntary movement. In attempt to interpret the functional significance of LMP one should, however, take into consideration also other possible cognitive operation occurring in this period. First, performance monitoring related to error detection could be considered. Nevertheless, contrary to our recent studies on post-movement potentials (Damborská et al., 2016; Kukleta et al., 2016) the simplicity of the task used in our current study practically excluded the implication of error detection. Second, existence of late stimulus-related operations (Damborská et al., 2012) could be considered, however, not in current self-initiated movement task. Third, attentional processes could be taken into account (Posner and Dehaene, 1994). Rektor et al. (1998) studied the potential occurring during voluntary limb movement, i.e. the movement-accompanying slow potential (MASP). Although with no ambition to study MASP in detail authors interpreted this evidently heterogenic phenomenon to be associated with "readiness to subsequent act" and "attention to action". In present study in order to more specifically address involvement of brain structures in process of comparison between the intended and performed action, we focused on sites generating one and only evoked potentials beginning at or after the peak of EMG activation. By using such temporal limitation, not only did we exclude every possible contamination by preceding processes associated with the late Bereitschaftspotential component, but we also eliminated contamination with electrophysiological correlates of through the whole task sustained attention. Brain sites involved in attentional processes could be rather supposed to be active for longer periods of a task (Damborská et al., 2012) than just suddenly switch on in the final epoch of the task. Fourth, various aspects of motor execution are supposed to occur during movement. The location of LMPs not sooner than at the peak of EMG activation and their persistence after cessation of EMG activity, however, favors the view that it could reflect only such aspects of executive functions that are associated with late processes, such as the comparison procedure and not for instance with initiation of the movement performance. Taken together the results of the current study imply that the brain sites generating the LMP could be involved in the late online movement and the post-movement comparisons of intended and actually performed actions. This evidence contributes to better understanding the physiology of movement in man which is a prerequisite for studies on pathophysiology of various movement

disorders.

The findings of present study go even beyond the questions concerning purely movement issues. The monitoring whether the intended goal of a behavior was really reached is the basic prerequisite of any successful interaction with the outer world. There is a well-founded opinion that the evolution brought still another use of this information. A series of experimental psychophysiological studies in healthy human subjects and selected patients demonstrated the crucial role of the accordance between an intention and its result for the creation of agentive experience (Farrer et al., 2003, 2004; Fourneret and Jeannerod, 1998; Fourneret et al., 2002; Franck et al., 2001; Knoblich and Kircher, 2004; Nielsen et al., 1965; Slachevsky et al., 2001; Ullsperger et al., 2014). The experience that we are in control of our own actions is in turn one of the key components of human consciousness. Seen from this point of view, the attempted description of large-scale network generating the LMPs could be considered as a step towards structural delineation of this significant component of human consciousness.

Acknowledgements

None of the authors have potential conflicts of interest to be disclosed.

The study was supported by the project “CEITEC – Central European Institute of Technology” (CZ.1.05/1.1.00/02.0068) from the European Regional Development Fund. The data were collected in Paris (Hôpital Ste. Anne, Service de Neurochirurgie; INSERM, U 97) by a currently no more existent research group headed by Michel Lamarche, with substantial contribution of Pierre Buser and Ivan Rektor.

References

Ball, T., Schreiber, A., Feige, B., Wagner, M., Lücking, C.H., Kristeva-Feige, R., 1999. The role of higher-order motor areas in voluntary movement as revealed by high-resolution EEG and fMRI. NeuroImage 10, 682–694.

Bötzel, K., Ecker, C., Schulze, S., 1997. Topography and dipole analysis of reafferent electrical brain activity following the Bereitschaftspotential. Exp. Brain Res. 114, 352–361.

Damborská, A., Brázdil, M., Rektor, I., Janoušová, E., Chládek, J., Kukleta, M., 2012. Late divergence of target and nontarget ERPs in a visual oddball task. Physiol. Res. 61, 307–318.

Damborská, A., Roman, R., Brázdil, M., Rektor, I., Kukleta, M., 2016. Post-movement processing in visual oddball task - evidence from intracerebral recording. Clin. Neurophysiol. 127, 1297–1306.

Deiber, M.P., Passingham, R.E., Colebatch, J.G., Friston, K.J., Nixon, P.D., Frackowiak, R.S.J., 1991. Cortical areas and the selection of movement: a study with positron emission tomography. Exp. Brain Res. 84, 393–402.

Deiber, M.P., Ibanez, V., Sadato, N., Hallett, M., 1996. Cerebral structures participating in motor preparation in humans: a positron emission tomography study. J. Neurophysiol. 75, 233–247.

Deiber, M.P., Honda, M., Ibañez, V., Sadato, N., Hallett, M., 1999. Mesial motor areas in self-initiated versus externally triggered movements examined with fMRI: effect of movement type and rate. J. Neurophysiol. 81, 3065–3077.

Farrer, C., Franck, N., Georgieff, N., Frith, C.D., Decety, J., Jeannerod, M., 2003. Modulating the experience of agency: a positron emission tomography study. NeuroImage 18, 324–333.

Farrer, C., Franck, N., Frith, C.D., Decety, J., Georgieff, N., D'Amato, T., et al., 2004. Neural correlates of action attribution in schizophrenia. Psychiatry Res. Neuroimaging 131, 31–44.

Fourneret, P., Jeannerod, M., 1998. Limited conscious monitoring of motor performance in normal subjects. Neuropsychologia 36, 1133–1140.

Fourneret, P., Paillard, J., Lamarre, Y., Cole, J., Jeannerod, M., 2002. Lack of conscious recognition of one's own actions in a haptically deafferented patient. Neuroreport 13, 541–547.

Franck, N., Farrer, C., Georgieff, N., Marie-Cardine, M., Daléry, J., D'Amato, T., et al., 2001. Defective recognition of one's own actions in patients with schizophrenia. Am. J. Psychiatry 158, 454–459.

Hallett, M., 1991. Topography of scalp-recorded motor potentials in human finger movements. J. Clin. Neurophysiol. 8, 331–341.

Jahanshahi, M., Jenkins, I.H., Brown, R.G., Marsden, C.D., Passingham, R.E., Brooks, D.J., 1995. Self-initiated versus externally triggered movements: I. An investigation using measurement of regional cerebral blood flow with PET and movement-related potentials in normal and Parkinson's disease subjects. Brain 118, 913–933.

Jeannerod, M., 2009. Le cerveau volontaire. Éditions Odile Jacob, Paris.

Jenkins, I.H., Jahanshahi, M., Jueptner, M., Passingham, R.E., Brooks, D.J., 2000. Self-initiated versus externally triggered movements. II. The effect of movement predictability on regional cerebral blood flow. Brain 123, 1216–1228.

Knoblich, G., Kircher, T.T.J., 2004. Deceiving oneself about being in control: conscious detection of changes in visuomotor coupling. J Exp Psychol Hum Percept Perform 30, 657–666.

Kornhuber, H.H., Deecke, L., 1965. Changes in the brain potential in voluntary movements and passive movements in man: readiness potential and reafferent potentials. Pflugers arch gesamte physiol menschen tiere 284, 1–17.

Kristeva-Feige, R., Rossi, S., Pizzella, V., Sabato, A., Tecchio, F., Feige, B., et al., 1996. Changes in movement-related brain activity during transient deafferentation: a neuromagnetic study. Brain Res. 714, 201–208.

Kukleta, M., Buser, P., Rektor, I., Lamarche, M., 1996. Readiness potentials related to self-initiated movement and to movement preceded by time estimation: a comparison. Physiol. Res. 45, 235–239.

Kukleta, M., Turak, B., Louvel, J., 2012. Intracerebral recordings of the Bereitschaftspotential demonstrate the heterogeneity of its components. Int. J. Psychophysiol. 83, 65–70.

Kukleta, M., Bob, P., Turak, B., Louvel, J., 2015. Large-scale synchronization related to structures manifesting simultaneous EEG baseline shifts in the pre-movement period. Act Nerv Super 57, 101–109.

Kukleta, M., Damborská, A., Roman, R., Rektor, I., Brázdil, M., 2016. The primary motor cortex is involved in the control of a non-motor cognitive action. Clin. Neurophysiol. 127, 1547–1550.

Lachaux, J.P., Rudrauf, D., Kahane, P., 2003. Intracranial EEG and human brain mapping. J. Physiol. Paris 97, 613–628.

Libet, B., Wright Jr., E.W., Gleason, C.A., 1982. Readiness-potentials preceding unrestricted ‘spontaneous’ vs. pre-planned voluntary acts. Electroencephalogr. Clin. Neurophysiol. 54, 322–335.

MacKinnon, C.D., Kapur, S., Hussey, D., Verrier, M.C., Houle, S., Tatton, W.G., 1996. Contributions of the mesial frontal cortex to the premovement potentials associated with intermittent hand movements in humans. Hum. Brain Mapp. 4, 1–22.

Menon, V., Freeman, W.J., Cutillo, B.A., Desmond, J.E., Ward, M.F., Bressler, S.L., et al., 1996. Spatio-temporal correlations in human gamma band electrocorticograms. Electroencephalogr. Clin. Neurophysiol. 98, 89–102.

Nielsen, T.I., Paetorius, N., Kuschel, R., 1965. Volitional aspects of voice performance: an experimental approach. Scand. J. Psychol. 6, 201–208.

Paradiso, G., Cunic, D., Saint-Cyr, J.A., Hoque, T., Lozano, A.M., Lang, A.E., et al., 2004. Involvement of human thalamus in the preparation of self-paced movement. Brain 127, 2717–2731.

Posner, M.I., Dehaene, S., 1994. Attentional networks. Trends Neurosci. 17, 75–79.

Rektor, I., 2000. Parallel information processing in motor systems: intracerebral recordings of readiness potential and CNV in human subjects. Neural Plast 7, 65–72.

Rektor, I., 2003. Intracerebral recordings of the Bereitschaftspotential and related potentials in cortical and subcortical structures in human subjects. In: Jahanshahi, M., Hallett, M. (Eds.), The Bereitschaftspotential. Movement-related Cortical Potentials. Kluwer Academic/Plenum Publishers, New York, pp. 61–77.

Rektor, I., Fève, A., Buser, P., Bathien, N., Lamarche, M., 1994. Intracerebral recording of movement related readiness potentials: an exploration in epileptic patients. Electroencephalogr. Clin. Neurophysiol. 90, 273–283.

Rektor, I., Louvel, J., Lamarche, M., 1998. Intracerebral recording of potentials accompanying simple limb movements: a SEEG study in epileptic patients. Electroencephalogr. Clin. Neurophysiol. 107, 277–286.

Rektor, I., Bareš, M., Kubová, D., 2001. Movement-related potentials in the basal ganglia: a SEEG readiness potential study. Clin. Neurophysiol. 112, 2146–2153.

Seiss, E., Hesse, C.W., Drane, S., Oostenveld, R., Wing, A.M., Praamstra, P., 2002. Proprioception-related evoked potentials: origin and sensitivity to movement parameters. NeuroImage 17, 461–468.

Shadmehr, R., Smith, M.A., Krakauer, J.W., 2010. Error correction, sensory prediction, and adaptation in motor control. Annu. Rev. Neurosci. 33, 89–108.

Shibasaki, H., 2012. Cortical activities associated with voluntary movements and involuntary movements. Clin. Neurophysiol. 123, 229–243.

Shibasaki, H., Hallett, M., 2006. What is the Bereitschaftspotential? Clin. Neurophysiol. 117, 2341–2356.

Shibasaki, H., Barrett, G., Halliday, E., Halliday, A.M., 1980a. Components of the movement-related cortical potential and their scalp topography. Electroencephalogr. Clin. Neurophysiol. 49, 213–226.

Shibasaki, H., Barrett, G., Halliday, E., Halliday, A.M., 1980b. Cortical potentials following voluntary and passive finger movements. Electroencephalogr. Clin. Neurophysiol. 50, 201–213.

Slachevsky, A., Pillon, B., Fourneret, P., Pradat-Diehl, P., Jeannerod, M., Dubois, B., 2001. Preserved adjustment but impaired awareness in a sensory-motor conflict following prefrontal lesions. J. Cogn. Neurosci. 13, 332–340.

Talairach, J., Szikla, G., Tournoux, P., Prossalentis, A., Bordas-Ferrer, M., Covello, L., 1967. Atlas d'Anatomie Stéréotaxique du Télencéphale. Masson & Cie, Paris.

Toro, C., Wang, B., Zeffiro, T., Thatcher, R.W., Hallett, M., 1994. Movement-related cortical potentials: source analysis and PET/MRI correlation. In: Thatcher, R.W., Hallett, M., Zeffiro, T., John, E.R., Huerta, M. (Eds.), Functional Neuroimaging: Technical Foundations. Academic Press, Orlando, FL, pp. 259–267.

Ullsperger, M., Danielmeier, C., Jocham, G., 2014. Neurophysiology of performance monitoring and adaptive behavior. Physiol. Rev. 94, 35–79.

4. Event-related potentials as biomarkers of impaired brain

Many neurological and psychiatric disorders are characterized by impairments in higher brain functions such as thinking, planning and deciding. Traumatic brain injury is regarded as an event involving an injury to the head due to trauma that produces a disruption of brain function and/or structure. If it is mild in severity, this type of trauma was previously thought to leave no long-term sequelae. Later on, however, electrophysiological studies provided evidence that a mild traumatic brain injury (mTBI) may lead to a wide variety of brain function alterations. João Gomes, who focused on this topic under my supervision within his Individual Project during his master's studies, reviewed event-related potential (ERP) studies conducted on mTBI patients (Gomes & Damborská, 2017 – Annex 8). In this paper, ERP changes after mTBI were reviewed with the aim to critically evaluate this electrophysiological technique as a possible diagnostic tool for impairments following the mTBI. We concluded that findings are still not consistent, and electrophysiological measures most suitable as markers of dysfunction have not been clearly established yet. Nevertheless, the ERP methodology is worth investigating as a promising tool that might, in the future, help individuals suffering from mTBI in terms of an early detection of functional brain abnormities as well as in terms of a longitudinal measurement of a treatment response.

Annex 8

Gomes, J. & **Damborská, A.** (2017). Event-related potentials as biomarkers of mild traumatic brain injury. *Activitas Nervosa Superior*,59 (3-4), 87-90.

Quantitative contribution: 50%

Content contribution: development of the initial idea, participation in writing the initial draft, corresponding author

Annex 8

Gomes, J. & **Damborská, A.** (2017). Event-related potentials as biomarkers of mild traumatic brain injury. *Activitas Nervosa Superior*,59 (3-4), 87-90.

Act Nerv Super (2017) 59:87–90
https://doi.org/10.1007/s41470-017-0011-2

REVIEW

Event-Related Potentials as Biomarkers of Mild Traumatic Brain Injury

João Gomes[1] · **Alena Damborská**[2,3,4]

Received: 3 October 2017 / Accepted: 1 November 2017 / Published online: 8 November 2017
© Springer International Publishing AG, part of Springer Nature 2017

Abstract Mild traumatic brain injury (mTBI) may lead to a wide variety of brain function alterations and is nowadays one of the least understood issues within neuroscience and sports medicine communities. Investigation and characterization of these functional abnormities are key to a better understanding of such changes. In current paper, a review of event-related potential (ERP) changes after mTBI is provided with the aim to critically evaluate this electrophysiological technique as a possible future diagnostic tool for impairments following the mTBI.

Keywords Mild traumatic brain injury · Event-related potential · Human

Introduction

Traumatic brain injury (TBI) is regarded as an event involving an injury to the head due to a blunt or penetrating trauma or from acceleration-deceleration forces that produces an immediately apparent disruption of brain function and/or structure. Much was said through recent years that if it is mild in severity, this type of trauma does not leave any long-term sequelae. With newer approaches such as neuropsychological tests and electrophysiological techniques, however, investigators have been finding long-lasting brain function anomalies in asymptomatic individuals that sustained mild TBI in the course of their lives (Slobounov et al. 2005, 2012; Nuwer et al. 2005; Thompson et al. 2005; Tallus et al. 2013). This anomalies are quite variable and non-specific, yielding cognitive impairments affecting global functions such as information processing, sleep, attention, and control and regulation of activity processes (Williams et al. 2008; Ashman et al. 2004; Kumar et al. 2009; Pontifex et al. 2009; Duncan et al. 2011). It then becomes imperative to regard mild traumatic brain injury (mTBI) as a problematic issue that should be fully understood and managed in the best way to avoid neuropsychiatric disorders or premature mortality, even due to suicide.

One way to do that is to try to find biomarkers that signal for brain function disruption, like scalp-recorded event-related potentials (ERPs). An ERP waveform is defined by its positive or negative polarity, amplitude, latency, scalp distribution, and relation to experimental variables. The amplitudes indicate the extent of allocation of neural resources to specific cognitive processes required to analyze, categorize, and recognize stimuli. The latencies reflect the speed of such mental processes. Altered ERP patterns might therefore indicate functional abnormities occurring after mTBI. Since controversy still exists in this field, a comprehensive evaluation of ERP studies targeting changes after mTBI is warranted. Current paper provides a review on available literature mainly targeting visual and auditory ERP changes after mTBI.

✉ Alena Damborská
adambor@med.muni.cz

[1] General Surgery Department, Amato Lusitano Hospital, Castelo Branco, Portugal

[2] CEITEC—Central European Institute of Technology, Brain and Mind Research Program, Masaryk University, Kamenice 735/5, CZ-625 00 Brno, Czech Republic

[3] Department of Psychiatry, Faculty of Medicine, Masaryk University, Brno, Czech Republic

[4] Functional Brain Mapping Laboratory, Departments of Clinical and Fundamental Neurosciences, University Medical School, Geneva, Switzerland

Visual ERP Approaches

Visual task ERP studies usually focus on investigating selective deficits in complex visual information processing. Throughout the years, investigators found mainly N2, N350, and P3 amplitude decrements in mTBI patients compared to that in control groups of individuals with no history of head trauma. Broglio et al. (2009) studied 90 participants, 46 of which with previous mTBI, using a three-stimulus oddball task. Their ERP study demonstrated significant decrements in the N2 and P3b amplitudes of the stimulus-locked ERP in mTBI subjects. Gosselin et al. (2011) compared 23 healthy individuals with 14 mTBI patients using a working memory task and showed decreased amplitude of N350 component. One year later, Gosselin et al. (2012) using again a working memory task demonstrated that the 44 patients within the mTBI group had a lower percentage of correct answers comparing to those within the control group on the behavioral performance, as well as smaller amplitudes of both frontal N350 and parietal P300 ERP components. P3 amplitude was also observed to be decreased in concussion victims among contact sports athletes (Dupuis et al. 2000), with no significant change in latency compared to healthy controls. In other studies, furthermore, symptomatic mTBI was found to be associated not only with amplitude reduction but also with delayed latency of cognitive ERPs for texture and cognitive paradigms (Lachapelle et al. 2008; Di Russo and Spinelli 2010; Li et al. 2016).

On the other hand, Potter and collaborators (Potter et al. 2002) reported more negative ERP deflections in the mild head-injured group in both congruent and incongruent conditions of Stroop task, consistent with the activation of the anterior cingulate gyrus. This finding is consistent with conclusion of Larson and collaborators (Larson et al. 2011) who suggested that mild TBI is associated with altered conflict adaptation and adjustment processes. Also, recent study of Mäki-Marttunen et al. (2015) reported rather increase than reduction in ERP amplitude. Authors studied emotional stimuli response in mTBI patients using a Go-NoGo task requiring cognitive control. The study demonstrated greater threat-related enhancement of the N2-P3 complex in mTBI group compared to that in control individuals. Authors concluded that mTBI might originate inefficient top-down control of bottom-up influences of emotion and might contribute to affective symptoms in mTBI.

It is evident that alterations on the ERP activity due to mTBI are not constant among visual ERP studies. Furthermore, Larson et al. (2012) recently showed no significant change in visual ERP amplitudes in mTBI patients and also reported comparable performance to non-injured individuals in some aspects of cognitive control.

Auditory ERP Approaches

Auditory task ERP studies focus on investigating selective deficits in complex auditory information processing. Differences disclosed in subjects with and without history of TBI are mainly in P3 amplitude.

Comparing 24 mild head-injured and 24 healthy control participants during a three-stimulus auditory target detection task, a putative "O-wave" or "reorienting negativity" following the P3a was reported to be more negative in the mild head-injured group (Potter et al. 2001). During oddball vigilance tasks, both easy and difficult ones, reduced P300 amplitudes were observed with no alterations of N1, P2, or N2 components in well-functioning university students who had experienced mTBI in average 6.4 years prior to the testing (Segalowitz et al. 2001). Thériault et al. (2009) demonstrated that asymptomatic athletes with concussion less than two years prior to the testing had reduced P3a and P3b amplitudes. So despite functioning normally in their life activities, they showed altered neuronal information processing. De Beaumont et al. (2009) compared 19 healthy former athletes, in late adulthood, who sustained their last sport-related concussion in early adulthood, with 21 healthy former athletes with no history of concussion, and also registered significantly delayed and decreased P3a/P3b components. Authors suggested the ERP changes to be long lasting since the P3 amplitude attenuation was observed more than three decades post-injury in individuals who sustained more than one concussion. These findings suggest slower allocation of attentional resources for memory processing and reduced frontal lobe function efficiency particularly affecting the ability to shift attentional resources to novel stimuli, yielding chronic cognitive and motor system changes. These ERP findings might point to sub-clinical alterations in cognitive-attentional allocation processes that could interfere with vocational outcome even years after injury. On the other hand, no significant differences in N2 and P3 wave parameters were observed in a standard auditory oddball task (Sivák et al. 2008). Authors interpreted their findings as such that ERPs are not sensitive enough to detect and/or quantify subtle objective neuropsychological changes in selected mTBI patients.

Summarizing, auditory ERP investigations show, similarly to the visual approaches, different P3 wave abnormities in mTBI patients, mainly in terms of amplitude reduction and also in latency increase. Anomalies in cognitive-attentional allocation processes are suggested in individuals with mTBI.

Discussion

Mainly, visual and auditory approaches have been used to try to prove pathognomonic changes linked to mTBI. Regarding visual approaches, the literature points to a decrease in P3

amplitude after mTBI, which can be found even years post-injury. N2 amplitude changes were also demonstrated. Concerning latency, some studies found it was delayed, but this was not a constant feature. Analyzing the auditory ERP changes reduced P300 amplitudes, both P3a and P3b subcomponents have been reported by several authors. Here again, latency alterations are not constant. Putting visual and auditory approaches together, both show mainly changes in the P300, pointing to different cognitive-attentional allocation processes in mTBI individuals, even asymptomatic ones. However, these ERP differences are not present in all the studies, making it a non-constant alteration in such individuals. The reason why the ERP investigation does not bring any consensus in mTBI research may arise from infinite possibilities of sequelae from different brain traumas and a wide variability in age, background, and medications within studied groups of individuals.

The usage of ERP analyses in mTBI patients has the advantage of being regarded as an "endogenous" approach, as ERPs are heavily influenced by higher level cognitive processes and not so much by physical characteristics of the stimulus. ERP analyses detect changes in cortical functions that normal hospital imaging methods do not encounter, as those are more structural than functional. Last but not least, advantage of ERP approach is its non-invasiveness with low-stress diagnostic burden towards patients. On the other hand, ERP testing requires time, highly competent personnel, and machinery, making it not an everyday hospital used methodology. And most importantly, despite ERP differences have been showed between healthy controls and mTBI patients, no solid and indisputable findings point to a faithful ERP usage when it comes to diagnosis of sequelae from head trauma. Besides mTBI, similar ERP changes might be actually encountered also in major depressive disorder, bipolar disorder, schizophrenia, or dementia indicating low specificity of the technique (Rapp et al. 2015).

In order to get a technique with which medical professionals can undoubtedly make a diagnosis of post-mTBI brain damage and plan for a proper follow-up, further investigations with similar criteria and approaches are needed. We propose for example to study groups of individuals with specific head injuries regarding location, frequency, and intensity of the trauma, as different injury events tend to lead to very different pathophysiological processes. Moreover, investigations should target individuals with different age intervals. For example, mTBI patients who sustained head trauma in similar years of their life might be studied in their 40s, 50s, or 60s to find out a possible delay in ERP abnormity occurence. The most valuable approach would be to investigate healthy individuals and then, if they sustain a mTBI, to compare their before and after trauma ERPs. This might be a non-profitable approach but perhaps the most valuable one. Other possible important aspects are genetics and environment. One should aim to study individuals with different cultural and geographic backgrounds, as these differences might as well hypothetically bring different neuropsychological brain adaptations to injury. Several recommendations for research on electrophysiological methods as mTBI diagnostic tools have been recently introduced by Rapp et al. (2015). Authors argued that reliability in a healthy population should be established and test-retest reliability studies should be conducted for each candidate electrophysiological measure. Furthermore, studies should compare well-characterized TBI patients with well-matched healthy controls to test for the clinical validity of each measure. Lastly, investigators should aim to expand the mathematical algorithms to try to find some novel ERP techniques that eventually would show pathognomic changes.

Conclusion

It is now known that mild traumatic head injuries might lead to long-term higher level cognitive sequelae. These can have an important impact on individuals' professional and social relations. Promising biomarkers that might help to detect such changes are changes in parameters of ERPs. In current paper, we reviewed studies that point to real ERP differences between mTBI patients and healthy controls. Although findings in the literature are not consistent and electrophysiological measures most suitable as markers of dysfunction have not been clearly established yet, the ERP approach represents a promising diagnostic tool for mTBI functional impairments. If here suggested additional studies are conducted, the ERP methodology might in future help individuals suffering from mTBI in terms of early detection of functional brain abnormities as well as in terms of longitudinal measurement of treatment response.

Compliance with Ethical Standards

Conflict of Interest The authors declare that they have conflict of interest.

Disclaimer The institutions to which authors are affiliated had no role in decision to publish or in preparation of the manuscript.

References

Ashman, T. A., Spielman, L. A., Hibbard, M. R., Silver, J. M., Chandna, T., & Gordon, W. A. (2004). Psychiatric challenges in the first 6 years after traumatic brain injury: cross-sequential analyses of axis I disorders. *Archives of Physical Medicine and Rehabilitation, 85*, S36–S42. https://doi.org/10.1016/j.apmr.2003.08.117.

Broglio, S. P., Pontifex, M. B., O'Connor, P., & Hillman, C. H. (2009). The persistent effects of concussion on neuroelectric indices of

attention. *Journal of Neurotrauma, 26*, 1463–1470. https://doi.org/10.1089/neu.2008.0766.

De Beaumont, L., Théoret, H., Mongeon, D., Messier, J., Leclerc, S., Tremblay, S., Ellemberg, D., & Lassonde, M. (2009). Brain function decline in healthy retired athletes who sustained their last sports concussion in early adulthood. *Brain, 132*, 695–708. https://doi.org/10.1093/brain/awn347.

Di Russo, F., & Spinelli, D. (2010). Sport is not always healthy: executive brain dysfunction in professional boxers. *Psychophysiology, 47*, 425–434. https://doi.org/10.1111/j.1469-8986.2009.00950.x.

Duncan, C. C., Summers, A. C., Perla, E. J., Coburn, K. L., & Mirsky, A. F. (2011). Evaluation of traumatic brain injury: brain potentials in diagnosis, function, and prognosis. *International Journal of Psychophysiology, 82*, 24–40. https://doi.org/10.1016/j.ijpsycho.2011.02.013.

Dupuis, F., Johnston, K. M., Lavoie, M., Lepore, F., & Lassonde, M. (2000). Concussions in athletes produce brain dysfunction as revealed by event-related potentials. *Neuroreport, 11*, 4087–4092.

Gosselin, N., Bottari, C., Chen, J. K., Petrides, M., Tinawi, S., De Guise, É., & Ptito, A. (2011). Electrophysiology and functional MRI in post-acute mild traumatic brain injury. *Journal of Neurotrauma, 28*, 329–341. https://doi.org/10.1089/neu.2010.1493.

Gosselin, N., Erg, C. B., Chen, J. K., Huntgeburth, S. C., Beaumont, L. D., Petrides, M., Cheung, B., & Ptito, A. (2012). Evaluating the cognitive consequences of mild traumatic brain injury and concussion by using electrophysiology. *Neurosurgical Focus, 33*, E7. https://doi.org/10.3171/2012.10.FOCUS12253.

Kumar, S., Rao, S. L., Chandramouli, B. A., & Pillai, S. V. (2009). Reduction of functional brain connectivity in mild traumatic brain injury during working memory. *Journal of Neurotrauma, 26*, 665–675.

Lachapelle, J., Bolduc-Teasdale, J., Ptito, A., & McKerral, M. (2008). Deficits in complex visual information processing after mild TBI: electrophysiological markers and vocational outcome prognosis. *Brain Injury, 22*, 265–274. https://doi.org/10.1080/02699050801938983.

Larson, M. J., Farrer, T. J., & Clayson, P. E. (2011). Cognitive control in mild traumatic brain injury: conflict monitoring and conflict adaptation. *International Journal of Psychophysiology, 82*, 69–78. https://doi.org/10.1016/j.ijpsycho.2011.02.018.

Larson M. J., Clayson P. E., Farrer T. J. (2012) Performance monitoring and cognitive control in individuals with mild traumatic brain injury. *Journal of the International Neuropsychological Society, 18*(2): 323–333.

Li, L., Arakaki, X., Tran, T., Harrington, M., Padhye, N., & Zouridakis, G. (2016). Brain activation profiles in mTBI: evidence from ERP activity of working memory response. Paper presented at the Proceedings of the Annual International Conference of the IEEE Engineering in Medicine and Biology Society, EMBS, 2016-October 1862–1865. doi:https://doi.org/10.1109/EMBC.2016.7591083.

Mäki-Marttunen, V., Kuusinen, V., Brause, M., Peräkylä, J., Polvivaara, M., Dos Santos Ribeiro, R., Öhman, J., & Hartikainen, K. M. (2015). Enhanced attention capture by emotional stimuli in mild traumatic brain injury. *Journal of Neurotrauma, 32*, 272–279. https://doi.org/10.1089/neu.2014.3557.

Nuwer, M. R., Hovda, D. A., Schrader, L. M., & Vespa, P. M. (2005). Routine and quantitative EEG in mild traumatic brain injury. *Clinical Neurophysiology, 116*, 2001–2025. https://doi.org/10.1016/j.clinph.2005.05.008.

Pontifex, M. B., O'Connor, P. M., Broglio, S. P., & Hillman, C. H. (2009). The association between mild traumatic brain injury history and cognitive control. *Neuropsychologia, 47*, 3210–3216. https://doi.org/10.1016/j.neuropsychologia.2009.07.021.

Potter, D. D., Bassett, M. R. A., Jory, S. H., & Barrett, K. (2001). Changes in event-related potentials in a three-stimulus auditory oddball task after mild head injury. *Neuropsychologia, 39*, 1464–1472. https://doi.org/10.1016/S0028-3932(01)00057-4.

Potter, D. D., Jory, S. H., Bassett, M. R. A., Barrett, K., & Mychalkiw, W. (2002). Effect of mild head injury on event-related potential correlates of Stroop task performance. *Journal of the International Neuropsychological Society, 8*, 828–837. https://doi.org/10.1017/S1355617702860118.

Rapp, P. E., Keyser, D. O., Albano, A., Hernandez, R., Gibson, D. B., Zambon, R. A., Hairston, D., Hughes, J. D., Krzstal, A., & Nichols, A. S. (2015). Traumatic brain injury detection using electrophysiological methods. Frontiers in Human Neuroscience, 9, 32p doi: https://doi.org/10.3389/fnhum.2015.00011.

Segalowitz, S. J., Bernstein, D. M., & Lawson, S. (2001). P300 event-related potential decrements in well-functioning university students with mild head injury. *Brain and Cognition, 45*, 342–356. https://doi.org/10.1006/brcg.2000.1263.

Sivák, Š., Kurča, E., Hladká, M., Zeleňák, K., Turčanová-Koprušáková, M., & Michalik, J. (2008). Early and delayed auditory oddball ERPs and brain MRI in patients with MTBI. *Brain Injury, 22*, 193–197. https://doi.org/10.1080/02699050801895431.

Slobounov, S., Sebastianelli, W., & Moss, R. (2005). Alteration of posture-related cortical potentials in mild traumatic brain injury. *Neuroscience Letters, 383*, 251–255. https://doi.org/10.1016/j.neulet.2005.04.039.

Slobounov, S., Sebastianelli, W., & Hallett, M. (2012). Residual brain dysfunction observed one year post-mild traumatic brain injury: combined EEG and balance study. *Clinical Neurophysiology, 123*, 1755–1761. https://doi.org/10.1016/j.clinph.2011.12.022.

Tallus, J., Lioumis, P., Hämäläinen, H., Kähkönen, S., & Tenovuo, O. (2013). Transcranial magnetic stimulation-electroencephalography responses in recovered and symptomatic mild traumatic brain injury. *Journal of Neurotrauma, 30*, 1270–1277. https://doi.org/10.1089/neu.2012.2760.

Thériault, M., De Beaumont, L., Gosselin, N., Filipinni, M., & Lassonde, M. (2009). Electrophysiological abnormalities in well functioning multiple concussed athletes. *Brain Injury, 23*, 899–906. https://doi.org/10.1080/02699050903283189.

Thompson, J., Sebastianelli, W., & Slobounov, S. (2005). EEG and postural correlates of mild traumatic brain injury in athletes. *Neuroscience Letters, 377*, 158–163. https://doi.org/10.1016/j.neulet.2004.11.090.

Williams, B. R., Lazic, S. E., & Ogilvie, R. D. (2008). Polysomnographic and quantitative EEG analysis of subjects with long-term insomnia complaints associated with mild traumatic brain injury. *Clinical Neurophysiology, 119*, 429–438. https://doi.org/10.1016/j.clinph.2007.11.003.

5. Resting-state brain electrophysiological activity

When people are awake and aware but not pursuing any particular goal, thought, or task, high levels of activity in many brain regions are observed. It means that at rest these regions are not only active but they are *more* active at rest than when a subject is carrying a specific cognitive task. These regions include the posterior cingulate cortex, the ventral anterior cingulate cortex, the medial prefrontal cortex, and the cortex at the junction of the temporal and parietal lobes. It has been shown that cognitive tasks induce an activation increase in other brain regions and this finding led to the proposal that the regions activated more at rest constitute a functionally linked network (Fox et al., 2005). Neuroscientists call this network, supporting a default mode of brain function, the *default mode* or *resting-state* network.

The puzzling question of neuroscience is the purpose of the resting-state brain activity. Why should some regions be highly active when the brain is doing nothing special? Is this activity related to mental "idling" or mental operations related to an inwardly focused attention contrary to an externally focused attention oriented to events in the surrounding environment? Although it is not clear yet what this network actually does, it was also observed in monkeys; thus, it probably carries some phylogenetically basic and likely important function whose impairment presumably might manifest in mental disorders. Neuroimaging studies have brought evidence about abnormal functioning of the resting-state network in several neurological and psychiatric disorders, e.g., less active in autism and more so in schizophrenia.

Studies included in this chapter of the habilitation thesis focused on the functional organization of resting-state networks of the human brain. Together with my colleagues, I studied subcortico-cortical interactions, large-scale brain network dynamics, and directed functional brain connectivity during resting state. All these studies were conducted in collaboration between the Masaryk University and University of Geneva. Patients were recruited at the 1st Department of Neurology at St. Anne's University Hospital in Brno, Department of Psychiatry at University Hospital Brno, and Department of Psychiatry at Geneva University Hospital.

Results of our simultaneous intracerebral and scalp EEG study on *subcortico-cortical interactions* (Damborská et al., 2021, – Annex 9, Chapter 5.1) represent the first report on functional linkage in the cross-frequency domain between the resting-state electrophysiological activity of the subthalamic nucleus and cortex in human. Our next three high-density scalp EEG studies contributed to the understanding of resting-state large-scale brain networks in *affective disorders*. We demonstrated interindividual differences in large-scale brain network dynamics related to depressive symptomatology (Damborská et al., 2019 b – Annex 10, Chapter 5.2) and brought the first evidence for disruption of resting-state brain network dynamics in euthymic patients with bipolar disorder (Damborská et al., 2019 c – Annex 11, Chapter 5.2). In the directed functional connectivity study (Damborská et al., 2020 – Annex 12, Chapter 5.2), we focused on cortico-striatal-pallidal-thalamic circuits during resting state in patients with depression. We showed a higher-than-normal functional connectivity arising from the right amygdala in depressive patients supporting the view that the amygdala plays an important role in the neurobiology of depression.

5.1 Resting-state subcortico-cortical interactions in human brain

The subthalamic nucleus (STN) is known to have a central position in basal ganglia-thalamo-cortical circuits and to be involved in motor-related neuropathologies such as Parkinson's disease (PD) (Bočková and Rektor 2019). Excessive synchronization of β (15–35 Hz) activity at multiple nodes throughout the basal ganglia-thalamo-cortical motor network is the most commonly reported electrophysiological abnormality of PD patients (Sharott et al., 2014). Nevertheless, several other studies have shown that abnormalities in multiple frequencies are associated with PD (for review see Bočková and Rektor 2019).

Interestingly, involvement of multiple frequencies was also reported during dopaminergic medication of PD patients. Modulations induced by dopaminergic medication have been observed within the subcortico-cortical networks in the θ/α range (Oswal et al., 2013), as well as in the β/γ frequency bands (Litvak et al., 2011). Bidirectional basal ganglia – cortex communication was reported to be differentially patterned across frequency bands and change with movement and dopaminergic input

(Lalo et al., 2008). Such subcortico-cortical coupling patterns observed under on-medication conditions make it possible to speculate whether this communication at different frequency bands is physiological or related to the pathophysiology of PD. The results of both nonhuman and human studies suggest that the coherence between the STN and scalp-recorded EEG activity in the sub-β and β bands might represent a pathological exaggeration of physiological activity (for review, see Brown and Williams 2005; Engel and Fries 2010).

It has been suggested that slow oscillations in the STN reflect top-down inputs from the medial prefrontal cortex, thus implementing behaviour control. It was unclear, however, whether the STN oscillations are related to cortical activity in a bottom-up manner. In our study (Damborská et al., 2021 – Annex 9), we brought the first evidence for coupling between the δ/θ phase of the STN and the amplitude of higher frequency bins of the scalp-recorded electrophysiological human brain activity. This result suggests the existence of a cross-frequency hierarchical functional linkage within the STN-cortical networks during resting conditions in human. On theoretical grounds, the coupling between the STN phase and cortical amplitude of neuronal activity represents a serious candidate for physiological functional interactions between these brain structures during resting conditions. The neuronal oscillations in the neocortex tend to couple hierarchically, with the phase of lower-frequency oscillations modulating the higher frequency amplitudes (Canolty et al., 2006). The lower-frequency phase determines momentary power in higher frequency activity. The coupling observed between the STN phase activity and the amplitude of the scalp-recorded activity could thus be considered as a manifestation of fluctuation of excitability in local neuronal assemblies in the cortex with rhythmic activity in the STN. This interpretation is in agreement with previously reported evidence of driving from the STN to the cortex under resting conditions (Williams 2002). Our results suggest that besides being involved in top-down processes, STN plays a role in bottom-up, i.e., from the STN to cortex, communication within the subcortico-cortical circuitries of the human brain during the resting state.

Annex 9

Damborská, A., Lamoš, M., Baláž, M., Deutschová, B., Brunet, D., Vulliemoz, S., Bočková, M., & Rektor, I. (2021) Resting-State Phase-Amplitude Coupling Between the

Human Subthalamic Nucleus and Cortical Activity: A Simultaneous Intracranial and Scalp EEG Study, *Brain Topography*, 34(3), 272-282.
IF(2021) = 4.275, rank Q2
Quantitative contribution: 70%
Content contribution: designing the study, participation in data acquisition, pre-processing, table and figure preparation, writing the initial draft, corresponding author

Annex 9

Damborská, A., Lamoš, M., Baláž, M., Deutschová, B., Brunet, D., Vulliemoz, S., Bočková, M., & Rektor, I. (2021) Resting-State Phase-Amplitude Coupling Between the Human Subthalamic Nucleus and Cortical Activity: A Simultaneous Intracranial and Scalp EEG Study, *Brain Topography*, 34(3), 272-282.

Brain Topography (2021) 34:272–282
https://doi.org/10.1007/s10548-021-00822-8

ORIGINAL PAPER

Resting-State Phase-Amplitude Coupling Between the Human Subthalamic Nucleus and Cortical Activity: A Simultaneous Intracranial and Scalp EEG Study

Alena Damborská[1,2,6] · Martin Lamoš[1] · Denis Brunet[2,3] · Serge Vulliemoz[3,4] · Martina Bočková[1,5] · Barbora Deutschová[1,5] · Marek Baláž[5] · Ivan Rektor[1,5]

Received: 19 November 2020 / Accepted: 18 January 2021 / Published online: 29 January 2021
© The Author(s), under exclusive licence to Springer Science+Business Media, LLC part of Springer Nature 2021

Abstract

It has been suggested that slow oscillations in the subthalamic nucleus (STN) reflect top-down inputs from the medial prefrontal cortex, thus implementing behavior control. It is unclear, however, whether the STN oscillations are related to cortical activity in a bottom-up manner. To assess resting-state subcortico-cortical interactions, we recorded simultaneous scalp electroencephalographic activity and local field potentials in the STN (LFP-STN) in 11 patients with Parkinson's disease implanted with deep brain stimulation electrodes in the on-medication state during rest. We assessed the cross-structural phase-amplitude coupling (PAC) between the STN and cortical activity within a wide frequency range of 1 to 100 Hz. The PAC was dominant between the δ/θ STN phase and β/γ cortical amplitude in most investigated scalp regions and between the δ cortical phase and θ/α STN amplitude in the frontal and temporal regions. The cross-frequency linkage between the slow oscillations of the LFP-STN activity and the amplitude of the scalp-recorded cortical activity at rest was demonstrated, and similar involvement of the left and right STNs in the coupling was observed. Our results suggest that the STN plays a role in both bottom-up and top-down processes within the subcortico-cortical circuitries of the human brain during the resting state. A relative left–right symmetry in the STN-cortex functional linkage was suggested. Practical treatment studies would be necessary to assess whether unilateral stimulation of the STN might be sufficient for treatment of Parkinson's disease.

Keywords Subthalamic nucleus · Subcortico-cortical interactions · Phase-amplitude coupling · Cross-structural coupling · Simultaneous intracranial and scalp EEG

Introduction

The subthalamic nucleus (STN) is known to have a central position in basal ganglia-thalamo-cortical circuits and to be involved in motor-related neuropathologies such as Parkinson's disease (Bočková and Rektor 2019). Excessive synchronization of β (15–35 Hz) activity at multiple nodes throughout the basal ganglia-thalamo-cortical motor network is the most commonly reported electrophysiological abnormality of Parkinson's disease (PD) patients (Sharott et al. 2014; Hammond et al. 2007; Oswal et al. 2013a; Chen et al. 2010; Stein and Bar-Gad 2013).

Several studies have shown that β is not the only frequency band that is associated with PD, suggesting that an integral view on electrophysiological brain activities throughout the entire frequency spectrum could help better understand parkinsonian pathophysiology (for review see Bočková and Rektor 2019). Lower (3–7 Hz) and higher

Handling Editor: Bin He.

✉ Alena Damborská
adambor@med.muni.cz

1 CEITEC – Central European Institute of Technology, Masaryk University, Brno, Czech Republic

2 Functional Brain Mapping Lab, University of Geneva, Geneva, Switzerland

3 CIBM – Center for Biomedical Imaging, Geneva, Switzerland

4 EEG and Epilepsy Unit, Neurology, University Hospital and Faculty of Medicine, Geneva, Switzerland

5 First Department of Neurology, St. Anne's University Hospital, Masaryk University, Brno, Czech Republic

6 CEITEC – Central European Institute of Technology, Brain and Mind Research Program, Masaryk University, Kamenice 753/5, 625 00 Brno, Czech Republic

(8–20) frequency oscillations were observed in the STN during resting conditions in PD patients in the off-medication state, and the existence of two different specific local functional organizations of oscillating neuronal populations in the STN was suggested (Moran et al. 2008). Several functional sub-loops were identified in PD patients in the off-medication state between the STN and cortical motor regions, defined in terms of coherence and distinguished by their frequency, cortical topography, and temporal relationships (Fogelson et al. 2006). Increased resting-state cortico-cortical functional connectivity in the α range (8–10 Hz) was suggested as a feature of PD from the earliest clinical stages onward (Stoffers et al. 2008). An increase in θ (4–8 Hz) and low α (8–10 Hz) power, as well as a decrease of β (13–30 Hz) and γ (30–48 Hz) power in resting-state oscillatory brain activity has been reported in de novo PD patients compared to healthy controls (Stoffers et al. 2007). Coupling between the β-phase (13–30 Hz) and γ-amplitude (50–200 Hz) in the primary motor cortex was reported to be exaggerated in PD patients compared with patients with craniocervical dystonia and subjects without any movement disorder (De Hemptinne et al. 2013).

Another important aspect of functional organization within the subcortico-cortical circuits is the involvement of multiple frequencies during the on-medication state of PD. Modulations induced by dopaminergic medication have been observed within the subcortico-cortical networks in the θ/α range (Alonso-Frech et al. 2006; Oswal et al. 2013b), as well as in the β/γ frequency bands (Marsden et al. 2001; Williams 2002; Lalo et al. 2008; Brown et al. 2001; Litvak et al. 2011). A bidirectional cortico-basal ganglia communication was reported that is differentially patterned across frequency bands and changes with movement and dopaminergic input (Lalo et al. 2008). Such cortico-subcortical coupling patterns observed under on-medication conditions make it possible to speculate whether this communication at different frequency bands is physiological or related to the pathophysiology of PD. The results of both nonhuman and human studies suggest that the coherence between the STN and electroencephalographic (EEG) scalp-recorded activity in the sub-β and β bands might represent a pathological exaggeration of a physiological activity (for review, see Hammond et al. 2007; Brown and Williams 2005; Engel and Fries 2010).

The communication-through-coherence hypothesis was formulated more than 10 years ago suggesting that communication between two neuronal groups depends on coherence within specific frequency bands (Fries 2005). Later, the authors of the gating-by-inhibition hypothesis proposed that the routing of information flow between brain regions is established by actively inhibiting the pathway not required for the task (Jensen and Mazaheri 2010). These two hypotheses were recently unified via a cross-frequency coupling phenomenon (Bonnefond et al. 2017). It suggests that communication between two regions is established by the phase synchronization of oscillations at lower frequencies (< 25 Hz), which serve as a temporal reference frame for information carried by high-frequency (> 40 Hz) activity. Specifically, high-frequency oscillations are expected to be nested within low-frequency oscillations, i.e. they would occur only during the excitability phase of the lower-frequency oscillations. Testing the proposed communication-by-nested-oscillation framework requires simultaneous recordings from different brain regions. The first support for this framework was provided by Saalmann et al. (2012), with intracranial recordings on nonhuman primates. The authors suggested that the pulvinar, a thalamic nucleus, regulates α synchrony between cortical areas according to attention allocation. Moreover, they observed the pulvinar-controlled cortical α activity modulating the cortical γ activity through cross-frequency coupling. Studies involving cross-frequency linkage within a given brain area have suggested a physiological role of these interactions in facilitating the transient coordination of cortical areas (Canolty et al. 2006; Lakatos et al. 2008; Lisman and Jensen 2013; Voytek et al. 2010). Nevertheless, the cross-frequency interactions between different brain regions are not yet fully understood in humans.

It has been suggested that slow oscillations in the subthalamic nucleus (STN) reflect top-down inputs from the medial prefrontal cortex, thus implementing behavior control (Cavanagh et al. 2011; Zavala et al. 2014; Kelley et al. 2018). It is unclear, however, whether the STN oscillations are related to cortical activity in a bottom-up manner. One of the best studied forms of cross-frequency coupling is phase-amplitude coupling (PAC), in which the amplitude of a higher frequency oscillation is coupled to the phase of a lower frequency oscillation (Canolty et al. 2006). To address both top-down and bottom-up human brain processes in the absence of overt stimuli and, particularly, to examine whether specific cross-frequency and cross-structural PAC patterns occur in the subcortico-cortical circuits, we investigated both "STN phase—cortical amplitude" and "cortical phase—STN amplitude" couplings of the resting-state electrophysiological activity. Specifically, we recorded local field potential (LFP) from bilateral STNs in combination with a simultaneous scalp EEG in PD patients. This enabled us to assess the spatial characteristics of coordinated cross-structural STN-cortical activity. Bearing in mind a possible role of multiple frequency band oscillations in communications between the STN and cortical neuronal groups (Hammond et al. 2007; Bočková and Rektor 2019; Brown and Williams 2005; Cavanagh et al. 2011), we analyzed interactions in electrophysiological activities in a wide frequency range of 1 to 100 Hz.

Focusing on the physiological rather than pathological cross-frequency cross-structural interactions in the

subcortico-cortical circuits, we examined the electrophysiological activity of PD patients under their usual anti-parkinsonian medication, where a reduced impairment compared to an off-medication state or to untreated patients could be expected. Nevertheless, suppressing PD symptoms with medication does not necessarily mean the brain networks are normal and their activity physiological.

Bilateral deep brain stimulation of subthalamic nucleus (STN-DBS) improves motor symptoms of PD. Interestingly, it has been shown that similar improvements can be achieved with unilateral STN-DBS in some patients (Germano et al. 2004; Slowinski et al. 2007); it has been suggested that these patients presenting such a "dominant STN" might not need bilateral STN-DBS surgery (Castrioto et al. 2011). Since the neural substrate of functional asymmetry of the STN is largely unknown, the analysis of cross-frequency interactions of the left and right STN with the scalp-recorded activity could yield great insight into the dynamics of the subcortico-cortical circuitry. To assess a possible functional asymmetry in the STN-cortical interactions, we compared the PACs for the left versus right STN.

Methods

Subjects

Eleven right-handed PD patients enrolled in an STN-DBS program participated in the study. All the participants were recruited at the First Department of Neurology, St. Anne's University Hospital, Masaryk University in Brno. They were implanted with STN-DBS four-contact electrodes bilaterally. Stereotactic coordinates, direct visualization of the lead location on postoperative MRI scan, and the antiparkinsonian effects of high-frequency stimulation confirmed the lead placement within the desired target region. Intervals of 4 to 5 days between the implantation and final internalization of DBS electrodes served for clinical assessment and testing of DBS efficacy. We used this period for simultaneous scalp and intracranial EEG recording. Patients were recorded on their usual anti-parkinsonian medication. The patient characteristics are given in Table 1.

Procedure

Subjects were lying in a light and sound attenuated room. They were instructed to move as little as possible and to refrain from extensive eye movements. One session of 10 min in the off-stimulation and on-medication state in resting conditions was recorded with eyes open.

Recording

Recording sessions were conducted 2 to 3 days after the surgery, after ensuring that the patients' general state was satisfactory and they could collaborate appropriately. The electrophysiological activity was recorded simultaneously intracranially and from the scalp using the BrainScope EEG system. The LFP data were obtained from four-contact DBS electrodes implanted bilaterally into the STN. The EEG data were collected in each patient using up to 62 Ag–AgCl electrodes (see Table 1) placed on the scalp according the International 10/10 System. The central scalp region was covered by postoperative bandages and thus not explored. The size and shape of this unexplored scalp region slightly differed amongst patients. All intracranial and scalp recordings were

Table 1 Patient characteristics

Subject no.	Age (years)	Sex	Duration of PD (years)	Medication	First manifestation	Rec. (Int.)	Length of data (s)
1	59	F	8	L-dopa	Right H–R	51 (11)	173
2	49	M	14	L-dopa	Right H–R, left T	57 (3)	300
3	56	F	7	L-dopa, Ent, Pra	Left T	58 (2)	300
4	51	M	9	L-dopa, Ent, Pra	Right T	60 (0)	300
5	63	F	12	L-dopa, Ent, Rop, Ama	Left H–R	52 (10)	260
6	63	M	16	L-dopa, Ent, Pra	Left T	53 (2)	240
7	60	M	6	L-dopa, Ent, Rop	Left H–R	47 (10)	280
8	70	M	8	L-dopa	Right H–R, right T	60 (0)	300
9	63	M	9	L-dopa, Rop	Right T	61 (5)	260
10	61	M	9	L-dopa, Ent, Rot	left T	62 (1)	258
11	54	M	6	L-dopa, Pra	Right H–R, right T	60 (4)	200

L-dopa levodopa, *Ent* entacapone, *Rop* ropinirole, *Pra* pramipexole, *Rot* rotigotine, *Ama* amantadine, *Rec. (Int.)* number of recording (interpolated) scalp electrodes, *H–R* hypokinesia and rigidity, *T* tremor

monopolar on-line referred to an average reference of all scalp electrodes, except for the most peripheral ones with a higher risk of possible muscle artifacts (F9, F10, FT9, FT10, T9, T10, TP9, TP10, P9, P10, Nz, Iz). Eye movements were recorded with electrodes placed above the right and below the left lateral canthi. The sampling rate was 5 kHz. Recordings were visually inspected and 3 to 5 min artifact-free simultaneous intracranial and scalp recordings in each subject were selected for further analysis.

Data Pre-processing

Intracranial data were band-pass filtered from 0.1 to 100 Hz with two Butterworth filters (one high-pass and one low-pass) of second-order, 12 dB/octave roll-off, and forward and backward passes for both of them. Data were then down-sampled to 250 Hz with a cascaded integrator comb method. Three bipolar montages from two neighboring contacts of the four-contact DBS electrode were calculated for each STN. The recording from one bipolar lead closest to each STN based on MRI scans and clinical outcome was selected and used for further analysis. Recordings from scalp EEG data were band-pass filtered from 0.1 to 100 Hz with the same second-order Butterworth filters, plus a notch filter at 50 Hz to remove power-line artifacts. Subsequently, in order to remove ballistocardiogram and oculomotor artifacts, the infomax-based Independent Component Analysis (Jung et al. 2000) was applied on all but one or two channels rejected due to abundant artifacts. Two to four independent components were removed in each patient. Only artifacts related to ballistocardiogram, saccadic eye movements, and eye blinking were removed, based on the waveform, topography, and time course of the component. Subsequently the data were back-reconstructed without these components and further analyzed. Every scalp electrode with a recording available in at least eight subjects was included into further analysis. Previously identified noisy channels and recordings from the electrodes that were missing at most in three subjects were interpolated using a 3-D spherical spline (Perrin et al. 1989). Thus, for each subject, a set of the same 53 channels was obtained that covered all scalp regions except for the central area (see Supplementary Fig. S1 online). The number of channels interpolated in each subject is given in Table 1. The scalp data were then down-sampled to 250 Hz with the same cascaded integrator comb method.

Phase-Amplitude Coupling Analysis

The PAC was calculated using the envelope-to-signal correlation technique (Bruns and Eckhorn 2004), which calculates a correlation between the amplitude envelope of the filtered high frequency signal and the filtered low frequency signal. Filtering was achieved via a convolution with complex Morlet's wavelets w (t, f_0) that have a Gaussian shape both in the time domain (SD σ_t) and in the frequency domain (SD σ_f) around its central frequency f_0 (Kronland-Martinet et al. 1987). The wavelet family we used was defined by $(f_0/\sigma_f) = 7$, with wavelet duration $2\sigma_t$ of about two periods of oscillatory activity at f_0. Parameter settings, pipeline for PAC calculation, and evaluation of PAC significance were adopted from the recommended settings of the PAC toolbox (Onslow et al. 2011). To conduct a significance evaluation of the PAC values found, we shuffled the high frequency amplitude envelope signal. This procedure retained the mean, variance and power spectrum of the original signal but removed the temporal relationship between amplitude values. A set of fifty shuffled signals was created and compared to the original low frequency signal in order to generate a distribution of PAC values. PAC values lying in the top 5% of this distribution were deemed significant. After that, resulting correlations were corrected for multiple comparisons by controlling the false discovery rate and PAC grams were constructed, in which only significant relationships were presented.

The PAC computation was performed between one bipolar intracranial contact and 53 scalp channels from 1 to 100 Hz by steps of 1 Hz in a time window of 1 to 5 min of the artifact-free EEG, depending on the subject. Resulting PAC-grams were then pooled in spectral and spatial modes. Six frequency bins are presented: δ [1–4] Hz, θ [5–8] Hz, α [9–12] Hz, β [13–25] Hz, $\gamma 1$ [26–45] Hz, $\gamma 2$ [46–100] Hz). Concerning the spatial mode, the resulting PAC-grams based on 53 scalp channels were pooled into 13 regional diagrams.

A paired *t* test was used to assess the differences in the PAC between the left and right STNs. The significance level was set to 5%. The false discovery rate correction adjusting *p*-values to *q*-values was performed to correct for multiple testing, in which we controlled both the PAC-grams (N = 6*6) and the number of regions (N = 13). The procedure was implemented using CARTOOL software by Denis Brunet (https://sites.google.com/site/fbmlab/home), in-house MATLAB solution, and MATLAB toolbox for PAC estimation (Onslow et al. 2011).

Results

The PAC was identified in all subjects between the STN and cortical activity in both directions (see Figs. 1 and 2). Particularly, significant cross-structural correlations were detected between the phase of the LFP in the STN and the scalp-recorded cortical amplitude of the EEG (Fig. 3). On the other hand, significant cross-structural correlations between the signals were also detected in the opposite direction, i.e. between the cortical phase and STN

amplitude. Both positive and negative correlations were detected among the δ [1–4 Hz], θ [5–8 Hz], α [9–12 Hz], β [13–25 Hz], γ1 [26–45 Hz], and γ2 [46–100 Hz] frequency bands. Distinct group-level patterns of cross-structural PACs were observed with the highest significant correlations exceeding an absolute R-value of $2 * 10^{-3}$ (Figs. 1 and 2). The highest significant positive correlations occurred for both STNs between the δ/θ STN phase and β/γ cortical amplitude and they were detected mainly in the frontal, parietal and occipital scalp regions. Additionally, the highest significant negative correlations occurred for both STNs between the δ STN phase and θ/α cortical amplitude and they were detected dominantly in the frontal region (Fig. 1). Concerning the cortical phase—STN amplitude coupling, the highest significant positive correlations occurred only in the frontal and temporal regions between the δ cortical phase and θ/α STN amplitude mainly for the right STN; the highest significant negative correlations were detected solely in the parietal region between the δ/θ cortical phase and α/β/γ1 STN amplitude for the right STN (Fig. 2).

Within the frequency bands, where significant PAC correlations were identified, the results of the paired *t*-test on the group level across all subjects did not show any significant differences between the left and right STNs, neither in the STN phase—cortical amplitude nor in the cortical phase—STN amplitude couplings.

Discussion

The evidence of coupling between the δ/θ phase of the STN and the amplitude of higher frequency bins of the scalp-recorded electrophysiological brain activity is the main finding of the study. This result suggests the existence of a cross-frequency hierarchical functional linkage within the STN-cortical networks during resting conditions in humans.

On theoretical grounds, the coupling between the STN phase and cortical amplitude of neuronal activity represents a serious candidate for physiological functional interactions between these brain structures during resting conditions. The neuronal oscillations in the neocortex tend to couple hierarchically, with the phase of lower-frequency oscillations modulating the higher frequency amplitudes (Canolty et al. 2006). The lower-frequency phase determines momentary power in higher frequency activity. The PAC observed between the LFP-STN activity and the amplitude of the scalp-recorded activity could thus be considered as a manifestation of fluctuations of excitability in local neuronal assemblies in the cortex with rhythmic activity in the STN. This interpretation is in agreement with previously reported evidence of driving from the STN to the cortex in resting conditions (Williams 2002). It has been suggested that in the presence of dopaminergic activity, the STN may produce a high frequency 70–85 Hz drive to the cerebral cortex during resting conditions (Williams, 2002), thus demonstrating its active involvement in subcortico-cortical interactions. These frequency ranges are highly divergent from the δ/θ and θ/α bands observed in our study. Nevertheless, an important role of slow oscillations was also reported within the STN-related large-scale brain networks. The δ/θ coherence between the STN and the activity over the medial frontal cortex was shown to be involved in conflict and error monitoring (Zavala et al. 2014, 2016). It has also been suggested that the STN δ/θ oscillations may reflect inputs from cortical structures such as the medial prefrontal cortex (Cavanagh et al. 2011; Zavala et al. 2014; Kelley et al. 2018) that projects into the STN through a hyperdirect pathway (Smith et al. 1998).

In the current study, only the frontal regions revealed both positive and negative highly significant correlations with the STN activity. Specifically, the δ STN phase correlated positively with the β/γ frontal cortical amplitude and negatively with the θ/α frontal cortical amplitude. This finding suggests specific subcortico-cortical interactions between the STN and frontal cortex during resting conditions, distinguishing the frontal cortex from other cortical regions. Furthermore, the coupling between the δ phase over the frontal scalp regions and the amplitude of the θ STN oscillations reported here supports the top-down influence of the frontal cortex on the STN. The top-down functional linkage suggested here between these two structures during rest extends the reported driving of STN oscillations by the midline frontal cortex low-frequency activity during conflict (Zavala et al. 2014).

Our results rely on cross-frequency cross-structural coupling rather than on the previously reported coherence within the δ/θ band (Cavanagh et al. 2011; Zavala et al. 2014). Thus, the resting-state scalp-recorded higher frequency activity demonstrated here modulated in amplitude via the δ/θ STN oscillations provides support for the communication-by-nested-oscillation framework (Bonnefond et al. 2017). Our findings suggest that cross-frequency interactions are essential for understanding how resting-state STN-cortical networks operate.

We showed that the PAC was not stronger for the left or right STN in any scalp region. Thus, our results suggest a similar involvement of the left and right STNs in subcortico-cortical interactions. A recent study reported that α/β band oscillations and PAC within the STN were greater in the more affected hemisphere in PD patients (Shreve et al. 2017). In contrast to the study by Shreve et al. (2017), our patients were recorded during the on-medication state, where a reduced influence of PD on brain activity could be expected due to the exogenous dopaminergic input that

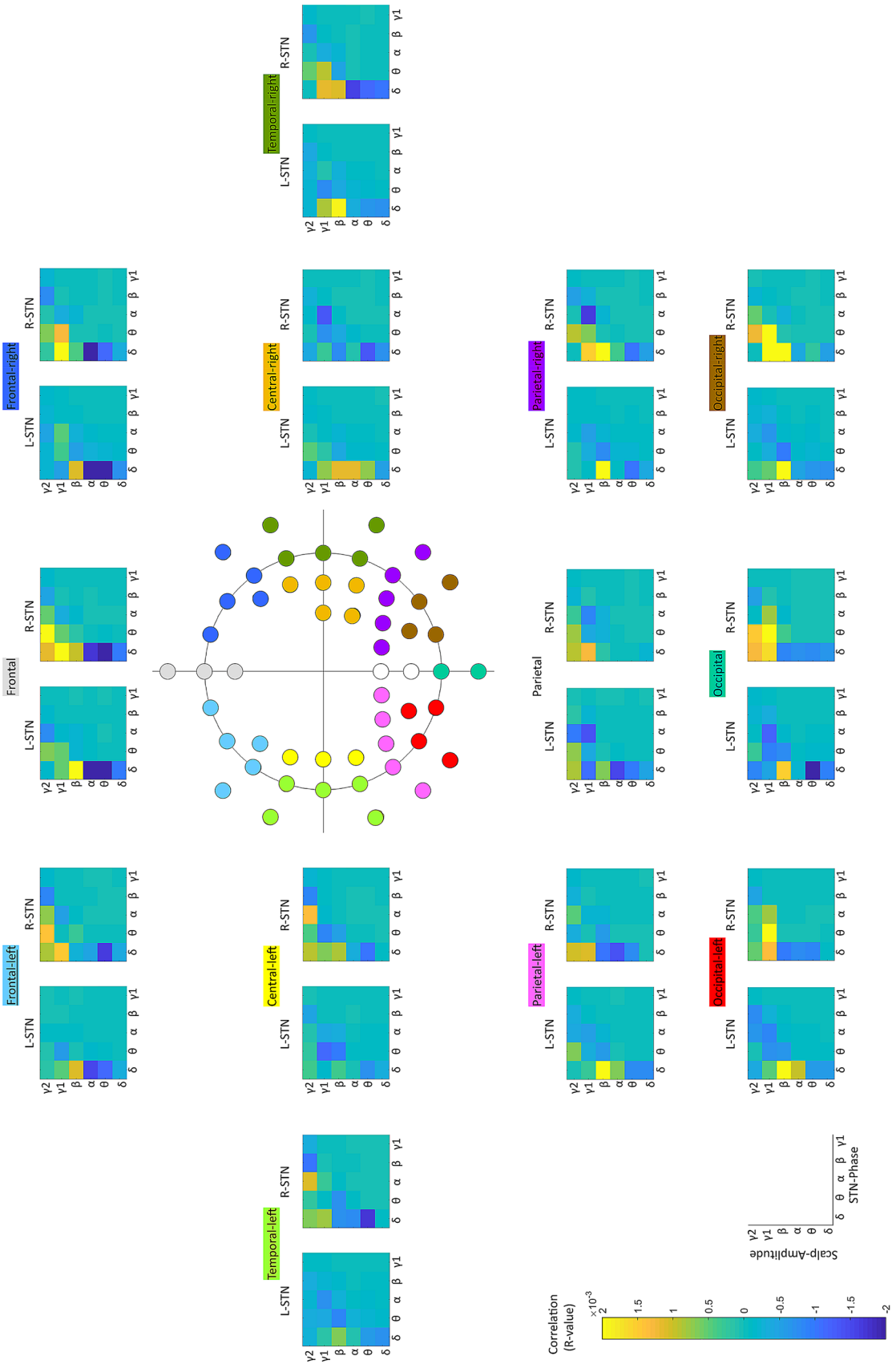

Fig. 1 Phase-amplitude coupling between the phase of the STN activity and the amplitude of the scalp-recorded activity averaged across 11 subjects. The color-coded regional pools out of 53 electrodes in the central scheme correspond to 13 highlighted phase-amplitude coupling diagrams. The highest positive significant correlations ($R > 2 * 10^{-3}$; bright yellow) occurred between the δ/θ STN phase and β/γ scalp amplitude, in most scalp regions for both STNs. The highest negative significant correlations ($R < -2 * 10^{-3}$; dark blue) occurred between the δ STN phase and θ/α scalp amplitude over the frontal cortex for both STNs and over the occipital cortex for the left STN. *STN* subthalamic nucleus, *L* left, *R* right

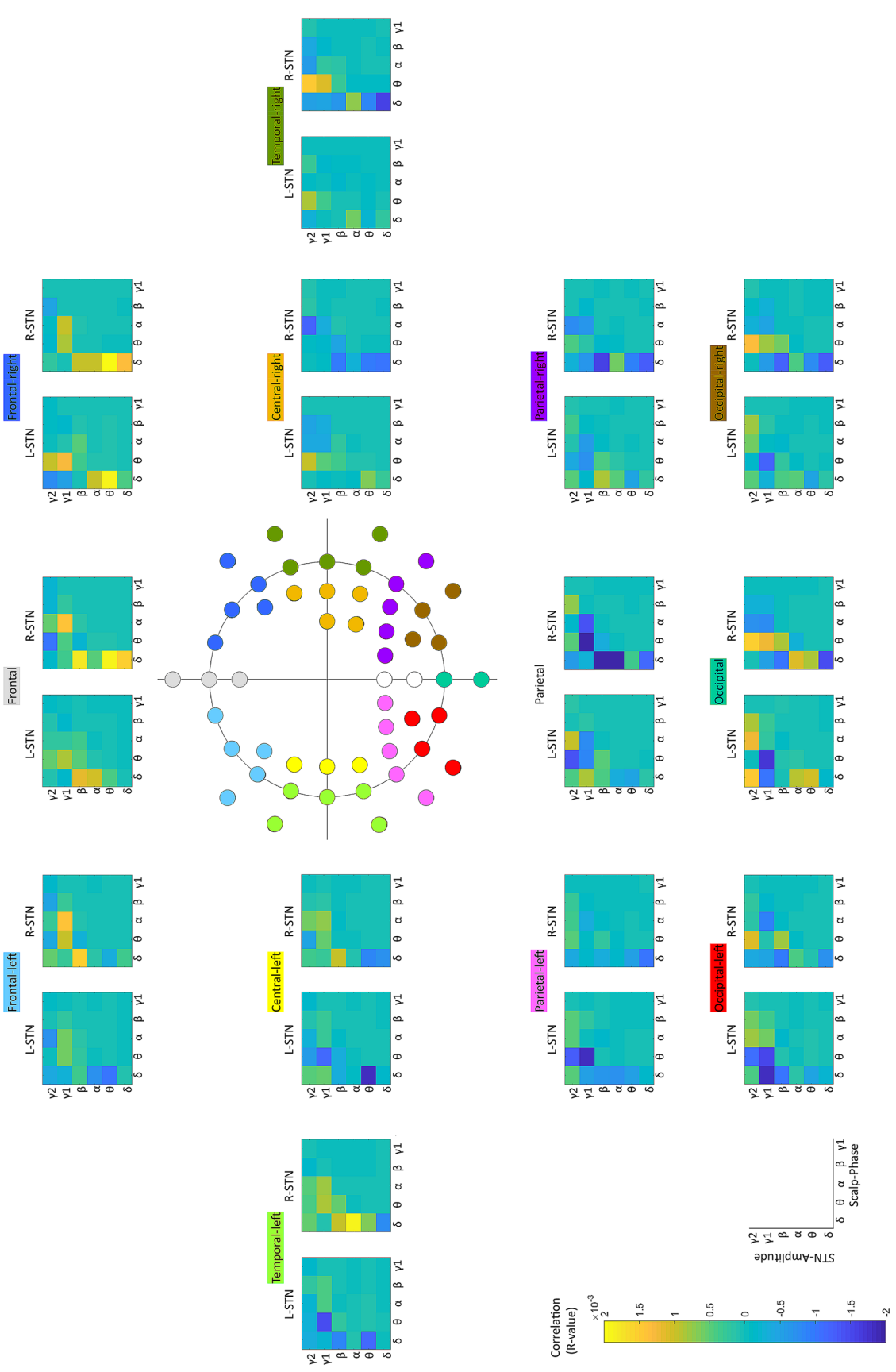

Fig. 2 Phase-amplitude coupling between the phase of the scalp recorded activity and the amplitude of the STN activity averaged across 11 subjects. The color-coded regional pools out of 53 electrodes in the central scheme correspond to 13 highlighted phase-amplitude coupling diagrams. The highest positive significant correlations ($R = 1.9 * 10^{-3}$; yellow) occurred between the δ scalp phase and θ/α STN amplitude, in the frontal and temporal regions mainly for the right STN. The highest negative significant correlations ($R < -2 * 10^{-3}$; dark blue) occurred between the δ/θ scalp phase and α/β/γ1 STN amplitude over the parietal cortex for the right STN. *STN* subthalamic nucleus, *L* left, *R* right

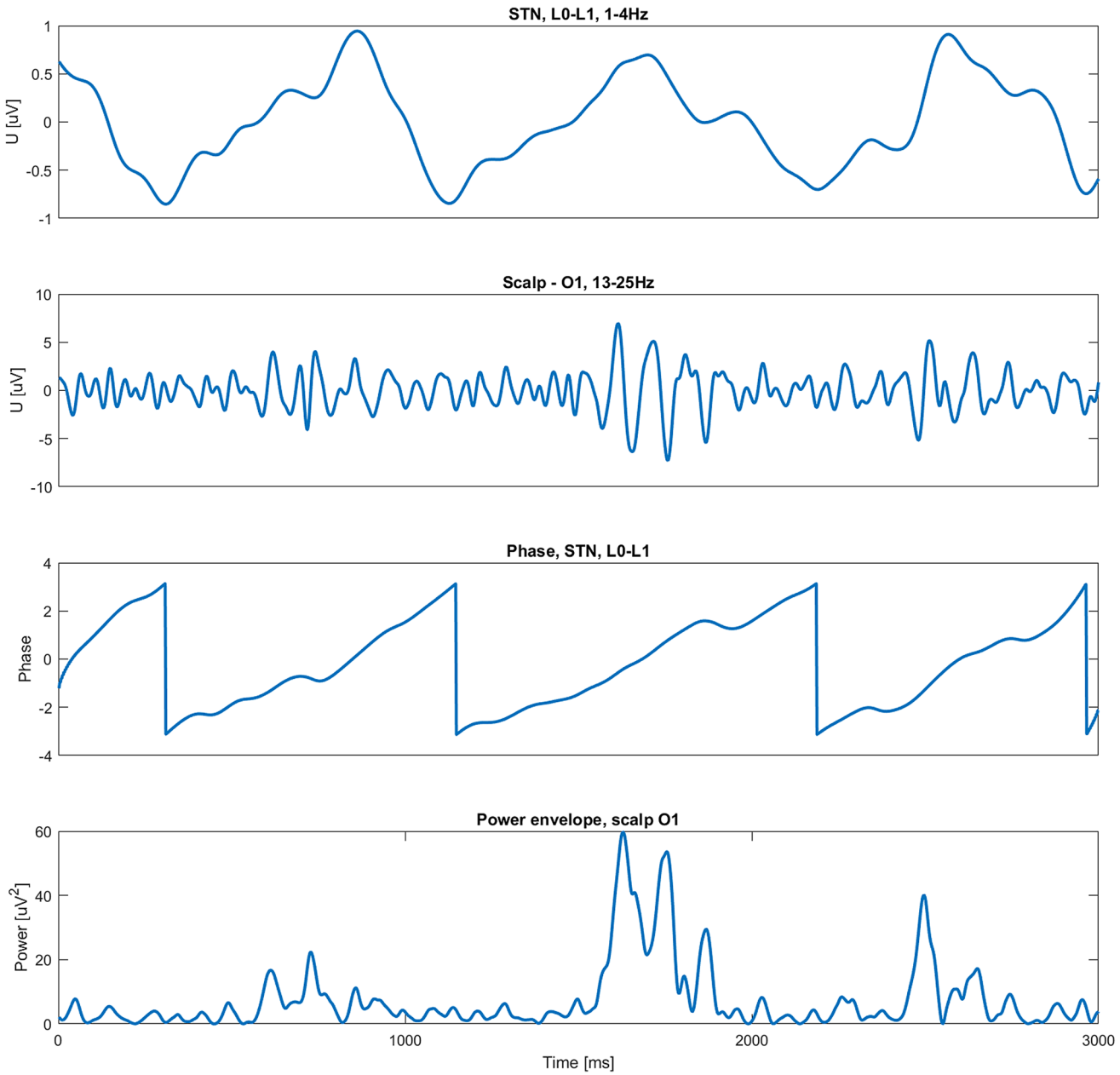

Fig. 3 Example of the phase-amplitude coupling between the STN and cortical activity—an empirical justification on data from subject 25. The local field potential signal and its phase in δ frequency range are presented in the first and third panels, respectively. The EEG-signal and its power envelope in β frequency range are presented in the second and fourth panels, respectively. Note periodic amplitude changes of the cortical activity (O1 channel) corresponding to the phase of the STN activity (L0-L1 channel). *STN* subthalamic nucleus, *L0–L1* bipolar lead in the left STN, *O1* the left occipital region electrode

is supposed to reverse the core deficit in PD. The fact that we observed no significant differences between the left and right STNs may represent electrophysiological evidence of relative symmetry in the STN-cortical functional linkage. Therefore, from the functional interaction perspective, both STNs might be similarly suitable for deep brain stimulation treatment of PD and one could even speculate that unilateral stimulation could be sufficient for treatment for PD at least in some patients. Practical treatment studies would be necessary to test the hypothesis of unilateral DBS efficacy.

We studied electrophysiological correlates of functional brain interactions on unique data that cannot be obtained from healthy humans due to ethical constraints. This approach proved to be fruitful in previous studies that investigated electrophysiological activity of large-scale brain

networks using intracranial data from epileptic (Damborská et al. 2012, 2016; Kukleta et al. 2009, 2010, 2017) and PD (Williams 2002; Zavala et al. 2013, 2014, 2015, 2016) patients. As in those studies, any inferences with regard to the normal functioning of the brain must be made with caution in the present study. We also admit that source imaging would have been better than correlation with electrode signals. This was, however, technically impossible given the missing signals close to the vertex. Large interpolation is another limitation of our study. In three patients (No. 1, 5, and 7; see Table 1) almost a quarter of the electrodes were interpolated. Such extensive interpolation might have led to erroneously reduced variability of PAC values among scalp regions. Furthermore, the PAC averaging employed here across different timescales (see the last column in Table 1) might have introduced unequal smoothing effects among subjects. Moreover, this averaging approach did not enable the study of the possible variability of PAC over time.

The results of the current study represent the first report on functional interaction in the cross-frequency domain between the STN low-frequency phase and cortical high-frequency amplitude in humans. This finding contributes to a better understanding of integrative processes reflecting fundamental self-organization within the brain. The cross-structural cross-frequency linkage in the STN-cortical circuits suggested here presents an interesting perspective for further research. If the cross-structural cross-frequency approach is applied both during on- and off-medication states, both before and after DBS stimulation, the relation to the clinical outcome could be evaluated, which could lead to new findings for a better understanding of the pathophysiology of PD.

Supplementary Information The online version of this article (https://doi.org/10.1007/s10548-021-00822-8) contains supplementary material, which is available to authorized users.

Acknowledgements The authors wish to thank Anne Johnson for providing language help.

Author Contributions A.D. designed the study, collected and preprocessed the data, and wrote the initial draft of the manuscript. M.L. analyzed the data. D.B. and S.V. served as consultants for the data analysis and clinical issues, respectively. B.D., M.Ba, and M.Bo collected the data. I.R. developed the initial idea. All authors reviewed the manuscript.

Funding The study was financially supported by the Czech Science Foundation Grant 21-25953S, by Grants FNS 192749 and CRSII5_170873, and by the Ministry of Education, Youth and Sports of the Czech Republic within the CEITEC 2020 (LQ1601) project.

Availability of Data and Material The data and material that support the findings of this study are available from the corresponding author upon reasonable request.

Code Availability The custom in-house MATLAB code is available from the corresponding author upon reasonable request. CARTOOL software by Denis Brunet is freely available https://sites.google.com/site/fbmlab/home.

Compliance with Ethical Standards

Competing interest The authors declare no competing interests.

Ethics Approval and Consent to Participate All participants gave their written informed consent prior to the experiment and the study received the approval of the ethics committee of St. Anne's Hospital in Brno. All experiments in this study were performed in accordance with relevant guidelines and regulations.

Consent for Publication Each author has read the complete manuscript and concurs with its content and publication.

References

Alonso-Frech F, Zamarbide I, Alegre M, Rodríguez-Oroz MC, Guridi J, Manrique M et al (2006) Slow oscillatory activity and levodopa-induced dyskinesias in Parkinson's disease. Brain 129:1748–1757. https://doi.org/10.1093/brain/awl103

Bočková M, Rektor I (2019) Impairment of brain functions in Parkinson's disease reflected by alterations in neural connectivity in EEG studies: a viewpoint. Clin Neurophysiol 130:239–247. https://doi.org/10.1016/j.clinph.2018.11.013

Bonnefond M, Kastner S, Jensen O (2017) Communication between brain areas based on nested oscillations. eNeuro. https://doi.org/10.1523/ENEURO.0153-16.2017

Brown P, Williams D (2005) Basal ganglia local field potential activity: character and functional significance in the human. Clin Neurophysiol 116:2510–2519. https://doi.org/10.1016/j.clinph.2005.05.009

Brown P, Oliviero A, Mazzone P, Insola A, Tonali P, Di Lazzaro V (2001) Dopamine dependency of oscillations between subthalamic nucleus and pallidum in Parkinson's disease. J Neurosci 21:1033–1038. https://doi.org/10.1523/jneurosci.21-03-01033.2001

Bruns A, Eckhorn R (2004) Task-related coupling from high- to low-frequency signals among visual cortical areas in human subdural recordings. Int J Psychophysiol 51:97–116

Canolty RT, Edwards E, Dalal SS, Soltani M, Nagarajan SS, Kirsch HE et al (2006) High gamma power is phase-locked to theta oscillations in human neocortex. Science 313:1626–1628. https://doi.org/10.1126/science.1128115

Castrioto A, Meaney C, Hamani C, Mazzella F, Poon YY, Lozano AM et al (2011) The Dominant-STN phenomenon in bilateral STN DBS for Parkinson's disease. Neurobiol Dis 41:131–137. https://doi.org/10.1016/j.nbd.2010.08.029

Cavanagh JF, Wiecki TV, Cohen MX, Figueroa CM, Samanta J, Sherman SJ, Frank MJ (2011) Subthalamic nucleus stimulation reverses mediofrontal influence over decision threshold. Nat Neurosci 14:1462–1467. https://doi.org/10.1038/nn.2925

Chen CC, Hsu YT, Chan HL, Chiou SM, Tu PH, Lee ST et al (2010) Complexity of subthalamic 13-35 Hz oscillatory activity directly correlates with clinical impairment in patients with Parkinson's disease. Exp Neurol 224:234–240. https://doi.org/10.1016/j.expneurol.2010.03.015

Damborská A, Brázdil M, Rektor I, Janoušová E, Chládek J, Kukleta M (2012) Late divergence of target and nontarget ERPs in a visual oddball task. Physiol Res 61:307–318

Damborská A, Roman R, Brázdil M, Rektor I, Kukleta M (2016) Post-movement processing in visual oddball task—evidence from intracerebral recording. Clin Neurophysiol 127:1297–1306. https://doi.org/10.1016/j.clinph.2015.08.014

De Hemptinne C, Ryapolova-Webb ES, Air EL, Garcia PA, Miller KJ, Ojemann JG et al (2013) Exaggerated phase-amplitude coupling in the primary motor cortex in Parkinson disease. Proc Natl Acad Sci USA 110:4780–4785

Engel AK, Fries P (2010) Beta-band oscillations-signalling the status quo? Curr Opin Neurobiol 20:156–165. https://doi.org/10.1016/j.conb.2010.02.015

Fogelson N, Williams D, Tijssen M, Van Bruggen G, Speelman H, Brown P (2006) Different functional loops between cerebral cortex and the subthalmic area in Parkinson's disease. Cereb Cortex 16:64–75. https://doi.org/10.1093/cercor/bhi084

Fries P (2005) A mechanism for cognitive dynamics: neuronal communication through neuronal coherence. Trends Cogn Sci 9:474–480. https://doi.org/10.1016/j.tics.2005.08.011

Germano IM, Gracies JM, Weisz DJ, Tse W, Koller WC, Olanow CW (2004) Unilateral stimulation of the subthalamic nucleus in Parkinson disease: a double-blind 12-month evaluation study. J Neurosurg 101:36–42. https://doi.org/10.3171/jns.2004.101.1.0036

Hammond C, Bergman H, Brown P (2007) Pathological synchronization in Parkinson's disease: networks, models and treatments. Trends Neurosci 30:357–364. https://doi.org/10.1016/j.tins.2007.05.004

Jensen O, Mazaheri A (2010) Shaping functional architecture by oscillatory alpha activity: gating by inhibition. Front Hum Neurosci. https://doi.org/10.3389/fnhum.2010.00186

Jung TP, Makeig S, Westerfield M, Townsend J, Courchesne E, Sejnowski TJ (2000) Removal of eye activity artifacts from visual event-related potentials in normal and clinical subjects. Clin Neurophysiol 111:1745–1758. https://doi.org/10.1016/S1388-2457(00)00386-2

Kelley R, Flouty O, Emmons EB, Kim Y, Kingyon J, Wessel JR et al (2018) A human prefrontal-subthalamic circuit for cognitive control. Brain 141:205–216

Kronland-Martinet R, Morlet J, Grossmann A (1987) Analysis of sound patterns through walvelet transforms. Int J Pattern Recognit Artif Intell 1:273–302

Kukleta M, Bob P, Brázdil M, Roman R, Rektor I (2009) Beta 2-band synchronization during a visual oddball task. Physiol Res 58:725–732

Kukleta M, Bob P, Brázdil M, Roman R, Rektor I (2010) The level of frontal-temporal beta-2 band EEG synchronization distinguishes anterior cingulate cortex from other frontal regions. Conscious Cogn 19:879–886. https://doi.org/10.1016/j.concog.2010.04.007

Kukleta M, Damborská A, Turak B, Louvel J (2017) Evoked potentials in final epoch of self-initiated hand movement: a study in patients with depth electrodes. Int J Psychophysiol 117:119–125. https://doi.org/10.1016/j.ijpsycho.2017.05.004

Lakatos P, Karmos G, Mehta AD, Ulbert I, Schroeder CE (2008) Entrainment of neuronal oscillations as a mechanism of attentional selection. Science 320:110–113. https://doi.org/10.1126/science.1154735

Lalo E, Thobois S, Sharott A, Polo G, Mertens P, Pogosyan A, Brown P (2008) Patterns of bidirectional communication between cortex and basal ganglia during movement in patients with Parkinson disease. J Neurosci 28:3008–3016. https://doi.org/10.1523/JNEUROSCI.5295-07.2008

Lisman JE, Jensen O (2013) The theta-gamma neural code. Neuron 77:1002–1016

Litvak V, Jha A, Eusebio A, Oostenveld R, Foltynie T, Limousin P et al (2011) Resting oscillatory cortico-subthalamic connectivity in patients with Parkinson's disease. Brain 134:359–374. https://doi.org/10.1093/brain/awq332

Marsden JF, Limousin-Dowsey P, Ashby P, Pollak P, Brown P (2001) Subthalamic nucleus, sensorimotor cortex and muscle interrelationships in Parkinson's disease. Brain 124:378–388. https://doi.org/10.1093/brain/124.2.378

Moran A, Bergman H, Israel Z, Bar-Gad I (2008) Subthalamic nucleus functional organization revealed by parkinsonian neuronal oscillations and synchrony. Brain 131:3395–3409. https://doi.org/10.1093/brain/awn270

Onslow ACE, Bogacz R, Jones MW (2011) Quantifying phase–amplitude coupling in neuronal network oscillations. Prog Biophys Mol Biol 105:49–57

Oswal A, Brown P, Litvak V (2013a) Synchronized neural oscillations and the pathophysiology of Parkinson's disease. Curr Opin Neurol 26:662–670. https://doi.org/10.1097/WCO.0000000000000034

Oswal A, Brown P, Litvak V (2013b) Movement related dynamics of subthalmo-cortical alpha connectivity in Parkinson's disease. Neuroimage 70:132–142. https://doi.org/10.1016/j.neuroimage.2012.12.041

Perrin F, Pernier J, Bertrand O, Echallier JF (1989) Spherical splines for scalp potential and current density mapping. Electroencephalogr Clin Neurophysiol 72:184–187. https://doi.org/10.1016/0013-4694(89)90180-6

Saalmann YB, Pinsk MA, Wang L, Li X, Kastner S (2012) The pulvinar regulates information transmission between cortical areas based on attention demands. Science 337:753–756

Sharott A, Gulberti A, Zittel S, Tudor-Jones AA, Fickel U, Münchau A et al (2014) Activity parameters of subthalamic nucleus neurons selectively predict motor symptom severity in Parkinson's disease. J Neurosci 34:6273–6285. https://doi.org/10.1523/JNEUROSCI.1803-13.2014

Shreve LA, Velisar A, Malekmohammadi M, Koop MM, Trager M, Quinn EJ et al (2017) Subthalamic oscillations and phase amplitude coupling are greater in the more affected hemisphere in Parkinson's disease. Clin Neurophysiol 128:128–137. https://doi.org/10.1016/j.clinph.2016.10.095

Slowinski JL, Putzke JD, Uitti RJ, Lucas JA, Turk MF, Kall BA, Wharen RE (2007) Unilateral deep brain stimulation of the subthalamic nucleus for Parkinson disease. J Neurosurg 106:626–632. https://doi.org/10.3171/jns.2007.106.4.626

Smith Y, Bevan MD, Shink E, Bolam JP (1998) Microcircuitry of the direct and indirect pathways of the basal ganglia. Neuroscience 86:353–387. https://doi.org/10.1016/S0306-4522(98)00004-9

Stein E, Bar-Gad I (2013) Beta oscillations in the cortico-basal ganglia loop during parkinsonism. Exp Neurol 245:52–59. https://doi.org/10.1016/j.expneurol.2012.07.023

Stoffers D, Bosboom JLW, Deijen JB, Wolters EC, Berendse HW, Stam CJ (2007) Slowing of oscillatory brain activity is a stable characteristic of Parkinson's disease without dementia. Brain 130:1847–1860

Stoffers D, Bosboom JLW, Deijen JB, Wolters EC, Stam CJ, Berendse HW (2008) Increased cortico-cortical functional connectivity in early-stage Parkinson's disease: an MEG study. Neuroimage 41:212–222. https://doi.org/10.1016/j.neuroimage.2008.02.027

Voytek B, Canolty RT, Shestyuk A, Crone NE, Parvizi J, Knight RT (2010) Shifts in gamma phase-amplitude coupling frequency from theta to alpha over posterior cortex during visual tasks. Front Hum Neurosci. https://doi.org/10.3389/fnhum.2010.00191

Williams D (2002) Dopamine-dependent changes in the functional connectivity between basal ganglia and cerebral cortex in humans. Brain 125:1558–1569. https://doi.org/10.1093/brain/awf156

Zavala B, Brittain JS, Jenkinson N, Ashkan K, Foltynie T, Limousin P et al (2013) Subthalamic nucleus local field potential activity

during the eriksen flanker task reveals a novel role for theta phase during conflict monitoring. J Neurosci 33:14758–14766. https://doi.org/10.1523/JNEUROSCI.1036-13.2013

Zavala BA, Tan H, Little S, Ashkan K, Hariz M, Foltynie T et al (2014) Midline frontal cortex low-frequency activity drives subthalamic nucleus oscillations during conflict. J Neurosci 34:7322–7333. https://doi.org/10.1523/JNEUROSCI.1169-14.2014

Zavala B, Damera S, Dong JW, Lungu C, Brown P, Zaghloul KA (2015) Human subthalamic nucleus theta and beta oscillations entrain neuronal firing during sensorimotor conflict. Cereb Cortex 27:496–508. https://doi.org/10.1093/cercor/bhv244

Zavala B, Tan H, Ashkan K, Foltynie T, Limousin P, Zrinzo L et al (2016) Human subthalamic nucleus-medial frontal cortex theta phase coherence is involved in conflict and error related cortical monitoring. Neuroimage 137:178–187. https://doi.org/10.1016/j.neuroimage.2016.05.031

Publisher's Note Springer Nature remains neutral with regard to jurisdictional claims in published maps and institutional affiliations.

5.2 Resting-state large-scale brain networks in affective disorders

Affective disorders, including major depressive disorder (MDD) and bipolar disorder (BD), are among the most serious psychiatric disorders with high prevalence and illness-related disability (Andrade et al., 2003). Evidence across resting-state functional magnetic resonance (fMRI) studies consistently points to an impairment of large-scale resting-state brain networks in affective disorders rather than a disruption of discrete brain regions (Gong & He, 2015; Iwabuchi et al., 2015; Kaiser et al., 2015). In general, large-scale networks dynamically re-organize themselves on sub-second temporal scales to enable efficient functioning (De Pasquale et al., 2018; Bressler & Menon, 2010). Fast temporal dynamics of large-scale neuronal networks, not accessible with the low temporal resolution of the fMRI technique, can be investigated by analyzing the temporal characteristics of "EEG microstates" (Michel & Koenig, 2018; Van de Ville et al., 2010). Assessment of the temporal characteristics of these microstates provides information about the dynamics of large-scale brain networks because this technique simultaneously considers signals recorded from all areas of the cortex. Since the temporal variation in resting-state brain network dynamics may be a significant biomarker of illness and therapeutic outcome (Hutchison et al., 2013; Chang & Glover, 2010), microstate analysis is a highly suitable tool for this purpose. Numerous studies demonstrated changes in EEG microstates in patients with neuropsychiatric disorders such as schizophrenia, dementia, panic disorder, and multiple sclerosis (Michel & Koenig, 2018). Nevertheless, until recently, microstates in depressive patients were investigated only in three studies (Strik et al., 1995; Ihl & Brinkmeyer, 1999; Atluri et al., 2018). No sooner than in our study (Damborská et al., 2019 b – Annex 10), it was shown that interindividual differences in resting-state microstate parameters could reflect altered large-scale brain network dynamics relevant to depressive symptomatology during a depressive episode. Our findings immediately inspired more than twenty research teams worldwide that cited our work when testing microstate features, as candidate biomarkers of te depressive syndrome within mental disorders (e.g., Murphy et al., 2020; He et al., 2021; Lei et al., 2022) and predictors of antidepressant treatment response (e.g., Yan et al., 2021; Lei et al., 2022).

Biomarkers that are investigated during a depressive episode, i.e., relapse of affective disorder, reflect the actual state of the impaired brain. On the contrary, trait

markers of affective disorders are studied during euthymia, i.e., the periods of remission, and can be considered as biomarkers of illness per se (Piguet et al., 2016; Berchio et al., 2017). In our next research, we focused on trait markers of affective disorders and performed the first resting-state microstate study on euthymic BD patients (Damborská et al., 2019 c - Annex 11). We observed an increased presence of A microstate, suggesting it to be an electrophysiological trait characteristic of BD. We suggested that the increased presence of A microstate in euthymic BD patients might be related to the hyperconnectivity of the underlying networks involving the temporal lobe, insula, mPFC, and occipital gyri (Custo et al., 2017; Bréchet et al., 2019).

A crucial role of the cortico-striatal-pallidal-thalamic and limbic circuits in the neurobiology of depression was repeatedly reported (Bora et al., 2012; Yang et al., 2017; Zhang et al., 2016). Neuroimaging studies have confirmed that depressive patients show structural impairments and functional dysbalances of brain networks that involve structures engaged in (a) emotions, i.e., amygdala, subgenual anterior cingulate, caudate, putamen and pallidum (Yang et al., 2017; Disner et al., 2011; Surguladze et al, 2005; Sheline et al., 2001; Siegle et al., 2007; Nugent et al., 2015; Knyazev et al., 2018; Lu et al., 2016; Kim et al., 2008); (b) self-referential processes, i.e., medial prefrontal cortex, precuneus, and posterior cingulate cortex (Sheline et al., 2010; Kühn & Gallinat, 2013); (c) memory, i.e., hippocampus, parahippocampal cortex (Lorenzetti et al., 2009); (d) visual processing, i.e., fusiform gyrus, lingual gyrus, and lateral temporal cortex (Veer et al., 2010); and (e) attention, i.e., dorsolateral prefrontal cortex, anterior cingulate cortex (ACC), thalamus, and insula (Knyazev et al., 2018; Lu et al., 2016; Kim et al., 2008; Hamilton et al., 2012). Moreover, post-mortem morphometric measurements revealed smaller volumes of the hypothalamus, pallidum, putamen and thalamus in patients with affective disorders (Bielau et al., 2005).

Even with the multitude of noninvasive methods used to treat depression, a significant portion of patients fail to respond, resulting in an estimated 1–3% prevalence of treatment-resistant depression (TRD) (Holtzheimer & Mayberg 2011). Nevertheless, growing evidence suggests that direct stimulation of deep brain structures involved in the neurobiology of depression improves symptoms of TRD (Drobisz & Damborská 2019 – Annex 14, Chapter 6). Connectivity properties of deep

brain structures potentially implicated in invasive deep brain stimulation (DBS) treatment are, however, not fully understood yet. Directionality of connections, which might be of interest when considering a structure as a potential DBS-target for treatment of TRD, can be inferred from functional brain mapping studies. There are several EEG-based connectivity studies focusing on depressive symptoms (Sun et al., 2008; Tang et al., 2011; Wang et al., 2015; Ferdek et al., 2016) that are, however, conducted only on a non-clinical population (Ferdek et al., 2016) or with connectivity parameters calculated at the sensor level (Sun et al., 2008; Tang et al., 2011; Wang et al., 2015). Authors of one of these studies (Ferdek et al., 2016) suggest an inability of the left dorsolateral prefrontal cortex to modulate the activation of the left temporal lobe structures to be a crucial condition for ruminative tendencies. Interestingly, an abnormal increase in directed functional connectivity arising from the right amygdala during resting condition was demonstrated in our recent study (Damborská et al., 2020 – Annex 12). This increased resting-state connectivity in depressive patients could reflect an abnormal functioning of the right amygdala. Such dysfunction might represent an impaired bottom-up signalling for top-down cortical modulation of limbic regions, leading to an abnormal affect regulation in depressive patients. Our findings support the view that the amygdala might play an important role in the neurobiology of depression. Nevertheless, practical treatment studies would be necessary to assess the amygdala as a potential future DBS target for treating depression.

Annex 10

Damborská, A., Tomescu, M.I., Honzírková, E., Barteček, R., Hořínková, J., Fedorová, S., Ondruš Š., Michel C.M. (2019b). EEG resting-state large-scale brain network dynamics are related to depressive symptoms. *Frontiers in Psychiatry*, 548 (10)
IF(2019) = 2.849, rank Q2
Quantitative contribution: 90%
Content contribution: development of the initial idea, design of the study, supervision on data acquisition, pre-processing, analysis, statistical evaluation, writing the initial draft, table and figure preparation, corresponding author

Annex 11

Damborská, A., Piguet, C., Aubry, J-M., Dayer, A.G., Michel C.M., Berchio, C. (2019c). Altered EEG resting-state large-scale brain network dynamics in euthymic bipolar disorder patients. *Frontiers in Psychiatry*, 826 (10)
IF(2019) = 2.849, rank Q2
Quantitative contribution: 80%

Content contribution: development of the initial idea, pre-processing, analysis, statistical evaluation, writing the initial draft, table and figure preparation, corresponding author

Annex 12

Damborská, A., Honzírková, E., Barteček R., Hořínková J., Fedorová, S., Ondruš, Š., Michel, C.M., Rubega, M. (2020). Altered directed functional connectivity of the right amygdala in depression: high-density EEG study. *Scientific Reports*, 4398 (10)
IF(2020) = 4.379, rank Q1
Quantitative contribution: 60%
Content contribution: development of the initial idea, design of the study, supervision on data acquisition, pre-processing, participation in writing the initial draft, participation in table and figure preparation, corresponding author

Annex 10

Damborská, A., Tomescu, M.I., Honzírková, E., Barteček, R., Hořínková, J., Fedorová, S., Ondruš Š., Michel C.M. (2019b). EEG resting-state large-scale brain network dynamics are related to depressive symptoms. *Frontiers in Psychiatry*, 548 (10)

frontiers in Psychiatry

ORIGINAL RESEARCH
published: 09 August 2019
doi: 10.3389/fpsyt.2019.00548

EEG Resting-State Large-Scale Brain Network Dynamics Are Related to Depressive Symptoms

Alena Damborská[1,2], Miralena I. Tomescu[1], Eliška Honzírková[2], Richard Barteček[2], Jana Hořínková[2], Sylvie Fedorová[2], Šimon Ondruš[2] and Christoph M. Michel[1,3]*

[1] Department of Basic Neurosciences, Campus Biotech, University of Geneva, Geneva, Switzerland, [2] Department of Psychiatry, Faculty of Medicine, Masaryk University and University Hospital Brno, Brno, Czechia, [3] Lemanic Biomedical Imaging Centre (CIBM), Geneva, Switzerland

Background: The few previous studies on resting-state electroencephalography (EEG) microstates in depressive patients suggest altered temporal characteristics of microstates compared to those of healthy subjects. We tested whether resting-state microstate temporal characteristics could capture large-scale brain network dynamic activity relevant to depressive symptomatology.

Methods: To evaluate a possible relationship between the resting-state large-scale brain network dynamics and depressive symptoms, we performed EEG microstate analysis in 19 patients with moderate to severe depression in bipolar affective disorder, depressive episode, and recurrent depressive disorder and in 19 healthy controls.

Results: Microstate analysis revealed six classes of microstates (A–F) in global clustering across all subjects. There were no between-group differences in the temporal characteristics of microstates. In the patient group, higher depressive symptomatology on the Montgomery–Åsberg Depression Rating Scale correlated with higher occurrence of microstate A (Spearman's rank correlation, $r = 0.70$, $p < 0.01$).

Conclusion: Our results suggest that the observed interindividual differences in resting-state EEG microstate parameters could reflect altered large-scale brain network dynamics relevant to depressive symptomatology during depressive episodes. Replication in larger cohort is needed to assess the utility of the microstate analysis approach in an objective depression assessment at the individual level.

Keywords: EEG microstates, large-scale brain networks, resting state, dynamic brain activity, major depressive disorder, bipolar disorder

OPEN ACCESS

Edited by:
Roberto Esposito, A.O. Ospedali Riuniti Marche Nord, Italy

Reviewed by:
Olga V. Martynova, Institute of Higher Nervous Activity and Neurophysiology (RAS), Russia
Jarod L. Roland, Washington University in St. Louis, United States

****Correspondence:***
Alena Damborská
adambor@med.muni.cz

Specialty section:
This article was submitted to Neuroimaging and Stimulation, a section of the journal Frontiers in Psychiatry

Received: *23 March 2019*
Accepted: *15 July 2019*
Published: *09 August 2019*

Citation:
Damborská A, Tomescu MI, Honzírková E, Barteček R, Hořínková J, Fedorová S, Ondruš Š and Michel CM (2019) EEG Resting-State Large-Scale Brain Network Dynamics Are Related to Depressive Symptoms. Front. Psychiatry 10:548. doi: 10.3389/fpsyt.2019.00548

INTRODUCTION

Major depressive disorder (MDD) and bipolar disorder are among the most serious psychiatric disorders with high prevalence and illness-related disability (1–3). Despite growing evidence for the spectrum concept of mood disorders (4), and even with the advanced neuroimaging methods developed in recent years, the underlying pathophysiological mechanisms of depression remain poorly understood. Evidence across resting-state functional magnetic resonance (fMRI) studies consistently points to an impairment of large-scale resting-state brain networks in MDD rather than a disruption of discrete brain regions (5–8). Consistent with the neurobiological model of depression (9),

numerous resting-state fMRI studies show decreased frontal cortex function and increased limbic system function in patients with MDD (10). Functional abnormalities in large-scale brain networks include hypoconnectivity within the frontoparietal network (7) and the reward circuitry, centered around the ventral striatum (11). Reduced functional connectivity in first-episode drug-naïve patients with MDD was also recently reported between the frontoparietal and cingulo-opercular networks (12). Moreover, hyperconnectivity of the default mode network (13) and amygdala hyperconnectivity with the affective salience network (14, 15) were shown to be characteristic features of depression.

In general, large-scale networks dynamically re-organize themselves on sub-second temporal scales to enable efficient functioning (16, 17). Fast temporal dynamics of large-scale neural networks, not accessible with the low temporal resolution of the fMRI technique, can be investigated by analyzing the temporal characteristics of "EEG microstates" (18, 19). Scalp EEG measures the electric potential generated by the neuronal activity in the brain with a temporal resolution in the millisecond range. A sufficient number of electrodes distributed over the scalp, i.e., high density-EEG (HD-EEG), allows for the reconstruction of a scalp potential map representing the global brain activity (20). Any change in the map topography reflects a change in the distribution and/or orientation of the active sources in the brain (21). Already in 1987 (22), Lehmann et al. observed that in spontaneous resting-state EEG, the topography of the scalp potential map remains stable for a short period of time and then rapidly switches to a new topography in which it remains stable again. Ignoring map polarity, the duration of these stable topographies is around 80–120 ms. Lehmann called these short periods of stability EEG microstates and attributed them to periods of synchronized activity within large-scale brain networks. For a recent review, see Ref. (19). Assessment of the temporal characteristics of these microstates provides information about the dynamics of large-scale brain networks, because this technique simultaneously considers signals recorded from all areas of the cortex. Since the temporal variation in resting-state brain network dynamics may be a significant biomarker of illness and therapeutic outcome (23–25), microstate analysis is a highly suitable tool for this purpose.

Numerous studies demonstrated changes in EEG microstates in patients with neuropsychiatric disorders such as schizophrenia, dementia, panic disorder, multiple sclerosis, and others [for reviews see Refs. (19, 26)]. Despite the potential of microstate analysis for detecting global brain dynamic impairment, microstates were not investigated in depressive patients, except for three studies that provided inconsistent results. Using adaptive segmentation of resting state EEG in depressive patients, two early studies showed abnormal microstate topographies and reduced overall average microstate duration (27) but unchanged numbers of different microstates per second (28). In a more recent study using a topographical atomize-agglomerate hierarchical clustering algorithm, abnormally increased overall microstate duration and decreased overall microstate occurrence per second were reported in treatment-resistant depression (29).

A better understanding of disruption and changes in brain network dynamics in depression is critical for developing novel and targeted treatments, e.g., deep brain stimulation in treatment-resistant depression (30). Furthermore, microstate features reflecting the disruption of brain network dynamics might be later tested as candidate biomarkers of depressive disorder and predictors of treatment response. Thus, the main goal of our study was to explore how resting-state microstate dynamics are affected in depressive patients as compared to healthy individuals. We hypothesized that patients with depression will show different microstate dynamics than healthy controls in terms of the temporal characteristics of EEG microstates such as duration, coverage, and occurrence. We also hypothesized that microstate dynamics will be related to the overall clinical severity of depression.

MATERIALS AND METHODS

Subjects

Data was collected from 19 depressive patients (age in years: mean = 53.0, standard deviation = 9.8; 6 females) and 19 healthy control (HC) subjects (age in years: mean = 51.4, standard deviation = 9.1; 6 females). Education was classified into three levels: 1 = no high school, 2 = high school, 3 = university studies in the depressed (mean = 1.9, standard deviation = 0.9) and HC (mean = 2.2, standard deviation = 0.7) groups. There were no differences in gender, and an independent sample *t*-test also showed no significant differences in age [*t*-value (df 36) = 0.45, $p > 0.05$] or education [*t*-value (df 36) = −1.5, $p > 0.05$] between the two groups. The patients were recruited at the Department of Psychiatry, Faculty of Medicine, Masaryk University and University Hospital Brno. The diagnostic process had two steps and was determined based on the clinical evaluation by two board-certified psychiatrists. First, the diagnosis was made according to the criteria for research of the International Classification of Disorders (ICD-10). Second, the diagnosis was confirmed by the Mini International Neuropsychiatric interview (M.I.N.I.) according to the *Diagnostic and Statistical Manual of Mental Disorders, Fifth Edition* (DSM-V). All patients were examined in the shortest time period after the admission and before the stabilisation of treatment, typically during their first week of hospitalization. All patients met the criteria for at least a moderate degree of depression within the following affective disorders: bipolar affective disorder (F31), depressive episode (F32), and recurrent depressive disorder (F33). Exclusion criteria for patients were any psychiatric or neurological comorbidity, IQ < 70, organic disorder with influence on the brain function, alcohol dependence, or other substance dependence. All patients were in the on-medication state with marked interindividual variability in specific medicaments received. The patient characteristics are summarized in **Table 1**. Control subjects were recruited by general practitioners from their database of clients. Control subjects underwent the M.I.N.I. by board-certified psychiatrists to ensure that they had no previous or current psychiatric disorder according to the DSM-V criteria. The scores on the Montgomery–Åsberg Depression Rating Scale (MADRS), a specific questionnaire validated for patients with mood disorders

TABLE 1 | Patient characteristics.

Patient	ICD-10 diagnose	Number of episodes	Illness duration (years)	MADRS score	CGI score	BZD	AD/AP/MS	Medication scale AD/AP/MS
1	F31.4	3	2	27	4	2	AD, AP, MS	3
2	F32.2	1	0.5	24	5	0	AD	2
3	F32.1	1	1	15	4	2	AD	2
4	F31.5	5	20	39	6	0	AP	2
5	F33.1	3	7	18	4	0	AD	1
6	F33.1	2	8	9	3	1.33	AD	1
7	F32.1	1	1	24	4	1.33	AD, AP	3
8	F31.4	4	27	29	5	2	AP	2
9	F33.3	2	5	36	6	1	AD, AP	4
10	F33.1	3	19	21	4	1	AD	1
11	F33.3	2	2	38	5	6	AD, AP	4
12	F33.2	2	1	39	5	3	AD, AP	4
13	F32.3	1	0.08	21	5	2	AD, AP	4
14	F33.2	5	21	32	5	0	AD, AP	3
15	F33.3	2	2	38	6	3	AD, AP	4
16	F32.3	1	0.08	37	6	2	AD, AP	4
17	F33.1	3	4	18	4	0	AD, AP	4
18	F31.3	2	16	28	4	0	AP, MS	4
19	F31.3	11	24	23	4	1	AP, MS	4

F31.3, Bipolar affective disorder, current episode mild or moderate depression; F31.4, Bipolar affective disorder, current episode severe depression without psychotic symptoms; F31.5, Bipolar affective disorder, current episode severe depression with psychotic symptoms; F32.1, Moderate depressive episode; F32.2, Severe depressive episode without psychotic symptoms; F32.3, Severe depressive episode with psychotic symptoms; F33.1, Recurrent depressive disorder, current episode moderate; F33.2, Recurrent depressive disorder, current episode severe without psychotic symptoms; F33.3, Recurrent depressive disorder, current episode severe with psychotic symptoms; BZD, benzodiazepine equivalent dose (31); AD, antidepressants (mirtazapine, citalopram, venlafaxine, vortioxetine, sertraline); AP, antipsychotics (risperidone, olanzapine, quetiapine, amisulpride, aripiprazole); MS, mood stabilizers (valproate, lamotrigine); medication scale AD/AP/MS: 1, one medication in sub-therapeutic doses; 2, one medication in therapeutic doses; 3, combination of medications with one in therapeutic doses; 4, combination of medications with more than one in therapeutic doses; MADRS (Montgomery–Åsberg Depression Rating Scale): score is between 0 and 60, the higher the score the higher the depressive symptom severity; CGI (Clinical Global Impression) scale: healthy (1) – most extremely ill (7). Four patients were undergoing the first (patient 3) and second (patients 4 and 9) week of electroconvulsive therapy and the first week of repetitive transcranial magnetic stimulation (patient 5). No clinical effect of these neurostimulation treatments was apparent.

(32), and Clinical Global Impression (CGI) (33), a general test validated for mental disorders, were used to evaluate the severity of depressive symptoms in patients. The status of depression was further described with lifetime count of depressive episodes and illness duration in years. Medication in 24 h preceding the EEG examination was also recorded (see **Table 1**). This study was carried out in accordance with the recommendations of Ethics Committee of University Hospital Brno with written informed consent from all subjects. All subjects gave written informed consent in accordance with the Declaration of Helsinki. The protocol was approved by the Ethics Committee of University Hospital Brno, Czech Republic.

EEG Recording and Pre-processing

Subjects were sitting in a comfortable upright position in an electrically shielded room with dimmed light. They were instructed to stay as calm as possible to keep their eyes closed and to relax for 15 min. They were asked to stay awake. All participants were monitored by the cameras, and in the event of signs of nodding off or EEG signs of drowsiness detected by online visual inspection, the recording was stopped. The EEG was recorded with a high density 128-channel system (EGI System 400; Electrical Geodesic Inc., OR, USA), a sampling rate of 1kHz, and Cz as acquisition reference.

Five minutes of the EEG data were selected based on visual assessment of the artifacts. The EEG was band-pass filtered between 1 and 40 Hz. Subsequently, in order to remove ballistocardiogram and oculo-motor artifacts, infomax-based Independent Component Analysis (34) was applied to all but one or two channels rejected due to abundant artifacts. Only components related to ballistocardiogram, saccadic eye movements, and eye blinking were removed based on the waveform, topography, and time course of the component. The cleaned EEG recording was down-sampled to 125 Hz, and the previously identified noisy channels were interpolated using a three-dimensional spherical spline (35) and re-referenced to the average reference. For subsequent analyses, the EEG data was reduced to 110 channels to remove muscular artifacts originating in the neck and face. All the preprocessing steps were done using the freely available Cartool Software 3.70, programmed by Denis Brunet Cartool (https://sites.google.com/site/cartoolcommunity/home) and MATLAB.

Microstate Analysis

The microstate analysis (see **Figure 1**) followed the standard procedure using *k*-means clustering method to estimate the optimal set of topographies explaining the EEG signal (36–38). The polarity of the maps was ignored in this clustering procedure. To determine the optimal number of clusters, we applied a meta-criterion that is a combination of seven independent optimization criteria [for details see Ref. (39)]. In order to improve the signal-to-noise ratio, only the data at the time points of the local

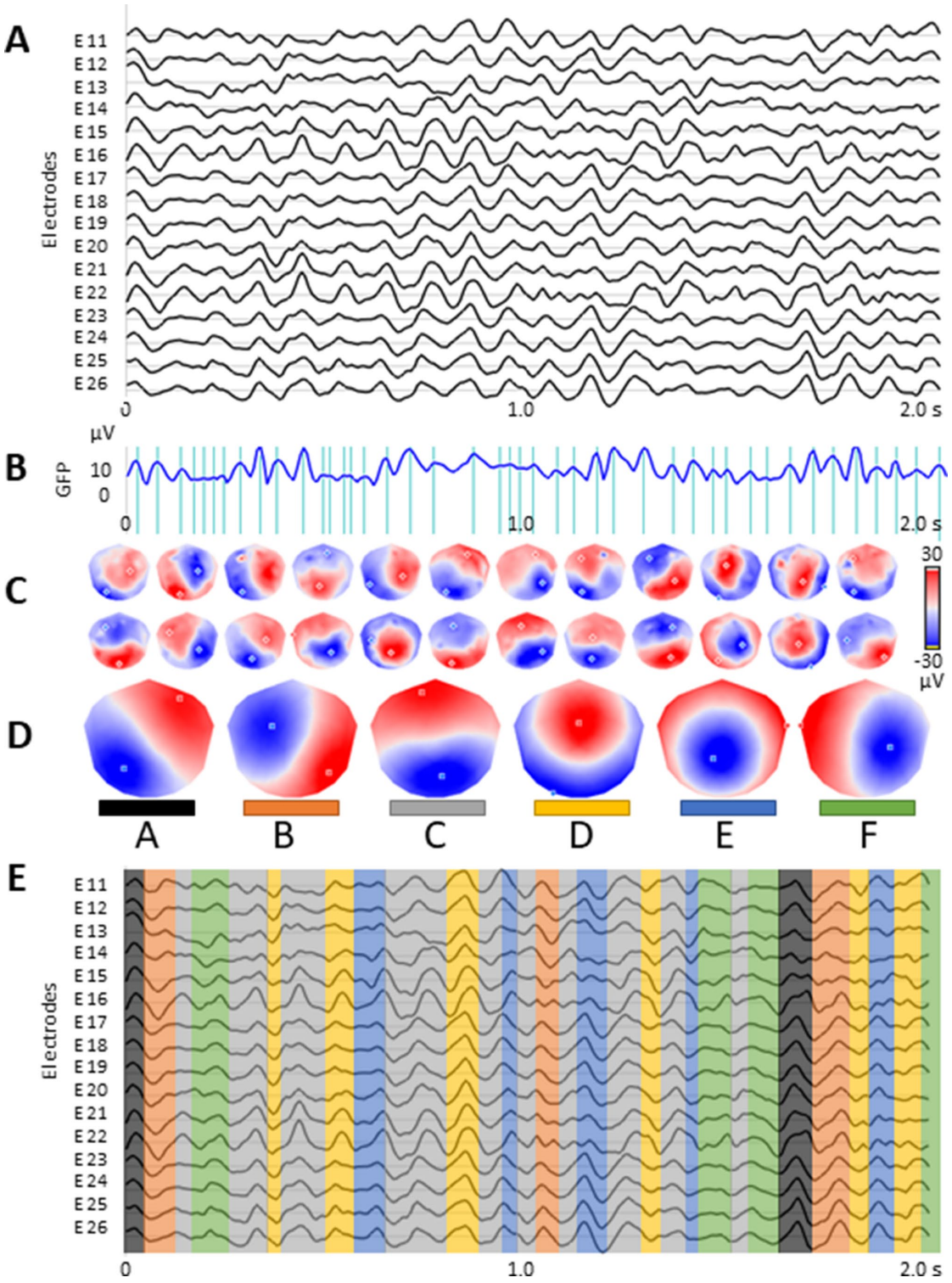

FIGURE 1 | Microstate analysis: **(A)** resting-state EEG from subsample of 16 out of 110 electrodes; **(B)** global field power (GFP) curve with the GFP peaks (vertical lines) in the same EEG period as shown in **(A)**; **(C)** potential maps at successive GFP peaks, indicated in **(B)**, from the first 1 s period of the recording; **(D)** set of six cluster maps best explaining the data as revealed by K-means clustering of the maps at the GFP peaks; **(E)** the original EEG recording shown in **(A)** with superimposed color-coded microstate segments. Note that each time point of the EEG recording was labelled with the cluster map, shown in **(D)**, with which the instant map correlated best. The duration of segments, occurrence, and coverage for all microstates were computed on thus labeled EEG recording.

maximum of the global field power (GFP) were clustered (38, 40–42). The GFP is a scalar measure of the strength of the scalp potential field and is calculated as the standard deviation of all electrodes at a given time point (36, 37, 43). The cluster analysis was first computed at the individual level and then at global level across all participants (patients and controls).

Spatial correlation was calculated between every map identified at the global level and the individual subject's topographical map in every instant of the pre-processed EEG recording. Each continuous time point of the subject's EEG (not only the GFP peaks) was then assigned to the microstate class of the highest correlation, again ignoring polarity (19, 36, 39, 44). Temporal smoothing parameters [window half size = 3, strength (Besag Factor) = 10] ensured that the noise during low GFP did not artificially interrupt the temporal segments of stable topography (36, 38). For each subject, three temporal parameters were then calculated for each of the previously identified microstates: i) occurrence, ii) coverage, and iii) duration. Occurrence indicates how many times a microstate class recurs in 1 s. The coverage represents the summed amount of time spent in a given microstate class. The duration in milliseconds for a given microstate class indicates the amount of time that a given microstate class is continuously present. In order to assess the extent to which the representative microstate topographies explain the original EEG data, the global explained variance (GEV) was calculated as the sum of the explained variances of each microstate weighted by the GFP. Microstate analysis was performed using the freely available Cartool Software 3.70, programmed by Denis Brunet Cartool (https://sites.google.com/site/cartoolcommunity/home).

Statistical Analysis

To investigate group differences, independent *t*-tests were used for temporal parameters of each microstate. Comparisons were corrected using the false discovery rate (FDR) method (45). In order to evaluate the possible relation of microstate dynamics to severity of depression, we computed Spearman's rank correlation coefficients of all microstate parameters with the MADRS and CGI scores and number of episodes. In order to evaluate possible influence of medication on microstate dynamics, we calculated Spearman's rank correlation coefficients between all microstate parameters and medication that patients received during 24 h preceding the EEG measurement. Intake of antidepressants, antipsychotics, and mood stabilizers was indicated as a single ordinal variable taking into account the number of medicaments and their dosages. Intake of benzodiazepines was expressed with the benzodiazepine equivalent dose (33). A significance level of $\alpha < 0.01$ was used for all correlations. Statistical evaluation of the results was performed by the routines included in the program package Statistica'13 (1984-2018, TIBCO, Software Inc, Version 13.4.0.14).

RESULTS

The meta-criterion used to determine the most dominant topographies revealed six microstates explaining 82.6% of the global variance. Four topographies resembled those previously reported in the literature as A, B, C, and D maps (19, 29, 40, 41) and two topographies resembled the recently identified (46) resting-state microstate maps. We labeled these maps as A–D, in accordance with previous literature, and as E and F (**Figure 2**).

The groups did not differ in any temporal parameter in any microstate. The depressive group was indistinguishable from the control group (all absolute *t*-values < 2.5). The FDR-corrected *p*-values (six comparisons for the six microstate classes) were not significant between the patients and controls for any microstate in the duration (A: $p = 0.39$; B: $p = 0.39$; C: $p = 0.30$; D: $p = 0.39$; E: $p = 0.77$; F: $p = 0.68$), occurrence (A: $p = 0.13$; B: $p = 0.92$; C: $p = 0.92$; D: $p = 0.92$; E: $p = 0.13$; F: $p = 0.29$), or coverage (A: $p = 0.44$; B: $p = 0.75$; C: $p = 0.44$; D: $p = 0.75$; E: $p = 0.16$; F: $p = 0.44$).

The results of Spearman's rank correlation revealed a positive association of the depression severity with the presence of microstate A but not with the presence of other microstates. The occurrence of microstate A significantly correlated with the MADRS scores ($r = 0.70$, $p < 0.01$; **Figure 3**), but not with the CGI score ($r = 0.40$), illness duration ($r = 0.06$), or the number of episodes ($r = 0.08$). There were no significant associations between the depression severity and the duration or coverage of microstate A (all absolute *r*-values < 0.55).

The results of Spearman's rank correlation revealed a significant positive association between the medication status and the presence of microstate E but not with the presence of other microstates. The occurrence of microstate E significantly correlated with the intake of antidepressants, antipsychotics, and mood stabilizers ($r = 0.65$, $p < 0.01$; **Figure 4**), but not with the intake of benzodiazepines ($r = 0.20$). There were no significant associations between the medication status and the duration or coverage of microstate E (all absolute *r*-values < 0.45).

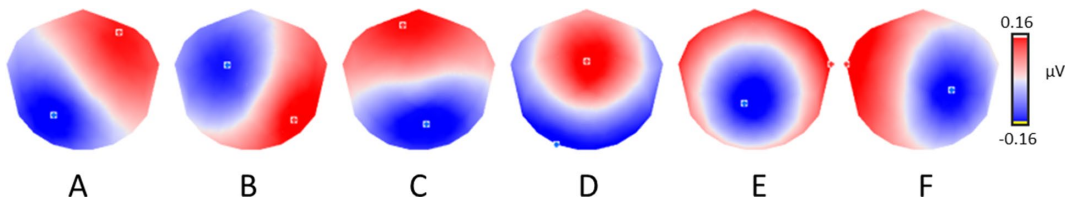

FIGURE 2 | The six microstate topographies identified in the global clustering across all subjects.

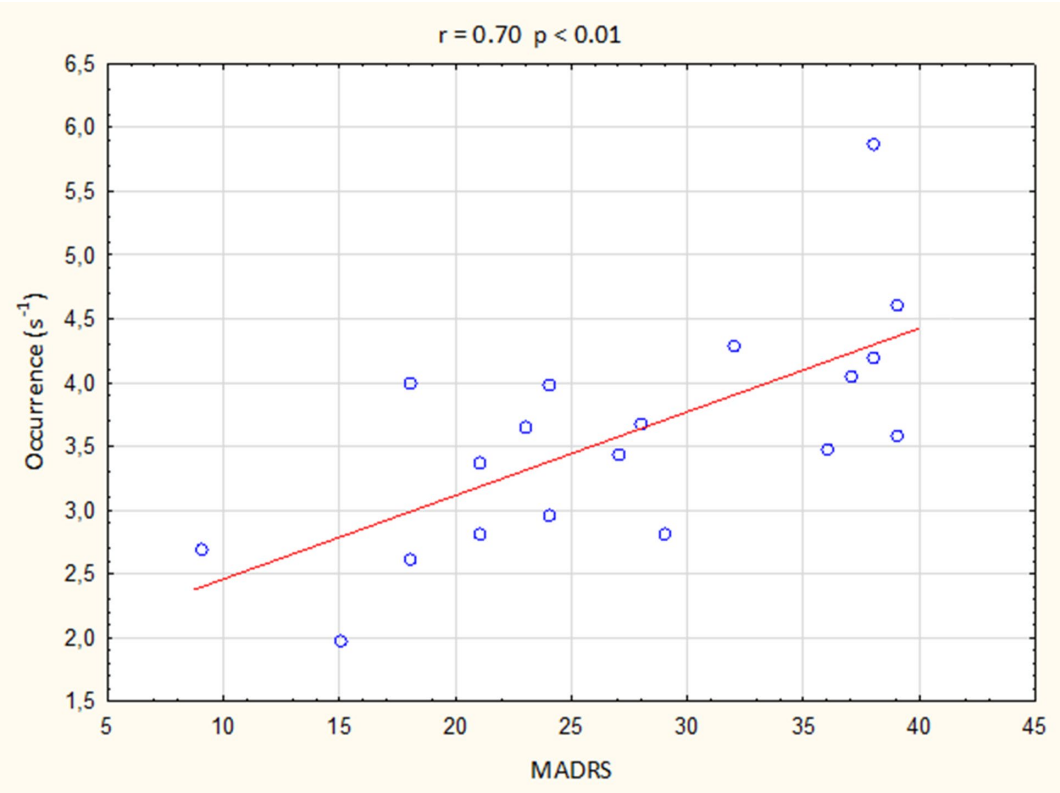

FIGURE 3 | Correlation between the occurrence of microstate A and Montgomery–Åsberg Depression Rating Scale (MADRS) score.

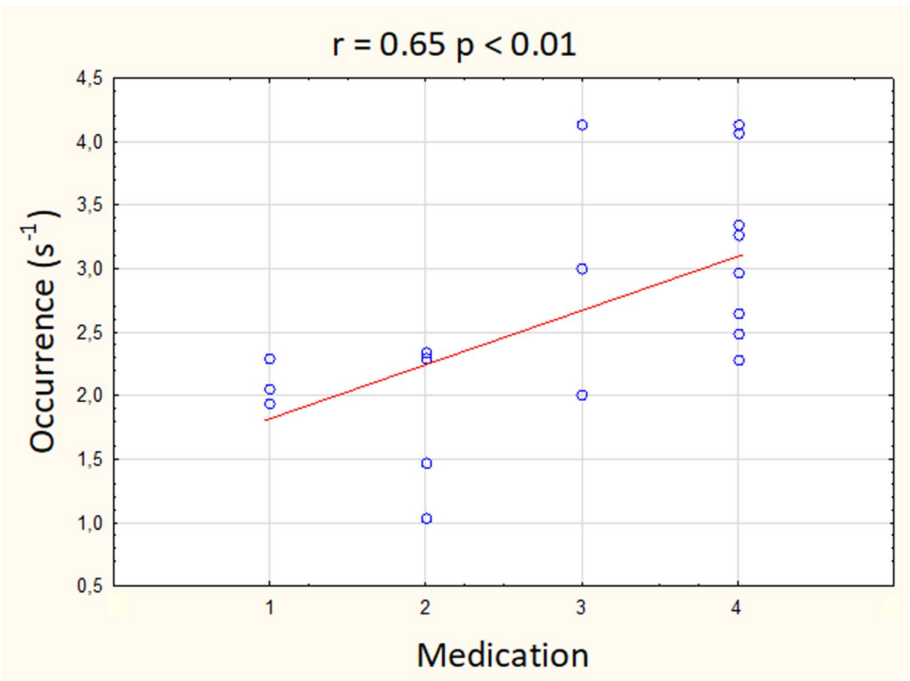

FIGURE 4 | Correlation between the occurrence of microstate E and the intake of antidepressants, antipsychotics, and mood stabilizers. Medication scale: 1, one medication in sub-therapeutic doses; 2, one medication in therapeutic doses; 3, combination of medications with one in therapeutic doses; 4, combination of medications with more than one in therapeutic doses.

DISCUSSION

In this report, the dynamics of resting-state large-scale brain network activity are depicted in the form of functional EEG brain microstates. We demonstrated that microstate temporal dynamics are sensitive to interindividual differences in depressive symptom severity in patients with moderate to severe depression. Particularly, we showed that severity of depressive symptoms correlated with higher occurrence of the microstate A. This finding suggests that microstate analysis-based neural markers might represent a largely untapped resource for understanding the neurobiology of depression. Since the between-group differences were absent in EEG dynamic, it is, however, unknown, if higher occurrence of microstate A is a complex expression of depressive symptomatology or if it reflects a latent risk factor. The here demonstrated symptom-related interindividual differences in microstate dynamics need further research to test its utility in an objective depression assessment. The present study is the first in a planned longitudinal study series with depressive patients recruited at the University Hospital Brno that will help further investigate the microstate parameters as possible predictors of treatment response to both medication and neurostimulation methods including the electroconvulsive therapy.

Only three studies examined microstate duration and/or occurrence in depressive patients. The earliest study showed lower duration in the depressive group than in controls (27). In a subsequent study, between-group differences in occurrence were found neither in young nor aged depressive patients as compared to healthy controls (28). Contrary to these early findings, longer duration and lower occurrence of microstates in treatment-resistant depressed patients as compared to healthy subjects were demonstrated recently (29). The authors suggested that the increased duration and decreased occurrence in microstates could reflect modulation of global brain dynamics with neurotropic medications previously taken by patients resistant to antidepressant treatment. In the current study, we found an increased microstate A occurrence with depression only as an effect related to the symptom severity and not as a between-group difference. This finding is, despite different analytical approaches used in the studies, consistent with the previously reported lowering of microstate occurrence following magnetic seizure therapy and electroconvulsive therapy that in fact might represent a normalization of occurrence with successful treatment (29).

Different methodological approaches might have, however, led to discrepant findings in terms of duration of microstates among the current and the three previous studies. The methodological differences include different frequency bands examined (28), different clustering algorithms applied (27–29), different numbers of maps used for backfitting to the EEG (29), and analyzing all data points (e.g., in current study) or only those with the local maxima of the global field power [e.g., in Ref. (29)].

Discrepant findings may also reflect the pathophysiologic heterogeneity of depression. Similarly to the current sample, the experimental group in the study by Strik et al. (27) included depressive patients who met the criteria for unipolar or bipolar mood disorders or for dysthymia. The other two studies both focused on unipolar depression (28, 29), the more recent one was even restricted only to the treatment-resistant form of depression (29). With respect to the symptom variations in patients meeting criteria for depression, currently based solely on the clinical interviews and diagnostic questionnaires, such heterogeneity in findings could be expected.

In the current study, the topography of microstate A strongly resembled the topography of one of the four canonical microstates, i.e., microstate A, earlier described in the literature (19, 26). Using resting-state fMRI, this microstate was previously linked to the auditory brain network (41), involving bilateral superior and middle temporal gyri, regions associated with phonological processing (47). In addition to this indirect identification of involved brain structures, the sources generating microstate scalp topographies were directly estimated (39, 46). The left temporal lobe and left insula were identified as the major generators of microstate A (47). Additionally, left-lateralized activity in the medial prefrontal cortex and the occipital gyri was most recently reported to underlie this microstate (39).

Evidence from the meta-analysis of functional neuroimaging studies suggests resting-state functional alterations in first-episode drug-naïve MDD patients in the fronto-limbic system, including the dorsolateral prefrontal cortex and putamen, and in the default mode network, namely, the precuneus and superior and middle temporal gyri (48). Altered activity in the superior temporal gyrus in patients with MDD was reported repeatedly in fMRI studies (49–52) and was also suggested to be responsible for the abnormal processing of negative mood and cognition in first-episode, drug-naïve patients with MDD (48). Our findings of positive associations of depressive symptoms with the occurrence of microstate A that is related to temporal lobe activity are thus in line with these studies.

It has been shown that benzodiazepines and antipsychotics may modulate microstate dynamics (53). Accordingly, we observed the effect of medication on the presence of microstate E. The topography of this microstate strongly resembled one of the newly reported microstates, the generators of which were identified in the dorsal anterior cingulate cortex, superior and middle frontal gyri, and insula (46). The cingulo-opercular network (CON), comprising regions in the thalamus as well as frontal operculum/anterior insula and anterior cingulate cortex, is considered to have a central role in sustaining alertness (54) or in general for maintaining perceptual readiness (55). An important role in the pathophysiological mechanisms of depression was suggested for the CON, whose disrupted functional connectivity was observed in first-episode drug-naïve patients with MDD (12). Since the medication status in our study was only roughly defined, it is rather questionable whether the observed correlation between the medication scoring and the occurrence of microstate E could be related to the pharmacological effect on the activity of structures constituting the CON.

In the current study, we decided to use the resting-state condition rather than employing any cognitive task. Depression affects not only emotional and cognitive mental operations but also motivational processes. Therefore, the task performance

differences between patients and healthy controls may relate to different levels of motivation rather than information processing per se. Using a resting-state condition makes it possible to avoid some task-related confounds and makes the application of non-invasive neuroimaging techniques a powerful tool for measuring baseline brain activity (56). Moreover, if the research outputs such as those presented here lead to developing a new diagnostic tool for depressive disorder, such a tool, based on evaluating the resting-state scalp EEG, will be easy to use and require only minimal cooperation from the patients.

It is important to note that our data may have limitations. First, our sample included mixed diagnoses, with both bipolar and unipolar disorders. The observed relationship between the microstate A occurrence and depressive symptomatology should therefore be considered as a state rather than as a trait marker of depression. Second, the low sample size and great variability in medication made it impossible to examine any potential influence of medication on the microstate parameters by comparing patients receiving a specific drug with those not receiving it. To summarize the various medications, an ordinal variable was used that is only a rough measurement of medication usage. Therefore, the observed relationship between the microstate E occurrence and medications should be viewed with caution.

CONCLUSIONS

The study presented here provides insights into global brain dynamics of the resting-state in depressive patients. The identified depressive symptom-related changes in resting-state large-scale brain dynamics suggest the utility of the microstate analysis approach in an objective depression assessment. On the other side, using this analysis at the individual level could prove challenging. To test the observed microstate changes as possible biomarkers of illness and/or treatment response at individual level is the next step for future research in depressive patients.

DATA AVAILABILITY

The raw data supporting the conclusions of this manuscript will be made available by the authors, without undue reservation, to any qualified researcher.

ETHICS STATEMENT

This study was carried out in accordance with the recommendations of Ethics Committee of University Hospital Brno with written informed consent from all subjects. All subjects gave written informed consent in accordance with the Declaration of Helsinki. The protocol was approved by the Ethics Committee of University Hospital in Brno, Czech Republic.

AUTHOR CONTRIBUTIONS

AD designed the study, performed the analysis, and wrote the initial draft. MT served as consultant for the data analysis. RB and JH were responsible for patient recruitment and clinical assessment. EH collected the HD-EEG data. SF and ŠO were involved in the clinical assessment. CM served as an advisor and was responsible for the overall oversight of the study. All authors revised the manuscript.

FUNDING

This project received funding from the European Union Horizon 2020 research and innovation program under the Marie Skłodowska-Curie grant agreement No. 739939. The study was also supported by Ministry of Health, Czech Republic – conceptual development of research organization (University Hospital Brno – FNBr, 65269705). These funding sources had no role in the design, collection, analysis, or interpretation of the study. CM was supported by the Swiss National Science Foundation (grant No. 320030_184677), by the National Centre of Competence in Research (NCCR) "SYNAPSY–The Synaptic Basis of Mental Diseases" (NCCR Synapsy Grant # "51NF40 – 185897), and by the Swiss National Science Foundation (Sinergia project CRSII5_170873).

ACKNOWLEDGMENTS

The authors wish to thank Anne Meredith Johnson for providing language help.

REFERENCES

1. Andrade L, Caraveo-Anduaga JJ, Berglund P, Bijl RV, De Graaf R, Vollebergh W, et al. The epidemiology of major depressive episodes: results from the International Consortium of Psychiatric Epidemiology (ICPE) Surveys. *Int J Methods Psychiatr Res* (2003) 12:3–21. doi: 10.1002/mpr.138
2. Eaton WW, Alexandre P, Bienvenu OJ, Clarke D, Martins SS, Nestadt G, et al. *The burden of mental disorders*. Public Mental Health, Oxford University Press, Oxford, UK (2012). doi: 10.1093/acprof:oso/9780195390445.003.0001
3. Cloutier M, Greene M, Guerin A, Touya M, Wu E. The economic burden of bipolar I disorder in the United States in 2015. *J Affective Disord* (2018) 226:45–51. doi: 10.1016/j.jad.2017.09.011
4. Angst J, Merikangas KR, Cui L, Van Meter A, Ajdacic-Gross V, Rössler W. Bipolar spectrum in major depressive disorders. *Eur Arch Psychiatry Clin Neurosci* (2018) 268:741–48. doi: 10.1007/s00406-018-0927-x
5. Gong Q, He Y. Depression, neuroimaging and connectomics: a selective overview. *Biol Psychiatry* (2015) 77:223–35. doi: 10.1016/j.biopsych.2014.08.009
6. Iwabuchi SJ, Krishnadas R, Li C, Auer DP, Radua J, Palaniyappan L. Localized connectivity in depression: a meta-analysis of resting state functional imaging studies. *Neurosci Biobehav Rev* (2015) 51:77–86. doi: 10.1016/j.neubiorev.2015.01.006
7. Kaiser RH, Andrews-Hanna JR, Wager TD, Pizzagalli DA. Large-scale network dysfunction in major depressive disorder: a meta-analysis of resting-state functional connectivity. *JAMA Psychiatry* (2015) 72:603–11. doi: 10.1001/jamapsychiatry.2015.0071
8. Peng D, Liddle EB, Iwabuchi SJ, Zhang C, Wu Z, Liu J, et al. Dissociated large-scale functional connectivity networks of the precuneus in medication-naïve first-episode depression. *Psychiatry Res Neuroimaging* (2015) 232:250–56. doi: 10.1016/j.pscychresns.2015.03.003

9. Mayberg HS. Limbic-cortical dysregulation: a proposed model of depression. *J Neuropsychiatry Clin Neurosci* (1997) 9:471–81. doi: 10.1176/jnp.9.3.471
10. Fischer AS, Keller CJ, Etkin A. The clinical applicability of functional connectivity in depression: pathways toward more targeted intervention. *Biol Psychiatry Cogn Neurosci Neuroimaging* (2016) 1:262–70. doi: 10.1016/j.bpsc.2016.02.004
11. Satterthwaite TD, Kable JW, Vandekar L, Katchmar N, Bassett DS, Baldassano CF, et al. Common and dissociable dysfunction of the reward system in bipolar and unipolar depression. *Neuropsychopharmacol* (2015) 40:2258–68. doi: 10.1038/npp.2015.75
12. Wu X, Lin P, Yang J, Song H, Yang R, Yang J. Dysfunction of the cingulo-opercular network in first-episode medication-naive patients with major depressive disorder. *J Affective Disord* (2016) 200:275–83. doi: 10.1016/j.jad.2016.04.046
13. Greicius MD, Flores BH, Menon V, Glover GH, Solvason HB, Kenna H, et al. Resting-state functional connectivity in major depression: abnormally increased contributions from subgenual cingulate cortex and thalamus. *Biol Psychiatry* (2007) 62:429–37. doi: 10.1016/j.biopsych.2006.09.020
14. Price JL, Drevets WC. Neurocircuitry of mood disorders. *Neuropsychopharmacol* (2010) 35:192–16. doi: 10.1038/npp.2009.104
15. Hamilton JP, Chen MC, Gotlib IH. Neural systems approaches to understanding major depressive disorder: an intrinsic functional organization perspective. *Neurobiol Dis* (2013) 52:4–11. doi: 10.1016/j.nbd.2012.01.015
16. de Pasquale. F, Corbetta M, Betti. V, Della Penna S. Cortical cores in network dynamics. *Neuroimage* (2018) 180:370–82. doi: 10.1016/j.neuroimage.2017.09.063
17. Bressler SL, Menon V. Large-scale brain networks in cognition: emerging methods and principles. *Trends Cogn Sci* (2010) 14(6):277–90. doi: 10.1016/j.tics.2010.04.004
18. Van De Ville D, Britz J, Michel CM. EEG microstate sequences in healthy humans at rest reveal scale-free dynamics. *Proc Natl Acad Sci* (2010) 107:18179–84. doi: 10.1073/pnas.1007841107
19. Michel CM, Koenig T. EEG microstates as a tool for studying the temporal dynamics of whole-brain neuronal networks: a review. *Neuroimage* (2018) 180:577–93. doi: 10.1016/j.neuroimage.2017.11.062
20. Michel CM, Murray MM. Towards the utilization of EEG as a brain imaging tool. *Neuroimage* (2012) 61:371–85. doi: 10.1016/j.neuroimage.2011.12.039
21. Lehmann D. Principles of spatial analysis. In: Gevins AS, Remont A, editors. *Methods of analysis of brain electrical and magnetic signals*. Elsevier (1987). p. 309–54.
22. Lehmann D, Ozaki H, Pal I. EEG alpha map series: brain micro-states by space-oriented adaptive segmentation. *Electroencephalogr Clin Neurophysiol* (1987) 67:271–88. doi: 10.1016/0013-4694(87)90025-3
23. Hutchison RM, Womelsdorf T, Allen EA, Bandettini PA, Calhoun VD, Corbetta M, et al. Dynamic functional connectivity: promise, issues, and interpretations. *NeuroImage* (2013) 80:360–78. doi: 10.1016/j.neuroimage.2013.05.079
24. Chang C, Glover GH. Time–frequency dynamics of resting-state brain connectivity measured with fMRI. *NeuroImage* (2010) 50:81–98. doi: 10.1016/j.neuroimage.2009.12.011
25. Honey CJ, Kötter R, Breakspear M, Sporns O. Network structure of cerebral cortex shapes functional connectivity on multiple time scales. *Proc Natl Acad Sci* (2007) 104:10240–45. doi: 10.1073/pnas.0701519104
26. Khanna A, Pascual-Leone A, Michel CM, Farzan F. Microstates in resting-state EEG: current status and future directions. *Neurosci Biobehav Rev* (2015) 49:105–13. doi: 10.1016/j.neubiorev.2014.12.010
27. Strik WK, Dierks T, Becker T, Lehmann D. Larger topographical variance and decreased duration of brain electric microstates in depression. *J Neural Transm* (1995) 99:213–22. doi: 10.1007/BF01271480
28. Ihl R, Brinkmeyer J. Differential diagnosis of aging, dementia of the Alzheimer type and depression with EEG-segmentation. *Dement Geriatr Cogn Disord* (1999) 10:64–9. doi: 10.1159/000017103
29. Atluri S, Wong W, Moreno S, Blumberger DM, Daskalakis ZJ, Farzan F. Selective modulation of brain network dynamics by seizure therapy in treatment-resistant depression. *NeuroImage Clin* (2018) 20:1176–90. doi: 10.1016/j.nicl.2018.10.015
30. Drobisz D, Damborská. A. Deep brain stimulation targets for treating depression. *Behav Brain Res* (2019) 359:266–73. doi: 10.1016/j.bbr.2018.11.004
31. Bazire S. Benzodiazepine equivalent doses. In: *Psychotropic Drug Directory*. Cheltenham, UK: Lloyd-Reinhold Communications (2014).
32. Williams JBW, Kobak KA. Development and reliability of a structured interview guide for the Montgomery Asberg Depression Rating Scale (SIGMA). *Br J Psychiatry* (2008) 192:52–8. doi: 10.1192/bjp.bp.106.032532
33. Guy W ed. *ECDEU Assessment Manual for Psychopharmacology*. Rockville, MD: US Department of Health, Education, and Welfare Public Health Service Alcohol, Drug Abuse, and Mental Health Administration (1976).
34. Jung T, Makeig S, Westerfield M, Townsend J, Courchesne E.c., Sejnowski TJ. Removal of eye activity artifacts from visual event-related potentials in normal and clinical subjects. *Clin Neurophysiol* (2000) 111:1745–58. doi: 10.1016/S1388-2457(00)00386-2
35. Perrin F, Pernier J, Bertrand O, Echallier JF. Spherical splines for scalp potential and current density mapping. *Electroencephalogr Clin Neurophysiol* (1989) 72:184–87. doi: 10.1016/0013-4694(89)90180-6
36. Brunet D, Murray MM, Michel CM. Spatiotemporal analysis of multichannel EEG: CARTOOL. *Comput Intell Neurosci* (2011) 813870:1–15. doi: 10.1155/2011/813870
37. Murray MM, Brunet D, Michel CM. Topographic ERP analyses: a step-by-step tutorial review. *Brain Topogr* (2008) 20:249–64. doi: 10.1007/s10548-008-0054-5
38. Pascual-Marqui RD, Michel CM, Lehmann D. Segmentation of brain electrical activity into microstates; model estimation and validation. *IEEE Trans Biomed Eng* (1995) 42:658–65. doi: 10.1109/10.391164
39. Bréchet L, Brunet D, Birot G, Gruetter R, Michel CM, Jorge J. Capturing the spatiotemporal dynamics of self-generated, task-initiated thoughts with EEG and fMRI. *Neuroimage* (2019) 194:82–92. doi: 10.1016/j.neuroimage.2019.03.029
40. Koenig T, Prichep L, Lehmann D, Sosa PV, Braeker E, Kleinlogel H, et al. Millisecond by millisecond, year by year: normative EEG microstates and developmental stages. *Neuroimage* (2002) 16:41–8. doi: 10.1006/nimg.2002.1070
41. Britz J, Van De Ville D, Michel CM. BOLD correlates of EEG topography reveal rapid resting-state network dynamics. *NeuroImage* (2010) 52:1162–70. doi: 10.1016/j.neuroimage.2010.02.052
42. Tomescu MI, Rihs TA, Becker R, Britz J, Custo A, Grouiller F, et al. Deviant dynamics of EEG resting state pattern in 22q11.2 deletion syndrome adolescents: a vulnerability marker of schizophrenia? *Schizophr Res* (2014) 157:175–81. doi: 10.1016/j.schres.2014.05.036
43. Michel CM, Brandeis D, Skrandies W, Pascual R, Strik WK, Dierks T. Global field power: a 'time-honoured' index for EEG/EP map analysis. *Int J Psychophysiol* (1993) 15:1–2. doi: 10.1016/0167-8760(93)90088-7
44. Santarnecchi E, Khanna AR, Musaeus CS, Benwell CSY, Davila P, Farzan F, et al. EEG microstate correlates of fluid intelligence and response to cognitive training. *Brain Topogr* (2017) 30:502–20. doi: 10.1007/s10548-017-0565-z
45. Benjamini Y. Discovering the false discovery rate. *J R Stat Soc Ser B Stat Methodol* (2010) 72:405–16. doi: 10.1111/j.1467-9868.2010.00746.x
46. Custo A, Van De Ville D, Wells WM, Tomescu MI, Brunet D, Michel CM. Electroencephalographic resting-state networks: source localization of microstates. *Brain Connect* (2017) 7:671–82. doi: 10.1089/brain.2016.0476
47. Buchsbaum BR, Hickok G, Humphries C. Role of left posterior superior temporal gyrus in phonological processing for speech perception and production. *Cogn Sci* (2001) 25:663–78. doi: 10.1207/s15516709cog2505_2
48. Zhong X, Pu W, Yao S. Functional alterations of fronto-limbic circuit and default mode network systems in first-episode, drug-naïve patients with major depressive disorder: a meta-analysis of resting-state fMRI data. *J Affective Disord* (2016) 206:280–86. doi: 10.1016/j.jad.2016.09.005
49. Ke Z, Qing G, Zhiliang L, Fei X, Xiao S, Huafu C, et al. Abnormal functional connectivity density in first-episode, drug-naïve adult patients with major depressive disorder. *J Affect Disord* (2016) 194:153–8. doi: 10.1016/j.jad.2015.12.081
50. Liu Z, Xu C, Xu Y, Wang Y, Zhao B, Lv Y, et al. Decreased regional homogeneity in insula and cerebellum: a resting-state fMRI study in patients with major depression and subjects at high risk for major depression. *Psychiatry Res* (2010) 182:211–15. doi: 10.1016/j.pscychresns.2010.03.004
51. Shen T, Qiu M, Li C, Zhang J, Wu Z, Wang B, et al. Altered spontaneous neural activity in first-episode, unmedicated patients with major depressive disorder. *Neuroreport* (2014) 25:1302–07. doi: 10.1097/WNR.0000000000000263

52. Tadayonnejad R, Yang S, Kumar A, Ajilore O. Clinical, cognitive, and functional connectivity correlations of resting-state intrinsic brain activity alterations in unmedicated depression. *J Affective Disord* (2015) 172:241–50. doi: 10.1016/j.jad.2014.10.017
53. Kinoshita T, Strik WK, Michel CM, Yagyu T, Saito M, Lehmann D. Microstate segmentation of spontaneous multichannel EEG map series under diazepam and sulpiride. *Pharmacopsychiatry* (1995) 28:51–5. doi: 10.1055/s-2007-979588
54. Coste CP, Kleinschmidt A. Cingulo-opercular network activity maintains alertness. *Neuroimage* (2016) 128:264–72. doi: 10.1016/j.neuroimage.2016.01.026
55. Sadaghiani S, D'Esposito M. Functional characterization of the cingulo-opercular network in the maintenance of tonic alertness. *Cereb Cortex* (2015) 25:2763–73. doi: 10.1093/cercor/bhu072
56. Gusnard DA, Raichle ME. Searching for a baseline: Functional imaging and the resting human brain. *Nat Rev Neurosci* (2001) 2:685–694.

Conflict of Interest Statement: The authors declare that the research was conducted in the absence of any commercial or financial relationships that could be construed as a potential conflict of interest.

Copyright © 2019 Damborská, Tomescu, Honzírková, Barteček, Hořínková, Fedorová, Ondruš and Michel. This is an open-access article distributed under the terms of the Creative Commons Attribution License (CC BY). The use, distribution or reproduction in other forums is permitted, provided the original author(s) and the copyright owner(s) are credited and that the original publication in this journal is cited, in accordance with accepted academic practice. No use, distribution or reproduction is permitted which does not comply with these terms.

Annex 11

Damborská, A., Piguet, C., Aubry, J-M., Dayer, A.G., Michel C.M., Berchio, C. (2019c). Altered EEG resting-state large-scale brain network dynamics in euthymic bipolar disorder patients. *Frontiers in Psychiatry*, 826 (10)

frontiers in Psychiatry

ORIGINAL RESEARCH
published: 15 November 2019
doi: 10.3389/fpsyt.2019.00826

Altered Electroencephalographic Resting-State Large-Scale Brain Network Dynamics in Euthymic Bipolar Disorder Patients

Alena Damborská[1,2], Camille Piguet[3], Jean-Michel Aubry[3,4], Alexandre G. Dayer[3,4], Christoph M. Michel[1,5] and Cristina Berchio[1,3]*

[1] Functional Brain Mapping Laboratory, Campus Biotech, Department of Basic Neurosciences, University of Geneva, Geneva, Switzerland, [2] Department of Psychiatry, Faculty of Medicine, Masaryk University and University Hospital Brno, Brno, Czechia, [3] Service of Psychiatric Specialties, Mood Disorders, Department of Psychiatry, Geneva University Hospital, Geneva, Switzerland, [4] Department of Psychiatry, University of Geneva, Geneva, Switzerland, [5] Lemanic Biomedical Imaging Centre (CIBM), Geneva, Switzerland

OPEN ACCESS

Edited by:
Paul Stokes,
King's College London,
United Kingdom

Reviewed by:
Emine Elif Tülay,
Üsküdar University,
Turkey
Bahar Güntekin,
Istanbul Medipol University,
Turkey

***Correspondence:**
Alena Damborská
adambor@med.muni.cz

Specialty section:
This article was submitted to Mood and Anxiety Disorders, a section of the journal Frontiers in Psychiatry

Received: 10 July 2019
Accepted: 18 October 2019
Published: 15 November 2019

Citation:
Damborská A, Piguet C, Aubry J-M, Dayer AG, Michel CM and Berchio C (2019) Altered Electroencephalographic Resting-State Large-Scale Brain Network Dynamics in Euthymic Bipolar Disorder Patients. Front. Psychiatry 10:826. doi: 10.3389/fpsyt.2019.00826

Background: Neuroimaging studies provided evidence for disrupted resting-state functional brain network activity in bipolar disorder (BD). Electroencephalographic (EEG) studies found altered temporal characteristics of functional EEG microstates during depressive episode within different affective disorders. Here we investigated whether euthymic patients with BD show deviant resting-state large-scale brain network dynamics as reflected by altered temporal characteristics of EEG microstates.

Methods: We used high-density EEG to explore between-group differences in duration, coverage, and occurrence of the resting-state functional EEG microstates in 17 euthymic adults with BD in on-medication state and 17 age- and gender-matched healthy controls. Two types of anxiety, state and trait, were assessed separately with scores ranging from 20 to 80.

Results: Microstate analysis revealed five microstates (A–E) in global clustering across all subjects. In patients compared to controls, we found increased occurrence and coverage of microstate A that did not significantly correlate with anxiety scores.

Conclusion: Our results provide neurophysiological evidence for altered large-scale brain network dynamics in BD patients and suggest the increased presence of A microstate to be an electrophysiological trait characteristic of BD.

Keywords: electroencephalographic microstate, large-scale brain networks, resting state, dynamic brain activity, bipolar disorder, high-density electroencephalography

INTRODUCTION

Bipolar disorder (BD) is a common and severe psychiatric disorder, with an important personal and societal burden (1, 2). The worldwide prevalence of BD is considered to range between 1 and 3% (3, 4). BD patients are frequently misdiagnosed and often identified at late stages of disease progression, which can lead to inadequate treatment (5) and worse functional prognosis (6). A better understanding of the underlying pathophysiology is needed to identify objective

biomarkers of BD that would improve diagnostic and/or treatment stratification of patients.

Possible candidates for neurobiological biomarkers in BD could arise from the abnormalities of functional brain networks. Evidence from brain imaging studies consistently points to abnormalities in circuits implicated in emotion regulation and reactivity. Particularly, attenuated frontal and enhanced limbic activations are reported in BD patients (7–9). Interestingly, regions implicated in the pathophysiology of the disease, such as the inferior frontal gyrus, the medial prefrontal cortex (mPFC), and the amygdala present altered activation patterns even in unaffected first-degree relatives of BD patients (10), pointing toward brain alterations that could underlie disease vulnerability. Moreover, evidence from functional magnetic resonance imaging (fMRI) studies showed aberrant resting-state functional connectivity between frontal and meso-limbic areas in BD when compared to healthy controls (11). A recently developed functional neuroanatomic model of BD suggests, more specifically, decreased connectivity between ventral prefrontal networks and limbic brain regions including the amygdala (12, 13). The functional connectivity abnormalities in BD in brain areas associated with emotion processing were shown to vary with mood state. A resting-state functional connectivity study of emotion regulation networks demonstrated that subgenual anterior cingulate cortex (sgACC)-amygdala coupling is critically affected during mood episodes, and that functional connectivity of sgACC plays a pivotal role in mood normalization through its interactions with the ventrolateral PFC and posterior cingulate cortex (14). Nevertheless, although different fMRI metrics allowed to report deviant patterns of large-scale networks and altered resting-state functional connectivity (14, 15) in BD, the precise temporal dynamics of the functional brain networks at rest remain to be determined.

Large-scale neural networks dynamically and rapidly re-organize themselves to enable efficient functioning (16, 17). Fast dynamics of the resting-state large-scale neural networks can be studied on sub-second temporal scales with EEG microstate analysis (18–20). EEG microstates are defined as short periods (60–120 ms) of quasi-stable electric potential scalp topography (21, 22). Therefore, microstate analysis can cluster the scalp topographies of the resting-state EEG activity into the set of a few microstate classes including the four canonical classes A–D (20) and more recent additional ones (23, 24). Since each microstate class topography reflects a coherent neuronal activity (25, 20), the temporal characteristics, such as duration, occurrence, and coverage, may be linked to the expression of spontaneous mental states and be representative of the contents of consciousness (26, 27). Numerous studies reported abnormalities in temporal properties of resting-state EEG microstates in neuropsychiatric disorders (for review see 25, 20). Evidence from microstate studies suggests that altered resting-state brain network dynamics may represent a marker of risk to develop neuropsychiatric disorders (28–30), predict clinical variables of an illness (31), or help to assess the efficacy of a treatment (32, 33). Only two studies investigated resting-state EEG in BD patients (34, 35). These studies examined patients during a depressive episode within different affective disorders. Adaptive segmentation of resting-state EEG showed abnormal microstate topographies and reduced overall average microstate duration in patients that met criteria for unipolar or bipolar mood disorders or for dysthymia (34). Using a *k*-means cluster analysis, an increased occurrence of microstate A with depression as an effect related to the symptom severity was observed during a period of depression in unipolar and bipolar patients (35).

Trait markers of BD based on neurobiological findings can be considered as biomarkers of illness (36, 37). These trait markers of BD can be studied during the periods of remission, or euthymia. No microstate study on spontaneous activity, however, has been performed on euthymic BD patients to the best of our knowledge. Thus, the main goal of the current study was to explore group differences between euthymic patients with BD and healthy controls in terms of resting-state EEG microstate dynamics. We hypothesized that BD patients during remission will show altered temporal characteristics of EEG microstates such as duration, coverage, and occurrence.

MATERIALS AND METHODS

Subjects

Data were collected from 17 euthymic adult patients with BD and 17 healthy control (HC) subjects. The patients were recruited from the Mood Disorders Unit at the Geneva University Hospital. A snowball convenience sampling was used for the selection of the BD patients. Control subjects were recruited by general advertisement. All subjects were clinically evaluated using clinical structured interview [DIGS: Diagnostic for Genetic Studies (38)]. BD was confirmed in the experimental group by the usual assessment of the specialized program, an interview with a psychiatrist, and a semi-structured interview and relevant questionnaires with a psychologist. Exclusion criteria for all participants were a history of head injury, current alcohol, or drug abuse. Additionally, a history of psychiatric or neurological illness and of any neurological comorbidity were exclusion criteria for controls and bipolar patients, respectively. Symptoms of mania and depression were evaluated using the Young Mania Rating Scale (YMRS) (39) and the Montgomery-Åsberg Depression Rating Scale (MADRS) (40), respectively. Participants were considered euthymic if they scored < 6 on YMRS and < 12 on MADRS at the time of the experiment, and were stable for at least 4 weeks before. All patients were medicated, receiving pharmacological therapy including antipsychotics, antidepressants, and mood stabilizers, and had to be under stable medication for at least 4 weeks. The experimental group included both BD I ($n = 10$) and BD II ($n = 7$) types.

To check for possible demographic or clinical differences between groups, subject characteristics such as age, education, or level of depression were compared between groups using independent *t*-tests. Anxiety is highly associated with BD (41, 42) and is a potential confounding variable when investigating microstate dynamics at rest. For example, decreased duration of EEG microstates at rest in patients with panic disorder has been reported (43). To check for possible differences in anxiety symptoms, all subjects were assessed with the State-Trait Anxiety

Inventory (STAI) (44). Anxiety as an emotional state (state-anxiety) and anxiety as a personal characteristic (trait-anxiety) were evaluated separately. Scores of both state- and trait-anxiety range from 20 to 80, higher values indicating greater anxiety. The scores were compared between patients and controls using independent *t*-tests.

This study was carried out in accordance with the recommendations of the Ethics Committee for Human Research of the Geneva University Hospital, with written informed consent from all subjects. All subjects gave written informed consent in accordance with the Declaration of Helsinki. The protocol was approved by the Ethics Committee for Human Research of the Geneva University Hospital, Switzerland.

Electroencephalographic Recording and Pre-Processing

The EEG was recorded with a high density 256-channel system (EGI System 200; Electrical Geodesic Inc., OR, USA), sampling rate of 1 kHz, and Cz as acquisition reference. Subjects were sitting in a comfortable upright position and were instructed to stay as calm as possible, to keep their eyes closed and to relax for 6 min. They were asked to stay awake.

To remove muscular artifacts originating in the neck and face the data were reduced to 204 channels. Two to four minutes of EEG data were selected based on visual assessment of the artifacts and band-pass filtered between 1 and 40 Hz. Subsequently, in order to remove ballistocardiogram and oculo-motor artifacts, Infomax-based independent component analysis (45) was applied on all but one or two channels rejected due to abundant artifacts. Only components related to physiological noise, such as ballistocardiogram, saccadic eye movements, and eye blinking, were removed based on the waveform, topography, and time course of the component. The cleaned EEG recordings were down-sampled to 125 Hz and the previously identified noisy channels were interpolated using a three-dimensional spherical spline (46), and re-referenced to the average reference. All the preprocessing steps were done using MATLAB and the freely available Cartool Software 3.70 (https://sites.google.com/site/cartoolcommunity/home), programmed by Denis Brunet.

Electroencephalographic Data Analysis

To estimate the optimal set of topographies explaining the EEG signal, a standard microstate analysis was performed using *k*-means clustering (see **Supplementary Figure 1**). The polarity of the maps was ignored in this procedure (18, 47, 48). To determine the optimal number of clusters, we applied a meta-criterion that is a combination of seven independent optimization criteria (for details see 24). In order to improve the signal-to-noise ratio, only the data at the time points of the local maximum of the Global Field Power (GFP) were clustered (18, 22, 28, 49). The GFP is a scalar measure of the strength of the scalp potential field and is calculated as the standard deviation of all electrodes at a given time point (47, 48, 50). The cluster analysis was first computed at the individual level yielding one set of representative maps for each subject. Clustering at the group level followed, in which the individual representative maps of patients and controls were clustered separately. Then all participants' representative maps were clustered at global level yielding one set of maps that represented the data of all subjects. This one set of global representative maps entered the fitting process and the presence of each global map in every subject was determined. This enabled us to compare groups in terms of the presence of these global maps in the original data, i.e., to compare the microstate temporal characteristics between patients and controls.

In order to retrieve the temporal characteristics of the microstates, the fitting procedure consisted in calculating the spatial correlation between every representative map identified at the global level across all subjects and the individual subject's scalp potential map in every instant of the pre-processed EEG recording. Each continuous time point of the subject's EEG (not only the GFP peaks) was then assigned to the microstate class of the highest correlation (winner-takes-all), again ignoring polarity (20, 24, 47, 51). Temporal smoothing parameters [window half size = 3, strength (Besag factor) = 10] ensured that the noise during low GFP did not artificially interrupt the temporal segments of stable topography (18, 47). These segments of stable topography assigned to a given microstate class were then evaluated. For each subject, three temporal parameters were calculated for each microstate class: i) occurrence, ii) coverage, and iii) duration. Occurrence indicates how many temporal segments of a given microstate class occur in 1 s. The coverage in percent represents the summed amount of time spent in a given microstate class as a portion of the whole analyzed period. The duration in milliseconds indicates the most common amount of time that a given microstate class is continuously present. The global explained variance for a specific microstate class was calculated by summing the squared spatial correlations between the representative map and its corresponding assigned scalp potential maps at each time point weighted by the GFP (48). Global explained variances of all microstate classes were then summed yielding the portion of data explained with the set of representative maps.

Microstate analysis was performed using the freely available Cartool Software 3.70, (https://sites.google.com/site/cartoolcommunity/home), programmed by Denis Brunet. Mann-Whitney U test was used to investigate group differences for temporal parameters of each microstate. Multiple comparisons were corrected using the false discovery rate (FDR) method (52).

Spearman's rank correlations were calculated between the MADRS, YMRS, STAI-state, and STAI-trait scores and significant microstate parameters to check for possible relationships between symptoms and microstate dynamics. Eyes closed spontaneous EEG dynamics are mostly dominated by alpha activity (53). To provide an estimate of the absolute alpha power of each group, individual EEG data were Fourier transformed (Hanning windowing function, common averge reference). Mann-Whitney U test was used to investigate group differences for mean alpha (8–14 Hz) power across 204 channels. To evaluate the role of the alpha rhythm in the appearance of the microstates, the Spearman's rank correlation was calculated between Alpha Power and those microstate parameters, in which significant group differences were found. All statistical evaluations were performed by the routines included in the

program package Statistica'13 (1984–2018, TIBCO, Software Inc, Version 13.4.0.14).

RESULTS

Clinical and Demographic Variables

There were no significant differences in age and level of education between the patient and the control groups. In both groups, very low mean scores on depression and mania symptoms were observed, which did not significantly differ between the two groups. BD patients showed higher scores on state and trait scales of the STAI. For all subject characteristics, see **Table 1**.

TABLE 1 | Subject characteristics.

Characteristic	Healthy controls (n = 17)	Bipolar patients (n = 17)	*t*-value	p-value
Age: mean ± SD	36.6 ± 14.5	35.9 ± 11.9	-0.17	0.87
Gender: male, *n*	12	12		
Handedness[a]: right, *n*	14	14		
Education[b]: mean ± SD	2.3 ± 0.6	2.4 ± 0.5	0.63	0.53
MADRS: mean ± SD	1.4± 1.6	2.3 ± 2.9	1.09	0.29
YMRS: mean ± SD	0.86 ± 1.4	0.76 ± 1.4	-0.18	0.86
STAI-state: mean ± SD	26.7 ± 4.8	36.9 ± 15.2	-2.13	0.04
STAI-trait: mean ± SD	27.4 ± 5.2	42.9 ± 13.3	-3.7	0.001

[a]*Edinburgh inventory (54);* [b]*Education levels: 1 = no high school, 2 = high school, 3 = university studies.*

Microstate Results

The meta-criterion used to determine the most dominant topographies revealed five resting-state microstate maps across patients, HCs, and all subjects, explaining 82.1, 83.1, and 82.2% of the global variance, respectively (**Figure 1**). The topographies resembled those previously reported as A, B, C, and D maps (20, 22, 25, 49) and one of the three recently identified additional maps (23). We labeled these scalp maps from A to E in accordance with the previous literature on microstates. The scalp topographies showed left posterior-right anterior orientation (map A), a right posterior-left anterior orientation (map B), an anterior-posterior orientation (map C), a fronto-central maximum (map D), and a parieto-occipital maximum (map E).

Since some microstate parameters showed a non-homogeneity of variances in the two groups (Levene's tests for the microstate C coverage and microstates A and C duration; $p < 0.01$), we decided to calculate Mann-Whitney U test to investigate group differences for temporal parameters of each microstate.

We found significant between-group differences for microstate classes A and B. Both microstates showed increased presence in patients in terms of occurrence and coverage. The two groups did not differ in any temporal parameter of microstates C, D, or E. The results of the temporal characteristics of each microstate are summarized in **Table 2** and **Figure 2**.

Clinical Correlations

Correlations with clinical parameters were calculated for those microstate parameters, in which significant group differences

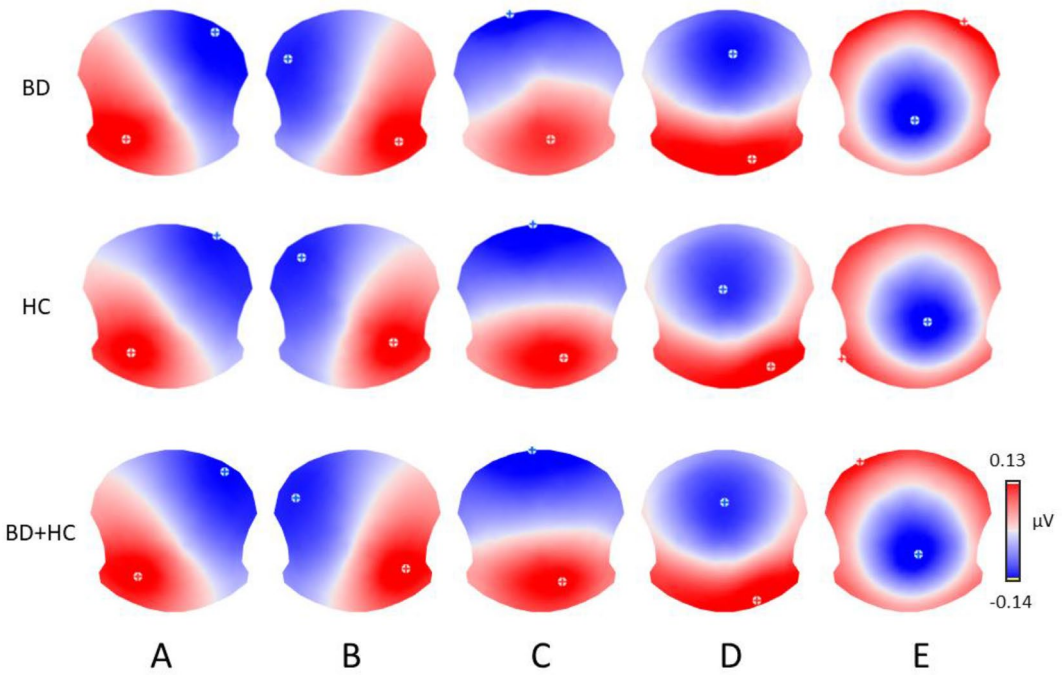

FIGURE 1 | The five microstate topographies **(A–E)** identified in the group clusterings across patients (BD) and healthy controls (HC) and in the global clustering across all subjects (BD+HC). Note that similar five dominant microstate topographies were identified in all three clusterings.

TABLE 2 | Mann-Whitney U test for group comparisons in the investigated microstate parameters.

Microstate	A	B	C	D	E
Occurrence (s^{-1})					
Patients (mean ± s.d.)	4.5 ± 1.1	3.9 ± 1.1	5.2 ± 1.1	3.9 ± 2.2	1.9 ± 1.2
Controls (mean ± s.d.)	3.4 ± 1.2	3.0 ± 1.1	5.0 ± 1.1	3.4 ± 2.1	2.0 ± 1.3
Z-value	2.51	2.51	–0.03	0.65	–0.14
Uncorrected p-value	0.01	0.01	0.97	0.51	0.89
FDR corrected p-value	0.03	0.03	0.97	0.85	0.97
Coverage (%)					
Patients (mean ± s.d.)	18.9 ± 6.5	16.0 ± 7.8	25.1 ± 8.6	18.5 ± 12.3	6.4 ± 5.1
Controls (mean ± s.d.)	13.3 ± 4.9	11.4 ± 6.0	34.7 ± 16.8	17.0 ± 12.0	7.0 ± 5.3
Z-value	2.62	2.79	–1.69	0.17	–0.21
Uncorrected p-value	0.009	0.005	0.09	0.86	0.84
FDR corrected p-value	0.02	0.02	0.15	0.86	0.86
Duration (ms)					
Patients (mean ± s.d.)	26 ± 4	25 ± 4	29 ± 4	26 ± 6	21 ± 4
Controls (mean ± s.d.)	24 ± 1	24 ± 3	35 ± 9	27 ± 6	22 ± 4
Z-value	1.38	1.03	–2.27	0.17	–0.69
Uncorrected p-value	0.17	0.30	0.02	0.86	0.49
FDR corrected p-value	0.42	0.50	0.12	0.86	0.61

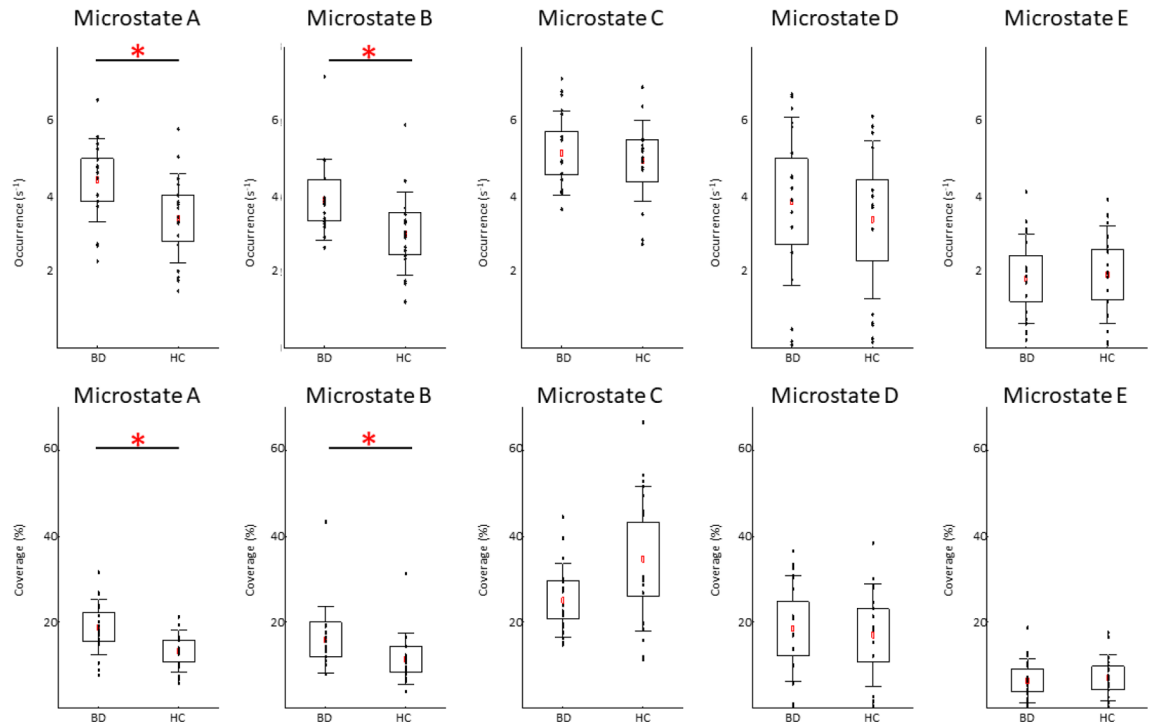

FIGURE 2 | Temporal dynamics of electroencephalographic microstates in patients with bipolar disorder (BD) and in healthy controls (HC). In each subplot, the raw data are plotted on top of the boxplot showing the mean (◘), 95% confidence interval (box plot area), 1 standard deviation (whiskers), and significant differences (*). In all plots, x-axes represent the subject group; y-axes represent the occurrence (upper plots) or coverage (lower plots). Note significantly increased occurrence and coverage of the microstate A and B in the BD compared to HC group (FDR corrected $p < 0.05$).

were found. The results of Spearman's rank correlation revealed a significant positive association between the coverage of the microstate B and the STAI-state ($r = 0.40$; $p < 0.05$) and STAI-trait ($r = 0.54$; $p < 0.05$) scores. The results of Spearman's rank correlation revealed a significant positive association between the occurrence of the microstate B and the STAI-trait ($r = 0.47$; $p < 0.05$) scores. The results of Spearman's rank correlation revealed no significant associations between the STAI-state or STAI-trait scores and the occurrence or coverage of the microstate A (all absolute r-values < 0.35).

The results of Spearman's rank correlation revealed no significant associations between the MADRS and YMRS scores and the occurrence or coverage of the microstate A and B (all absolute r-values < 0.30).

Alpha Rhythm

The Mann-Whitney U test showed significantly decreased alpha power ($p < 0.03$, Z-value 2.7) in the BD compared to HC group (see **Figure 3**). The results of Spearman's rank correlation revealed no significant associations between the alpha power and occurrence or coverage of microstates A and B (all absolute r-values < 0.40).

DISCUSSION

Our study presents the first evidence for altered resting-state EEG microstate dynamics in euthymic patients with BD. Patients were stable and did not significantly differ in their depressive or manic symptomatology from HCs at the time of experiment. Despite this fact, they showed abnormally increased presence of microstates A and B, the latter correlating with the anxiety level.

In an earlier combined fMRI-EEG study the microstate A was associated with the auditory network (49). Moreover, generators of the functional EEG microstates were estimated in recent studies, where sources of the microstate A showed left-lateralized activity in the temporal lobe, insula, mPFC, and occipital gyri (23, 24).

In the fMRI literature as well, resting-state functional connectivity alterations of the insula (55), the auditory network (56), and the mPFC (57) were reported in BD patients. Verbal episodic memory deficits and language-related symptoms in BD patients were suggested to be associated with a diminished functional connectivity within the auditory/temporal gyrus and to be compensated by increased fronto-temporal functional connectivity (56). The mPFC was also identified as a major locus of shared abnormality in BD and schizophrenia (58), showing reduced default mode network connectivity from the mPFC to the hippocampus and fusiform gyrus, as well as increased connectivity between the mPFC and primary visual cortex in BD. Hypoconnectivity of the default mode network from the left posterior cingulate cortex to the bilateral mPFC and bilateral precuneus, and reduced salience connectivity of the left sgACC to the right inferior temporal gyrus in BD patients (57) was observed in unmedicated BD patients. In euthymic BD subjects compared to HCs, resting-state functional connectivity of the insula (59) and amygdala (60) to other brain regions was reported to be increased and decreased, respectively. In summary, the evidence from fMRI studies shows both hypoconnectivity (57, 58) and hyperconnectivity (56, 58, 59) pointing to complex alterations of functional resting-state networks. Our findings of increased presence of the microstate A in euthymic BD patients might be related to the hyperconnectivity of the underlying networks that involve the temporal lobe, insula, mPFC, and occipital gyri.

Anxiety symptoms were previously associated with greater severity and impairment in BD (41) and euthymic bipolar patients tend to present high residual level of anxiety (61), as it was the case here. No significant correlation was found between the increased anxiety scores and the increased occurrence or coverage of the microstate A. Our results therefore indicate that this alteration of microstate dynamics might represent a characteristic feature of

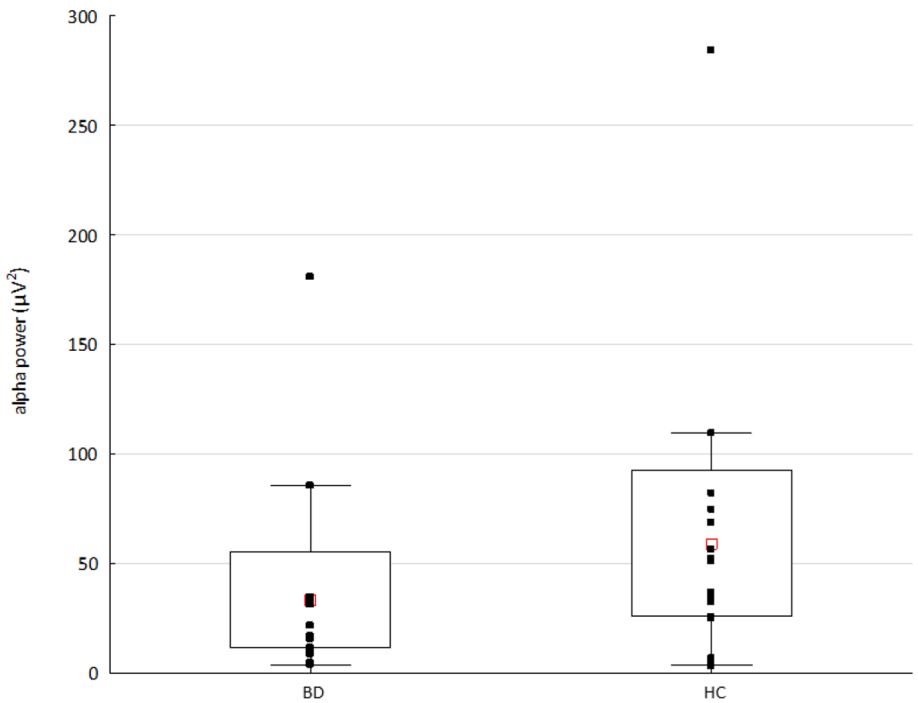

FIGURE 3 | The alpha power in patients with bipolar disorder (BD) and healthy controls (HC). Raw data are plotted on top of each boxplot showing the mean (▫), 95% confidence interval (box plot area), and non-outlier range (whiskers). The x-axis represents the subject group; the y-axis represents the average alpha (8–14 Hz) power across 204 channels. Note significantly decreased alpha power in the BD compared to HC group ($p < 0.03$, Z value 2.7).

BD that is not affected by anxiety. The demonstrated alterations in microstate A dynamics during clinical remission might reflect i) an impaired resting-state large-scale brain network dynamics as a trait characteristic of the disorder and/or ii) a compensatory mechanism needed for clinical stabilization of the disorder.

Our study is the first to examine EEG microstate dynamics of spontaneous activity in BD patients during remission. The here demonstrated group difference of BD patients *vs*. controls, is not congruent with the previously reported reduced duration of the EEG microstates during a depressive episode (34). The experimental group in that study was not restricted to bipolar patients, however, and included also patients who met the criteria for unipolar depression or dysthymia. Moreover, authors examined the overall microstate duration and did not examine distinct microstates separately. These and other aspects, such as different clustering methods used, make it difficult to compare our findings with that early evidence of disrupted microstate dynamics in depression. Nevertheless, in our recent resting-state study we showed positive associations of depressive symptoms with the occurrence of microstate A in a heterogenous group of patients with affective disorders (35).

The microstate B was previously associated with the visual network (23, 24, 49, 62) and thoughts related to the conscious experience of an episodic autobiographic memory, i.e., mental visualization of the scene (24). In our group of BD patients, we found an abnormally increased presence of microstate B that was associated with a higher anxiety. In particular, the occurence together with coverage and only the coverage were positively correlated with scores of trait and state anxiety, respectively. The observed change in microstate B dynamics might be, therefore, more related to a relatively stable disposition than to the actual emotional state. Previous studies also suggest that anxiety may influence visual processing (63, 64) and that connections between amygdala and visual cortex might underlie enhanced visual processing of emotionally salient stimuli in patients with social phobia (65). Our finding of increased presence of microstate B positively associated with anxiety level in euthymic BD patients is consistent with these observations. Additionally, a more regular appearance for microstate B and increased overall temporal dependencies among microstates were recently reported in mood and anxiety disorders, suggesting a decreased dynamicity in switching between different brain states in these psychiatric conditions (66). Another microstate study on anxiety disorders reported a decreased overall resting-state microstate duration in panic disorder (43). That early study, however, did not assess temporal characteristics of different microstates separately and it is therefore difficult to compare those findings with our observations. Further evidence is needed to determine, whether the increased presence of microstate B in our experimental group is a characteristic feature of BD or anxiety, or whether it is related to both conditions.

We found an unchanged duration but a higher occurence and coverage of A and B microstates in BD patients. In other words, an unchanged sustainability in time and still increased presence of these microstates in patients compared to HCs were observed. Possible explanation for this finding appears to be a redundance in activation of the sensory and autobiographic memory networks during spontaneous mentation in euthymic BD patients. Changes in A and B microstate occurence, duration, and coverage have been reported in several psychiatric conditions such as schizophrenia, dementia, narcolepsy, multiple sclerosis, panic disorder, etc. (for review see 20). In schizophrenia patients, both increased (30) and decreased (67, 68) durations of microstate B as well as increased occurrence of microstate A (68) were reported. Increases in duration and occurrence of microstates A and B were also observed in patients with multiple sclerosis, moreover predicting depression scores and other clinical variables (31). It was suggested that multiple sclerosis affects the "sensory" (visual, auditory) rather than the higher-order (salience, central executive) functional networks (20). Our findings of impaired dynamics in microstates A and B suggest a similar interpretation for the BD. Although the pathophysiology in multiple sclerosis differes from that in depression, the increased presence of A and B microstates might reflect aberrant temporal functioning of sensory-related and memory networks in both diseases. Evidence from fMRI studies points to topographical dysbalances between the default mode and sensorimotor networks in BD patients with opposing patterns in depression and mania (69). Cyclothymic and depressive temperaments were associated with opposite changes in the sensorimotor network variability in the resting state signal measured by fractional standard deviation of blood-oxygen-level dependent signal (70). Our findings of altered microstates A and B dynamics is consistent with this fMRI evidence of impaired sensorimotor network in affective disorders, and moreover suggests that neural correlates of these deficits are prominent even during the euthymic state in BD patients.

It is known that EEG microstate dynamics during eyes closed and eyes open resting-state is different. Manipulations of visual input showed increased occurrence and coverage of microstate B and shorter duration of microstate A in the eyes open condition in healthy young adults (71). Further studies are needed to investigate, whether the here observed abnormalities of the A and B microstates in BD patients are still present in the eyes open condition.

BD patients were previously shown to display lower alpha power as compared to HCs (72), as it was the case here. We failed, however, to find any significant correlation between the altered microstate dynamics and decreased alpha power. Our findings, therefore, further support the previously reported independence of microstates from EEG frequency power fluctuations (49).

In summary, results of the current study seem to indicate that dysfunctional activity of resting-state brain networks underlying microstates A and B is a detectable impairment in BD during an euthymic state. The presence of microstate A and B represents measures that might be implicated in clinical practice, although using these parameters for early identification of BD at individual level could prove challenging. If future studies confirm the same pattern in prodromal or vulnerable subjects, it could help detection of at-risk subjects and therefore the possiblility for early intervention. The present study has, however, some limitations. Our low sample size made it impossible to examine any potential influence of medication on the microstate parameters by comparing patients receiving a specific drug with those not receiving it. Possible effects of medication on our results should be therefore taken into account. Due to the same reason, it was

not possible to examine any potential influence of subtypes of BD on microstate results.

CONCLUSIONS

Our study described altered EEG resting-state microstate temporal parameters in euthymic bipolar patients. Our findings provide an insight into the resting-state global brain network dynamics in BD. Since the increased presence of microstate A is not unique to BD patients, having been reported also in other psychiatric disorders (see 20), it might be considered only as a non-specific electrophysiological marker of BD. Moreover, studies examining possible interactions between microstate dynamics and BD symptoms are needed to better understand the dysfunction of large-scale brain network resting-state dynamics in this affective disorder.

DATA AVAILABILITY STATEMENT

The raw data supporting the conclusions of this manuscript will be made available by the authors, without undue reservation, to any qualified researcher.

ETHICS STATEMENT

The studies involving human participants were reviewed and approved by Ethics Committee for Human Research of the Geneva University Hospital. The patients/participants provided their written informed consent to participate in this study.

AUTHOR CONTRIBUTIONS

AD designed the study, performed the analysis, and wrote the initial draft. J-MA, AD, and CP were responsible for clinical assessment. CM served as an advisor. CB collected the HD-EEG data and was responsible for the overall oversight of the study. All authors revised the manuscript.

FUNDING

This study was supported by the European Union Horizon 2020 research and innovation program under the Marie Skłodowska-Curie grant agreement No. 739939, by the Swiss National Science Foundation (grant No. 320030_184677), and by the National Centre of Competence in Research (NCCR) "SYNAPSY—The Synaptic Basis of Mental Diseases" (NCCR Synapsy Grant # "51NF40-185897). The funding sources had no role in the design, collection, analysis, or interpretation of the study.

ACKNOWLEDGMENTS

Special thanks go to Anne-Lise Kung, psychologist, for her involvement in clinical data collection.

SUPPLEMENTARY MATERIAL

The Supplementary Material for this article can be found online at: https://www.frontiersin.org/articles/10.3389/fpsyt.2019.00826/full#supplementary-material

SUPPLEMENTARY FIGURE 1 | Microstate analysis: **(A)** resting-state EEG from subsample of 16 out of 204 electrodes; **(B)** global field power (GFP) curve with the GFP peaks (vertical lines) in the same EEG period as shown in (A); **(C)** potential maps at successive GFP peaks, indicated in (B), from the first 1 s period of the recording; **(D)** set of five cluster maps best explaining the data as revealed by *k*-means clustering of the maps at the GFP peaks; **(E)** the original EEG recording shown in (A) with superimposed color-coded microstate segments. Note that each time point of the EEG recording was labelled with the cluster map, shown in (D), with which the instant map correlated best. The duration of segments, occurrence, and coverage for all microstates were computed on thus labeled EEG recording.

REFERENCES

1. Cloutier M, Greene M, Guerin A, Touya M, Wu E. The economic burden of bipolar I disorder in the United States in 2015. *J Affect Disord* (2018) 226:45–51. doi: 10.1016/j.jad.2017.09.011
2. Eaton WW, Alexandre P, Bienvenu OJ, Clarke D, Martins SS, Nestadt G, et al. The burden of mental disorders. In: Eaton WW, editor. *Public Mental Health*. Oxford, UK: Oxford University Press (2012). doi: 10.1093/acprof:oso/9780195390445.003.0001.
3. Merikangas KR, Jin R, He JP, Kessler RC, Lee S, Sampson NA, et al. Prevalence and correlates of bipolar spectrum disorder in the World Mental health survey initiative. *Arch Gen Psychiatry* (2011) 68:241–51. doi: 10.1001/archgenpsychiatry.2011.12
4. Ferrari AJ, Stockings E, Khoo JP, Erskine HE, Degenhardt L, Vos T, et al. The prevalence and burden of bipolar disorder: findings from the Global Burden of disease study 2013. *Bipolar Disord.* (2016) 18:440–50. doi: 10.1111/bdi.12423
5. Hirschfeld RMA. Screening for bipolar disorder. *Am J Managed Care* (2007) 13:S164–9.
6. Vieta E, Salagre E, Grande I, Carvalho AF, Fernandes BS, Berk M, et al. Early intervention in Bipolar disorder. *Am J Psychiatry* (2018) 175:411–26. doi: 10.1176/appi.ajp.2017.17090972
7. Chen CH, Suckling J, Lennox BR, Ooi C, Bullmore ET. A quantitative meta-analysis of fMRI studies in bipolar disorder. *Bipolar Disord* (2011) 13:1–15. doi: 10.1111/j.1399-5618.2011.00893.x
8. Houenou J, Frommberger J, Carde S, Glasbrenner M, Diener C, Leboyer M, et al. Neuroimaging-based markers of bipolar disorder: evidence from two meta-analyses. *J Affect Disord* (2011) 132:344–55. doi: 10.1016/j.jad.2011.03.016
9. Kupferschmidt DA, Zakzanis KK. Toward a functional neuroanatomical signature of bipolar disorder: quantitative evidence from the neuroimaging literature. *Psychiatry Res Neuroimaging* (2011) 193:71–9. doi: 10.1016/j.pscychresns.2011.02.011
10. Piguet C, Fodoulian L, Aubry JM, Vuilleumier P, Houenou J. Bipolar disorder: functional neuroimaging markers in relatives. *Neurosci Biobehav. Rev* (2015) 57:284–96. doi: 10.1016/j.neubiorev.2015.08.015
11. Vargas C, López-Jaramillo C, Vieta E. A systematic literature review of resting state network-functional MRI in bipolar disorder. *J Affect Disord* (2013) 150:727–35. doi: 10.1016/j.jad.2013.05.083
12. Strakowski SM, Adler CM, Almeida J, Altshuler LL, Blumberg HP, Chang KD, et al. The functional neuroanatomy of bipolar disorder: A consensus model. *Bipolar Disord* (2012) 14:313–25. doi: 10.1111/j.1399-5618.2012.01022.x

13. Chase HW, Phillips ML. Elucidating neural network functional connectivity abnormalities in bipolar disorder: toward a harmonized methodological approach. *Biol Psychiatry Cogn. Neurosci Neuroimaging* (2016) 1:288–98. doi: 10.1016/j.bpsc.2015.12.006
14. Rey G, Piguet C, Benders A, Favre S, Eickhoff SB, Aubry JM, et al. Resting-state functional connectivity of emotion regulation networks in euthymic and non-euthymic bipolar disorder patients. *Eur Psychiatry* (2016) 34:56–63. doi: 10.1016/j.eurpsy.2015.12.005
15. Wang Y, Zhong S, Jia Y, Sun Y, Wang B, Liu T, et al. Disrupted resting-state functional connectivity in nonmedicated bipolar disorder. *Radiology* (2016) 280:529–36. doi: 10.1148/radiol.2016151641
16. de Pasquale. F, Corbetta M, Betti. V, Penna Della. Cortical cores in network dynamics. *Neuroimage* (2018) 180:370–82:S. doi: 10.1016/j.neuroimage.2017.09.063
17. Bressler SL, Menon V. Large-scale brain networks in cognition: emerging methods and principles. *Trends Cogn. Sci* (2010) 14:277–90. doi: 10.1016/j.tics.2010.04.004
18. Pascual-Marqui RD, Michel CM, Lehmann D. Segmentation of brain electrical activity into microstates; model estimation and validation. *IEEE Trans Biomed Eng.* (1995) 42:658–65. doi: 10.1109/10.391164
19. Van De Ville D, Britz J, Michel CM. EEG microstate sequences in healthy humans at rest reveal scale-free dynamics. *Proc Natl Acad Sci* (2010) 107:18179–84. doi: 10.1073/pnas.1007841107
20. Michel CM, Koenig T. EEG microstates as a tool for studying the temporal dynamics of whole-brain neuronal networks: a review. *Neuroimage* (2018) 180:577–93. doi: 10.1016/j.neuroimage.2017.11.062
21. Lehmann D, Ozaki H, Pal I. EEG alpha map series: brain micro-states by space-oriented adaptive segmentation. *Electroencephalogr. Clin Neurophysiol.* (1987) 67:271–88. doi: 10.1016/0013-4694(87)90025-3
22. Koenig T, Prichep L, Lehmann D, Sosa PV, Braeker E, Kleinlogel H, et al. Millisecond by millisecond, year by year: normative EEG microstates and developmental stages. *Neuroimage* (2002) 16:41–8. doi: 10.1006/nimg.2002.1070
23. Custo A, Van De Ville D, Wells WM, Tomescu MI, Brunet D, Michel CM. Electroencephalographic resting-state networks: source localization of microstates. *Brain Connectivity* (2017) 7:671–82. doi: 10.1089/brain.2016.0476
24. Bréchet L, Brunet D, Birot G, Gruetter R, Michel CM, Jorge J. Capturing the spatiotemporal dynamics of self-generated, task-initiated thoughts with EEG and fMRI. *Neuroimage* (2019) 194:82–92. doi: 10.1016/j.neuroimage.2019.03.029
25. Khanna A, Pascual-Leone A, Michel CM, Farzan F. Microstates in resting-state EEG: Current status and future directions. *Neurosci Biobehav. Rev* (2015) 49:105–13. doi: 10.1016/j.neubiorev.2014.12.010
26. Changeux JP, Michel CM. Mechanism of neural integration at the brain-scale Level. In: Grillner S, Graybiel, AM, editors. *Microcircuits*. Cambridge, Mass, USA: MIT Press (2004). p. 347–70.
27. Lehmann D. Brain Electric microstates and cognition: the atoms of thought. In: John ER, Harmony T, Prichep LS, Valdés-Sosa M, Valdés-Sosa PA, editors. *Machinery of the Mind*. Birkhäuser, Boston, MA, USA (1990). p. 209–24. doi: 10.1007/978-1-4757-1083-0_10
28. Tomescu MI, Rihs TA, Becker R, Britz J, Custo A, Grouiller F, et al. Deviant dynamics of EEG resting state pattern in 22q11.2 deletion syndrome adolescents: a vulnerability marker of schizophrenia? *Schizophr. Res* (2014) 157:175–81. doi: 10.1016/j.schres.2014.05.036
29. Tomescu MI, Rihs TA, Roinishvili M, Karahanoglu FI, Schneider M, Menghetti S, et al. Schizophrenia patients and 22q11.2 deletion syndrome adolescents at risk express the same deviant patterns of resting state EEG microstates: a candidate endophenotype of schizophrenia. *Schizophr. Res Cogn.* (2015) 2:159–65. doi: 10.1016/j.scog.2015.04.005
30. Andreou C, Faber PL, Leicht G, Schoettle D, Polomac N, Hanganu-Opatz IL, et al. Resting-state connectivity in the prodromal phase of schizophrenia: Insights from EEG microstates. *Schizophr. Res* (2014) 152:513–20. doi: 10.1016/j.schres.2013.12.008
31. Gschwind M, Hardmeier M, Van De Ville D, Tomescu MI, Penner I, Naegelin Y, et al. Fluctuations of spontaneous EEG topographies predict disease state in relapsing-remitting multiple sclerosis. *NeuroImage Clin* (2016) 12:466–77. doi: 10.1016/j.nicl.2016.08.008
32. Atluri S, Wong W, Moreno S, Blumberger DM, Daskalakis ZJ, Farzan F. Selective modulation of brain network dynamics by seizure therapy in treatment-resistant depression. *NeuroImage Clin* (2018) 20:1176–90. doi: 10.1016/j.nicl.2018.10.015
33. Sverak T, Albrechtova L, Lamos M, Rektorova I, Ustohal L. Intensive repetitive transcranial magnetic stimulation changes EEG microstates in schizophrenia: A pilot study. *Schizophr. Res* (2018) 193:451–2. doi: 10.1016/j.schres.2017.06.044
34. Strik WK, Dierks T, Becker T, Lehmann D. Larger topographical variance and decreased duration of brain electric microstates in depression. *J Neural Transm* (1995) 99:213–22. doi: 10.1007/BF01271480
35. Damborská A, Tomescu MI, Honzírková E, Barteček R, Hořínková J. Fedorová, S, et al. EEG resting-state large-scale brain network dynamics are related to depressive symptoms. *Front Psychiatry* (2019) 548:10. doi: 10.3389/fpsyt.2019.00548
36. Piguet C, Dayer A, Aubry JM. Biomarkers and vulnerability to bipolar disorders. *Schweiz Arch Neurol Psychiatr* (2016) 167:57–67. doi: 10.4414/sanp.2016.00387
37. Berchio C, Piguet C, Michel CM, Cordera P, Rihs TA, Dayer AG, et al. Dysfunctional gaze processing in bipolar disorder. *NeuroImage Clin* (2017) 16:545–56. doi: 10.1016/j.nicl.2017.09.006
38. Nurnberger JI Jr., Blehar MC, Kaufmann CA, York-Cooler C, Simpson SG, Harkavy-Friedman J, et al. Diagnostic interview for genetic studies: Rationale, unique features, and training. *Arch Gen Psychiatry* (1994) 51:849–59. doi: 10.1001/archpsyc.1994.03950110009002
39. Young RC, Biggs JT, Ziegler VE, Meyer DA. A rating scale for mania: reliability, validity and sensitivity. *Br J Psychiatry* (1978) 133:429–35. doi: 10.1192/bjp.133.5.429
40. Williams JBW, Kobak KA. Development and reliability of a structured interview guide for the Montgomery Asberg depression rating scale (sigma). *Br J Psychiatry* (2008) 192:52–8. doi: 10.1192/bjp.bp.106.032532
41. Simon NM, Otto MW, Wisniewski SR, Fossey M, Sagduyu K, Frank E, et al. Anxiety disorder comorbidity in bipolar disorder patients: data from the first 500 participants in the Systematic Treatment Enhancement Program for Bipolar Disorder (STEP-BD). *Am J Psychiatry* (2004) 161:2222–9. doi: 10.1176/appi.ajp.161.12.2222
42. Simon NM, Zalta AK, Otto MW, Ostacher MJ, Fischmann D, Chow CW, et al. The association of comorbid anxiety disorders with suicide attempts and suicidal ideation in outpatients with bipolar disorder. *J Psychiatr Res* (2007) 41:255–64. doi: 10.1016/j.jpsychires.2006.08.004
43. Wiedemann G, Stevens A, Pauli P, Dengler W. Decreased duration and altered topography of electroencephalographic microstates in patients with panic disorder. *Psychiatry Res Neuroimaging* (1998) 84:37–48. doi: 10.1016/S0925-4927(98)00044-4
44. Spielberger CD, Gorsuch RL, Lushene RE, (1970). *Manual for the State-Trait Anxiety Inventory*. Palo Alto, CA, USA: Consulting Psychologists Press.
45. Jung T, Makeig S, Westerfield M, Townsend J, CourchesneE.c, et al. Removal of eye activity artifacts from visual event-related potentials in normal and clinical subjects. *Clin Neurophysiol.* (2000) 111:1745–58. doi: 10.1016/S1388-2457(00)00386-2
46. Perrin F, Pernier J, Bertrand O, Echallier JF. Spherical splines for scalp potential and current density mapping. *Electroencephalogr. Clin Neurophysiol.* (1989) 72:184–7. doi: 10.1016/0013-4694(89)90180-6
47. Brunet D, Murray M, Michel CM. Spatiotemporal analysis of multichannel EEG: CARTOOL. *Comput Intell. Neurosci* (2011) 2011, 813870. doi: 10.1155/2011/813870.
48. Murray MM, Brunet D, Michel CM. Topographic ERP analyses: a step-by-step tutorial review. *Brain Topogr.* (2008) 20:249–64. doi: 10.1007/s10548-008-0054-5
49. Britz J, Van De Ville D, Michel CM. BOLD correlates of EEG topography reveal rapid resting-state network dynamics. *NeuroImage* (2010) 52:1162–70. doi: 10.1016/j.neuroimage.2010.02.052
50. Michel CM, Brandeis D, Skrandies W, Pascual R, Strik WK, Dierks T, et al. Global field power: a 'time-honoured' index for EEG/EP map analysis. *Int J Psychophysiol.* (1993) 15:1–2. doi: 10.1016/0167-8760(93)90088-7
51. Santarnecchi E, Khanna AR, Musaeus CS, Benwell CSY, Davila P, Farzan F, et al. EEG microstate correlates of fluid intelligence and response to cognitive training. *Brain Topogr.* (2017) 30:502–20. doi: 10.1007/s10548-017-0565-z

52. Benjamini Y. Discovering the false discovery rate. *J R Stat Soc Ser B Stat Methodol* (2010) 72:405–16. doi: 10.1111/j.1467-9868.2010.00746.x
53. Niedermeyer E. *Niedermeyer's electroencephalography: basic principles, clinical applications, and related fields*. Philadelphia , PA, USA: Lippincott Williams & Wilkins (2011).
54. Oldfield RC. The assessment and analysis of handedness: The Edinburgh inventory. *Neuropsychologia* (1971) 9:97–113. doi: 10.1016/0028-3932(71)90067-4
55. Yin Z, Chang M, Wei S, Jiang X, Zhou Y, Cui L, et al. Decreased functional connectivity in insular subregions in depressive episodes of bipolar disorder and major depressive disorder. *Front Neurosci* (2018) 12, 842. doi: 10.3389/fnins.2018.00842.
56. Reinke B, Van de Ven V, Matura S, Linden DEJ, Oertel-Knöchel V. Altered intrinsic functional connectivity in language-related brain regions in association with verbal memory performance in euthymic bipolar patients. *Brain Sci* (2013) 3:1357–73. doi: 10.3390/brainsci3031357
57. Gong J, Chen G, Jia Y, Zhong S, Zhao L, Luo X, et al. Disrupted functional connectivity within the default mode network and salience network in unmedicated bipolar II disorder. *Prog Neuro-Psychopharmacol. Biol Psychiatry* (2019) 88:11–8. doi: 10.1016/j.pnpbp.2018.06.012
58. Öngür D, Lundy M, Greenhouse I, Shinn AK, Menon V, Cohen BM, et al. Default mode network abnormalities in bipolar disorder and schizophrenia. *Psychiatry Res Neuroimaging* (2010) 183:59–68. doi: 10.1016/j.pscychresns.2010.04.008
59. Minuzzi L, Syan SK, Smith M, Hall A, Hall GBC, Frey BN. Structural and functional changes in the somatosensory cortex in euthymic females with bipolar disorder. *Aust New Z J Psychiatry* (2018) 52:1075–83. doi: 10.1177/0004867417746001
60. Li G, Liu P, Andari E, Zhang A, Zhang K. The role of amygdala in patients with euthymic bipolar disorder during resting state. *Front Psychiatry* (2018) 9, 445. doi: 10.3389/fpsyt.2018.00445
61. Albert U, Rosso G, Maina G, Bogetto F. Impact of anxiety disorder comorbidity on quality of life in euthymic bipolar disorder patients: differences between bipolar I and II subtypes. *J Affect Disord* (2008) 105:297–303. doi: 10.1016/j.jad.2007.05.020
62. Custo A, Vulliemoz S, Grouiller F, Van De Ville D, Michel C. EEG source imaging of brain states using spatiotemporal regression. *Neuroimage* (2014) 96:106–16. doi: 10.1016/j.neuroimage.2014.04.002
63. Phelps EA, Ling S, Carrasco M. Emotion facilitates perception and potentiates the perceptual benefits of attention. *Psychol Sci* (2006) 17:292–9. doi: 10.1111/j.1467-9280.2006.01701.x
64. Laretzaki G, Plainis S, Argyropoulos S, Pallikaris IG, Bitsios P. Threat and anxiety affect visual contrast perception. *J Psychopharmacol* (2010) 24:667–75. doi: 10.1177/0269881108098823
65. Goldin PR, Manber T, Hakimi S, Canli T, Gross JJ. Neural bases of social anxiety disorder: Emotional reactivity and cognitive regulation during social and physical threat. *Arch Gen Psychiatry* (2009) 66:170–80. doi: 10.1001/archgenpsychiatry.2008.525
66. Al Zoubi O, Mayeli A, Tsuchiyagaito A, Misaki M, Zotev V, Refai H, et al. EEG microstates temporal dynamics differentiate individuals with mood and anxiety disorders from healthy subjects. *Front Hum Neurosci* (2019) 13, 56. doi: 10.3389/fnhum.2019.00056
67. Nishida K, Morishima Y, Yoshimura M, Isotani T, Irisawa S, Jann K, et al. EEG microstates associated with salience and frontoparietal networks in frontotemporal dementia, schizophrenia and Alzheimer's disease. *Clin Neurophysiol.* (2013) 124:1106–14. doi: 10.1016/j.clinph.2013.01.005
68. Lehmann D, Faber PL, Galderisi S, Herrmann WM, Kinoshita T, Koukkou M, et al. EEG microstate duration and syntax in acute, medication-naïve, first-episode schizophrenia: a multi-center study. *Psychiatry Res Neuroimaging* (2005) 138:141–56. doi: 10.1016/j.pscychresns.2004.05.007
69. Martino M, Magioncalda P, Huang Z, Conio B, Piaggio N, Duncan NW, et al. Contrasting variability patterns in the default mode and sensorimotor networks balance in bipolar depression and mania. *Proc Natl Acad Sci USA* (2016) 113:4824–9. doi: 10.1073/pnas.1517558113
70. Conio B, Magioncalda P, Martino M, Tumati S, Capobianco L, Escelsior A, et al. Opposing patterns of neuronal variability in the sensorimotor network mediate cyclothymic and depressive temperaments. *Hum Brain Mapp.* (2019) 40:1344–52. doi: 10.1002/hbm.24453
71. Seitzman BA, Abell M, Bartley SC, Erickson MA, Bolbecker AR, Hetrick WP. Cognitive manipulation of brain electric microstates. *Neuroimage* (2017) 146:533–43. doi: 10.1016/j.neuroimage.2016.10.002
72. Basar E, Güntekin B, Atagün I, Turp Gölbas B, Tülay E, Özerdem A. Brain's alpha activity is highly reduced in euthymic bipolar disorder patients. *Cogn. Neurodynamics* (2012) 6:11–20. doi: 10.1007/s11571-011-9172-y

Conflict of Interest: The authors declare that the research was conducted in the absence of any commercial or financial relationships that could be construed as a potential conflict of interest.

Copyright © 2019 Damborská, Piguet, Aubry, Dayer, Michel and Berchio. This is an open-access article distributed under the terms of the Creative Commons Attribution License (CC BY). The use, distribution or reproduction in other forums is permitted, provided the original author(s) and the copyright owner(s) are credited and that the original publication in this journal is cited, in accordance with accepted academic practice. No use, distribution or reproduction is permitted which does not comply with these terms.

Annex 12

Damborská, A., Honzírková, E., Barteček R., Hořínková J., Fedorová, S., Ondruš, Š., Michel, C.M., Rubega, M. (2020). Altered directed functional connectivity of the right amygdala in depression: high-density EEG study. *Scientific Reports*, 4398 (10)

SCIENTIFIC REPORTS
nature research

OPEN

Altered directed functional connectivity of the right amygdala in depression: high-density EEG study

Alena Damborská[1,2,3,6*], Eliška Honzírková[2], Richard Barteček[2,3], Jana Hořínková[2,3], Sylvie Fedorová[2,3], Šimon Ondruš[2,3], Christoph M. Michel[1,4] & Maria Rubega[1,5,6]

The cortico-striatal-pallidal-thalamic and limbic circuits are suggested to play a crucial role in the pathophysiology of depression. Stimulation of deep brain targets might improve symptoms in treatment-resistant depression. However, a better understanding of connectivity properties of deep brain structures potentially implicated in deep brain stimulation (DBS) treatment is needed. Using high-density EEG, we explored the directed functional connectivity at rest in 25 healthy subjects and 26 patients with moderate to severe depression within the bipolar affective disorder, depressive episode, and recurrent depressive disorder. We computed the Partial Directed Coherence on the source EEG signals focusing on the amygdala, anterior cingulate, putamen, pallidum, caudate, and thalamus. The global efficiency for the whole brain and the local efficiency, clustering coefficient, outflow, and strength for the selected structures were calculated. In the right amygdala, all the network metrics were significantly higher ($p < 0.001$) in patients than in controls. The global efficiency was significantly higher ($p < 0.05$) in patients than in controls, showed no correlation with status of depression, but decreased with increasing medication intake ($R^2 = 0.59$ and $p = 1.52e\text{-}05$). The amygdala seems to play an important role in neurobiology of depression. Practical treatment studies would be necessary to assess the amygdala as a potential future DBS target for treating depression.

Affective disorders belong to the most common and most serious psychiatric disorders[1]. A crucial role of the cortico-striatal-pallidal-thalamic and limbic circuits in the neurobiology of depression was repeatedly reported[2–4]. Magnetic resonance imaging, functional magnetic resonance imaging (fMRI), magnetoencephalographic, and electroencephalographic (EEG) studies have confirmed that depressive patients show structural impairments and functional dysbalances of brain networks that involve structures engaged in (a) emotions, i.e. amygdala, subgenual anterior cingulate, caudate, putamen and pallidum[3,5–12]; (b) self-referential processes, i.e. medial prefrontal cortex, precuneus, and posterior cingulate cortex[13,14]; (c) memory, i.e. hippocampus, parahippocampal cortex[15]; (d) visual processing, i.e. fusiform gyrus, lingual gyrus, and lateral temporal cortex[16]; and (e) attention, i.e. dorsolateral prefrontal cortex, anterior cingulate cortex (ACC), thalamus, and insula[10–12,17]. Moreover, post-mortem morphometric measurements revealed smaller volumes of the hypothalamus, pallidum, putamen and thalamus in patients with affective disorders[18].

Many depressive patients fail to respond to pharmacological therapy resulting in 1–3% prevalence of treatment-resistant depression (TRD)[19]. One of the newest therapeutic approaches for TRD is an invasive direct electrical stimulation of relevant deep brain structures[20]. Both unipolar and bipolar depression patients might benefit from deep brain stimulation (DBS) treatment[21], although an optimal approach, including selection of an optimal target structure, has yet to be established. Selection of the brain structures, that are currently being tested as DBS targets for treating depression[20], is mostly supported with the evidence from lesional[22,23], animal[24–30], and neuroimaging[31–38] studies. The latter approach provides evidence from a network perspective[39,40] showing

[1]Department of Basic Neurosciences, University of Geneva, Campus Biotech, Geneva, Switzerland. [2]Department of Psychiatry, Faculty of Medicine, Masaryk University, Brno, Czech Republic. [3]Department of Psychiatry, University Hospital Brno, Brno, Czech Republic. [4]Lemanic Biomedical Imaging Centre (CIBM), Lausanne and Geneva, Switzerland. [5]Present address: Department of Neuroscience, University of Padova, Padova, Italy. [6]These authors contributed equally: Alena Damborská and Maria Rubega. *email: adambor@med.muni.cz

dysbalances in the intrinsic functional architecture of the brain. During a resting state, patients with depression as compared to healthy controls show hyperconnectivity within the default mode network[13,33,38], hypoconnectivity within the frontoparietal network[41,42], hyperconnectivity between the default mode and frontoparietal networks[43], and dysbalances in connectivity within the salience[44,45] and dorsal attention[46] networks. Functional connectivity anomalies between the hippocampus, cortical and subcortical regions[47] similar to those observed in humans with depression, were also observed in a genetic rat model of major depression. The pathophysiological basis of depression, however, still remains incompletely understood. Particularly, better understanding of the connectivity properties of deep brain structures potentially implicated in DBS treatment could have an important value.

Neuroimaging techniques, such as fMRI and EEG, allow to investigate the integration of functionally specialized brain regions in a network. Inferring the dynamical interactions among simultaneously recorded brain signals can reveal useful information in abnormal connectivity patterns due to pathologies.

The connectivity studies based on fMRI are usually based on correlation analyses without providing knowledge about the direction of the information flow between the examined regions. Understanding the directionality is, however, crucial when searching for suitable DBS targets for treating TRD, because the antidepressant effect of DBS treatment might be caused by changes in the activity of remote structures that receive inputs from the stimulated region. For example, it has been hypothesized that DBS applied in the nucleus accumbens might influence the activity in the ventral (subgenual ACC, orbitofrontal and insular cortices) and dorsal (dorsal ACC, prefrontal and premotor cortices) subnetworks of the depression neurocircuitry[48]. Causal link between a functional inhibition of the lateral habenula and reduction of the default mode network hyperconnectivity was shown on a rat model of depression[30], which might explain the therapeutic effect of the lateral habenula DBS in TRD patients[49]. In other words, the functional inhibition of a deep brain structure via DBS might cure depression through reduction of the hyperconnectivity in the large-scale brain network. Another example of a particular role of the stimulated structure in the large-scale neural communication is the ACC, whose possible integrative role in cognitive processing[50,51] might explain the most recently reported high efficacy of DBS to subgenual ACC in treating depression[52].

The growing interest in investigating the dynamical causal interactions that characterize resting-state or task-related brain networks has increased the use of adaptive estimation algorithms during recent years. Particularly, Granger causality based on adaptive filtering algorithms is a well suited procedure to study dynamical networks consisting of highly non-stationary neural signals such as EEG signals[53,54]. The adaptive filtering enables to deal with time-varying multivariate time-series and test direct causal links among brain regions. A signal x is said to Granger-cause another signal y if the history of x contains information that helps to predict y above and beyond the information contained in the history of y alone[55].

Aberrant functional EEG-based connectivity in depressive patients was reported in studies where network metrics were computed directly between sensor recordings[56–61]. Since each EEG channel is a linear mixture of simultaneously active neural and other electrophysiological sources, whose activities are volume conducted to the scalp electrodes, the utility of such observations on the sensor level is limited[62,63]. This limitation is particularly remarkable in connectivity studies which aim to identify the real active relations between brain regions. Connectivity analysis performed in the source space enables to partially overcome this issue[62]. Indeed, Partial Directed Coherence estimators do not take into account zero-lag interactions that describe the instantaneous propagation of activity, considering the zero-phase connectivity as noise added to lagged connectivity patterns of interest. For this reason, directed functional connectivity analysis based on electrical source imaging proved to be a promising tool to study the dynamics of spontaneous brain activity in healthy subjects and in various brain disorders[64–66]. Despite this fact, the electromagnetic imaging has not been yet used in patients with depression to study the directed connectivity of resting-state networks.

In the current study, we explored the directed functional connectivity at rest in depression using high-density EEG. We computed the Partial Directed Coherence on the source EEG signals focusing on the role of the amygdala, anterior cingulate, putamen, pallidum, caudate, and thalamus in large-scale brain network activities. We hypothesized that the resting-state directed functional connectivity in these deep brain structures might be disrupted in patients with depression compared to healthy controls.

Results

In line with the aim of the study we focused on resting-state electrophysiological activity of twelve regions of interest (ROIs) of selected deep brain structures. Further details on results on the ROIs of the whole brain are reported in the Supplementary Information.

Power spectra. We found an overall increase in power in theta and alpha frequency bands in patients compared to controls at both the *population* and *single-subject* levels. At the *population* level, significantly higher power ($p < 0.05$) in patients was found in all investigated subcortical regions in both frequency bands (see Fig. 1). At the *single-subject* level, a significantly higher power ($p < 0.05$) in patients than in controls was observed in the [4–12] Hz frequency range bilaterally in the thalamus, pallidum, putamen, and caudate. Moreover, a significant left-lateralized power increase ($p < 0.05$) in patients vs controls was observed in the anterior cingulate and amygdala in this frequency range (see Fig. 2b).

We found a significantly decreased power in delta [1–4] Hz and beta [12–18] Hz frequency bands in patients compared to controls in all investigated ROIs, when evaluating the results at the *population* level (Fig. 1). At the *single-subject* level, delta power was significantly decreased in patients vs controls in the right caudate, putamen, and pallidum (Fig. 2a). There was no significant difference in beta power between the two groups in any investigated ROI at the *single-subject* level (see Fig. 2c).

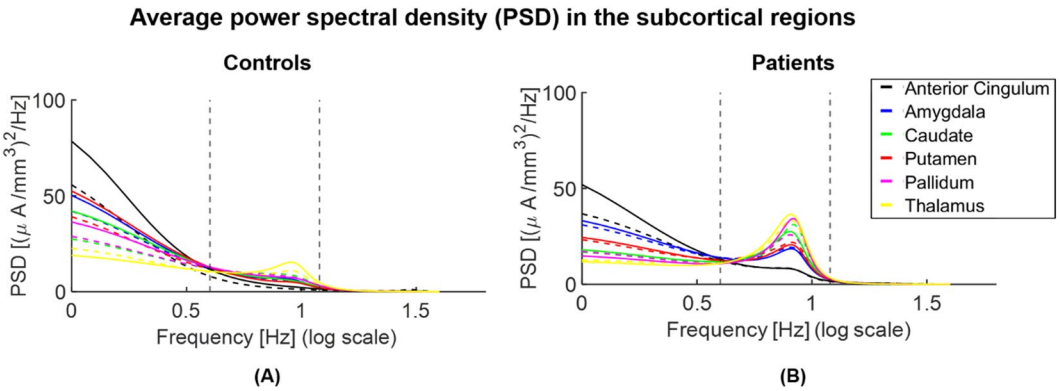

Figure 1. Parametric power spectral density (PSD) of the *population subjects* representing controls (**A**) vs patients (**B**) in the subcortical regions of interest. Power significantly increases within the interval [4–12] Hz (indicated with vertical dashed lines) in theta ([4–8] Hz) and alpha ([8–12] Hz) bands and decreases in delta ([1–4] Hz) and beta ([12–18] Hz) bands in patients compared to controls ($p < 0.05$) in the subcortical regions of interest. Continuous and dashed lines indicate the results for structures in the right and left hemispheres, respectively.

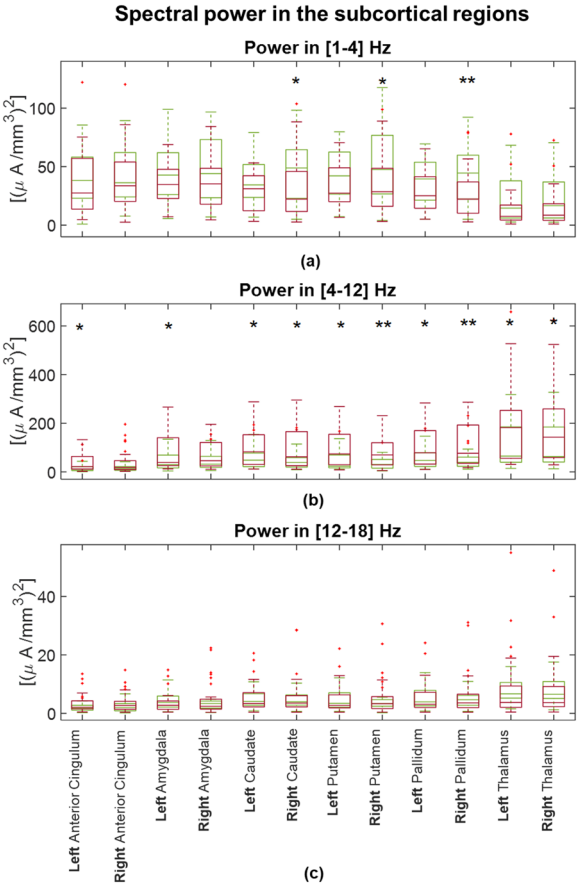

Figure 2. Boxplots to graphical illustrate the distribution of power of controls (green boxes) and patients (red boxes) in (**a**) [1–4] Hz, (**b**) [4–12] Hz and (**c**) [12–18] Hz. One star (*) stands for significant statistical difference with $p < 0.05$ and two stars (**) for $p < 0.001$. Power in [4–12] Hz significantly increases in patients compared to controls in all examined anatomical brain structures.

Network metrics. The connectivity network measures that we performed in the [4–12] Hz frequency range, showed increased values in patients compared to controls at both levels. At the *population* level, the local efficiency measured in patients was higher than in controls in all examined subcortical ROIs (see Fig. 3). At the *single-subject* level, the global efficiency was significantly higher ($p < 0.05$) in patients (mean ± standard

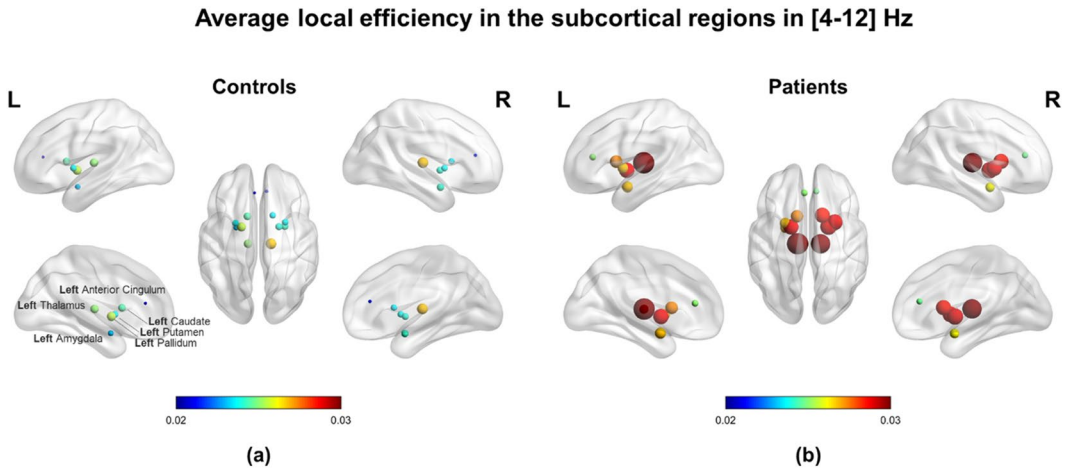

Figure 3. Local efficiency computed in the two *population subjects* representing (**a**) controls and (**b**) patients. Note that all subcortical regions of interest (ROIs) revealed higher values for patients than controls corresponding to the same tendency observed in all ROIs of the brain at the *single-subject* level (see Supplementary Figs. S1, S2). The efficiency for each ROI is represented by a sphere centered on the cortical region, whose radius is linearly related to the magnitude. Such information is also coded through a color scale.

deviation: 0.0129 ± 0.0021) than in controls (mean $\pm$ standard deviation: 0.0126 ± 0.0019). Considering all brain regions, the local efficiency tended to be higher in patients compared to controls (see Supplementary Fig. S2) but the significant differences corresponded only to the right precentral, amygdala and caudate regions ($p < 0.05$). We observed significant correlations between the local efficiency and power in the [4–12] Hz frequency range in subcortical ROIs but it was not generalized among all twelve subcortical ROIs (see Supplementary Fig. S3). No significant correlations were found between the local efficiency and power in delta and beta bands. All the network measures computed on the twelve selected ROIs showed significantly higher values in patients than in controls in the right amygdala. The strength, local efficiency, and clustering coefficient of the right caudate were significantly higher in patients than controls, while there was no significant difference between the groups in the outflow from this ROI. There were no significant differences in any network metric in the anterior cingulate, thalamus, pallidum, or putamen (see Fig. 4).

There were no statistical differences in the network metrics estimated between the left and right hemisphere in each subject. The laterality indices showed that neither controls, nor patients had a lateralization in connectivity results of the six investigated deep brain structures. No significant differences in the laterality indices were observed comparing controls and patients.

Effect of medication on network impairments. We found no correlation of the connectivity results with the intake of benzodiazepines, while there was a significant relationship between the global efficiency as predictor of the intake of AD/AP/MS medication ($AD/AP/MS \sim 1 + GE + GE^2$; Root Mean Squared Error: 0.716; $R^2 = 0.59$; F-statistic vs. constant model: 18.7, $p = 1.52e-05$). The global efficiency decreased with increasing medication score (see Fig. 5). We observed no significant correlation ($R^2 < 0.05$ and $p > 0.8$) between the connectivity results and any of the parameters that describe the status of depression (MADRS score, CGI score, illness duration, and the number of episodes) or the demographic profile (age and education level).

Discussion

In this study, we investigated resting-state network alterations using iPDC on source signals of high-density EEG in patients with depression compared to healthy controls. We explored the directed functional connectivity of the amygdala, anterior cingulate, putamen, pallidum, caudate, and thalamus, among them and with all the other brain regions in the time and frequency domain. We exploited the Kalman filter algorithm[67] assuming that resting state EEG segments were multiple realizations of the same process. Although we collapsed the temporal dimension to evaluate the network metrics, we decided to use a time-varying adaptive algorithm instead of a stationary autoregressive model to take into account the possible non-stationarity of the EEG signal and to more accurately capture this variability before collapsing the time with a summary measure, e.g., the median.

To sum up, we demonstrated that in patients with moderate to severe depression: (1) the directed functional connectivity was significantly increased compared to controls in the right amygdala and the right caudate; (2) the power in theta and alpha frequency bands was significantly increased compared to controls in all investigated brain anatomical structures; (3) higher medication intake was associated with lower overall driving from the investigated regions.

Increased right amygdala directed functional connectivity in depression. The most robust finding in our study was an abnormally increased directed functional connectivity in the right amygdala during resting-state in depressive patients. Even though the left-right asymmetry was not demonstrated by the laterality indices, a right-lateralized hyper-connectivity, as revealed with all the computed network metrics, was observed

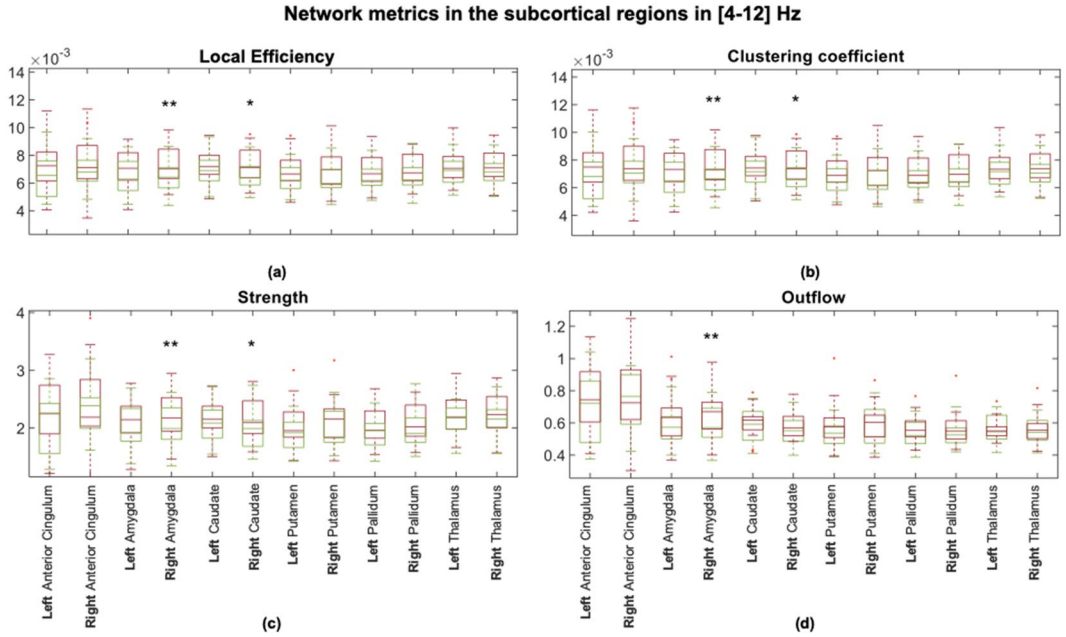

Figure 4. Boxplots to graphically illustrate the distribution of (**a**) local efficiency, (**b**) clustering coefficient, (**c**) strength, and (**d**) outflow in controls (green boxes) and patients (red boxes). One star (*) stands for significant statistical difference with $p < 0.05$ and two stars (**) for $p < 0.001$. All network metrics that refer to the right amygdala significantly differ between controls and patients ($p < 0.001$), applying the Bonferroni correction ($p < 0.05/12 \rightarrow p < 0.0042$).

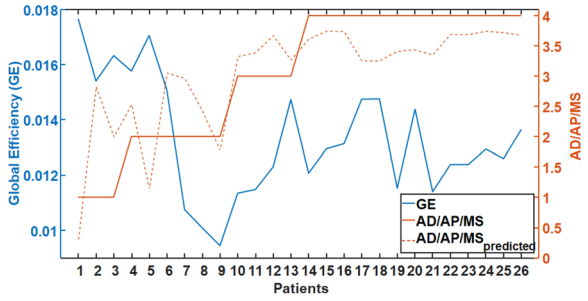

Figure 5. Relationship between the intake of antidepressants/antipsychotics/mood stabilizers (AD/AP/MS) and the global efficiency (GE). Note that higher medication intake is associated with lower GE. The orange dotted line stands for the predicted value of AD/AP/MS for each patient using GE as predictor. For values of the AD/AP/MS medication scale the reader is referred to the legend of Table 2.

in the amygdala. We observed an increase in outgoing connections from the right amygdala as reflected with significantly higher outflow and strength in patients compared to controls. Moreover, we found a hyper-connectivity in the local networks of the right amygdala as reflected with significantly higher local efficiency and clustering coefficient in patients compared to controls.

We also found a significantly higher global efficiency in patients compared to healthy controls. This network feature had the same trend at the population level. Namely, we observed abnormally increased local efficiency of all examined deep brain structures in depressive patients. The efficiency measures the ability of a neural network to integrate and combine information. The deeper regions have a key role as hubs of the large-scale brain networks, so changes in their local connectivity properties might have also led to connectivity changes in the whole brain.

The amygdala is involved in processing salient stimuli[68,69] and has been implicated as one of the central hubs within the affective salience network[70–72]. There is converging evidence from the neuroimaging studies that points to an abnormally increased connectivity and heightened activation of the amygdala in major depressive disorder (MDD) patients[73,74]. Reduced connectivity[75,76] and anomalous subregional functional resting-state connectivity of the amygdala[77] were also reported. Distinct network dysfunctions in MDD were suggested to underlie adult-specific amygdala resting-state fMRI connectivity impairment within the affective network, presumably reflecting an emotional dysregulation in MDD[76]. Hyperconnectivity between the amygdala, default mode

network and salience network was also found to be related to depressive symptoms suggesting to underlie the poststroke depression in temporal lobe lesions[78]. Unfortunately, the directionality of connections, which might be of interest when considering a structure as a potential DBS-target for treatment of TRD, cannot be inferred from these functional studies. There are only rare EEG-based connectivity studies focusing on depressive symptoms[58–60,79] that are, however, conducted only on a non-clinical population[79] or with connectivity parameters calculated at the sensor level[57–61]. Authors of one of these studies[79] suggested an inability of the left dorsolateral prefrontal cortex to modulate the activation of the left temporal lobe structures to be a crucial condition for ruminative tendencies. Interestingly, in the current study we demonstrated an abnormal increase in directed functional connectivity arising from the right amygdala. This increased connectivity in depressive patients could reflect an abnormal functioning of the right amygdala. Such dysfunction might represent an impaired bottom-up signaling for top-down cortical modulation of limbic regions, leading to an abnormal affect regulation in depressive patients.

The increased functional connectivity in amygdala is likely related to structural changes observed in depression. Enlarged amygdala volumes was found in first-episode depressive patients that positively correlated with severity of depression[80]. Higher grey matter volume was detected in bilateral amygdala of TRD patients compared to non-TRD patients, irrespective whether the patients presented bipolar or unipolar features and was suggested to reflect vulnerability to chronicity, revealed by medication resistance[81]. Larger right amygdala volume was, however, also suggested to be associated with greater chances of remission in bipolar disorder[82].

In our study we aimed to investigate the directed functional connectivity in amygdala to provide knowledge on neurobiology of depression that is needed to evaluate this structure as a possible candidate for DBS treatment in depression. Despite myriad of DBS targets for treating depression tested in humans[20], the amygdala is not among them. The possible safety and utility of DBS in the amygdala could only be inferred from studies, in which the amygdala-DBS was performed for other neuropsychiatric diagnoses, such as epilepsy[83–86], post-traumatic stress disorder[87,88], and autism[89]. In one of these studies transient stimulation-related positive shift in mood was observed[84]. Particularly, the stimulation of the right amygdala induced a transient decrease in the negative affective bias, i.e. the tendency to interpret ambiguous or positive events as relatively negative. In this case study, an epileptic patient with MDD rated the emotional facial expressions as more positive with stimulation than without. The stimulation effect might have been associated with a transient normalization of likely impaired function of the right amygdala in that patient. We can only speculate, whether this dysfunction was in terms of hyper-connectivity similar to that observed in our study and whether it was temporally decreased by inhibitory effect of the stimulation.

Increased right caudate directed functional connectivity in depression. We demonstrated that during resting state, patients had significantly higher right caudate directed functional connectivity than healthy controls. Despite no significant difference between groups in the caudate outflow, we observed an abnormally increased strength of outgoing connections from the right caudate in patients. Moreover, we found a hyper-connectivity in the local networks of the right caudate as reflected with significantly higher local efficiency and clustering coefficient in patients compared to controls. Caudate hyperactivation and increased caudate-amygdala and caudate-hippocampus fMRI connectivity during stress was previously reported in remitted individuals with recurrent depression[90]. The here observed EEG-based functional caudate hyperconnectivity suggests striatal dysfunction even during resting-state in depressed patients. Our finding is consistent with a compelling evidence directly associating cortico-basal ganglia functional abnormalities with primary bipolar and unipolar spectrum disorders[91]. Deficits in resting-state default-mode network connectivity with the bilateral caudate were suggested to be an early manifestation of MDD[92]. Reduced grey matter volume in the bilateral caudate[12,93–95], diffusion tensor imaging-based hypoconnectivity between the right caudate and middle frontal gyrus[96], and altered functional connectivity of the right caudate with the frontal regions[94] was observed in MDD patients. In a post-mortem morphometric study in late-life depressive subjects, reduction in neuronal density was found in both the dorsolateral and ventromedial areas of the caudate nucleus[97]. Associations between increased white matter lesion volumes and a decreased right caudate volume in the late-life depression was reported[98]. In mild to moderately depressed patients no change in caudate gray matter volumes were found[99] suggesting inverse correlation between the caudate volume and severity of depression.

We found no significant differences in any network metric in the putamen, pallidum, thalamus, and anterior cingulate. It is possible, however, that examining these structures as a whole might be insensitive to different changes in their relevant subregions. Only the medial part of the thalamus is expected to play a role in the experience of affect[73,100]. Reduced activity in the dorsal ACC but increased activity in the subgenual ACC have been found in acute depression in functional imaging studies[101,102]. Moreover, we must take into account the limitations of our methodological approach, i.e. the source localization of the EEG activity in the subcortical regions. We have to keep in mind that the spatial resolution in detecting and distinguishing neighboring brain regions is about 24 mm[103]. Therefore, our results in the caudate, putamen and pallidum are probably overlapping due to smearing of the sources. Keeping in mind these limitations and with respect to the lower robustness of our findings in the caudate, we can just encourage researchers to further investigate the neuropathophysiology of depression associated with the caudate nucleus functioning. More evidence from neuroimaging studies is needed to provide arguments for the next caudate-DBS tests in treating TRD. In an early case study, DBS of the ventral caudate nucleus markedly improved symptoms of depression in a patient with MDD and comorbid obsessive-compulsive disorder[104]. No change in depressive symptoms, however, was recently observed during the stimulation of the caudate in a study of three TRD patients[105] and authors concluded the caudate to be less promising DBS target than the nucleus accumbens.

Increased theta and alpha powers in depression. We found a significantly higher power in the theta and alpha frequency bands in the depressed compared to the healthy control group in all the investigated subcortical structures consistently at both the population and single-subject levels. The power decrease in the beta and delta frequency bands was observed only in the right striatum at both levels.

Our findings might be in line with previous observations in the sensor space of the scalp EEG. Abnormally high power in alpha[106–108] and theta[106,108,109] frequency bands in parietal and occipital regions were found in depressed patients, lower than normal beta and delta power were also reported[108]. Recent evidence points, however, to opposite power changes showing that theta and alpha power might decrease, while beta power increases in depression[110]. Moreover, the same study reported negative association of the posterior alpha power with the depression severity. While changes in cortical theta and alpha activity were suggested to be inversely related to the level of cortical activation, enhancement of the cortical beta power was suggested to reflect higher level of anxiety symptoms in depressed patients[106]. To the best of our knowledge there is only one study that directly recorded electrophysiological activity in subcortical structures in depressive patients. In this study, a larger alpha activity in MDD patients compared with obsessive compulsive disorder was found in the limbic DBS targets (the anterior cingulate and the bed nucleus of the stria terminalis)[111]. Moreover, in the same study, the increased alpha power correlated with severity of depressive symptoms. Nevertheless, in spite of parallels with prior reports, the current link between the power changes in subcortical structures and depression awaits replication.

Lower network impairments with more medication. We found an inverse relationship between the intake of medication and the impairment of the investigated networks. Particularly, increased intake of antidepressants, antipsychotics, and mood stabilizers was associated with reduction of the global efficiency. This finding might be related to the pharmacological effect on the brain activity, i.e. a change towards the normalization of the hyper-connectivity in the cortico-striatal-pallidal-thalamic and limbic networks. The low sample size and great variability in medication made it, however, impossible to examine any potential influence of medication on the network impairments by comparing patients receiving a specific drug with those not receiving it. To summarize the various medications, an ordinal variable was used that is only a rough measurement of medication usage. Moreover, the duration of the illness rather than the duration of the specific drug intake was considered in our study. Only doses of medication actually taken at the time of experiment were taken into consideration. The possible accumulated effect of specific drugs on connectivity results, thus, cannot be assessed. Therefore, the observed relationship between the global efficiency and medication should be viewed with caution. Interestingly, we have not found significant correlation between the global efficiency and intake of benzodiazepines. This negative finding suggests that even though benzodiazepines are known to have an effect on electrophysiological correlates of brain functions, the network properties might not be influenced. There were no significant correlations between the connectivity results and depressive symptom severity or other parameters describing the status of depression within the patient group. We suppose that heterogeneity of our dataset, in which patients with different disorders were included, might underlie this observation. We also found no relation between the connectivity results and education level or age. This finding suggests independence of the observed impairment on these demographic variables, however, the current sample size might be insufficient for such investigations.

Limitations of the study. We here report sources of scalp-recorded electrophysiological brain activity in deep brain structures. We are aware of the limitations of EEG in sensing deep brain structures. However, previous work using simulations and source reconstruction provided indirect evidence for the detectability of subcortical sources in non-invasive EEG and magnetoencephalographic recordings[112–115]. Moreover, recent simultaneous scalp and intracranial recordings directly demonstrated that activity in deep brain structures spread to the scalp[103,116]. While Seeber and colleagues[103] used individual head models that improve source localization precision, a generic head model was used in the magnetoencephalographic study by Pizzo *et al.*[116], similar to the approach used in our study. Nevertheless, the results that we report have to be interpreted with caution and need further validation by intracranial recordings in future studies.

Conclusions

We found an overall increase in power in theta and alpha frequency bands in depressive patients compared to healthy controls in the subcortical regions constituting the cortico-striatal-pallidal-thalamic and limbic circuits. The network measures showed a higher than normal functional connectivity arising from the right amygdala in depressive patients. The amygdala seems to play an important role in neurobiology of depression. Resting-state EEG directed functional connectivity is a useful tool for studying abnormal brain activity in depression.

Methods

Subjects. Data were collected from 26 depressive patients and 25 healthy controls. The two groups were matched by gender and there were no significant differences in age or education (see Table 1). On a subsample of this dataset we recently showed that the severity of depressive symptoms correlates with resting-state microstate dynamics[117]. The patients were recruited at the Department of Psychiatry, Faculty of Medicine, Masaryk University and University Hospital Brno, Czech Republic. The diagnostic process had two steps and was determined based on the clinical evaluation by two board-certified psychiatrists. First, the diagnosis was made according to the criteria for research of the International Classification of Disorders (ICD-10). Second, the diagnosis was confirmed by the Mini International Neuropsychiatric Interview (M.I.N.I.) according to the Diagnostic and Statistical Manual (DSM-V). All patients were examined in the shortest time period after the admission and before the stabilization of treatment, typically during their first week of hospitalization. All patients met the criteria for at least a moderate degree of depression within the following affective disorders: bipolar affective disorder (F31), depressive episode (F32), recurrent depressive disorder (F33). Exclusion criteria for patients

Characteristic	Patients (n = 26)	Controls (n = 25)	*t*-value	df	p-value
Age: mean ± SD	51.9 ± 9.1	49.5 ± 8.7	0.97	49	0.34
Gender: female, *n*	11	10			
Education[a]: mean ± SD	1.9 ± 0.9	2.3 ± 0.7	−1.70	49	0.10

Table 1. Demographic data. [a]Education was classified into three levels: 1 = no high school, 2 = high school, 3 = university studies.

were any psychiatric or neurological comorbidity, IQ <70, organic disorder with influence on the brain function, alcohol dependence or other substance dependence. All patients were in the on-medication state with marked interindividual variability in specific medicaments received. Control subjects were recruited by general practitioners from their database of clients. Control subjects underwent the M.I.N.I. by board-certified psychiatrists, to ensure that they had no previous or current psychiatric disorder according to the DSM-V criteria. The scores on the Montgomery-Åsberg Depression Rating Scale (MADRS), a specific questionnaire validated for patients with mood disorders[118] and the Clinical Global Impression (CGI)[119], a general test validated for mental disorders, were used to evaluate the severity of depressive symptoms in patients. The status of depression was further described with life time count of depressive episodes and illness duration. Medication in 24 hours preceding the EEG examination was also recorded (see Table 2). This study was carried out in accordance with the recommendations of Ethics Committee of University Hospital Brno with written informed consent from all subjects.

EEG - data acquisition and pre-processing steps. Subjects were sitting in a comfortable upright position in an electrically shielded room with dimmed light. They were instructed to stay as calm as possible, to keep their eyes closed and to relax for 15 minutes. They were asked to stay awake. All participants were monitored by the cameras and in the event of signs of nodding off or EEG signs of drowsiness detected by visual inspection, the recording was stopped. The EEG was recorded with a high density 128-channel system (EGI System 400; Electrical Geodesic Inc., OR, USA), $f_s = 1$ kHz, and Cz as acquisition reference.

Five minutes of EEG data were selected and visually assessed. Noisy channels with abundant artifacts were identified. EEG signal was band-pass filtered between 1 and 40 Hz with a 2nd-order Butterworth filter avoiding phase-distortion. Subsequently, in order to remove physiological artifacts, e.g. ballistocardiogram and oculo-motor artifacts, infomax-based Independent Component Analysis[120] was applied on all but one or two noisy channels. Only components related to ballistocardiogram, saccadic eye movements, and eye blinking were removed based on the waveform, topography and time course of the component. Then, the cleaned EEG recording was down-sampled at $f_s = 250$ Hz and the previously identified noisy channels were interpolated using a three-dimensional spherical spline[121], and re-referenced to the average reference. For the following analyses, thirty 2-s EEG epochs free of artifacts were selected per subject. All the pre-processing steps were done using the freely available Cartool Software 3.70, programmed by Denis Brunet[122] and custom functions in MATLAB® R2018b.

EEG source estimation. We applied the LAURA algorithm implemented in Cartool[122] to compute the source reconstruction taking into account the patient's age to calibrate the skull conductivity[123–125]. The method restricts the solution space to the gray matter of the brain. Then, the cortex was parcellated into the 90 Automated Anatomical Labeling brain regions[126]. The dipoles in each ROI were represented with one unique time-series by a singular-value decomposition[127].

Time-variant multivariate autoregressive modeling. The cortical waveforms computed after applying the singular-value decomposition, were fitted against a time-variant (tv) multivariate (MV) autoregressive (AR) model to overcome the problem of non-stationarity of the EEG data. If the EEG data are available as several trials of the same length, the cortical waveforms computed from the EEG data generates a collection of realizations of a multivariate stochastic process which can be combined in a multivariate, multi-trial time series[67,127,128]. The tv-MVAR matrices containing the model coefficients were computed in the framework of a MATLAB toolbox (code available upon reasonable request to the authors) that implements the adaptive Kalman filtering and information Partial Directed Coherence (iPDC) in the source space[67,129,130]. The model order of the tv-MVAR and the Kalman filter adaptation constant were chosen applying the method proposed by Rubega and colleagues[128], i.e., evaluating the partial derivatives of a residual minimization function obtained varying simultaneously both p ($p \in [1, 15]$) and c ($c \in [0, 0.03]$). By means of the model coefficients, we computed the parametric spectral power density and the iPDC absolute values for each subject. For each patient, we obtained a 4-dimensional matrix [ROIs × ROIs × frequency × time] that represented the directed information flow from one ROI to another for each frequency at each time sample. In this way we performed the analysis on the *single-subject* level to compare the two groups quantitatively.

Since the features in the power spectra were consistent among subjects in the same population (patients vs controls), we also performed the analysis on the *population* level. A *population subject* was built by estimating the tv-MVAR model, where each trial in the input was a different subject. One power spectral density matrix and one connectivity matrix [ROIs × ROIs × frequency × time] were obtained for each group (controls and patients). In other words, subjects were combined as trials, assuming respectively humans as multiple realizations of their own brain processes, with the purpose to show that the two approaches, i.e., *single subject* and *population*, give

Patient	ICD-10 diagnose	Number of episodes	Illness duration (years)	MADRS score	CGI score	BZD	ADP/ AP/MS	AD/AP/MS medication scale
1	F31.4	3	2	27	4	2	AD, AP, MS	3
2	F32.2	1	0.5	24	5	0	AD	2
3	F32.1	1	1	15	4	2	AD	2
4	F31.5	5	20	39	6	0	AP	2
5	F33.1	3	7	18	4	0	AD	1
6	F33.1	2	8	9	3	1.33	AD	1
7	F32.1	1	1	24	4	1.33	AD, AP	3
8	F31.4	4	27	29	5	2	AP	2
9	F33.3	2	5	36	6	1	AD, AP	4
10	F33.1	3	19	21	4	1	AD	1
11	F33.3	2	2	38	5	6	AD, AP	4
12	F33.2	2	1	39	5	3	AD, AP	4
13	F32.3	1	0.08	21	5	2	AD, AP	4
14	F33.2	5	21	32	5	0	AD, AP	3
15	F33.3	2	2	38	6	3	AD, AP	4
16	F32.3	1	0.08	37	6	2	AD, AP	4
17	F33.1	3	4	18	4	0	AD, AP	4
18	F31.3	2	16	28	4	0	AP, MS	4
19	F31.3	11	24	23	4	1	AP, MS	4
20	F32.2	0	0,17	23	4	1	AD, AP	4
21	F33.1	1	9	34	5	2	AD	2
22	F32.3	0	0,04	37	6	1	AD, AP	4
23	F33.3	1	11	49	6	3	AD, AP	4
24	F33.1	3	20	23	4	0	AD	2
25	F33.1	5	24	26	4	2	AD, AP, MS	4
26	F32.1	0	0,17	23	4	3	AD, AP	3

Table 2. Patient characteristics. F31.3 - Bipolar affective disorder, current episode mild or moderate depression; F31.4 - Bipolar affective disorder, current episode severe depression without psychotic symptoms; F31.5 - Bipolar affective disorder, current episode severe depression with psychotic symptoms; F32.1 - Moderate depressive episode; F32.2 - Severe depressive episode without psychotic symptoms; F32.3 - Severe depressive episode with psychotic symptoms; F33.1 - Recurrent depressive disorder, current episode moderate; F33.2 - Recurrent depressive disorder, current episode severe without psychotic symptoms; F33.3 - Recurrent depressive disorder, current episode severe with psychotic symptoms; BZD - benzodiazepine equivalent dose[139]; AD - antidepressants (mirtazapine, citalopram, venlafaxine, vortioxetine, sertraline, trazodone); AP - antipsychotics (risperidone, olanzapine, quetiapine, amisulpride, aripiprazole); MS - mood stabilizers (valproate, lamotrigine, carbamazepine); AD/AP/MS medication scale: 1 – one medication in sub-therapeutic doses, 2 – one medication in therapeutic doses, 3 – combination of medications with one in therapeutic doses, 4 – combination of medications with more than one in therapeutic doses; MADRS (Montgomery–Åsberg Depression Rating Scale): score is between 0 and 60, the higher the score the higher the depressive symptom severity; CGI (Clinical Global Impression scale): healthy (1) – most extremely ill (7). Four patients were undergoing the first (patient 3) and second (patient 4 and 9) week of electroconvulsive therapy and the first week of repetitive transcranial magnetic stimulation (patient 5). No clinical effect of these neurostimulation treatments was apparent.

equivalent results in differentiating patients vs controls. In the last decade, population-based approaches were successfully exploited in computer simulations engineered to evaluate the safety and limitations of closed-loop control treatment algorithms[131,132]. Population-based approaches for MVAR/PDC modelling are currently lacking and this might be considered a first attempt justified by the consistent features estimated in the frequency domain among subjects belonging to the same population (patients vs controls). Further details on the connectivity estimation are reported in the Supplementary Information.

Network metrics. In order to study the peculiarities of the brain network in patients vs controls, the brain was represented as a digraph defined by a collection of nodes and directed links (directional edges). Nodes in the brain network represent brain regions, i.e., the 90 ROIs, while the directed links represent the values computed by iPDC. Thus, the weight of such link can vary in the interval [0–1] and it represents the amount of mutual information flowing between ROIs. We defined twelve ROIs, including the bilateral amygdala, anterior cingulum, thalamus, putamen, caudate, and pallidum, to examine the directed functional connectivity between these seeds and the whole brain. Significant differences in power between patients and controls were observed in the *single-subject* level in alpha and theta frequency bands in all these six anatomical structures. Therefore,

we restricted the network analysis to this [4–12] Hz frequency range. To evaluate how much the system is fault tolerant and how much the communication is efficient, the global efficiency for the whole brain and the local efficiency, clustering coefficient, strength and outflow for each of these twelve investigated ROIs were computed. To compute all the graph measures, the scripts and functions implemented on the freely available MATLAB toolbox[133] were customized.

Global efficiency. Global efficiency is defined as the average minimum path length between two nodes in the network. This measure is inversely related to topological distance between nodes and is typically interpreted as a measure of the capacity for parallel information transfer and integrated processing[134].

Local efficiency. Local efficiency is defined as the average efficiency of the local subgraphs[135], i.e. the global efficiency computed on the neighborhood of the node. It reflects the ability of a network to transmit information at the local level. This quantity plays a role similar to the clustering coefficient since it reveals how much the system is fault tolerant, i.e., it shows how efficient the communication is between the first neighbors of i when i is removed.

$$\overrightarrow{E_{loc}} = \frac{1}{2n}\sum_{i\in N}\frac{\sum_{j,h\in N, j\neq i}(a_{ij}+a_{ji})(a_{ih}+a_{hi})([\overrightarrow{d_{jh}}(N_i)]^{-1}+[\overrightarrow{d_{hj}}(N_i)]^{-1})}{(k_i^{out}+k_i^{in})(k_i^{out}+k_i^{in}-1)-2\sum_{j\in N}a_{ij}a_{ji}} \quad (1)$$

where k_i^{out} is the out-degree of node i, k_i^{in} is the in-degree of node i, and a_{ij} is the connection status between node i and node j, i.e., $a_{ij} = 1$ if the link between i and j exists, $a_{ij} = 0$ otherwise. N is the set of nodes in the network. n is the number of nodes and $\overrightarrow{d_{jh}}(N_i)$ is the length of the shortest directed path between j (any node in the network) and h (any node that neighbors with i).

Clustering coefficient. Clustering coefficient reflects the prevalence of clustered connectivity around an individual brain region[136]:

$$cc_i = \frac{2t_i}{k_i(k_i-1)} \quad (2)$$

where t_i are the number of triangles around the node i, and k_i is the degree of node i, i.e., the number of links connected to node i. In our case of a weighted directed network, a weighted directed version of clustering coefficient was used[137]:

$$\overrightarrow{cc_i} = \frac{\overrightarrow{t_i}}{(k_i^{out}+k_i^{in})(k_i^{out}+k_i^{in}-1)-2\sum_{j\in N}a_{ij}a_{ji}} \quad (3)$$

where $\overrightarrow{t_i}$ are the number of directed triangles around the node i, k_i^{out} is the out-degree of node i, k_i^{in} is the in-degree of node i, and a_{ij} is the connection status between the nodes i and j, i.e., $a_{ij} = 1$ if the link between i and j exists, $a_{ij} = 0$ otherwise. N is the set of nodes in the network.

Strength and outflow. Finally, the connectivity patterns between the different cortical regions were summarized by representing the strength that quantifies for each node the sum of weights of all links connected to the node and the total outflow from a region toward the others, generated by the sum of all the statistically significant links obtained by application of the iPDC. The greatest amount of information outflow depicts the ROI as one of the main sources (drivers) of functional connections to the other ROIs[138].

Laterality. For all the network metrics explained in the previous paragraph, we also computed a laterality index, which is defined as $\frac{Left_{metric}-Right_{metric}}{Left_{metric}+Right_{metric}}$ to test if the measures significantly differentiate between the two hemispheres. Laterality index and all network metrics were calculated for both groups.

Statistical analysis. To assess whether or not the changes in the network metrics were statistically significant between patients and controls, paired Student's t-tests were computed under the hypothesis of normal distribution of samples (Lilliefors test), otherwise Wilcoxon rank-sign tests were considered. To test whether the age and education level predict the values of the spectral power distribution and the network metrics in patients, a multiple linear regression was performed. We also tested the influence of the clinical data on the connectivity results. A multiple linear regression was performed exploiting correlation of the connectivity results with four variables describing the status of depression and two variables describing the medication status in terms of the intake of benzodiazepines (BZP), antidepressants, antipsychotics, and mood stabilizers (AD/AP/MS). These six clinical variables are provided for each patient in Table 2. We checked through the following multiple linear regression models (4) (5), if the response variable Y depends on a number of predictor variables X_i:

$$Y = \beta_0 + \beta_1 X_1 + \ldots \beta_k X_k + \varepsilon \quad (4)$$

$$Y = \beta_0 + \beta_1 X + \beta_2 X^2 + \varepsilon \quad (5)$$

where the ε are the residual terms of the model and $\beta_0, \beta_1, \beta_2, \ldots, \beta_k$ are the k regression coefficients. Both the clinical data and the power and network metrics were used once as predictors and once as response variables.

Ethics statement. All participants gave their written informed consent prior to the experiment and the study received the approval of the Ethics Committee of University Hospital Brno in Brno, Czech Republic. All experiments of this study were performed in accordance with relevant guidelines and regulations.

Received: 19 July 2019; Accepted: 19 February 2020;
Published online: 10 March 2020

References

1. Andrade, L. *et al*. The epidemiology of major depressive episodes: results from the International Consortium of Psychiatric Epidemiology (ICPE) surveys. *Int. J. Methods Psychiatr. Res.* **12**, 3–21 (2003).
2. Bora, E., Harrison, B. J., Davey, C. G., Yü Cel, M. & Pantelis, C. Meta-analysis of volumetric abnormalities in cortico-striatal-pallidal-thalamic circuits in major depressive disorder., https://doi.org/10.1017/S0033291711001668
3. Yang, J. *et al*. Amygdala Atrophy and Its Functional Disconnection with the Cortico-Striatal-Pallidal-Thalamic Circuit in Major Depressive Disorder in Females. *PLoS One* **12**, e0168239 (2017).
4. Zhang, B. *et al*. Mapping anhedonia-specific dysfunction in a transdiagnostic approach: an ALE meta-analysis. *Brain Imaging Behav.* **10**, 920–939 (2016).
5. Disner, S. G., Beevers, C. G., Haigh, E. A. P. & Beck, A. T. Neural mechanisms of the cognitive model of depression. *Nat. Rev. Neurosci.* **12**, 467–477 (2011).
6. Surguladze, S. *et al*. A differential pattern of neural response toward sad versus happy facial expressions in major depressive disorder. *Biol. Psychiatry* **57**, 201–209 (2005).
7. Sheline, Y. I. *et al*. Increased amygdala response to masked emotional faces in depressed subjects resolves with antidepressant treatment: an fMRI study. *Biol. Psychiatry* **50**, 651–658 (2001).
8. Siegle, G. J., Thompson, W., Carter, C. S., Steinhauer, S. R. & Thase, M. E. Increased Amygdala and Decreased Dorsolateral Prefrontal BOLD Responses in Unipolar Depression: Related and Independent Features. *Biol. Psychiatry* **61**, 198–209 (2007).
9. Nugent, A. C., Robinson, S. E., Coppola, R., Furey, M. L. & Zarate, C. A. Group differences in MEG-ICA derived resting state networks: Application to major depressive disorder. *Neuroimage* **118**, 1–12 (2015).
10. Knyazev, G. G. *et al*. Task-positive and task-negative networks in major depressive disorder: A combined fMRI and EEG study. *J. Affect. Disord.* **235**, 211–219 (2018).
11. Lu, Y. *et al*. The volumetric and shape changes of the putamen and thalamus in first episode, untreated major depressive disorder. *NeuroImage. Clin.* **11**, 658–666 (2016).
12. Kim, M. J., Hamilton, J. P. & Gotlib, I. H. Reduced caudate gray matter volume in women with major depressive disorder. *Psychiatry Res. Neuroimaging* **164**, 114–122 (2008).
13. Sheline, Y. I., Price, J. L., Yan, Z. & Mintun, M. A. Resting-state functional MRI in depression unmasks increased connectivity between networks via the dorsal nexus. *Proc. Natl. Acad. Sci.* **107**, 11020–11025 (2010).
14. Kuhn, S. & Gallinat, J. Resting-State Brain Activity in Schizophrenia and Major Depression: A Quantitative Meta-Analysis. *Schizophr. Bull.* **39**, 358–365 (2013).
15. Lorenzetti, V., Allen, N. B., Fornito, A. & Yücel, M. Structural brain abnormalities in major depressive disorder: A selective review of recent MRI studies. *J. Affect. Disord.* **117**, 1–17 (2009).
16. Veer, I. M. Whole brain resting-state analysis reveals decreased functional connectivity in major depression. *Front. Syst. Neurosci.* **4**, 41 (2010).
17. Hamilton, J. P. *et al*. Functional Neuroimaging of Major Depressive Disorder: A Meta-Analysis and New Integration of Baseline Activation and Neural Response Data. *Am. J. Psychiatry* **169**, 693–703 (2012).
18. Bielau, H. *et al*. Volume deficits of subcortical nuclei in mood disorders. *Eur. Arch. Psychiatry Clin. Neurosci.* **255**, 401–412 (2005).
19. Holtzheimer, P. E. & Mayberg, H. S. Stuck in a rut: rethinking depression and its treatment. *Trends Neurosci.* **34**, 1–9 (2011).
20. Drobisz, D. & Damborská, A. Deep brain stimulation targets for treating depression. *Behav. Brain Res.* **359**, 266–273 (2019).
21. Holtzheimer, P. E. *et al*. Subcallosal Cingulate Deep Brain Stimulation for Treatment-Resistant Unipolar and Bipolar Depression. *Arch. Gen. Psychiatry* **69**, 150 (2012).
22. Knight, G. Stereotactic Tractotomy in The Surgical Treatment of Mental Illness. *J. Neurol. Neurosurg. Psychiatry* **28**, 304–310 (1965).
23. Dougherty, D. D. *et al*. Cerebral metabolic correlates as potential predictors of response to anterior cingulotomy for treatment of major depression. *J. Neurosurg.* **99**, 1010–1017 (2003).
24. Hamani, C. *et al*. Deep brain stimulation in rats: Different targets induce similar antidepressant-like effects but influence different circuits. *Neurobiol. Dis.* **71**, 205–214 (2014).
25. Hamani, C. & Nóbrega, J. N. Deep brain stimulation in clinical trials and animal models of depression. *Eur. J. Neurosci.* **32**, 1109–1117 (2010).
26. Hamani, C. *et al*. Antidepressant-Like Effects of Medial Prefrontal Cortex Deep Brain Stimulation in Rats. *Biol. Psychiatry* **67**, 117–124 (2010).
27. Moshe, H. *et al*. Prelimbic Stimulation Ameliorates Depressive-Like Behaviors and Increases Regional BDNF Expression in a Novel Drug-Resistant Animal Model of Depression. *Brain Stimul.* **9**, 243–250 (2016).
28. Thiele, S., Furlanetti, L., Pfeiffer, L. M., Coenen, V. A. & Döbrössy, M. D. The effects of bilateral, continuous, and chronic Deep Brain Stimulation of the medial forebrain bundle in a rodent model of depression. *Exp. Neurol.* **303**, 153–161 (2018).
29. Rummel, J. *et al*. Testing different paradigms to optimize antidepressant deep brain stimulation in different rat models of depression. *J. Psychiatr. Res.* **81**, 36–45 (2016).
30. Clemm Von Hohenberg, C. *et al*. Lateral habenula perturbation reduces default-mode network connectivity in a rat model of depression. *Transl. Psychiatry* **8**, 68 (2018).
31. Baeken, C., Duprat, R., Wu, G. R., De Raedt, R. & van Heeringen, K. Subgenual Anterior Cingulate–Medial Orbitofrontal Functional Connectivity in Medication-Resistant Major Depression: A Neurobiological Marker for Accelerated Intermittent Theta Burst Stimulation Treatment? *Biol. Psychiatry Cogn. Neurosci. Neuroimaging* **2**, 556–565 (2017).
32. Johansen-Berg, H. *et al*. Anatomical connectivity of the subgenual cingulate region targeted with deep brain stimulation for treatment-resistant depression. *Cereb. Cortex* **18**, 1374–1383 (2008).
33. Greicius, M. D. *et al*. Resting-State Functional Connectivity in Major Depression: Abnormally Increased Contributions from Subgenual Cingulate Cortex and Thalamus. *Biol. Psychiatry* **62**, 429–437 (2007).
34. Riva-Posse, P. *et al*. Defining critical white matter pathways mediating successful subcallosal cingulate deep brain stimulation for treatment-resistant depression. *Biol. Psychiatry* **76**, 963–969 (2014).
35. Quevedo, K. *et al*. Ventral Striatum Functional Connectivity during Rewards and Losses and Symptomatology in Depressed Patients. *Biol. Psychol.* **123**, 62–73 (2017).

36. Gutman, D. A., Holtzheimer, P. E., Behrens, T. E. J., Johansen-Berg, H. & Mayberg, H. S. A Tractography Analysis of Two Deep Brain Stimulation White Matter Targets for Depression. *Biol. Psychiatry* **65**, 276–282 (2009).
37. Bracht, T. *et al*. White matter microstructure alterations of the medial forebrain bundle in melancholic depression. *J. Affect. Disord.* **155**, 186–193 (2014).
38. Kaiser, R. H., Andrews-Hanna, J. R., Wager, T. D. & Pizzagalli, D. A. Large-scale network dysfunction in major depressive disorder: A meta-analysis of resting-state functional connectivity. *JAMA Psychiatry* **72**, 603–611 (2015).
39. Smith, S. M. *et al*. Functional connectomics from resting-state fMRI. *Trends in Cognitive Sciences* **17**, 666–682 (2013).
40. Fox, M. D. & Raichle, M. E. Spontaneous fluctuations in brain activity observed with functional magnetic resonance imaging. *Nature Reviews Neuroscience* **8**, 700–711 (2007).
41. Hamilton, J. P. *et al*. Default-Mode and Task-Positive Network Activity in Major Depressive Disorder: Implications for Adaptive and Maladaptive Rumination. *Biol. Psychiatry* **70**, 327–333 (2011).
42. Lui, S. *et al*. Resting-state functional connectivity in treatment-resistant depression. *Am. J. Psychiatry* **168**, 642–648 (2011).
43. Whitton, A. E. *et al*. Electroencephalography Source Functional Connectivity Reveals Abnormal High-Frequency Communication Among Large-Scale Functional Networks in Depression. *Biol. Psychiatry Cogn. Neurosci. Neuroimaging* **3**, 50–58 (2018).
44. Sikora, M. *et al*. Salience Network Functional Connectivity Predicts Placebo Effects in Major Depression. *Biol. Psychiatry Cogn. Neurosci. Neuroimaging* **1**, 68–76 (2016).
45. Gong, J. Y. *et al*. Disrupted functional connectivity within the default mode network and salience network in unmedicated bipolar II disorder. *Prog. Neuro-Psychopharmacology Biol. Psychiatry* **88**, 11–18 (2019).
46. Sacchet, M. D. *et al*. Large-scale hypoconnectivity between resting-state functional networks in unmedicated adolescent major depressive disorder. *Neuropsychopharmacology* **41**, 2951–2960 (2016).
47. Williams, K. A., Mehta, N. S., Redei, E. E., Wang, L. & Procissi, D. Aberrant resting-state functional connectivity in a genetic rat model of depression. *Psychiatry Res. - Neuroimaging* **222**, 111–113 (2014).
48. Kopell, B. H., Greenberg, B. & Rezai, A. R. Deep Brain Stimulation for Psychiatric Disorders. *J. Clin. Neurophysiol.* **21**, 51–67 (2004).
49. Sartorius, A. *et al*. Remission of Major Depression Under Deep Brain Stimulation of the Lateral Habenula in a Therapy-Refractory Patient. *Biological Psychiatry* **67**, e9-e11 (2010).
50. Kukleta, M., Bob, P., Brázdil, M., Roman, R. & Rektor, I. The level of frontal-temporal beta-2 band EEG synchronization distinguishes anterior cingulate cortex from other frontal regions. *Conscious. Cogn.* **19**, 879–886 (2010).
51. Brázdil, M. *et al*. Directional functional coupling of cerebral rhythms between anterior cingulate and dorsolateral prefrontal areas during rare stimuli: A directed transfer function analysis of human depth EEG signal. *Hum. Brain Mapp.* **30**, 138–146 (2009).
52. Kibleur, A. *et al*. Stimulation of subgenual cingulate area decreases limbic top-down effect on ventral visual stream: A DBS-EEG pilot study. *Neuroimage* **146**, 544–553 (2017).
53. Pereda, E., Quiroga, R. Q. & Bhattacharya, J. Nonlinear multivariate analysis of neurophysiological signals. *Prog. Neurobiol.* **77**, 1–37 (2005).
54. Seth, A. K., Barrett, A. B. & Barnett, L. Granger Causality Analysis in Neuroscience and Neuroimaging. *J. Neurosci.* **35**, 3293–3297 (2015).
55. Granger, C. W. J. Investigating Causal Relations by Econometric Models and Cross-spectral Methods. *Econometrica* **37**, 424–438 (1969).
56. Leistritz, L. *et al*. Connectivity Analysis of Somatosensory Evoked Potentials in Patients with Major Depression. *Methods Inf. Med.* **49**, 484–491 (2010).
57. Sun, Y., Sijung, H., Chambers, J., Yisheng Z. & Tong, S. Graphic patterns of cortical functional connectivity of depressed patients on the basis of EEG measurements. in *2011 Annual International Conference of the IEEE Engineering in Medicine and Biology Society* 1419–1422, https://doi.org/10.1109/IEMBS.2011.6090334 (IEEE, 2011).
58. Tang, Y. *et al*. The altered cortical connectivity during spatial search for facial expressions in major depressive disorder. *Prog. Neuro-Psychopharmacology Biol. Psychiatry* **35**, 1891–1900 (2011).
59. Mao, W., Li, Y., Tang, Y., Li, H. & Wang, J. The coherence changes in the depressed patients in response to different facial expressions. In *Lecture Notes in Computer Science (including subseries Lecture Notes in Artificial Intelligence and Lecture Notes in Bioinformatics)* **6064 LNCS**, 392–399 (2010).
60. Wang, C. *et al*. The brain network research of poststroke depression based on partial directed coherence (PDC). *Chinese J. Biomed. Eng.* **34**, 385–391 (2015).
61. Sun, Y., Li, Y., Zhu, Y., Chen, X. & Tong, S. Electroencephalographic differences between depressed and control subjects: An aspect of interdependence analysis. *Brain Res. Bull.* **76**, 559–564 (2008).
62. Schoffelen, J.-M. & Gross, J. Source connectivity analysis with MEG and EEG. *Hum. Brain Mapp.* **30**, 1857–1865 (2009).
63. He, B. *et al*. Electrophysiological Brain Connectivity: Theory and Implementation. *IEEE Trans. Biomed. Eng.* **66**, 2115–2137 (2019).
64. Coito, A., Michel, C. M., van Mierlo, P., Vulliemoz, S. & Plomp, G. Directed Functional Brain Connectivity Based on EEG Source Imaging: Methodology and Application to Temporal Lobe Epilepsy. *IEEE Trans. Biomed. Eng.* **63**, 2619–2628 (2016).
65. Sperdin, H. F. *et al*. Early alterations of social brain networks in young children with autism. *Elife* **7**, e31670 (2018).
66. Coito, A., Michel, C. M., Vulliemoz, S. & Plomp, G. Directed functional connections underlying spontaneous brain activity. *Hum. Brain Mapp.* **40**, 879–888 (2019).
67. Milde, T. *et al*. A new Kalman filter approach for the estimation of high-dimensional time-variant multivariate AR models and its application in analysis of laser-evoked brain potentials. *Neuroimage* **50**, 960–969 (2010).
68. Pessoa, L. & Adolphs, R. Emotion processing and the amygdala: from a 'low road' to 'many roads' of evaluating biological significance. *Nat. Rev. Neurosci.* **11**, 773–782 (2010).
69. Zheng, J. *et al*. Amygdala-hippocampal dynamics during salient information processing. *Nat. Commun.* **8**, 14413 (2017).
70. Freese, J. L. & Amaral, D. G. *Neuroanatomy of the primate amygdala. - PsycNET*. (Guilford Press, 2009).
71. Kober, H. *et al*. Functional grouping and cortical–subcortical interactions in emotion: A meta-analysis of neuroimaging studies. *Neuroimage* **42**, 998–1031 (2008).
72. Thomas Yeo, B. T. *et al*. The organization of the human cerebral cortex estimated by intrinsic functional connectivity. *J. Neurophysiol.* **106**, 1125–1165 (2011).
73. Price, J. L. & Drevets, W. C. Neurocircuitry of Mood Disorders. *Neuropsychopharmacology* **35**, 192–216 (2010).
74. Hamilton, J. P., Chen, M. C. & Gotlib, I. H. Neural systems approaches to understanding major depressive disorder: An intrinsic functional organization perspective. *Neurobiol. Dis.* **52**, 4–11 (2013).
75. Ramasubbu, R. *et al*. Reduced Intrinsic Connectivity of Amygdala in Adults with Major Depressive Disorder. *Front. Psychiatry* **5**, 17 (2014).
76. Tang, S. *et al*. Abnormal amygdala resting-state functional connectivity in adults and adolescents with major depressive disorder: A comparative meta-analysis. *EBioMedicine* **36**, 436–445 (2018).
77. Tang, S. *et al*. Anomalous functional connectivity of amygdala subregional networks in major depressive disorder. *Depress. Anxiety* **36**, 712–722 (2019).
78. Zhang, X. F., He, X., Wu, L., Liu, C. J. & Wu, W. Altered Functional Connectivity of Amygdala with the Fronto-Limbic-Striatal Circuit in Temporal Lobe Lesion as a Proposed Mechanism for Poststroke Depression. *Am. J. Phys. Med. Rehabil.* **98**, 303–310 (2019).

79. Ferdek, M. A., van Rijn, C. M. & Wyczesany, M. Depressive rumination and the emotional control circuit: An EEG localization and effective connectivity study. *Cogn. Affect. Behav. Neurosci.* **16**, 1099–1113 (2016).
80. van Eijndhoven, P. *et al*. Amygdala Volume Marks the Acute State in the Early Course of Depression. *Biol. Psychiatry* **65**, 812–818 (2009).
81. Sandu, A.-L. *et al*. Amygdala and regional volumes in treatment-resistant *versus* nontreatment-resistant depression patients. *Depress. Anxiety* **34**, 1065–1071 (2017).
82. Bauer, I. E. *et al*. Amygdala enlargement in unaffected offspring of bipolar parents. *J. Psychiatr. Res.* **59**, 200–205 (2014).
83. Inman, C. S. *et al*. Direct electrical stimulation of the amygdala enhances declarative memory in humans. *Proc. Natl. Acad. Sci.* **115**, 98–103 (2018).
84. Bijanki, K. R. *et al*. Case Report: Stimulation of the Right Amygdala Induces Transient Changes in Affective Bias. *Brain Stimul.* **7**, 690–693 (2014).
85. Tyrand, R., Seeck, M., Pollo, C. & Boëx, C. Effects of amygdala–hippocampal stimulation on synchronization. *Epilepsy Res.* **108**, 327–330 (2014).
86. Tyrand, R. *et al*. Effects of amygdala–hippocampal stimulation on interictal epileptic discharges. *Epilepsy Res.* **99**, 87–93 (2012).
87. Langevin, J.-P. *et al*. Deep Brain Stimulation of the Basolateral Amygdala: Targeting Technique and Electrodiagnostic Findings. *Brain Sci.* **6**, 28 (2016).
88. Koek, R. J. *et al*. Deep brain stimulation of the basolateral amygdala for treatment-refractory combat post-traumatic stress disorder (PTSD): study protocol for a pilot randomized controlled trial with blinded, staggered onset of stimulation. *Trials* **15**, 356 (2014).
89. Sturm, V. *et al*. DBS in the basolateral amygdala improves symptoms of autism and related self-injurious behavior: a case report and hypothesis on the pathogenesis of the disorder. *Front. Hum. Neurosci.* **6**, 341 (2013).
90. Admon, R. *et al*. Striatal hypersensitivity during stress in remitted individuals with recurrent depression. *Biol. Psychiatry* **78**, 67–76 (2015).
91. Marchand, W. R. & Yurgelun-Todd, D. Striatal structure and function in mood disorders: a comprehensive review. *Bipolar Disord.* **12**, 764–785 (2010).
92. Bluhm, R. *et al*. Resting state default-mode network connectivity in early depression using a seed region-of-interest analysis: Decreased connectivity with caudate nucleus. *Psychiatry Clin. Neurosci.* **63**, 754–761 (2009).
93. Butters, M. A. *et al*. Three-Dimensional Surface Mapping of the Caudate Nucleus in Late-Life Depression. *Am. J. Geriatr. Psychiatry* **17**, 4–12 (2009).
94. Ma, C. *et al*. Resting-State Functional Connectivity Bias of Middle Temporal Gyrus and Caudate with Altered Gray Matter Volume in Major Depression. *PLoS One* **7**, e45263 (2012).
95. Krishnan, K. R. R. Magnetic Resonance Imaging of the Caudate Nuclei in Depression. *Arch. Gen. Psychiatry* **49**, 553 (1992).
96. Tymofiyeva, O. *et al*. DTI-based connectome analysis of adolescents with major depressive disorder reveals hypoconnectivity of the right caudate. *J. Affect. Disord.* **207**, 18–25 (2017).
97. Khundakar, A., Morris, C., Oakley, A. & Thomas, A. J. Morphometric Analysis of Neuronal and Glial Cell Pathology in the Caudate Nucleus in Late-Life Depression. *Am. J. Geriatr. Psychiatry* **19**, 132–141 (2011).
98. Hannestad, J. *et al*. White matter lesion volumes and caudate volumes in late-life depression. *Int. J. Geriatr. Psychiatry* **21**, 1193–1198 (2006).
99. Pillay, S. A quantitative magnetic resonance imaging study of caudate and lenticular nucleus gray matter volume in primary unipolar major depression: relationship to treatment response and clinical severity. *Psychiatry Res. Neuroimaging* **84**, 61–74 (1998).
100. Price, J. L. & Drevets, W. C. Neural circuits underlying the pathophysiology of mood disorders. *Trends Cogn. Sci.* **16**, 61–71 (2012).
101. Limbic-cortical dysregulation: a proposed model of depression. *J. Neuropsychiatry Clin. Neurosci.* **9**, 471–481 (1997).
102. Pizzagalli, D. A. Frontocingulate Dysfunction in Depression: Toward Biomarkers of Treatment Response. *Neuropsychopharmacology* **36**, 183–206 (2011).
103. Seeber, M. *et al*. Subcortical electrophysiological activity is detectable with high-density EEG source imaging. *Nat. Commun.* **10**, 753 (2019).
104. Aouizerate, B. *et al*. Deep brain stimulation of the ventral caudate nucleus in the treatment of obsessive—compulsive disorder and major depression. *J. Neurosurg.* **101**, 682–686 (2004).
105. Millet, B. *et al*. Limbic versus cognitive target for deep brain stimulation in treatment-resistant depression: Accumbens more promising than caudate. *Eur. Neuropsychopharmacol.* **24**, 1229–1239 (2014).
106. Grin-Yatsenko, V. A., Baas, I., Ponomarev, V. A. & Kropotov, J. D. EEG Power Spectra at Early Stages of Depressive Disorders. *J. Clin. Neurophysiol.* **26**, 401–406 (2009).
107. Pollock, V. E. & Schneider, L. S. Topographic Quantitative EEG in Elderly Subjects with Major Depression. *Psychophysiology* **27**, 438–444 (1990).
108. Roemer, R. A., Shagass, C., Dubin, W., Jaffe, R. & Siegal, L. Quantitative EEG in elderly depressives. *Brain Topogr.* **4**, 285–290 (1992).
109. Kwon, J. S., Youn, T. & Jung, H. Y. Right hemisphere abnormalities in major depression: Quantitative electroencephalographic findings before and after treatment. *J. Affect. Disord.* **40**, 169–173 (1996).
110. Jiang, H. *et al*. Predictability of depression severity based on posterior alpha oscillations. *Clin. Neurophysiol.* **127**, 2108–2114 (2016).
111. Neumann, W.-J. *et al*. Different patterns of local field potentials from limbic DBS targets in patients with major depressive and obsessive compulsive disorder. *Mol. Psychiatry* **19**, 1186–1192 (2014).
112. Mégevand, P. *et al*. Electric source imaging of interictal activity accurately localises the seizure onset zone. *J. Neurol. Neurosurg. Psychiatry* **85**, 38–43 (2014).
113. Michel, C. M. *et al*. 128-Channel EEG source imaging in epilepsy: Clinical yield and localization precision. *J. Clin. Neurophysiol.* **21**, 71–83 (2004).
114. Attal, Y. & Schwartz, D. Assessment of Subcortical Source Localization Using Deep Brain Activity Imaging Model with Minimum Norm Operators: A MEG Study. *PLoS One* **8**, 59856 (2013).
115. Krishnaswamy, P. *et al*. Sparsity enables estimation of both subcortical and cortical activity from MEG and EEG. *Proc. Natl. Acad. Sci. USA* **114**, E10465–E10474 (2017).
116. Pizzo, F. *et al*. Deep brain activities can be detected with magnetoencephalography. *Nat. Commun.* **10**, 971 (2019).
117. Damborská, A. *et al*. EEG Resting-State Large-Scale Brain Network Dynamics Are Related to Depressive Symptoms. *Front. Psychiatry* **10**, 548 (2019).
118. Williams, J. B. W. & Kobak, K. A. Development and reliability of a structured interview guide for the Montgomery-Åsberg Depression Rating Scale (SIGMA). *Br. J. Psychiatry* **192**, 52–58 (2008).
119. Guy, W. *ECDEU assessment manual for psychopharmacology*. (U.S. Dept. of Health Education and Welfare Public Health Service Alcohol Drug Abuse and Mental Health Administration National Institute of Mental Health Psychopharmacology Research Branch, 1976).
120. Jung, T.-P. *et al*. Removal of eye activity artifacts from visual event-related potentials in normal and clinical subjects. *Clin. Neurophysiol.* **111**, 1745–1758 (2000).
121. Perrin, F., Pernier, J., Bertrand, O. & Echallier, J. F. Spherical splines for scalp potential and current density mapping. *Electroencephalogr. Clin. Neurophysiol.* **72**, 184–187 (1989).

122. The Cartool Community group. Available: cartoolcommunity.unige.ch.
123. Grave de Peralta Menendez, R., Murray, M. M., Michel, C. M., Martuzzi, R. & Gonzalez Andino, S. L. Electrical neuroimaging based on biophysical constraints. *Neuroimage* **21**, 527–539 (2004).
124. Michel, C. M. & Brunet, D. EEG Source Imaging: A Practical Review of the Analysis Steps. *Front. Neurol.* **10**, 325 (2019).
125. Spinelli, L., Andino, S. G., Lantz, G., Seeck, M. & Michel, C. M. Electromagnetic Inverse Solutions in Anatomically Constrained Spherical Head Models. *Brain Topogr.* **13**, 115–125 (2000).
126. Tzourio-Mazoyer, N. *et al.* Automated Anatomical Labeling of Activations in SPM Using a Macroscopic Anatomical Parcellation of the MNI MRI Single-Subject Brain. *Neuroimage* **15**, 273–289 (2002).
127. Rubega, M. *et al.* Estimating EEG Source Dipole Orientation Based on Singular-value Decomposition for Connectivity Analysis. *Brain Topogr.* **32**, 704–719, https://doi.org/10.1007/s10548-018-0691-2, (2018)
128. Rubega M. *et al.* Time-varying effective EEG source connectivity: The optimization of model parameters. In *41st Annual International Conference of the IEEE Engineering in Medicine and Biology Society (EMBC), IEEE* (2019).
129. Takahashi, D. Y., Baccalá, L. A. & Sameshima, K. Information theoretic interpretation of frequency domain connectivity measures. *Biol. Cybern.* **103**, 463–469 (2010).
130. Sameshima, K., Baccala, L. A. & Baccala, L. A. *Methods in Brain Connectivity Inference through Multivariate Time Series Analysis*. **20145078**, (CRC Press, 2014).
131. Vettoretti, M., Facchinetti, A., Sparacino, G. & Cobelli, C. Type-1 Diabetes Patient Decision Simulator for In Silico Testing Safety and Effectiveness of Insulin Treatments. *IEEE Trans. Biomed. Eng.* **65**, 1281–1290 (2018).
132. Man, C. D. *et al.* The UVA/PADOVA Type 1 Diabetes Simulator. *J. Diabetes Sci. Technol.* **8**, 26–34 (2014).
133. Available, http://www.brain-connectivity-toolbox.net.
134. Bullmore, E. & Sporns, O. The economy of brain network organization. *Nat. Rev. Neurosci.* **13**, 336–349 (2012).
135. Latora, V. & Marchiori, M. Efficient Behavior of Small-World Networks. *Phys. Rev. Lett.* **87**, 198701 (2001).
136. Watts, D. J. & Strogatz, S. H. Collective dynamics of 'small-world' networks. *Nature* **393**, 440–442 (1998).
137. Fagiolo, G. Clustering in complex directed networks. *Phys. Rev. E* **76**, 026107 (2007).
138. Babiloni, F. *et al.* Estimation of the cortical functional connectivity with the multimodal integration of high-resolution EEG and fMRI data by directed transfer function. *Neuroimage* **24**, 118–131 (2005).
139. Bazire, S. *Benzodiazepine equivalent doses. Psychotropic Drug Directory*. (Lloyd-Reinhold Communications, 2014).

Acknowledgements

This study was supported by the European Union Horizon 2020 research and innovation program under the Marie Skłodowska-Curie grant agreement No. 739939, by Ministry of Health, Czech Republic - conceptual development of research organization (University Hospital Brno - FNBr, 65269705), by the Swiss National Science Foundation (grant No. 320030_184677), and by the National Centre of Competence in Research (NCCR) "SYNAPSY–The Synaptic Basis of Mental Diseases" (NCCR Synapsy Grant # "51NF40 – 185897). C.M.M. and M.R. were supported by the Swiss National Science Foundation (Sinergia project CRSII5_170873). The funding sources had no role in the design, collection, analysis, or interpretation of the study. The authors wish to thank Martin Seeber, Patrik Wahlberg, David Pascucci, and Gijs Plomp for providing useful comments on the manuscript.

Author contributions

A.D. – designed the study, performed the preprocessing, and wrote the initial draft; R.B. and J.H. – were responsible for patient recruitment and clinical assessment; E.H. – collected the EEG data; S.F. and Š.O. – were involved in the clinical assessment; C.M.M. – served as an advisor, M.R. – performed the analysis, wrote the initial draft, and was responsible for the overall oversight of the study. All authors revised the manuscript.

Competing interests

The authors declare no competing interests.

Additional information

Supplementary information is available for this paper at https://doi.org/10.1038/s41598-020-61264-z.

Correspondence and requests for materials should be addressed to A.D.

Reprints and permissions information is available at www.nature.com/reprints.

Publisher's note Springer Nature remains neutral with regard to jurisdictional claims in published maps and institutional affiliations.

Open Access This article is licensed under a Creative Commons Attribution 4.0 International License, which permits use, sharing, adaptation, distribution and reproduction in any medium or format, as long as you give appropriate credit to the original author(s) and the source, provide a link to the Creative Commons license, and indicate if changes were made. The images or other third party material in this article are included in the article's Creative Commons license, unless indicated otherwise in a credit line to the material. If material is not included in the article's Creative Commons license and your intended use is not permitted by statutory regulation or exceeds the permitted use, you will need to obtain permission directly from the copyright holder. To view a copy of this license, visit http://creativecommons.org/licenses/by/4.0/.

© The Author(s) 2020

Supplementary information for Annex 12 paper that is also available at https://doi.org/10.1038/s41598-020-61264-z.

Further insights on connectivity estimation

On one hand, modifications on the EEG power spectral density in the canonical rhythms (delta, theta, alpha, beta and gamma) permit to infer information on brain activity in different areas. On the other hand, mathematical models may help to elucidate the relationship among brain electric potentials allowing the quantitative analysis of the connections among the different brain regions.

Most of the studies have used approaches based on the definition of Partial Directed Coherence (PDC), i.e., a frequency domain representation of Granger-causality. The originally defined PDC is not scale invariant, i.e., arbitrary changes in the amplitudes of one time series can lead to substantial changes in PDC values. This deficiency was first addressed by introducing the notion of generalized PDC (gPDC) and then by introducing information PDC (iPDC). This weighted multivariate directed dependence measure aims to compute the relationship among partialized signals, inferring the mutual information rates between process portions[1]. The main feature is to adequately consider the prediction error covariance matrix in its formulation to weight the relationships among signals into correctly scaled information measurements, when stationarity zero-mean white noise processes also called innovation processes are either strongly correlated or when their variances differ considerably in size. $iPDC$ properly accounts for size effects in gauging connection strength, given its ability to express information flow in rigorous fashion, as reported in detail in[1 2].

In particular, $iPDC$ is a multivariate spectral measure to compute only the directed influences between any given pair of signals (i, j) of a multivariate dataset. This information is condensed in a complex function $iPDC_{i \leftarrow j}(f)$ of the frequency f, which measures the relative interaction of the signal j with regard to signal i as compared to all j's interactions to other signals in the multivariate dataset. While we refer the reader to[1] for further mathematical details, the procedure for computing $iPDC$ is briefly described by the following two steps.

In the first step, the cortical waveforms $\tilde{x}$ computed after applying the projection method described in [3], are fitted against a *time-variant* (tv) multivariate autoregressive (MVAR) model to overcome the problem of non-stationarity of the EEG data. When the EEG data are available as several trials of the same length, the cortical waveforms computed from the EEG data generates a collection of realizations of a multivariate stochastic process, which can be combined in a multivariate, multi-trial time series:

$$\widetilde{\boldsymbol{X}}(t) = \begin{bmatrix} \widetilde{\boldsymbol{x}}_1^{(1)}(t) & \cdots & \widetilde{\boldsymbol{x}}_d^{(1)}(t) \\ \vdots & \ddots & \vdots \\ \widetilde{\boldsymbol{x}}_1^{(K)}(t) & \cdots & \widetilde{\boldsymbol{x}}_d^{(K)}(t) \end{bmatrix} \quad t = t_1, .., t_N \qquad (1)$$

where t refers to the time points, N the length of the time-series, K the number of trials and d the number of ROIs.

Then the data in $\widetilde{\boldsymbol{X}}$ are fitted against a tv-MVAR model in the general form:

$$\widetilde{\boldsymbol{X}}(t) = -\sum_{r=1}^{p} \boldsymbol{A_r}(t)\boldsymbol{X}(t-r) + \boldsymbol{W}(t) \qquad (2)$$

where $A_r(t)$ are the $[d\ x\ d]$ AR matrices containing the model coefficients, $W(t)$ is the innovation process with covariance matrix $\sum_w$, and p is the model order, usually estimated by means of the Akaike Information Criteria for MVAR processes[3]. The General Linear Kalman filter approach is applied with the aim to estimate the coefficients of the time-variant AR matrices and the covariance matrix $\sum_w$ [4].

As the MVAR model is estimated, for each time-point t, having defined the complex matrix $\boldsymbol{B}(f)$ as:

$$\boldsymbol{B}(f) = \boldsymbol{I_d} - \sum_{r=1}^{p} \boldsymbol{A_r} e^{-j2\pi f} \qquad (3)$$

where I_d is the identity matrix and j is the imaginary unit in this equation, the $iPDC$ complex function from the time-series j to the time-series i is obtained by:

$$iPDC_{i \leftarrow j}(f) = \sigma_{w_{ii}}^{-1/2} \frac{b_{ij}(f)}{\sqrt{\boldsymbol{b_j^H}(f)\boldsymbol{\Sigma_w^{-1}}\boldsymbol{b_j}(f)}} \qquad (4)$$

where $\boldsymbol{b}_j\ (f)$ and $b_{ij}\ (f)$ are respectively the j-th column and the (j,i)-th element of matrix $\boldsymbol{B}(f)$, σ_{w_ii} is the (i,i)-th element of the innovation covariance matrix $\sum_w$, and the apex H in $\boldsymbol{b}_j^H$ stands for Hermitian transpose, i.e., obtained from $\boldsymbol{b}_j$ by taking the transpose and then the complex conjugate of its components.

The complex function $iPDC_{i \leftarrow j}(f)$ of eq. (4) is usually analyzed in terms of its absolute value.

From the complex matrix computed in eq. (3), it is possible to estimate the parametric spectral power density (PSD):

$$PSD(f) = \boldsymbol{H}(f)\boldsymbol{\Sigma}_w\boldsymbol{H}(f)^T \qquad (5)$$

where $\boldsymbol{H}(f)$ is the signal transfer function equal to the inverse of $\boldsymbol{B}(f)$.

Results on all regions of interest

Both the frequency analysis and the network analysis were computed for all source waveforms in the 90 regions of interest (ROIs) considered in the mathematical model for computing the iPDC matrix. The main assumption in the tv-MVAR model to compute the tv-iPDC is based on the hypothesis that all the source waveforms are included in the model itself. In the paper, the results reported are restricted to the pre-selection of twelve areas (the pre-selection is only in the visualization of the results, not in their computation) to answer to the main question of the work: Which structure within the cortico-striatal-pallidal-thalamic and limbic circuits reveals a disrupted resting-state directed functional connectivity? The twelve deep brain structures were selected to consider their potential implication in the deep brain stimulation treating treatment-resistant depression.

Here, the labels of the considered macroscopic brain structures are listed following the order of the AAL atlas: (1) left precentral gyrus; (2) right precentral gyrus; (3) left superior frontal gyrus; (4) right superior frontal gyrus; (5) left superior frontal gyrus, orbital part; (6) right superior frontal gyrus, orbital part; (7) left middle frontal gyrus; (8) right middle frontal gyrus; (9) left middle frontal gyrus, orbital part; (10) right middle frontal gyrus, orbital part; (11) left inferior frontal gyrus, pars opercularis; (12) right inferior frontal gyrus, pars opercularis; (13) left inferior frontal gyrus, pars triangularis; (14) right inferior frontal gyrus, pars triangularis; (15) left inferior frontal gyrus, pars orbitalis; (16) right inferior frontal gyrus, pars orbitalis; (17) left rolandic operculum; (18) right rolandic operculum; (19) left supplementary motor area; (20) right supplementary motor area; (21) left olfactory cortex; (22) right olfactory cortex; (23) left medial frontal gyrus; (24) right medial frontal gyrus; (25) left medial orbitofrontal cortex; (26) right medial orbitofrontal cortex; (27) left gyrus rectus; (28) right gyrus rectus; (29) left insula; (30) right insula; (31) left anterior cingulate gyrus; (32) right anterior cingulate gyrus; (33) left midcingulate area; (34) right midcingulate area; (35) left posterior cingulate gyrus; (36) right posterior cingulate gyrus; (37) left hippocampus; (38) right hippocampus; (39) left parahippocampal gyrus; (40) right parahippocampal gyrus; (41) left amygdala; (42) right amygdala; (43) left calcarine sulcus; (44) right calcarine sulcus; (45) left cuneus; (46) right cuneus; (47) left lingual gyrus; (48) right lingual gyrus; (49) left superior occipital gyrus; (50) right superior occipital gyrus; (51) left middle occipital gyrus; (52) right middle occipital gyrus; (53) left inferior occipital cortex; (54) right inferior occipital cortex; (55) left fusiform gyrus; (56) right fusiform gyrus; (57) left postcentral gyrus; (58) right postcentral gyrus; (59) left superior parietal lobule; (60) right superior parietal lobule; (61) left inferior parietal lobule; (62) right inferior parietal lobule; (63) left supramarginal gyrus; (64) right supramarginal gyrus; (65) left angular gyrus; (66) right angular gyrus; (67) left precuneus; (68) right precuneus; (69) left paracentral lobule; (70) right paracentral lobule; (71) left caudate nucleus; (72) right caudate nucleus; (73) left putamen; (74) right putamen; (75) left globus pallidus; (76) right globus pallidus; (77) left thalamus; (78) right thalamus; (79) left transverse temporal gyrus; (80) right transverse temporal gyrus; (81) left superior temporal gyrus; (82) right superior temporal gyrus; (83) left superior temporal pole; (84) right superior temporal pole; (85) left middle temporal gyrus; (86) right middle temporal gyrus; (87) left middle temporal pole; (88) right middle temporal pole; (89) left inferior temporal gyrus; (90) right inferior temporal gyrus.

From Supplementary Fig. S1, it is possible to qualitatively notice differences in the connectivity relationships among the 90 ROIs of the tv-MVAR model of Eq. 2. In order to quantitatively estimate

the differences between controls and patients at the *population* level, graph metrics were extrapolated from this kind of matrices.

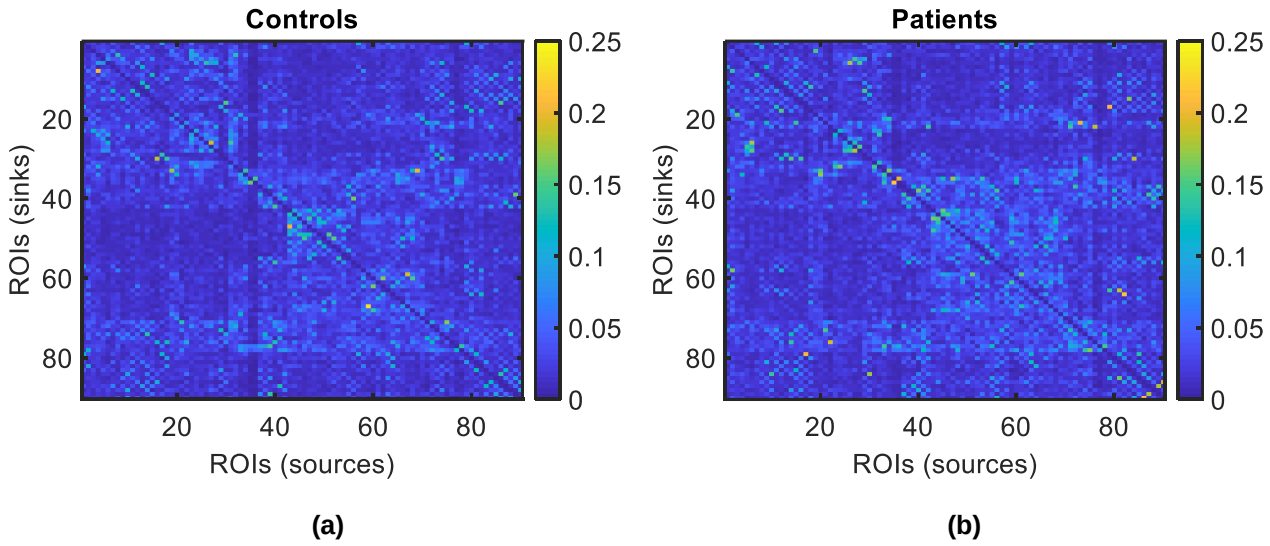

Supplementary Fig. S1: Absolute values of iPDC at the *population* level. Magnitude of iPDC values computed in two *population* subjects (i.e., each trial in input of the tv-MVAR model of Eq. 2 corresponds to the source waveforms computed from a different subject) representing (a) controls and (b) patients. The values reported were averaged over time and frequency. The ROIs are listed following the order of the AAL atlas. The direction of the reported information flow goes from the x-axis, i.e, ROIs (sources), to y-axis, i.e, the ROIs (sinks).

In Supplementary Fig. S2, we reported the values of the local efficiency for all the sources considered in the model at the *single-subject* level. Besides the right amygdala and caudate, also the right cuneus resulted significantly different between controls and patients ($p<0.001$).

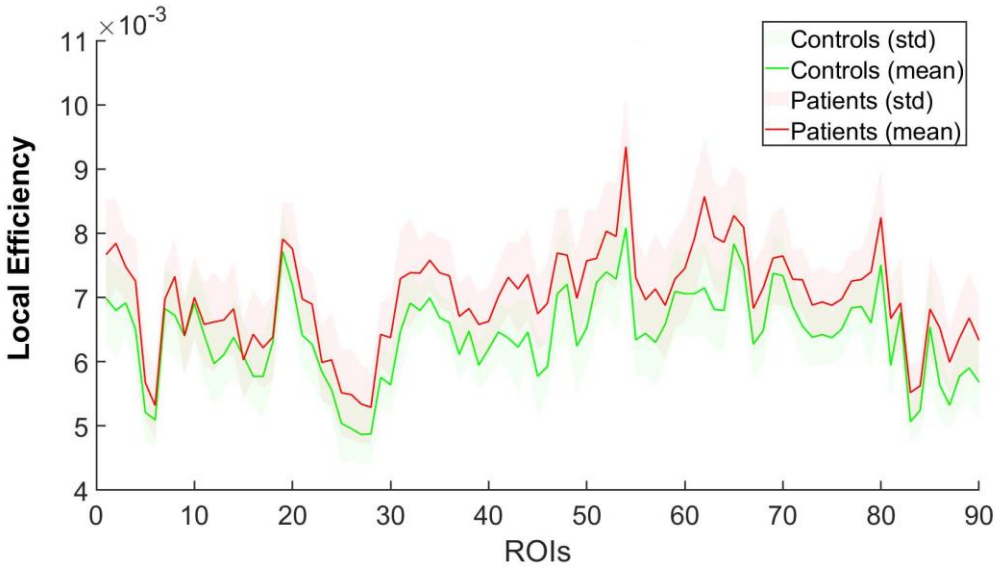

Supplementary Fig. S2: Local Efficiency at the *single-subject* level. Mean and standard deviation (std) of the values of local efficiency for each ROI in controls (green) and patients (red). The ROIs are listed following the order of the AAL atlas.

We found an overall increase in the PSD and in the network metrics comparing patients and controls, but the differences resulted significant only in the subset of the twelve ROIs reported in the paper. We also checked if there was a correlation between the results in the power spectra and the network metrics, no significant correlation was found between the power in delta and beta band and the network metrics. A correlation was found between the local efficiency and power in theta-alpha band, but it was not generalized to all the ROIs (Supplementary Fig. S3).

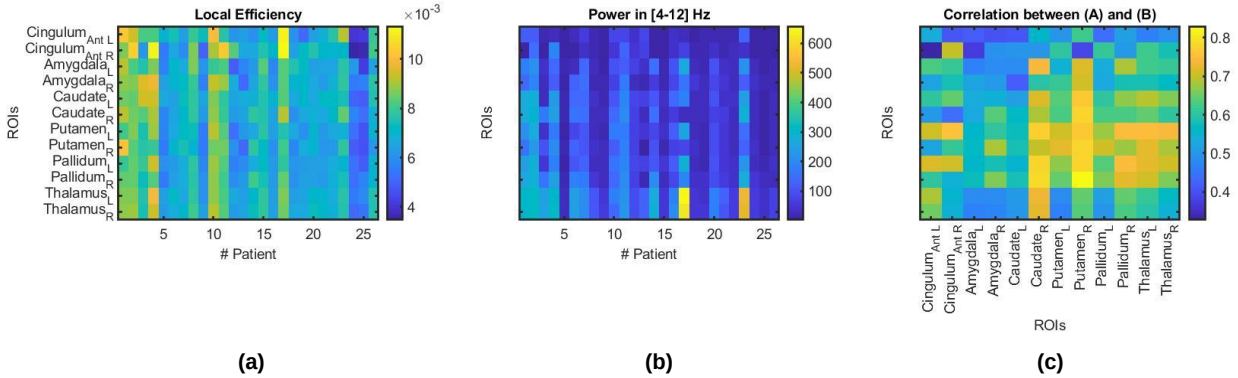

Supplementary Fig. S3: Correlation between the local efficiency and power in the twelve selected ROIs. (a) Values of local efficiency for each patient. The color code stands for the intensity of local efficiency; (b) Values of power in [4-12] Hz for each patient. The color code stands for the value of the power in $(\mu A/mm^3)^2$; (c) Correlation between the values of (a) local efficiency and the values of (b) power in [4-12] Hz in all the patients for each ROI. The color code stands for the r-value of

correlation. All y -axes report the ROIs in the left (L) and right (R) hemispheres as labeled in (a), x-axes report the patient number or ROIs.

References

1. Takahashi, D. Y., Baccalá, L. A. & Sameshima, K. Information theoretic interpretation of frequency domain connectivity measures. *Biol. Cybern.* **103**, 463–469 (2010).

2. Sameshima, K., Baccala, L. A. & Baccala, L. A. *Methods in Brain Connectivity Inference through Multivariate Time Series Analysis*. **20145078**, (CRC Press, 2014).

3. Akaike, H. Information Theory and an Extension of the Maximum Likelihood Principle. in 199–213 (Springer, New York, NY, 1998). doi:10.1007/978-1-4612-1694-0_15

4. Milde, T. *et al.* A new Kalman filter approach for the estimation of high-dimensional time-variant multivariate AR models and its application in analysis of laser-evoked brain potentials. *Neuroimage* **50**, 960–969 (2010).

6. Deep brain stimulation in neuropsychiatry

Deep brain stimulation (DBS) is a neuromodulatory technique that uses electrodes implanted in the brain to deliver adjustable electrical stimuli to specific brain regions to relieve symptoms associated with dysregulated neuronal circuitry (Lozano & Eltahawy, 2004). In the last several decades, DBS was applied to a number of neuropsychiatric conditions, including pain, motor, mood and cognitive disorders (Fig. 8).

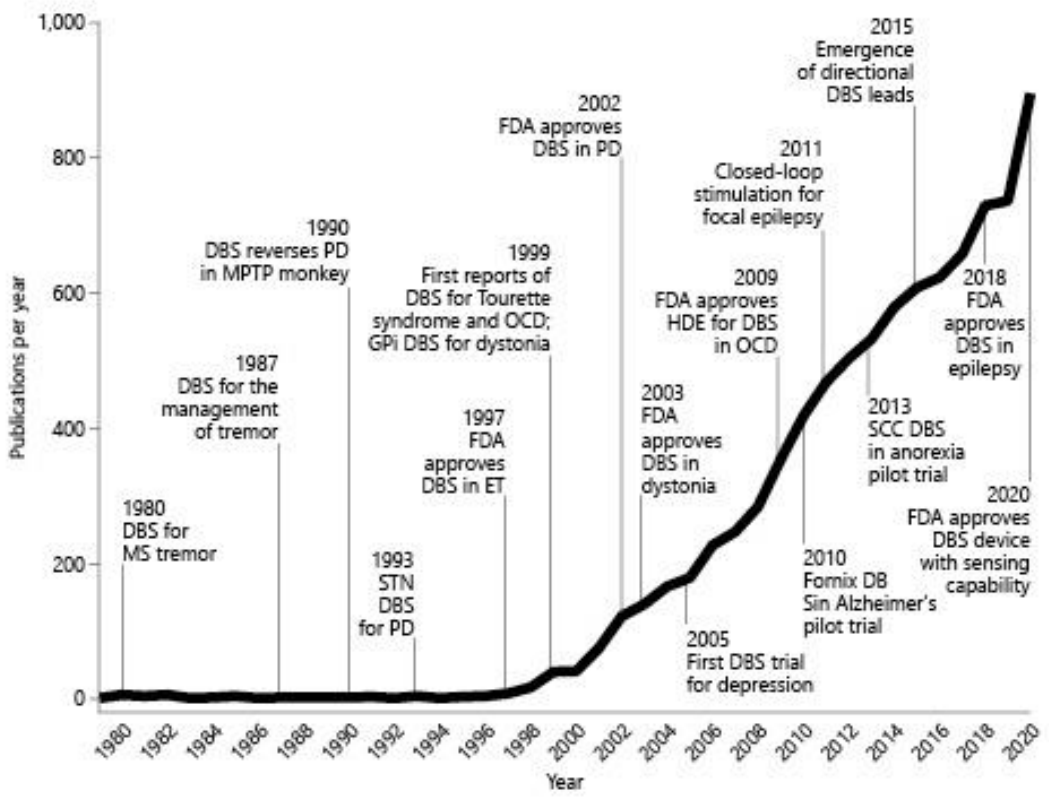

Figure 8 Timeline and yearly growth in the number of DBS publications. Around 8,696 studies were published between 1979 and 2020 with major DBS milestones highlighted. (From Harmsen et al., 2022, Fig. 2)

Throughout the years, this technique has reached advances in recording and stimulation possibilities, and in hardware and software technology. Nevertheless, to reach optimal results of DBS therapy, a number of aspects must be carefully considered. Inês Ludovico was interested in DBS therapy for Parkinson's disease (PD) and, under my supervision, focused on this topic within her Individual Project during

her master's studies. In our joint review paper, we provide an overview of DBS procedure with a special focus on complications of this therapeutic approach applied in PD patients (Ludovico & Damborská, 2017 – Annex 13).

Since 2005 DBS has become a new therapeutic approach for depression (Fig. 8). There is preliminary evidence for the efficacy and safety of DBS for pharmacoresistant depression in the subgenual anterior cingulate cortex, the ventral capsule/ventral striatum, the nucleus accumbens, the lateral habenula, the inferior thalamic peduncle, the medial forebrain bundle, and the bed nucleus of the stria terminalis. Optimal brain stimulation targets, however, have not yet been determined. Dominik Drobisz, assessed the knowledge gathered through DBS studies on depression, focusing on this topic under my supervision within his Individual Project during his master's studies. In our review we provide updated knowledge substantiating the suitability of each of the current and potential future DBS targets for treating depression (Drobisz & Damborská, 2019 – Annex 14). We show that the evidence for the efficacy and safety of DBS in depression is still weak, and the search for optimal target brain structures should continue. Despite myriad DBS targets for treating depression tested in human, the amygdala is not among them. From this perspective, our recent finding of higher-than-normal functional connectivity arising from the right amygdala in depressive patients (Damborská et al., 2020 – Annex 12, Chapter 5.2) contributes to the knowledge that is needed to evaluate deep brain structures as possible candidates for DBS treatment in depression.

Annex 13

Ludovico, I.C. & **Damborská, A.** (2017). Deep brain stimulation in Parkinson's disease: Overview and complications. *Activitas Nervosa Superior*, 59(1), 4-11. doi:10.1007/s41470-017-0003-2

Quantitative contribution: 50%

Content contribution: development of the initial idea, participation in writing the initial draft, corresponding author

Annex 14

Drobisz D. & **Damborská A.** (2019). Deep brain stimulation targets for treating depression, *Behavioural Brain Research*, 359 (1), 266-273.

IF(2019) = 2.977, rank Q2

Quantitative contribution: 50%

Content contribution: development of the initial idea, participation in writing the initial draft, figure preparation, corresponding author

Annex 13

Ludovico, I.C. & **Damborská, A.** (2017). Deep brain stimulation in Parkinson's disease: Overview and complications. *Activitas Nervosa Superior*, 59(1), 4-11. doi:10.1007/s41470-017-0003-2

Act Nerv Super (2017) 59:4–11
DOI 10.1007/s41470-017-0003-2

REVIEW ARTICLE

Deep Brain Stimulation in Parkinson's Disease: Overview and Complications

Inês Ludovico[1] · **Alena Damborská**[1,2]

Received: 5 March 2017 / Accepted: 30 March 2017 / Published online: 18 May 2017
© Springer International Publishing 2017

Abstract Deep brain stimulation (DBS) of basal ganglia has become a frequently performed surgery in patients with advanced Parkinson's disease. Throughout the years, this technique has reached advances in imaging techniques, neurophysiological recording possibilities, and in hardware and software technology. Nevertheless, to reach optimal results of DBS therapy, a number of aspects must be carefully considered. In current paper, overview of DBS procedure is provided with special focus on complications of this, an even so ever more promising therapeutic approach.

Keywords Parkinson's disease · Deep brain stimulation · High-frequency electrical stimulation · Functional inhibition

Introduction

Although nowadays there are still many areas of uncertainty concerning Parkinson's disease and its pathophysiological mechanisms, it is well known that it results from a neurodegenerative process with predominant loss of dopaminergic neurons in the substantia nigra pars compacta and consequent depletion of dopamine, neurotransmitter essential for the modulation of motor activity. The disease is characterized by clinical tetrad of motor dysfunction, including tremor, rigidity, bradykinesia, and postural instability. Besides motor impairments, also behavioral abnormalities, sleep disturbance, and autonomic problems frequently occur (Mehanna and Jankovic 2010; Mehanna 2015).

Concerning the therapeutical options, dopamine replacement therapy is the gold standard method. However, long-term dopamine replacement therapy is showing to have serious adverse effects such as motor fluctuations and levodopa-induced dyskinesia that arise commonly after 5 to 10 years of drug treatment occurring at the peak dose or when the medication is kicking in or wearing off (Mehanna and Jankovic 2010). Motor fluctuations occur when the duration of each medication dose is too short, so patients have a partial relief of their motor symptoms, "on" state, unexpectedly followed by the appearance of the parkinsonian symptoms due to ineffective pharmacological therapy, "off"-state (Silberstein et al. 2009).

In order to overcome the limitations of levodopa replacement therapy, deep brain stimulation (DBS) has become a frequently performed surgery in specifically selected candidates (Kocabicak and Temel 2013). Even this method, however, faces complications, thus DBS therapy becomes a delicate topic to be considered when approaching Parkinson's disease patients. In current paper, overview of DBS in Parkinson's disease patients is provided with special focus on complications of this, an even so ever more promising therapeutic approach.

Mechanisms of DBS Action

The exact mechanism of action of DBS is unknown. However, there is evidence that continuous high-frequency stimulation of overactive targets and induces local inhibition of this disordered basal ganglia nuclei activity. This inhibitory effect is thought to induce normalization of function in motor networks (Silberstein et al. 2009).

✉ Alena Damborská
adambor@med.muni.cz

[1] Department of Psychiatry, University Hospital and Masaryk University, Jihlavská 20, Brno, Czech Republic

[2] Brain and Mind Research Program, Central European Institute of Technology CEITEC, Masaryk University, Kamenice 5, Brno, Czech Republic

It is now clear that the effects of DBS extend beyond functional inhibition, since it has been shown that high-frequency stimulation of the structures surrounding the targeted nuclei invokes excitation rather than inhibition (Bolanowski and Zwislocki 1984). Also, a recent study in primates found that the stimulation of subthalamic nucleus had downstream effects on other nuclei and induced firing of GPint neurons (Hashimoto et al. 2003).

Areas of uncertainty include the need of an explanation on how does certain areas of the brain tissue respond with excitatory effects to high-frequency stimulation, while others respond to it with inhibitory effects. It is also unclear which exact neural elements are affected by DBS stimulation and its effects on the function of the basal ganglia-thalamocortical circuit (Lozano and Mahant 2004).

Extensive research on this matter is being done in order to reveal the mechanisms beyond this area of uncertainty, thus allowing a considerable improvement in DBS surgery technique in the near future.

Deep Brain Stimulation in Parkinson's Disease

DBS technique is based on inducing high-frequency electrical stimulation of specific basal ganglia nuclei targets, namely the subthalamic nucleus and the globus pallidus internus, by means of inhibition of its overactivity and restoration of adequate movement. It aims to mimic the effect of a lesion, without the need for destroying brain tissue thus being a reversible procedure. It is accomplished by permanently implanting an electrode, uni or bilaterally onto the target area and connecting it to an internal pulse generator that can be later reprogrammed telemetrically by the physician in order to better adapt to the course of the disease, minimizing the side effects and improving the efficacy (Volkmann 2007). To reach optimal results of DBS therapy following aspects must be carefully considered, such as patient selection and choosing optimal target for stimulation.

Patient Selection

The major benefits of DBS are to smooth the motor fluctuations, reduce dyskinesia, and suppress tremor in people that have medication-refractory tremor, as well as improvement of quality of life and performance in the activities of daily living (Silberstein et al. 2009). A careful selection of the patients that will undergo DBS is, however, a crucial determinant of favorable outcomes, concerning that about a third of DBS surgery failures is attributed to an inappropriate patient selection (Pollak 2013).

The team that evaluates the condition of the patient to undergo DBS should include a neurologist, neurosurgeon, neuropsychologist, neuroradiologist, psychiatrist, and a nurse specialized in Parkinson's disease (Kocabicak and Temel 2013).

Patients suffering from idiopathic Parkinson's disease, preferably with early-onset, and with good pre-operative levodopa response but severe motor complications due to long-term exposure to drug replacement therapy, would represent the perfect candidates to undergo DBS (Volkmann 2007; Pollak 2013). Before proceed to surgery, patients must have tried all the main medications at optimal doses and still keep impaired in their activities of daily living and quality of life due to motor fluctuations and dyskinesia. It must be, however, taken into account that medication-refractory symptoms such as postural instability, freezing, or dysarthria do not respond to DBS (Benabid et al. 2001).

Dementia, acute psychosis, major depression, cognitive impairment and, other relevant psychiatric illnesses are usually exclusion criteria, since those symptoms tend to get exacerbated after DBS surgery (Volkmann 2007). DBS is also contraindicated in patients with important medical comorbidities that might bring elevated risk during surgery, such as ischemic heart disease or taking anticoagulants (Silberstein et al. 2009).

Even if young age patients with early-onset idiopathic Parkinson's disease are the preferred candidates, people with advanced age should not be excluded. Nevertheless, older patients must be carefully evaluated, since in this group of patients levodopa-resistant symptoms are more often, surgical risk is higher and more frequent, motor rehabilitation is slower, and comorbidities may be limitative (Volkmann 2007).

Choosing Optimal Target for Stimulation

Although the mechanism that leads to the loss of dopaminergic neurons in the substantia nigra is still not quite well understood, there is evidence that bradykinesia could result from the overactivity of both subthalamic nucleus and globus pallidus. These basal ganglia became promising targets for medical and surgical therapy (Bergman et al. 1990; Hariz and Fodstad 2000; Lintas et al. 2012). Greater divergence, however, comes out in which of these targets to choose. Clinical trials including patients stimulated in either subthalamic nucleus or globus pallidus internus (STN-DBS or GPint-DBS, respectively) have demonstrated that both targets are equally effective in improving Parkinson's disease motor symptoms and dyskinesia (Anderson et al. 2005; Odekerken et al. 2013). Moreover, significant dose reduction in dopaminergic medication was shown in patients with STN-DBS, although cognitive and behavioral complications and exacerbation of pre-existing psychiatric illness occurred exclusively in that same group (Anderson et al. 2005). Therefore, GPint-DBS should be preferred in patients with pre-existing psychiatric illness. Besides that, in patients in which levodopa-

induced dyskinesia is the main complaint, GPint stimulation may bring advantages because of its direct anti-dyskinetic effect (Mehanna 2015). In addition, opposing to STN-DBS, the GPint-DBS requires less intensive follow-up and programming, also due to the lack of complications associated with levodopa withdrawal (Lozano and Mahant 2004).

In conclusion, the choice of the target must be determined for each patient on an individual basis, dependent on symptom profile, patient comorbidities, and the experience of the surgical unit.

DBS Surgery Technique

DBS implantation is a highly specialized surgery technique requiring cooperation of wide team of experts, including neurologist, neurosurgeon, neurophysiologist, anesthesiologist, and psychologist. Here, we mention the main steps of the procedure, (for detailed description see Grosset et al. 2009).

Stereotactic Localization of the Target

Patients considered adequate candidates for DBS are admitted to the neurology ward a few days before surgery. One day before DBS surgery, a preoperative MRI scan is performed, and the patient stops taking anti-parkinsonian medication 12 h before the procedure. On the day of the surgery, the patient receives a local anesthesia and a stereotactic frame is firmly placed above the skull, parallel to the line between the nose wing and the tragus. Then, a stereotactic CT is taken and an image fusion technique is used, where the stereotactic CT image is fused to the preoperatively acquired MRI, and targeting is performed based on those fused images, allowing to establish strict coordinates. The patient is then placed in supine position and a local anesthesia is applied, which requires the presence of a psychologist or specialized nurse, as well as two neurosurgeons to double check the correct positioning of the stereotactic frame and to confirm the coordinates (Kocabicak and Temel 2013).

Implantation of the DBS electrode

A 3-cm incision is made and a 1.8-cm diameter burr hole is drilled in the skull at the stereotactically targeted entry site. It is very important to penetrate the brain through a gyrus and not through a sulcus since it can lead to an improper descent of the electrode as well as greater probability of perforating a blood vessel. Although not supported by all groups in the surgical technique of DBS (Nakajima et al. 2011), after the incision has been made, microelectrode recording for precise physiological location of the target site is recommended previous to definite lead implantation (Benabid et al. 1994). A microelectrode is an instrument with a diameter measured in microns, generally used to get as close as possible to the basal ganglia nuclei and record their electrical activity. The microelectrode descends to 10 mm above the target and from there it makes a small step descent until the deepest anatomical level of the target, recording all the electrophysiological activity along the way. The trajectory with the largest electrical activity is chosen for definite DBS lead implantation (Starr et al. 2002; Kocabicak and Temel 2013).

Verification of the Electrode Position

Once the final coordinates are set, the surgeon proceeds to final lead implantation and verifies its correct placement by an intraoperative X-ray. Macrostimulation follows to verify its effectiveness by rating the symptom improvements (bradykinesia, tremor, and rigidity). Adverse effects of stimulation are also assessed, such as muscle contractions due to internal capsule stimulation; paresthesia from stimulation of the sensory thalamus or medial lemniscus; diplopia from oculomotor stimulation; or mood changes from stimulation of limbic pathways. Once finally electrodes are at the correct positions, they are fixed with an antibiotic-containing acrylic fixation ring in order to prevent future intracranial hardware infections (Kocabicak and Temel 2013).

Stimulator Implantation and Internalization of the Electrode

A few days after final electrode implantation (usually 1 to 2 days after), under general anesthesia, an internal pulse generator (IPG) is implanted subcutaneously in a pocket under the clavicle or in the abdominal region. A dual stimulator is usually preferred when the DBS lead implantation is a bilateral procedure. However, some centers prefer the implantation of two single IPG on both sides of the body.

After both final lead implantation and IPG implantation procedures are completed, an extension cable is tunneled under the scalp skin from the internal pulse generator into the DBS lead, and connected via a connector device in order to fully complete the DBS system (Kocabicak and Temel 2013).

Follow-up Care

After DBS surgery, an intensive follow-up care is mandatory in order to rate the clinical improvement of symptoms, while looking for neurological deficits or procedure-related complications and in order to make adjustments on the medication dosage. There are many centers that prefer to wait a few weeks before programming the device so that the brain edema and inflammation around the DBS lead have time to resolve. The system is then activated by the physician and set in one of the several possible combinations, in such way that it improves the patient's

parkinsonian symptoms as much as possible, while having minimal side effects. Later on, along the course of disease, and according to follow-up routine motor and neuropsychological evaluations, the device can be reprogrammed as often as necessary by telemetry. The initial voltage of stimulation is chosen according to the symptoms, usually 2.0 to 3.5 V and it is progressively increased over a few days, in parallel with the reduction of medications. The electrical parameters should be adjusted and the patient should be evaluated again after 3 months and then once a year (Benabid et al. 2001).

At the time of the evaluation, the physician should perform a complete neurological examination, and note the actual levodopa dosage, duration of "on" time (under stimulator effect, where no motor symptoms or dyskinesia should occur), and interview the patient's relatives in order to assess eventual psychological changes.

Clinical Outcomes

Concerning the pallidal stimulation, higher efficacy of bilateral GPint stimulation has been shown in comparison with unilateral stimulation in improvement of Parkinson's disease cardinal symptoms. Bilateral GPint stimulation has been shown to improve drug-induced dyskinesia by 80% and gait disturbance by 40% (Lozano et al. 2002). Bilateral procedures also improve "off-state" motor scores and reduce the severity of "on/off" motor fluctuations (Ghika et al. 1998). A recent study reported that a great improvement in dyskinesia and quality of life was maintained after 3 years of postsurgical follow-up (Durif et al. 1999). It is important to take into account that unilateral pallidal stimulation is safer concerning the cognitive perspective, while bilateral procedures are more prone to insurgence of side-effects such as confusion, depression, and dementia, as well speech and gait disturbances (Hariz 2002).

Considering subthalamic nucleus DBS, there is also evidence of being more effective if bilaterally implanted, rather than unilaterally. Great improvements in motor symptoms have been reported. Tremor is the cardinal sign that benefits the most with subthalamic nucleus DBS, with improvements ranging from 55–90%. It has greater efficacy in reducing tremor, in contrast with medication effect, possibly because it influences additional neural circuits which are independent from dopaminergic transmission (Blahak et al. 2007). Bradykinesia and rigidity are both improved by 52–72%, while axial symptoms and gait disturbances also showed improvement with bilateral subthalamic nucleus DBS. Also improvements in deglutition, olfactory dysfunction, orthostatic hypotension, and dysautonomia were reported (Stemper et al. 2006).

Several studies on unilateral subthalamic nucleus DBS, however, also confirmed improvements in axial symptoms and a bilateral decrease in rigidity and bradykinesia, improvements in quality of life, mental flexibility, and decrease in requirement for medication (Chung et al. 2006; Slowinski et al. 2007; Tabbal et al. 2008).

Complications of DBS Treatment

DBS treatment has proven its success in the control of major symptoms of Parkinson's disease. However, being a high degree precision procedure with elevated complexity, it tends to be a complication-prone operation (Chan et al. 2009). Numerous surgery-related, hardware-related, and stimulation-related complications may arise during the procedure or postoperatively, during the follow-up period (Vergani et al. 2010).

Major complications include the ones that result from the surgical procedure but the morbidity and mortality are rare. Less serious transient or modifiable, but more common complications include the ones resultant from hardware device or stimulation-related complications (Deuschl et al. 2006).

Surgery-Related Complications

The two most commonly encountered procedure-related complications are the intracranial hemorrhage (ICH) and lead malpositioning. The risk of developing intracranial hemorrhage, either subdural, subarachnoid, intraventricular, or intracerebral, is increased by the number of micro or macrostimulation electrode tracking during surgery, as well as by uncontrolled hypertension, presence of brain atrophy, or the use of anticoagulants. The ICH is usually a silent condition but occasionally might cause long-term disability or even death (Lozano and Mahant 2004). The risk of ICH complication, however, is acceptable. Several recent large studies reported ICH in less than 6% of cases (Mehanna 2015; Vergani et al. 2010; Xiaowu et al. 2010); although more frequently recommended, bilateral DBS shows usually higher risk of ICH (Lozano and Mahant 2004).

Microelectrode recording (MER) is used nowadays in order to improve the accuracy of the physiological target location, by recording of cellular discharges within the basal ganglia cells (Chan et al. 2009). On the other hand, it is thought to create an increased risk of ICH, and its value in DBS targeting is still a matter of debate. There are two concerns about MER: one is that it involves multiple penetrations into the brain in order to proper record the target; another one is that the sharp tip of the microelectrode is more prone to rupture a small artery than the blunt-tipped macroelectrode (Xiaowu et al. 2010).

Many reports have found that MRI planning together with intraoperative stimulation is enough to verify the target location in most of the cases. MER was suggested it may increase the risk of ICH without enhancing the accuracy. However, the value of MER varies according to the target site, being more

useful in GPint location and less valuable in detecting subthalamic nucleus (Hariz and Fodstad 2000).

A meticulous surgical planning, composite MRI targeting, and passing the microelectrode slowly at a measured increment of 0.1 mm at each time (Chan et al. 2009), careful management of coagulation dysfunction and hypertension prior to surgery (Kocabicak and Temel 2013), a proper trajectory planning, and the reduction of number of MERs would minimize the risk of ICH during surgery (Xiaowu et al. 2010).

Concerning lead malpositioning, it is the second most common surgical complication being, however, quite a rare event (Chou et al. 2007; Vergani et al. 2010). Malposition of the electrode implies surgical failure, since stimulation will not show any beneficial effects and might cause adverse effects.

Hardware-Related Complications

DBS hardware comprises an internal pulse generator (IPG), an extension electrode, and a stimulation electrode. The IPG is implanted subcutaneously in the infraclavicular region and fixed to the fascia of pectoris muscle by sutures. The extension electrode connects the IPG to the stimulation electrode, running under the scalp skin. The connector makes the connection between the extension cable and the stimulation electrode and it is usually placed in the retroauricular region. The stimulation electrode penetrates deep into the brain target nuclei, being anchored to the skull by a special anchoring device or a burr hole cap in order to prevent its migration. Several types of hardware-related complications may occur.

Infection

Infection is the most commonly encountered hardware-complication, ranging from 1.5 to 22%, and it occurs usually after 4 weeks of implantation (Chan et al. 2009; Vergani et al. 2010; Lockshin and Lockshin 2011). The most common site of infection is the retroauricular connector, followed by the burr hole site and the IPG pocket; while the main encountered pathogens are Gram-positive cocci, mainly *Staphylococcus aureus*. Also a rare occurrence of transient symptomatic post-operative edema surrounding the electrode was described in only 23 patients worldwide, being the edema in general unilateral and accompanied by symptoms such as headache, neurological deficit, or seizures. The etiological cause of such edema is still uncertain Lefaucheur et al. 2013). Infections due to implantation of DBS device can result in prolonged hospitalization, long-term antibiotic use, or even removal of the device in more severe situations.

Lead Migration

Lead migration accounts for 4–5% of the cases and electrode caps and anchoring devices are used in order to prevent such event (Kocabicak and Temel 2013). In most cases, it occurs an upward migration of the lead, due to a bad anchorage to the skull. However, a strange case of downward displacement of the left lead into the pons has been reported in a 53-year-old male, after 10 years of DBS system implantation. MRI technique helped in the final conclusion of a possible stretching of the electrode, by an unknown mechanism (Iacopino et al. 2015). One of the mechanisms that can lead to delayed displacement of DBS electrode is a head trauma (Chan et al. 2009; Vergani et al. 2010). A technique of lead anchorage using a miniplate and two screws has been reported. However, if loosely anchored it tends to migrate since it cannot withstand the head and neck motions. Nowadays, there is a more reliable anchorage device called Navigus that reduced the probability of lead migration to almost zero (Chan et al. 2009).

Lead Fracture

Risk of lead fracture is also a reality. A review of 84 cases was performed and revealed a 5.1% incidence rate of fracture (Mohit et al. 2004). Most of the fractures occurred in the supraclavicular region, while others occurred in the paramastoid region along the connector site. Lead fracture was reported also without any history of trauma (Chan et al. 2009; Vergani et al. 2010).

Major symptoms of lead fracture are related to the feeling of a sudden loss of stimulation after several months/years of device implantation. Most patients present with lapses in tremor control and episodic electric-shock feelings on the contralateral side of the body (Mohit et al. 2004). Diagnosis of lead fracture can be presumed by the symptoms presented or by a verification of high current drainage that soon leads to battery exhaustion (Chan et al. 2009), but confirmed only by X-ray imaging, that would localize the exact place of breakage. Lead replacement is necessary in order to restore normal function of the individual (Mohit et al. 2004).

Rare Hardware-Related Complications

A study was performed in seven patients that suffered from stimulation failure as a consequence of disruption of the lead electrical system, which resulted in an open circuit. The open circuit was detected by verifying an increase in impedance of the electrical system, after noting patient's loss of clinical benefit (Guridi et al. 2012). Another rare complication occurred in a 58-year-old patient that had several hospital admissions for repeated sterile wound necrosis at the IPG site due to allergy. Coating the IPG with a silicone cap was necessary and no further allergic reactions were registered. Other rarer hardware complications were also reported such as early battery exhaustion (Vergani et al. 2010).

Stimulation-Related Complications

Stimulation-related complications may occur when the lead is stimulating the target or its adjacent structures with suboptimal stimulation parameters. Most of these complications are easily reversible by adjustments on parameters of stimulation (Chan et al. 2009).

The most common stimulation-related side effects occur at the level of behavior, but non-behavioral symptoms have also been reported. Behavioral changes are mainly translated by mild changes in emotional and cognitive parameters and many patients might experience either mood enhancement or mood depression. But more severe changes such as mania (believed to be due to stimulation by an electrode surpassing the substantia nigra pars reticulata), depression, psychosis, and suicidal attempt have also been reported (Kocabicak and Temel 2013). Other reported psychiatric complications included anxiety, apathy, and impulse control disorders, such as aggression or obsessive-compulsive disorder (Mehanna 2015) Pre-existing psychiatric illness may then become exacerbated after undergoing DBS surgery (Lozano and Mahant 2004).

Non-behavioral side effects include those such as dyskinesia, worsening of axial symptoms, speech disturbance (Lozano and Mahant 2004), dystonia (Grosset et al. 2009), paresthesia (Lozano and Mahant 2004; Grosset et al. 2009), diplopia (Grosset et al. 2009), hemiballismus (Kocabicak and Temel 2013), and eyelid opening apraxia (Chan et al. 2009).

A curious phenomenon of weight gain has been reported in many patients undergoing subthalamic nucleus DBS. A possible explanation for such event is that the patients maintained the same energy input but had a decrease in energy expenditure, thus resulting in an energy surplus and consequent weight gain; however, the exact mechanism is still uncertain (Strowd et al. 2016).

Ideally, these side effects could be avoided by optimal placement of the lead, so it would not influence other vicinity structures. A combined use of anatomical localization by imaging techniques together with the intraoperative microelectrode recording technique revealed to be of great efficacy. It could also be used bipolar stimulation settings in order to create smaller fields of stimulation, thus avoiding the spreading to adjacent structures (Mehanna 2015).

Conclusion

It is now known that the correct functioning of the basal ganglia motor circuitry is fundamental for modulation of motor activities and an imbalance between the direct and indirect pathways can lead to inability to perform a fine and organized movement. The loss of dopaminergic neurons induces the malfunctioning of the basal ganglia motor circuitry, and the cardinal symptoms of Parkinson's disease gradually arise.

DBS surgery is becoming the treatment of choice, especially for patients suffering from idiopathic Parkinson's disease, preferably with early-onset, and with good pre-operative levodopa response but severe motor complications due to long-term exposure to drug replacement therapy. Patients should be screened for psychiatric disorders and cognitive impairment since those conditions may worsen with surgery. Most well-selected patients who undergo DBS with no complications can expect substantial improvement of their condition.

The most commonly targeted nuclei are the GPint and subthalamic nucleus that can be either targeted unilaterally or bilaterally. However the choice of the target is still controversial and it must be determined for each patient individually, depending on symptom profile, patient comorbidities and the experience of the surgical unit.

A better understanding of the mechanism of action of DBS is also mandatory, so it can lead to improvements in the clinical outcomes, including the treatment of symptoms that are currently refractory to DBS.

Despite the fact that DBS therapy is being refined over the past few years, a high degree of precision is needed and it has an elevated complexity, thus being a complication-prone operation. Complication rates are variable in the literature and data regarding the long-term follow-up complications is still scarce.

Concerning surgery-related complications, intracranial hemorrhage deserves to be mentioned. Its risk is increased by the MER tracking during surgery, as well as by uncontrolled hypertension, presence of brain atrophy or the use of anticoagulants. MER is one of the hardest features to control, thus being a major contributor to the development of intracranial hemorrhage during surgical procedure. The major concerns related to microelectrode recording are the multiple penetrations into the brain and the sharpness of the microelectrode tip, which makes it more prone to rupture the small blood vessels. So a meticulous surgical planning, including proper trajectory planning prior to surgery are of extreme importance when MER is performed.

The hardware-related complications include the hardware infections, lead migration, and lead fracture. Infections occur most often in the retroauricular connector by Gram-positive cocci. Since they can result in prolonged hospitalization, long-term antibiotic use, or even removal of the device in more severe situations, it is mandatory an adequate antibiotic prophylaxis as well as a proper management of the surgical wounds. Lead migration accounts for 4–5% of the hardware complications and electrode caps and anchoring devices are used in order to prevent such event. Lead fractures occur in the supraclavicular region, usually due to a trauma. However, it was reported to occur also without history of trauma. Lead replacement is always necessary in those situations.

Concerning stimulation-related complications, these occur mainly at behavioral level and include: mild changes in

emotional and cognitive parameters and, in rarer situations, mania, depression, psychosis, and suicidal attempt have been reported. Thankfully, these complications are easily reversible by adjustments on stimulation parameters. They can be avoided by an optimal placement of the lead, so it does not influence other vicinity structures. Imaging techniques together with microelectrode recording, or bipolar stimulation settings are also good viable options nowadays.As most of the complications reported were disabling but reversible, and non-life threatening, nowadays DBS proves itself to be a relatively safe procedure.

However, the scarceness of articles and reviews concerning DBS complications makes it a challenging procedure for all the neurosurgical team. Larger studies should be performed, as well as refinements in the imaging methods and in the surgical technique itself, in order to make it a more accurate, safer and economic treatment, while minimizing its tendency to complications.

Acknowledgments This work was supported by the project "CEITEC—Central European Institute of Technology" (CZ.1.05/1.1.00/02.0068) from the European Regional Development Fund and the grant project no.16-33798A from the Ministry of Health Research Program of the Ministry of Health of Czech Republic. The funders had no role in decision to publish, or in preparation of the manuscript.

Compliance with ethical standards

Conflict of interest The authors declare that they have no potential conflict of interest.

References

Anderson, V. C., Burchiel, K. J., Hogarth, P., Favre, J., & Hammerstad, J. P. (2005). Pallidal vs. subthalamic nucleus deep brain stimulation in Parkinson disease. *Archives of Neurology, 62*, 554–560. doi:10.1001/archneur.62.4.554.

Benabid, A. L., Pollak, P., Gross, C., Hoffmann, D., Benazzouz, A., Gao, D. M., Laurent, A., Gentil, M., & Perret, J. (1994). Acute and long-term effects of subthalamic nucleus stimulation of Parkinson's disease. *Stereotactic and Functional Neurosurgery, 62*, 76–84. doi:10.1159/000098600.

Benabid, A. L., Koudsie, A., Benazzouz, A., Piallat, B., Krack, P., Limousin-Dowsey, P., Lebas, J. F., & Pollak, P. (2001). Deep brain stimulation for Parkinson's disease. *Advances in Neurology, 86*, 405–412.

Bergman, H., Wichmann, T., & DeLong, M. R. (1990). Reversal of experimental parkinsonism by lesions of the subthalamic nucleus. *Science, 249*, 1436–1438.

Blahak, C., Wöhrle, J. C., Capelle, H. H., Bäzner, H., Grips, E., Weigel, R., Hennerici, M. G., & Krauss, J. K. (2007). Tremor reduction by subthalamic nucleus stimulation and medication in advanced Parkinson's disease. *Journal of Neurology, 254*, 169–178. doi:10.1007/s00415-006-0305-x.

Bolanowski Jr., S. J., & Zwislocki, J. J. (1984). Intensity and frequency characteristics of pacinian corpuscles. I. Action potentials. *Journal of Neurophysiology, 51*, 793–811.

Chan, D. T. M., Zhu, X. L., Yeung, J. H. M., Mok, V. C. T., Wong, E., Lau, C., & Poon, W. S. (2009). Complications of deep brain stimulation: a collective review. *Asian Journal of Surgery, 32*, 258–263. doi:10.1016/S1015-9584(09)60404-8.

Chou, Y. C., Lin, S. Z., Hsieh, W. A., Lin, S. H., Lee, C. C., Hsin, Y. L., Yen, P.-S., Lee, C. W., Chiu, W.-T., & Chen, S. Y. (2007). Surgical and hardware complications in subthalamic nucleus deep brain stimulation. *Journal of Clinical Neuroscience, 14*(7), 643–649. doi:10.1016/j.jocn.2006.02.016.

Chung, S. J., Jeon, S. R., Kim, S. R., Sung, Y. H., & Lee, M. C. (2006). Bilateral effects of unilateral subthalamic nucleus deep brain stimulation in advanced parkinson's disease. *European Neurology, 56*, 127–132. doi:10.1159/000095704.

Deuschl, G., Herzog, J., Kleiner-Fisman, G., Kubu, C., Lozano, A. M., Lyons, K. E., Rodriguez-Oroz, M. C., Tamma, F. G., Tröster, A. I., Vitek, J. L., Volkmann, J., & Voon, V. (2006). Deep brain stimulation: postoperative issues. *Movement Disorders, 21*, S219–S237. doi:10.1002/mds.20957.

Durif, F., Lemaire, J. J., Debilly, B., & Dordain, G. (1999). Acute and chronic effects of anteromedial globus pallidus stimulation in Parkinson's disease. *Journal of Neurology Neurosurgery and Psychiatry, 67*, 315–322.

Ghika, J., Villemure, J. G., Fankhauser, H., Favre, J., Assal, G., & Ghika-Schmid, F. (1998). Efficiency and safety of bilateral contemporaneous pallidal stimulation (deep brain stimulation) in levodopa-responsive patients with Parkinson's disease with severe motor fluctuations: a 2-year follow-up review. *Journal of Neurosurgery, 89*, 713–718.

Grosset, D. G., Grosset, K. A., Okun, M. S., & Fernandez, H. H. (Eds.). (2009). *Parkinson's disease*. London: Manson Publishing.

Guridi, J., Rodriguez-Oroz, M. C., Alegre, M., & Obeso, J. A. (2012). Hardware complications in deep brain stimulation: electrode impedance and loss of clinical benefit. *Parkinsonism and Related Disorders, 18*, 765–769. doi:10.1016/j.parkreldis.2012.03.014.

Hariz, M. I. (2002). Complications of deep brain stimulation surgery. *Movement Disorders, 17*, S162–S166. doi:10.1002/mds.10159.

Hariz, M. I., & Fodstad, H. (2000). Do microelectrode techniques increase accuracy or decrease risks in pallidotomy and deep brain stimulation? A critical review of the literature. *Stereotactic and Functional Neurosurgery, 72*, 157–169.

Hashimoto, T., Elder, C. M., Okun, M. S., Patrick, S. K., & Vitek, J. L. (2003). Stimulation of the subthalamic nucleus changes the firing pattern of pallidal neurons. *Journal of Neuroscience, 23*, 1916–1923.

Iacopino, D. G., Maugeri, R., Giugno, A., & Giller, C. A. (2015). A strange case of downward displacement of a deep brain stimulation electrode 10 years following implantation: the gliding movement of snakes theory. *World Neurosurgery, 84*, 591 e1–591 e5. doi:10.1016/j.wneu.2015.03.047.

Kocabicak, E., & Temel, Y. (2013). Deep brain stimulation of the subthalamic nucleus in Parkinson's disease: surgical technique, tips, tricks and complications. *Clinical Neurology and Neurosurgery, 115*, 2318–2323. doi:10.1016/j.clineuro.2013.08.020.

Lefaucheur, R., Derrey, S., Borden, A., Wallon, D., Ozkul, O., Gérardin, E., & Maltête, D. (2013). Post-operative edema surrounding the electrode: an unusual complication of deep brain stimulation. *Brain Stimulation, 6*, 459–460. doi:10.1016/j.brs.2012.05.012.

Lintas, A., Silkis, I. G., Albéri, L., & Villa, A. E. P. (2012). Dopamine deficiency increases synchronized activity in the rat subthalamic nucleus. *Brain Research, 1434*, 142–151. doi:10.1016/j.brainres.2011.09.005.

Lockshin, N. A., & Lockshin, B. N. (2011). Skin ulceration secondary to deep brain stimulation device leads. *Journal of the American Academy of Dermatology, 65*, e122–e123. doi:10.1016/j.jaad.2011.03.025.

Lozano, A. M., & Mahant, N. (2004). Deep brain stimulation surgery for Parkinson's disease: mechanisms and consequences. *Parkinsonism and Related Disorders, 10*, S49–S58. doi:10.1016/j.parkreldis.2003.12.006.

Lozano, A. M., Dostrovsky, J., Chen, R., & Ashby, P. (2002). Deep brain stimulation for Parkinson's disease: disrupting the disruption. *Lancet Neurology, 1*, 225–231. doi:10.1016/S1474-4422(02)00101-1.

Mehanna, R. (2015). Deep brain stimulation for Parkinson's disease. In R. Mehanna (Ed.), *Deep brain stimulation*. Huston: Nova Science Publishers, Inc..

Mehanna, R., & Jankovic, J. (2010). Respiratory problems in neurologic movement disorders. *Parkinsonism and Related Disorders, 16*, 628–638. doi:10.1016/j.parkreldis.2010.07.004.

Mohit, A. A., Samii, A., Slimp, J. C., Grady, M. S., & Goodkin, R. (2004). Mechanical failure of the electrode wire in deep brain stimulation. *Parkinsonism and Related Disorders, 10*, 153–156. doi:10.1016/j.parkreldis.2003.11.001.

Nakajima, T., Zrinzo, L., Foltynie, T., Olmos, I. A., Taylor, C., Hariz, M. I., & Limousin, P. (2011). MRI-guided subthalamic nucleus deep brain stimulation without microelectrode recording: can we dispense with surgery under local anaesthesia? *Stereotactic and Functional Neurosurgery, 89*, 318–325. doi:10.1159/000330379.

Odekerken, V. J. J., van Laar, T., Staal, M. J., Mosch, A., Hoffmann, C. F. E., Nijssen, P. C. G., Beute, G. N., van Vugt, J. P. P., Lenders, M. W. P. M., Contarino, M. F., Mink, M. S. J., Bour, L. J., van den Munckhof, P., Schmand, B. A., de Haan, R. J., Schuurman, P. R., & de Bie, R. M. A. (2013). Subthalamic nucleus versus globus pallidus bilateral deep brain stimulation for advanced Parkinson's disease (NSTAPS study): a randomised controlled trial. *The Lancet Neurology, 12*, 37–44. doi:10.1016/S1474-4422(12)70264-8.

Pollak, P. (2013). Deep brain stimulation for Parkinson's disease—patient selection. *Handook of Clinical Neurology, 116*, 97–105. doi:10.1016/B978-0-444-53497-2.00009-7.

Silberstein, P., Bittar, R. G., Boyle, R., Cook, R., Coyne, T., O'Sullivan, D., Pell, M., Peppard, R., Rodrigues, J., Silburn, P., Stell, R., & Watson, P. (2009). Deep brain stimulation for Parkinson's disease: Australian referral guidelines. *Journal of Clinical Neuroscience, 16*, 1001–1008. doi:10.1016/j.jocn.2008.11.026.

Slowinski, J. L., Putzke, J. D., Uitti, R. J., Lucas, J. A., Turk, M. F., Kall, B. A., & Wharen, R. E. (2007). Unilateral deep brain stimulation of the subthalamic nucleus for Parkinson disease. *Journal of Neurosurgery, 106*, 626–632. doi:10.3171/jns.2007.106.4.626.

Starr, P. A., Christine, C. W., Theodosopoulos, P. V., Lindsey, N., Byrd, D., Mosley, A., & Marks Jr., W. J. (2002). Implantation of deep brain stimulators into the subthalamic nucleus: technical approach and magnetic resonance imaging-verified lead locations. *Journal of Neurosurgery, 97*, 370–387.

Stemper, B., Berić, A., Welsch, G., Haendl, T., Sterio, D., & Hilz, M. J. (2006). Deep brain stimulation improves orthostatic regulation of patients with Parkinson disease. *Neurology, 67*, 1781–1785. doi:10.1212/01.wnl.0000244416.30605.f1.

Strowd, R. E., Herco, M., Passmore-Griffin, L., Avery, B., Haq, I., Tatter, S. B., et al. (2016). Association between subthalamic nucleus deep brain stimulation and weight gain: results of a case-control study. *Clinical Neurology and Neurosurgery, 140*, 38–42. doi:10.1016/j.clineuro.2015.11.002.

Tabbal, S. D., Ushe, M., Mink, J. W., Revilla, F. J., Wernle, A. R., Hong, M., Karimi, M., & Perlmutter, J. S. (2008). Unilateral subthalamic nucleus stimulation has a measurable ipsilateral effect on rigidity and bradykinesia in Parkinson disease. *Experimental Neurology, 211*(1), 234–242. doi:10.1016/j.expneurol.2008.01.024.

Vergani, F., Landi, A., Pirillo, D., Cilia, R., Antonini, A., & Sganzerla, E. P. (2010). Surgical, medical, and hardware adverse events in a series of 141 patients undergoing subthalamic deep brain stimulation for Parkinson disease. *World Neurosurgery, 73*, 338–344. doi:10.1016/j.wneu.2010.01.017.

Volkmann, J. (2007). Deep brain stimulation for Parkinson's disease. *Parkinsonism and Related Disorders, 13*, S462–S465. doi:10.1016/S1353-8020(08)70050-6.

Xiaowu, H., Xiufeng, J., Xiaoping, Z., Bin, H., Laixing, W., Yiqun, C., Jinchuan, L., Aiguo, J., & Jianmin, L. (2010). Risks of intracranial hemorrhage in patients with Parkinson's disease receiving deep brain stimulation and ablation. *Parkinsonism and Related Disorders, 16*, 96–100. doi:10.1016/j.parkreldis.2009.07.013.

Annex 14

Drobisz D. & **Damborská A.** (2019). Deep brain stimulation targets for treating depression, *Behavioural Brain Research*, 359 (1), 266-273.

Behavioural Brain Research 359 (2019) 266–273

Contents lists available at ScienceDirect

Behavioural Brain Research

journal homepage: www.elsevier.com/locate/bbr

Review

Deep brain stimulation targets for treating depression

Dominik Drobisz[a,1], Alena Damborská[a,b,c,*,1]

[a] Department of Psychiatry, University Hospital and Masaryk University, Brno, Czech Republic
[b] Department of Basic Neurosciences, University of Geneva, Campus Biotech, Geneva, Switzerland
[c] CEITEC – Central European Institute of Technology, Brain and Mind Research Program, Masaryk University, Brno, Czech Republic

ARTICLE INFO

Keywords:
Deep brain stimulation
Treatment-resistant depression
Major depressive disorder

ABSTRACT

Deep brain stimulation (DBS) is a new therapeutic approach for treatment-resistant depression (TRD). There is a preliminary evidence of the efficacy and safety of DBS for TRD in the subgenual anterior cingulate cortex, the ventral capsule/ventral striatum, the nucleus accumbens, the lateral habenula, the inferior thalamic peduncle, the medial forebrain bundle, and the bed nucleus of the stria terminalis. Optimal stimulation targets, however, have not yet been determined. Here we provide updated knowledge substantiating the suitability of each of the current and potential future DBS targets for treating depression. In this review, we discuss the future outlook for DBS treatment of depression in light of the fact that antidepressant effects of DBS can be achieved using different targets.

1. Introduction

According to the World Mental Health survey [1] the prevalence of unipolar depression expressed as a percentage of the whole population is 14.6% and 11.1% in the high- and low-income countries, respectively. Moreover, WHO studies continuously show a trend toward the increasing prevalence as the low-income countries continue to develop [2]. Major depressive disorder (MDD) by nature has a great impact on quality of life. The total disability-adjusted life years (DALY) attributed to major depression was evaluated at 4.3%, placing depression in third position among other diseases. The WHO forecast for 2030 sets major depression as the leading contributor to the whole of the DALY global burden, with a 6.2% projection. The total mortality ratio of patients with MDD is two times higher than the rest of the population [3].

Even with the multitude of methods used to treat depression, a significant portion of patients fails to respond, resulting in an estimated 1–3% prevalence of treatment-resistant depression (TRD) [4]. The most widely used therapeutic alternatives for pharmacologically refractory depression are electroconvulsive therapy (ECT), repetitive transcranial magnetic stimulation (rTMS) and transcranial magnetic stimulation, with ECT being the oldest technique and showing the best results [5]. However, even ECT is efficacious in only about half of TRD cases [5]. Despite several complications [6], deep brain stimulation (DBS) is commonly used in treating Parkinson's disease (PD) [7–9]; it is now also being applied, though off-label only, in the treatment of major depression. An optimal approach has yet to be established, as the neuropathophysiology of depression remains weakly defined, and the mechanism of DBS seems to be dependent on the stimulation site [10–14]. The best targets, parameters of stimulation, and stimulation protocols have not yet been determined. DBS shows preliminary evidence for antidepressant effects largely in the open-label studies and is still considered investigational in the treatment guidelines [15]. Defining the electrophysiological biomarkers indicating the suitability and efficacy of the treatment should be the next priority. In this review, we present the neuroanatomical brain structures that have been tested for treating depression with DBS. We provide an updated knowledge substantiating the suitability of each of the current and potential future DBS targets for treating depression. We show that the evidence for the efficacy and safety of DBS in depression is still weak and the search for optimal target brain structures should continue. Reliable biomarkers of brain abnormality in depression might help determine the suitability and efficacy of DBS treatment and personalized medicine might be the future outlook for DBS treatment of depression.

2. Current deep brain stimulation targets for treatment-resistant depression

The brain structures that have been used as DBS targets in treating severe depression, proving the safety and efficacy of the electric stimulation, are the subgenual anterior cingulate cortex (sACC), the

* Corresponding author at: Department of Basic Neurosciences, University of Geneva, Campus Biotech, Geneva, Switzerland.
E-mail address: Alena.Damborska@unige.ch (A. Damborská).
[1] The authors contributed equally to this work.

https://doi.org/10.1016/j.bbr.2018.11.004
Received 24 May 2018; Received in revised form 10 September 2018; Accepted 5 November 2018
Available online 08 November 2018
0166-4328/ © 2018 The Authors. Published by Elsevier B.V. This is an open access article under the CC BY license (http://creativecommons.org/licenses/BY/4.0/).

Table 1
Outcomes of deep brain stimulation studies for depression using different brain targets.

Target and study	N	Follow-up period (months)	Mean age at surgery (years)	Mean age of MDD onset (years)	Response rate (%)	Remission rate (%)	Primary measure
Subgenual cingulate gyrus							
Mayberg [39]	6	6	47	29.5	67	33	$HDRS_{17}$
Lozano [40]	20	12	47.4	27.1	55	35	$HDRS_{17}$
Lozano [41]	21	12	47.3	27.3	29	–	$HDRS_{17}$
Kennedy [42]	20	39	47.3	27.1	64	43	$HDRS_{17}$
Neimat [21]	1	30	55	9	100	100	$HDRS_{17}$
Puigdemont [101]	8	12	47.4	24.9	63	50	$HDRS_{17}$
Merkl [99]	6	6	50.67	23.67	50	33	$HDRS_{24}$
Puigdemont [102]	8	12	–	–	63	50	$HDRS_{17}$
Ramasubbu [44]	4	9	50.25	–	50	0	$HDRS_{17}$
Sun [100]	20	4 - 76	45.35	–	60	40	$HDRS_{17}$
Hilimire [103]	7	6	–	–	86	29	$HDRS_{17}$
McNeely [98]	6	12	46	29.5	66	33	$HDRS_{17}$
Kibleur [104]	5	9 - 72	52	–	100	60	$HDRS_{17}$
Riva-Posse [43]	11	12	–	–	82	55	HDRS
Guinjoan [22]	1	18	60	39	100	100	$HDRS_{17}$
Holtzheimer [105]	10	24	40	20.3	92	58	$HDRS_{17}$
Ventral capsule/ventral striatum							
Strong [53]	1	48	43	–	100	100	MADRS
Malone [50]	15	23	46.3	25.3	53	40	$HDRS_{24}$
Malone [51]	17	37	46.3	25.3	71	35	MADRS
Dougherty [52]	30	12	47.7	22.8	20	13	MADRS
Bergfeld [54]	25	13	53.2	28.5	40	20	$HDRS_{17}$
Nucleus accumbens							
Schlaepfer [59]	3	0.5 - 2	46.7	–	33	–	$HDRS_{24}$
Bewernick [57]	10	12 - 36	48.6	31.7	50	30	$HDRS_{28}$
Bewernick [58]	11	12 - 48	48.4	32.6	45	9	$HDRS_{28}$
Millet [60]	4	15	52	–	75	25	$HDRS_{17}$
Inferior thalamic peduncle							
Jiménez [73]	1	24	49	29	–	–	HDRS
Raymaekers [20]	1	96	52	47	100	100	$HDRS_{17}$
Lateral habenula							
Sartorius [67]	1	15	64	18	100	100	$HDRS_{21}$
Medial forebrain bundle							
Schlaepfer [18]	7	3-8	42.6	30	86	57	$HDRS_{24}$
Fenoy [82]	3	6.5	46.3	16.5	67	33	$HDRS_{29}$
Bed nucleus of the stria terminalis							
Raymaekers [20]	7	36	50	35.3	71	29	$HDRS_{17}$
Blomstedt [19]	1	12	60	–	100	100	HDRS

N = Number of participants; $HDRS_n$ = Hamilton Depression Rating Scale with indicated number 'n' of questionnaire items; MADRS = Montgomery-Asberg Depression Rating Scale; '–' data not provided; Note: outcome of identical patients are reported in some ACC-DBS studies [38,39,41] in different time points of the follow-up.

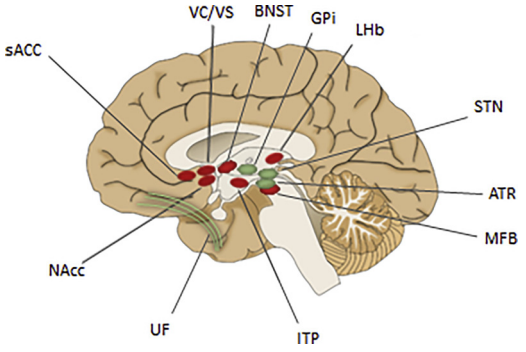

Fig. 1. Current (red) and candidate (green) deep brain stimulation targets for treatment-resistant depression. sACC – subgenual anterior cingulate cortex, VC/VS – ventral capsule/ventral striatum, BNST – bed nucleus of the stria terminalis, GPi – globus pallidus pars interna, LHb – lateral habenula, STN – subthalamic nucleus, ATR – anterior thalamic radiation, MFB –medial forebrain bundle, ITP – inferior thalamic peduncle, UF – uncinate fasciculus, NAcc – nucleus accumbens. Adopted and modified with permission from Anderson et al. [16].

ventral capsule/ventral striatum (VC/VS), the nucleus accumbens (NAcc), the lateral habenula (LHb), and the inferior thalamic peduncle (ITP) [for review see 16]. The medial forebrain bundle (MFB) [17,18] and the bed nucleus of the stria terminalis (BNST) [19,20] have also been recently used. An overview of studies that tested different targets for DBS in TRD is given in Table 1; Fig. 1 illustrates the anatomical locations of these targets. The selection of these structures has been supported mainly by neuroimaging and lesional studies. DBS studies themselves have also inspired the use of some targets through tests on animal models or use in humans for other neuropsychiatric diagnoses, in which improvement in mood was observed as a positive side effect. Some targets have been chosen based on the knowledge of their anatomical and functional position within supposed dysfunctional neural circuits in mood disorders or of their role in neurotransmitter systems.

2.1. Subgenual anterior cingulate cortex

Numerous accounts have linked altered states of the sACC, also referred to as Brodmann area 25, to MDD or/and feelings of sadness. In the sACC in healthy subjects, a change of mood towards less or more happy was shown to correlate with increased or decreased regional cerebral blood flow, respectively [23,24]. An increased regional cerebral metabolic rate of glucose (CMRGlc) in the left sACC was reported

to indicate a higher chance for successful cingulotomy in treating TRD [25] and for successful treatment with accelerated high-frequency rTMS. Moreover, the CMRGlc of the responsive subgroup was shown to decrease in time during rTMS [26].

Neural connections of the sACC correspond to its involvement in the large-scale neural networks that are dysfunctional in depressed patients, either directly or through a downstream connected structure [27]. The white matter of the sACC is connected to the medial frontal cortex, the anterior and posterior cingulate cortex, the anterior medial temporal lobe, the dorsal medial thalamus, the hypothalamus, the NAcc and the brainstem nuclei [28–30]. Dysfunctions of the subcortico-cortical and limbic neural networks are proposed as a basis of the pathophysiology of depression and hence the causes of anhedonia and dysphoria [14,31–33]. Substantial findings indicate increased involvement of the sACC in the brain default mode network (DMN), and subsequently altered states of DMN are linked to major depression [34–37]. Riva-Posse and colleagues [38] distinguished three major pathways most probably contributing to the clinical effect of the sACC-DBS. The first path consists of the forceps minor and medial aspect of the uncinate fascicle connecting the sACC with the medial frontal cortex. The second pathway leads via the cingulate bundle and connects the sACC with the rostral and dorsal anterior cingulate cortex, and the mid-cingulate cortex. Finally, the short descending midline fibres connect the sACC with the NAcc, caudate, putamen, and anterior thalamus.

Several human trials have investigated the efficacy of the DBS of sACC in the context of alleviating TRD (Table 1). An immediate anti-dysphoric effect of the stimulation of sACC has been reported [39,40] and replicated in different institutions [41]. As for the long-term effect of the stimulation, considerable responsiveness and remission rates that were observed one year after DBS implantation [40] lasted several years [42]. The efficacy of DBS in sACC was shown to increase with individualized target identification and contact selection and with the use of optimal stimulation parameters. In their recent study, Riva-Posse and colleagues [43] used a prospective connectomic approach for sACC DBS surgery. They used the group probabilistic tractography map as a 'connectome blueprint' to plan surgical targeting in 11 participants with TRD. At one year, 82% of the participants were responders and 55% were in remission, suggesting the utility of this approach for future sACC DBS studies. As to the stimulation parameters, the stimulation efficacy was observed to increase with the pulse duration [44].

2.2. Ventral capsule/ventral striatum

Increased functional connectivity of the ventral striatum (VS) with various brain areas was linked to the symptoms of depression [45]. For example, intensified connections from the left VS to the left caudate have been associated with anhedonia. Higher connections from the left VS to the right mid and superior prefrontal cortex and anterior cingulate cortex were reported to be associated with higher suicidality, while depression severity correlates with the connectivity of the left VS to the right precuneus and left caudate and mid-cingulate. Hwang and colleagues [46] found that an increase in functional connectivity between the VS and the DMN is positively associated with the Center for epidemiologic Studies Depression Scale (CES-D) score. The tractography of the anterior limb of the internal capsule revealed rich projections to the entire thalamus, hypothalamus, brainstem, frontal pole, medial temporal lobe, and the NAcc [29], which are sites associated with depressive syndrome [46].

Decreased interest in and performance of activities in depressed subjects as compared to healthy subjects was shown to be associated with lesser bilateral VS activation in response to positive stimuli [47].

Capsulotomies performed for obsessive-compulsive disorder (OCD) decreased patient scores in the Hamilton Depression Rating Scale (HDRS) and other neuropsychological scores [48]. Aouizerate and colleagues [49] performed a successful DBS trial with patients with OCD and concomitant MDD, with results showing decreases in both OCD and depression severity. In these ablative and stimulation studies, the improvement in depressive symptomatology might occur due to the amelioration or resolution of the OCD. The efficacy of DBS in VC/VS was, however, demonstrated in patients who received DBS for TRD [50–54], even though the results of the randomized controlled phase of the most recent VC/VS-DBS studies are contradictory. While Bergfeld et al. [54] reported significant reduction of depressive symptoms, Dougherty et al. [52] found no significant differences between the active and sham DBS. Slightly different position of the electrode, insufficient duration of the optimization phase and too short period for the evaluation of DBS settings might have led to negative results in the earlier study, as argued by the authors of the more recent study [54]. Interestingly, the two VC/VS-DBS studies differed also in the gender ratio with 57% [52] compared to 32% [54] of male participants, suggesting some influence of gender on the treatment efficacy. However, to the best of our knowledge there are no direct reports suggesting less efficacy of the VC/VS-DBS in men with TRD.

2.3. Nucleus accumbens

The NAcc is known for its established role in the neurocircuitry of pleasure and reward [32,55]; there are findings of increased activation of the NAcc to a presented reward and decreased activity in reaction to a punishment [56]. The trials of its stimulation in treating refractory depression have therefore a solid rationale. What further cements the link between depressive states and the NAcc are structural and functional correlates between the nucleus and the level of anhedonia, a cardinal symptom of depression. The more severe the anhedonia, the smaller the nucleus, and the lesser the activation of the NAcc to a reward [56]. Thus, a change in the activity of the nucleus could decrease the depressive symptomatology. The theoretical reasoning for stimulating the NAcc has been verified on several occasions [57–60]. Stimulation of the NAcc showed a reduced mean HDRS at every point of Bewernick's study [57], a year after the implantation surgery, 50% of the subjects were classified as responsive. An immediate effect of the stimulation was demonstrated in increased reward-seeking thoughts [59]. PET imaging performed by Schlaepfer and colleagues [59] after NAcc stimulation showed a bilateral increase in metabolic activity in the dorsolateral prefrontal cortex, a structure usually hypoactive in depression [61]. Additionally, decreased activity was observed throughout the study in the ventromedial prefrontal cortex, which has been reported to be hyperactive in depression [61]. Thus, a reversal of pathological activity as a result of NAcc stimulation was observed alongside with the cessation of depressive symptoms [59].

2.4. Lateral habenula

The LHb is known to play a key role during the acquisition of reward-related information [62]. The LHb activity corresponds negatively to the anticipation of a reward and the reception of a reward, the firing in the LHb neurons is increased in the opposite situations, namely the anticipation of a non-reward situation and the omission of a reward. The LHb causes inhibition of the ventral striatum dopamine neurons, which are active during the anticipation and reception of rewards. Shelton and colleagues [63] showed that the LHb is activated as a response to a noxious stimulus. An increase in LHb activity could therefore explain some symptoms of depression, such as increased pain sensation [64] and lowered reward-seeking behaviour [32]. In accordance with this theory, a rapid depletion of plasma tryptophan, a drug used to mitigate the exacerbation of depressive symptoms, showed increased blood flow in the habenular area [65].

In order to alleviate depression, DBS of the LHb should cause functional inhibition of the LHb. In rats, chronic DBS caused better performance in open-field tests and increased serum and brain tissue monoamines [66]. DBS of the LHb caused remission after 4 months of stimulation in a patient with MDD, supporting a critical role of this

structure in depression [67].

2.5. Inferior thalamic peduncle

The ITP is a bundle of fibres that reciprocally interconnect the intralaminar nucleus and the thalamic reticular nucleus with the orbitofrontal cortex (OFC) [68]. The OFC is widely accepted as playing a key role in the non-reward attractor theory of depression [69]. Lesioning of the ITP, which happens during stereotactic tractotomy of the broader area, showed the amelioration of depressive symptoms [70]. Low frequency (6 Hz) electric stimulation of the ITP and nucleus reticularis thalami caused a synchronization of the electroencephalographic (EEG) signal recorded in the frontopolar region. This suggest the existence of direct connections to the OFC. Higher frequency stimulation (60 Hz) caused desynchronization in the EEG signal of the same area [71]. Because high frequency stimulation causes EEG outputs similar to that of the simultaneous application of glutamate and *N*-methyl-D-aspartate into the cortex, Velasco and colleagues [71] hypothesized that this kind of stimulation can activate a glutamatergic system related to the arousal and the cholinergic system. In a case report, DBS of the ITP was shown to have a long-lasting antidepressant effect [72,73]. In a recent study, one patient that was stimulated in ITP continued to experience a substantial decrease in depressive symptoms 8 years after the implantation [20].

2.6. Medial forebrain bundle

The MFB consists of two distinct tracts both of which are connected to various parts of the limbic system: the inferomedial MFB (imMFB) and the superolateral MFB (slMFB). Both parts form a common trunk, which sprouts caudally to the ventral tegmental area, goes to the dentate nucleus of the cerebellum, leaves the cerebellum via the superior cerebellar peduncle, connects to the upper pons, retrobulbar area, and the periaqueductal grey, splits into the mentioned sole tracts in the ventral tegmental area, and finally the imMFB goes as far as to the lateral hypothalamus, while the slMFB passes through the thalamus into the anterior limb of the internal capsule [74]. It has been proposed that the MFB forms a part of the systems of seeking, panic, and reward [74,75]. As those systems are dysfunctional in MDD [32,55,76], it seems that the MFB plays a crucial role in the pathophysiology of depression. Alterations of the MFB, such as reduced fractional anisotropy in patients with the melancholic subtype of MDD [77] were observed to correlate with depressive symptomatology. Further investigations on animal models of depression showed a significant reversal of depressive-like symptoms after DBS of MFB [78–80]. While lower levels of dopamine were observed in some rat models of depression [80], electric stimulation of the MFB in rats was suggested to increase the number of D2 receptors in the prefrontal cortex and the number of dopamine transporters in the hippocampus [78]. The overall effect on depressive state, anxiety, and drive is rapid [81], as demonstrated in the increase in forced swim test scoring. It is, however, inconclusive whether the changed dopamine levels are causal for the observed change in behaviour and more importantly whether this phenomenon is of any significance in human neurocircuitry. In humans, the stimulation of the slMFB was observed to increase appetitive motivation and to improve mood immediately intraoperatively [18,82]. Significant changes in depression scores were seen as soon as in the seventh day of the stimulation. There have been even hints of a marker for suitability of DBS in certain depressive patients, as responsive groups were reported to have stronger connectivity between the location of the stimulation and the medial prefrontal cortex [82]. Casting doubt on the similarity of the actual action of stimulation in rat models and humans, and hence of the changed dopamine levels, Bregman and colleagues [81] pointed out that dopamine axons in MFB in both rats and humans are mostly non-myelinated. Therefore, the stimulation in commonly used parameters cannot recruit dopaminergic axons. In support of this point, no increase in dopamine release during DBS of MFB in rats was observed [81]. The antidepressant effect might be delivered by other types of axons in humans.

2.7. Bed nucleus of the stria terminalis

BNST is located in the basal forebrain, serves as a major output pathway of the amygdala and has a complex role in regulating stress response. Dysfunction in this structure was suggested to play an important role in anxiety disorders, partly through serotonergic activity [83]. To date, only two studies have reported the efficacy of DBS for TRD in BNST. In a recent case study a patient, with severe MDD and comorbid anorexia nervosa, was treated with DBS in the MFB and subsequently, two years after the first DBS procedure, in the BNST [19]. While DBS MFB had to be discontinued due to blurred vision as a side effect, very profound gradual improvements were seen after DBS BNST. In a double-blind crossover study the effects of DBS in the BNST and the ITP were assessed in seven TRD patients [20]. The outcomes during the two crossover periods performed within the first 16 months after the surgery suggested better effects of BNST to ITP stimulation. Three years after the DBS implantation all patients were stimulated at BNST. Five out of seven patients were responders and two were in remission. Due to limited number of investigations efficacy of DBS in the two targets was not compared. The authors concluded that both BNST and ITP stimulation may alleviate depressive symptoms in patients with TRD. The clinical outcomes of seven MDD patients undergoing DBS BNST in another study [84] have not been presented yet. The authors rather searched for electrophysiological biomarkers of depression. Based on the finding that relative alpha-power recorded in the BNST and the MFB correlate significantly with the self-reported disease severity in MDD patients, the authors suggested that alpha activity in the limbic system might be a signature of symptom severity in MDD.

3. Candidate deep brain stimulation targets for treatment-resistant depression

Based on their anatomical proximity to the previously tested sites, we can speculate that some other brain structures might be considered as possible new targets for the DBS for treating depression. These candidate structures include anterior thalamic radiation (ATR), uncinate fasciculus (UF), subthalamic nucleus (STN), and globus pallidus pars interna (GPi). Fig. 1 illustrates the anatomical locations of these targets.

3.1. Anterior thalamic radiation

The ATR goes medially to the slMFB and ends at the anterior limb of the internal capsule, and it connects the dorsomedial thalamus, anterior thalamic nucleus, temporo-mesial region, and brain stem through the mamillo-thalamic tract. It is thought to be in a kind of antagonistic relationship with the slMFB, as its increased activation has been ascribed to an activation of the grief or/and the panic system; thus, in combination with the slMFB it forms a kind of a homeostatic system [17,74,85].

3.2. Uncinate fasciculus

The UF connects the prefrontal regions associated with emotions with the middle temporal lobe and hence the hippocampus and amygdala [86]. The most convincing evidence of the possible role of UF in the pathophysiology of MDD are the observed abnormalities in structural connectivity of UF in patients with MDD [87–90]. Decreased fractional anisotropy and an increased apparent diffusion coefficient between the sites connected with UF were found in depressive patients [88]. Moreover, the structural changes showed a relationship to depression severity, as reported in this diffusion tensor imaging study.

Another marker of the severity of depression linked to the UF is the decreased functional connectivity between the supragenual cingulate and extended amygdala [90].

3.3. Subthalamic nucleus and globus pallidus pars interna

Both structures form a part of the basal ganglia motor, oculomotor, associative and limbic functional loops. Their stimulation is commonly used in the treatment of PD, mostly with the intention of influencing the motor loop dysfunction that manifests in the motor symptoms of PD [7–9]. Even though the intent is to specifically target the motor subunit of the STN in DBS for PD, the adjacent limbic subunit is too close to exclude the influence of stimulation on this site [91–94]. Recent observations of a decrease in scoring in depression during stimulation of the STN for treating PD support this view [95–97]. As to the efficacy of the stimulation in terms of depression, STN and GPi seem to have nearly the same results [96].

4. The search for optimal target brain structures for DBS in depression should continue

The existing clinical trials of DBS for TRD have provided evidence of efficacy and safety for various brain targets. The fact that the trials stimulating different sites were chiefly performed by different scientific teams makes any meta-analysis difficult. They used different inclusion criteria, applied various outcome measures, and had slightly different follow-up management. Nevertheless, bearing in mind the limitations of the available data, similar efficacy and safety can be seen regardless of the choice of the target structure. Typically one third of the patients achieved complete remission, another third showed improvements and yet another third experienced no benefit in studies using sACC [39,40,42,98–100], VC/VS [50] or NAcc [57] as target structures. Recent studies using sACC report higher response or remission rates [43,101–105] and thus favour the sACC over other targets.

In general, the evidence of efficacy is, however, somewhat weak for many reasons. Most of the studies involve few patients, with several even being case reports. Most studies are open-label, and thus fail to control for placebo effects, lacking control sham stimulation or control groups with the best medical therapy. Another drawback of the evidence is the very fact that complete remission rates do not exceed 30% in most studies. The reason the efficacy is not higher might be due to an undesirable study design, insufficient sample size, inappropriate patient selection, inadequate stimulation parameters, suboptimal target selection, or unfavourable electrode positions within the target structure.

To move forward in the effective DBS treatment of TRD, evidence from randomized double-blind crossover active-sham designed studies is highly appreciated. When designing such trials, optimization phase of sufficient duration, such as 6 months, with the possibility to evaluate DBS parameter setting over at least one week should precede the crossover phase [54]. That way, the highest possible efficacy in the active arm of the clinical trial is likely to be ensured, being a prerequisite for subsequent result evaluation in such study. Rapid worsening when stimulation is discontinued may preclude, however, using long time intervals due to ethical concerns [50,105]. From this respect, the animal studies aimed at testing various DBS targets for treating depression are far more suitable with the advantage that they allow for higher control over variables that cannot be influenced in humans [106]. Antidepressant-like effect of DBS was observed in rats stimulated in ventromedial prefrontal cortex (vmPFC, rodent analogue of subgenual cingulate) [107–109], MFB [110], and NAcc [108]. Besides identifying targets for effective DBS, animal studies may also directly compare the DBS efficacy while systematically testing different brain regions. VmPFC was recently reported to outperform Nacc-DBS in the antidepressant-like effect [111]. Furthermore, animal studies might address the mechanisms underlying DBS. Functional inactivation of local neuronal populations through DBS, activation of fiber pathways near the stimulating electrodes as well as serotonergic reserve were suggested to be involved in antidepressant-like effect of vmPFC-DBS [107].

In our view, the fundamental condition for DBS treatment of depression is the proper target selection. To find an optimal node that would reduce or even completely remove the functional abnormality in TRD would be crucial. Testing new targets for DBS might help in this respect. In searching for an optimal DBS target, it is necessary, however, to consider the possibility that in general there is no one and only optimal DBS target for the treatment of depression. The fact that the antidepressant effect of stimulation can be achieved using different targets supports the view that depression is a neurocircuitry disease involving the disruption of multiple large-scale neural networks rather than an impairment of a single brain structure. Aberrancies in the cortico-striato-thalamo-cortical loops have been suggested in the aetiology of MDD [14,112]. This neurocircuitry of depression is considered to involve the dorsal (prefrontal, dorsal anterior cingulate and premotor cortices), ventral (sACC, orbitofrontal, and insular cortices), and modulatory (pregenual ACC, amygdala, and the hypothalamic-pituitary axis) components [112]. Each DBS-TRD target structure has its own unique anatomical and functional position within these networks, which determines its ability to improve the depressive symptomatology during stimulation. For instance, it was hypothesized that DBS applied in an area where fibres from the ventral and dorsal compartments converge, such as the NAcc, might enable simultaneous excitation and inhibition in the dorsal and ventral compartments, respectively [112] influencing the dysbalanced neural system in a complex manner. Another example of a particular role of the stimulated structure in the large-scale communication is the ACC, whose possible integrative functions in cognitive processing [113] might explain the most recently reported high efficacy of DBS to sACC in treating depression [104].

The evidence for involvement of the medial and dorsolateral prefrontal cortex, the cingulate cortex, limbic and paralimbic regions in pathogenesis of depression [114–116] allows one to speculate, whether direct stimulation of multiple brain targets within the impaired network might be beneficial. Stimulation of multiple regions is already being performed by non-invasive approaches such as ECT and rTMS, which proved their efficacy in treating depression [116–118]. The ECT directly involves robust nonfocal electric stimulation of the brain. Even the rTMS, mainly performed over the left and/or right dorsolateral prefrontal cortices, has been shown to be biologically active not only locally but also at remote sites, presumably through transsynaptic connections [119–121,116]. Although the mechanism of action of ECT is not yet fully understood, beneficial plasticity mechanisms (e.g.neurogenesis, dendritogenesis, synapse formation) are speculated to occur following ECT [122,123]. For antidepressant effect, mainly the hippocampal neurogenesis seems to be necessary [124,125]. Indeed, depression has been linked to chronic stress [126,127] that is supposed to produce alterations in memory functions of the hippocampus [128]. It is known that low and high frequency electrical stimulation of neurons can cause long-term depression (LTD) and long-term potentiation (LTP), respectively. These physiological phenomena are considered to be involved in dynamic changes in neuronal networks underlying the learning and memory processes. If DBS of multiple brain structures involved in TRD could induce neuroplasticity analogous to the LTD or LTP this might restore these impaired networks.

It is also possible that different targets should be used in different subtypes or stages of MDD due to the existence of different underlying brain abnormalities. Despite the myriad of targets tested, neurobiological markers of these abnormalities, however, have not been identified yet. In a recent resting-state connectivity study based on EEG data, different network patterns were found in temporal lobe epilepsy patients and controls [129]. In this study, the outflow from the anterior cingulate cortex was lower in temporal lobe epilepsy patients with learning deficits or depression than in patients without impairments and then controls. These resting-state connectivity alterations were

suggested to constitute an important biomarker of temporal lobe epilepsy. We believe that identifying similar electrophysiological markers in TRD could help better identify the target structures for DBS treatment of depression.

In addition to efficacy and safety, practical aspects of stimulation such as battery longevity should influence the judgement on the suitability of a given target structure. The stimulation parameters are very high in the habenula and the IC/VC, which would lead to more frequent battery changes, an action which is not only more expensive but also riskier for the patients due to potential infection during each surgery. Rechargeable batteries have been suggested to solve this problem [130,51].

Taken together, a consensus on optimal DBS target/s for treating depression has not been reached yet, hence leaving the door for future investigations in this field still open.

5. Personalized medicine for DBS treatment in depression

In line with the concept of abnormal neurocircuitry in MDD, the observed variability in depressive symptomatology suggests the existence of variability in structural and/or functional abnormalities within the involved brain networks. Reliable biomarkers of these abnormalities are needed to determine the suitability and efficacy of DBS treatment. Personalized DBS treatment that would consider the specific needs of each patient thus could increase the overall efficacy of the DBS approach. To personalize DBS treatment, we need an individualized DBS protocol and a precise evaluation of patient impairment. First, within the efforts towards developing an individualized DBS protocol, establishing a registry for future clinical studies has recently been proposed by Morishita and colleagues [131]. They suggest that data from future clinical DBS studies for TRD be collected in an organized manner, creating a common register of variables related to the clinical status before the treatment, parameters of stimulation, precise positioning of the electrode within the brain structure, and postoperative outcomes, including side effects. Based on this accumulated data, rigorous meta-analyses would be performed and the DBS protocol could then be individualized to match the pre-surgical clinical characteristics of each patient. Recent study by Zhou and colleagues is the first step [132]. Second, to get the exact evaluation of each patient impairment an objective measure of the brain abnormality would be necessary, one that would allow for distinguishing among different subtypes of MDD and could also serve as a standard measure of treatment efficacy. Current diagnostic tools such as structured diagnostic interviews and psychometric methods seem to be insufficient in this respect, since they do not directly measure the structural or functional brain abnormalities and rather focus on the resulting symptomatology of the disease. Besides that, the use of more direct neuroimaging tools, such as standard clinical magnetic resonance imaging and electroencephalography, is mainly restricted to differential diagnostics of depression. It only serves to detect or exclude severe brain lesions and epilepsy.

In the search for an objective biomarker of brain abnormality in MDD, the EEG 'microstate' analysis might represent a possible solution [133]. This method is supposed to be a promising neurophysiological tool for understanding and assessing brain network dynamics on a subsecond timescale. A series of quasi-stable microstates, each characterized by a unique topography of electric potentials over the whole scalp, can be assessed to provide potential utility in detecting neurophysiological impairments. In early studies using adaptive segmentation to examine microstates in patients with depression, microstates exhibited abnormal topographies and reduced overall average microstate duration [134] but unchanged numbers of different microstates per second [135], compared to controls. These findings suggest that the resting-state EEG microstate analysis may offer a novel approach in diagnostics, making it possible to identify individually unique patterns of resting-state electrophysiological brain activity.

6. Conclusion

In conclusion, DBS in MDD should be still considered as an experimental therapy. Many questions remain. What is the neurobiology of treatment-resistant depression? What is/are the optimal target brain structure/s for deep brain stimulation in depression? What are the suitable biomarkers of brain abnormalities in depression? Will personalized medicine increase the efficacy of DBS therapies for treatment-resistant depression? Despite these still open questions, the advantages of electrical stimulation of brain structures over previously used lesioning procedures is evident right now. It is fully reversible and enables adjustments to interindividual and intraindividual variabilities of needs that rise from the existence of disease subtypes and disease progression. This method is promising and it may soon develop into a standard tool for treating depression resistant to other therapeutic approaches.

Declaration of interest

The authors have nothing to declare and have no conflict of interest.

Acknowledgements

This project received funding from the European Union Horizon 2020 research and innovation programme under the Marie Skłodowska-Curie grant agreement No. 739939 and was financially supported by Ministry of Education, Youths and Sports of the Czech Republic within CEITEC 2020 (LQ1601) project. The authors wish to thank Anne Meredith Johnson for providing language help.

References

[1] E. Bromet, et al., Cross-national epidemiology of DSM-IV major depressive episode, BMC Med. 9 (2011) 90.
[2] WHO, The Global Burden of Disease 2004 Update. Geneva, Switzerland, (2008).
[3] U. Ösby, et al., Excess mortality in bipolar and unipolar disorder in Sweden, Arch. Gen. Psychiatry 58 (2001) 844–850.
[4] P.E. Holtzheimer, H.S. Mayberg, Stuck in a rut: rethinking depression and its treatment, Trends Neurosci. 34 (2011) 1–9.
[5] A. Minichino, et al., ECT, rTMS, and deep TMS in pharmacoresistant drug-free patients with unipolar depression: a comparative review, Neuropsychiatr. Dis. Treat. 8 (2012) 55–64.
[6] I. Ludovico, A. Damborská, Deep brain stimulation in parkinson's disease: overview and complications, Act. Nerv. Super. (Praha) 59 (2017) 4–11.
[7] A.L. Benabid, et al., Combined (thalamotomy and stimulation) stereotactic surgery of the VIM thalamic nucleus for bilateral Parkinson disease, Appl. Neurophysiol. 50 (1987) 344–346.
[8] A. Castrioto, et al., Ten-year outcome of subthalamic stimulation in Parkinson disease: a blinded evaluation, Arch. Neurol. 68 (2011) 1550–1556.
[9] G. Deuschl, et al., A randomized trial of deep-brain stimulation for Parkinson's disease, New Engl. J. Med. Surg. Collat. Branches Sci. 355 (2006) 896–908.
[10] M.E. Anderson, et al., Effects of high-frequency stimulation in the internal globus pallidus on the activity of thalamic neurons in the awake monkey, J. Neurophysiol. 89 (2003) 1150–1160.
[11] C. Bosch, et al., Subthalamic nucleus high-frequency stimulation generates a concomitant synaptic excitation-inhibition in substantia nigra pars reticulata, J. Physiol. (Paris) 589 (2011) 4189–4207.
[12] L. Garcia, et al., Dual effect of high-frequency stimulation on subthalamic neuron activity, J. Neurosci. 23 (2003) 8743–8751.
[13] T. Hashimoto, et al., Stimulation of the subthalamic nucleus changes the firing pattern of pallidal neurons, J. Neurosci. 23 (2003) 1916–1923.
[14] H.S. Mayberg, Limbic-cortical dysregulation: a proposed model of depression, J. Neuropsychiatry Clin. Neurosci. 9 (1997) 471–481.
[15] R.V. Milev, et al., Canadian network for mood and anxiety treatments (CANMAT) 2016 clinical guidelines for the management of adults with major depressive disorder: section 4. Neurostimulation treatments, Can. J. Psychiatry 61 (2016) 561–575.
[16] R.J. Anderson, et al., Deep brain stimulation for treatment-resistant depression: efficacy, safety and mechanisms of action, Neurosci. Biobehav. Rev. 36 (2012) 1920–1933.
[17] V.A. Coenen, et al., Reply to: medial forebrain bundle stimulation - speed access to an old or entry into a new depression neurocircuit? Biol. Psychiatry 74 (2013) e45–e46.
[18] T.E. Schlaepfer, et al., Rapid effects of deep brain stimulation for treatment-resistant major depression, Biol. Psychiatry 73 (2013) 1204–1212.
[19] P. Blomstedt, et al., Deep brain stimulation in the bed nucleus of the stria

terminalis and medial forebrain bundle in a patient with major depressive disorder and anorexia nervosa, Clin. Case Rep. 5 (2017) 679–684.
[20] S. Raymaekers, et al., Deep brain stimulation for treatment-resistant major depressive disorder: a comparison of two targets and long-term follow-up, Transl. Psychiatry 7 (2017) e1251.
[21] J.S. Neimat, et al., Neural stimulation successfully treats depression in patients with prior ablative cingulotomy, Am. J. Psychiatry 165 (2008) 687–693.
[22] S.M. Guinjoan, et al., Asymmetrical contribution of brain structures to treatment-resistant depression as illustrated by effects of right subgenual cingulum stimulation, J. Neuropsychiatry Clin. Neurosci. 22 (2010) 265–277.
[23] H.S. Mayberg, et al., Reciprocal limbic-cortical function and negative mood: converging PET findings in depression and normal sadness, Am. J. Psychiatry 156 (1999) 675–682.
[24] P.S. Talbot, S.J. Cooper, Anterior cingulate and subgenual prefrontal blood flow changes following tryptophan depletion in healthy males, Neuropsychopharmacol. 31 (2006) 1757–1767.
[25] D.D. Dougherty, et al., Cerebral metabolic correlates as potential predictors of response to anterior cingulotomy for treatment of major depression, J. Neurosurg. 99 (2003) 1010–1017.
[26] C. Baeken, et al., The impact of accelerated HF-rTMS on the subgenual anterior cingulate cortex in refractory unipolar major depression: insights from 18FDG PET brain imaging, Brain Stimul. 8 (2015) 808–815.
[27] C. Hamani, et al., The subcallosal cingulate gyrus in the context of major depression, Biol. Psychiatry 69 (2011) 301–308.
[28] W.C. Drevets, et al., The subgenual anterior cingulate cortex in mood disorders, CNS Spectr. 13 (2008) 663–681.
[29] D.A. Gutman, et al., A tractography analysis of two deep brain stimulation white matter targets for depression, Biol. Psychiatry 65 (2009) 276–282.
[30] H. Johansen-Berg, et al., Anatomical connectivity of the subgenual cingulate region targeted with deep brain stimulation for treatment-resistant depression, Cereb. Cortex 18 (2008) 1374–1383.
[31] J.W. Dalley, et al., Neurobehavioral mechanisms of impulsivity: fronto-striatal systems and functional neurochemistry, Pharmacol. Biochem. Behav. 90 (2008) 250–260.
[32] A.J.M. Loonen, S.A. Ivanova, Circuits regulating pleasure and happiness—mechanisms of depression, Front. Human Neurosci. 10 (2016) 571.
[33] H.S. Mayberg, Targeted electrode-based modulation of neural circuits for depression, J. Clin. Invest. 119 (2009) 717–725.
[34] S.J. Broyd, Default-mode brain dysfunction in mental disorders: a systematic review, Neurosci. Biobehav. Rev. 33 (2009) 279–296.
[35] M.D. Greicius, et al., Resting-state functional connectivity in major depression: abnormally increased contributions from subgenual cingulate cortex and thalamus, Biol. Psychiatry 62 (2007) 429–437.
[36] V. Menon, Large-scale brain networks and psychopathology: a unifying triple network model, Trends Cogn. Sci. (Regul. Ed.) 15 (2011) 483–506.
[37] M. Van Den Heuvel, et al., Microstructural organization of the cingulum tract and the level of default mode functional connectivity, J. Neurosci. 28 (2008) 10844–10851.
[38] P. Riva-Posse, et al., Defining critical white matter pathways mediating successful subcallosal cingulate deep brain stimulation for treatment-resistant depression, Biol. Psychiatry 76 (2014) 963–969.
[39] H.S. Mayberg, et al., Deep brain stimulation for treatment-resistant depression, Neuron 45 (2005) 651–660.
[40] A.M. Lozano, et al., Subcallosal cingulate gyrus deep brain stimulation for treatment-resistant depression, Biol. Psychiatry 64 (2008) 461–467.
[41] A.M. Lozano, et al., A multicenter pilot study of subcallosal cingulate area deep brain stimulation for treatment-resistant depression: clinical article, J. Neurosurg. 116 (2012) 315–322.
[42] S.H. Kennedy, et al., Deep brain stimulation for treatment-resistant depression: follow-up after 3 to 6 years, Am. J. Psychiatry 168 (2011) 502–510.
[43] P. Riva-Posse, et al., A connectomic approach for subcallosal cingulate deep brain stimulation surgery: prospective targeting in treatment-resistant depression, Mol. Psychiatry 23 (2018) 843–849.
[44] R. Ramasubbu, et al., Double-blind optimization of subcallosal cingulate deep brain stimulation for treatment-resistant depression: a pilot study, J. Psychiatry Neurosci. 38 (2013) 325–332.
[45] K. Quevedo, et al., Ventral striatum functional connectivity during rewards and losses and symptomatology in depressed patients, Biol. Psychol. 123 (2017) 62–73.
[46] J.W. Hwang, et al., Enhanced default mode network connectivity with ventral striatum in subthreshold depression individuals, J. Psychiatr. Res. 76 (2016) 111–120.
[47] J. Epstein, et al., Lack of ventral striatal response to positive stimuli in depressed versus normal subjects, Am. J. Psychiatry 163 (2006) 1784–1790.
[48] S. Zhan, et al., Long-term follow-up of bilateral anterior capsulotomy in patients with refractory obsessive-compulsive disorder, Clin. Neurol. Neurosurg. 119 (2014) 91–95.
[49] B. Aouizerate, et al., Deep brain stimulation of the ventral caudate nucleus in the treatment of obsessive-compulsive disorder and major depression: case report, J. Neurosurg. 101 (2004) 682–686.
[50] D.A. Malone Jr.et al., Deep brain stimulation of the ventral Capsule/Ventral striatum for treatment-resistant depression, Biol. Psychiatry 65 (2009) 267–275.
[51] D.A. Malone Jr., Use of deep brain stimulation in treatment-resistant depression, Clevel. Clin. J. Med. 77 (2010) S77–S80.
[52] D.D. Dougherty, et al., A randomized sham-controlled trial of deep brain stimulation of the ventral Capsule/Ventral striatum for chronic treatment-resistant depression, Biol. Psychiatry 78 (2015) 240–248.
[53] D.R. Strong, Reversible increase in smoking after withdrawal of ventral capsule/ventral striatum deep brain stimulation in a depressed smoker, J. Addict. Med. 6 (2012) 94–95.
[54] I.O. Bergfeld, et al., Deep brain stimulation of the ventral anterior limb of the internal capsule for treatment-resistant depression, JAMA Psychiatry 73 (2016) 456–464.
[55] K.C. Berridge, M.L. Kringelbach, Affective neuroscience of pleasure: reward in humans and animals, Psychopharmacology 199 (2008) 457–480.
[56] J. Wacker, et al., The role of the nucleus accumbens and rostral anterior cingulate cortex in anhedonia: integration of resting EEG, fMRI, and volumetric techniques, Neuroimage 46 (2009) 327–337.
[57] B.H. Bewernick, et al., Nucleus accumbens deep brain stimulation decreases ratings of depression and anxiety in treatment-resistant depression, Biol. Psychiatry 67 (2010) 110–116.
[58] B.H. Bewernick, et al., Long-term effects of nucleus accumbens deep brain stimulation in treatment-resistant depression: evidence for sustained efficacy, Neuropsychopharmacol. 37 (2012) 1975–1985.
[59] T.E. Schlaepfer, et al., Deep brain stimulation to reward circuitry alleviates anhedonia in refractory major depression, Neuropsychopharmacology 33 (2008) 368–377.
[60] B. Millet, et al., Limbic versus cognitive target for deep brain stimulation in treatment-resistant depression: accumbens more promising than caudate, Eur. Neuropsychopharmacol. 24 (2014) 1229–1239.
[61] M. Koenigs, J. Grafman, The functional neuroanatomy of depression: distinct roles for ventromedial and dorsolateral prefrontal cortex, Behav. Brain Res. 201 (2009) 239–243.
[62] M. Matsumoto, O. Hikosaka, Lateral habenula as a source of negative reward signals in dopamine neurons, Nature 447 (2007) 1111–1115.
[63] L. Shelton, et al., Mapping pain activation and connectivity of the human habenula, J. Neurophysiol. 107 (2012) 2633–2648.
[64] M. Hermesdorf, et al., Pain sensitivity in patients with major depression: differential effect of pain sensitivity measures, somatic cofactors, and disease characteristics, J. Pain 17 (2016) 606–616.
[65] J.S. Morris, et al., Covariation of activity in habenula and dorsal raphe nuclei following tryptophan depletion, Neuroimage 10 (1999) 163–172.
[66] H. Meng, et al., Chronic deep brain stimulation of the lateral habenula nucleus in a rat model of depression, Brain Res. 1422 (2011) 32–38.
[67] A. Sartorius, et al., Remission of major depression under deep brain stimulation of the lateral habenula in a therapy-refractory patient, Biol. Psychiatry 67 (2010) e9–e11.
[68] J.D. Schmahmann, D.N. Pandya (Eds.), Fiber Pathways of the Brain, Oxford University Press, 2006.
[69] E.T. Rolls, A non-reward attractor theory of depression, Neurosci. Biobehav. Rev. 68 (2016) 47–58.
[70] G. Knight, Stereotactic tractotomy in the surgical treatment of mental illness, J. Neurol. Neurosurg. Psychiatr. 28 (1965) 304–310.
[71] M. Velasco, et al., Electrocortical and behavioral responses elicited by acute electrical stimulation of inferior thalamic peduncle and nucleus reticularis thalami in a patient with major depression disorder, Clin. Neurophysiol. 117 (2006) 320–327.
[72] F. Jiménez, et al., A patient with a resistant major depression disorder treated with deep brain stimulation in the inferior thalamic peduncle, Neurosurgery 57 (2005) 585–592.
[73] F. Jiménez, et al., Neuromodulation of the inferior thalamic peduncle for major depression and obsessive-compulsive disorder, Acta Neurochir. Suppl. (Wien) 97 (2007) 393–398.
[74] V.A. Coenen, et al., Human medial forebrain bundle (MFB) and anterior thalamic radiation (ATR): imaging of two major subcortical pathways and the dynamic balance of opposite affects in understanding depression, J. Neuropsychiatry Clin. Neurosci. 24 (2012) 223–236.
[75] M.A. Waraczynski, The central extended amygdala network as a proposed circuit underlying reward valuation, Neurosci. Biobehav. Rev. 30 (2006) 472–496.
[76] T.D. Satterthwaite, et al., Common and dissociable dysfunction of the reward system in bipolar and unipolar depression, Neuropsychopharmacology 40 (2015) 2258–2268.
[77] T. Bracht, et al., White matter microstructure alterations of the medial forebrain bundle in melancholic depression, J. Affect. Disord. 155 (2014) 186–193.
[78] M.P. Dandekar, et al., Increased dopamine receptor expression and anti-depressant response following deep brain stimulation of the medial forebrain bundle, J. Affect. Disord. 217 (2017) 80–88.
[79] H. Edemann-Callesen, et al., Medial forebrain bundle deep brain stimulation has symptom-specific anti-depressant effects in rats and as opposed to ventromedial prefrontal cortex stimulation interacts with the reward system, Brain Stimul. 8 (2015) 714–723.
[80] L.L. Furlanetti, et al., Ventral tegmental area dopaminergic lesion-induced depressive phenotype in the rat is reversed by deep brain stimulation of the medial forebrain bundle, Behav. Brain Res. 299 (2016) 132–140.
[81] T. Bregman, et al., Antidepressant-like effects of medial forebrain bundle deep brain stimulation in rats are not associated with accumbens dopamine release, Brain Stimul. 8 (2015) 708–713.
[82] A.J. Fenoy, et al., Deep brain stimulation of the medial forebrain bundle: distinctive responses in resistant depression, J. Affect. Disord. 203 (2016) 143–151.
[83] M.A. Lebow, A. Chen, Overshadowed by the amygdala: the bed nucleus of the stria terminalis emerges as key to psychiatric disorders, Mol. Psychiatry 21 (2016) 450–463.

[84] W.J. Neumann, et al., Different patterns of local field potentials from limbic DBS targets in patients with major depressive and obsessive compulsive disorder, Mol. Psychiatry 19 (2014) 1186–1192.
[85] T. Bracht, et al., A review of white matter microstructure alterations of pathways of the reward circuit in depression, J. Affect. Disord. 187 (2015) 45–53.
[86] J. Hau, et al., Revisiting the human uncinate fasciculus, its subcomponents and asymmetries with stem-based tractography and microdissection validation, Brain Struct. Funct. 222 (2017) 1645–1662.
[87] A. Carballedo, et al., Reduced fractional anisotropy in the uncinate fasciculus in patients with major depression carrying the met-allele of the Val66Met brain-derived neurotrophic factor genotype, Am. J. Med. Genet. B Neuropsychiatr. Genet. 159B (2012) 537–548.
[88] R.B. Dalby, et al., Depression severity is correlated to the integrity of white matter fiber tracts in late-onset major depression, Psychiatry Res. Neuroimaging 184 (2010) 38–48.
[89] B. De Kwaasteniet, et al., Relation between structural and functional connectivity in major depressive disorder, Biol. Psychiatry 74 (2013) 40–47.
[90] S.C. Matthews, et al., Decreased functional coupling of the amygdala and supragenual cingulate is related to increased depression in unmedicated individuals with current major depressive disorder, J. Affect. Disord. 111 (2008) 13–20.
[91] A.L. Benabid, et al., Acute and long-term effects of subthalamic nucleus stimulation of Parkinson's disease, Stereotactic Funct. Neurosurg. 62 (1994) 76–84.
[92] S. Hemm, et al., Deep brain stimulation in movement disorders: stereotactic coregistration of two-dimensional electrical field modeling and magnetic resonance imaging, J. Neurosurg. 103 (2005) 949–955.
[93] C.C. McIntyre, et al., Cellular effects of deep brain stimulation: model-based analysis of activation and inhibition, J. Neurophysiol. 91 (2004) 1457–1469.
[94] Y.R. Wu, et al., Does stimulation of the GPi control dyskinesia by activating inhibitory axons? Mov. Disord. 16 (2001) 208–216.
[95] E.L. Birchall, et al., The effect of unilateral subthalamic nucleus deep brain stimulation on depression in Parkinson's disease, Brain Stimul. 10 (2017) 651–656.
[96] H.L. Combs, et al., Cognition and depression following deep brain stimulation of the subthalamic nucleus and globus pallidus pars internus in parkinson's disease: a meta-analysis, Neuropsychol. Rev. 25 (2015) 439–454.
[97] J.F.A.D. Santos, et al., Tackling psychosocial maladjustment in Parkinson's disease patients following subthalamic deep-brain stimulation: a randomised clinical trial, PLoS One 12 (2017) e0174512.
[98] H.E. McNeely, et al., Neuropsychological impact of Cg25 deep brain stimulation for treatment-resistant depression: preliminary results over 12 months, J. Nerv. Ment. Dis. 196 (2008) 405–410.
[99] A. Merkl, et al., Antidepressant effects after short-term and chronic stimulation of the subgenual cingulate gyrus in treatment-resistant depression, Exp. Neurol. 249 (2013) 160–168.
[100] Y. Sun, et al., Deep brain stimulation modulates gamma oscillations and theta-gamma coupling in treatment resistant depression, Brain Stimul. 8 (2015) 1033–1042.
[101] D. Puigdemont, et al., Deep brain stimulation of the subcallosal cingulate gyrus: further evidence in treatment-resistant major depression, Int. J. Neuropsychopharmacol. 15 (2012) 121–133.
[102] D. Puigdemont, et al., A randomized double-blind crossover trial of deep brain stimulation of the subcallosal cingulate gyrus in patients with treatment-resistant depression: a pilot study of relapse prevention, J. Psychiatry Neurosci. 40 (2015) 224–231.
[103] M.R. Hilimire, et al., Effects of subcallosal cingulate deep brain stimulation on negative self-bias in patients with treatment-resistant depression, Brain Stimul. 8 (2015) 185–191.
[104] A. Kibleur, et al., Stimulation of subgenual cingulate area decreases limbic top-down effect on ventral visual stream: a DBS-EEG pilot study, Neuroimage 146 (2017) 544–553.
[105] P.E. Holtzheimer, et al., Subcallosal cingulate deep brain stimulation for treatment-resistant unipolar and bipolar depression, Arch. Gen. Psychiatry 69 (2012) 150–158.
[106] C. Hamani, J.N. Nóbrega, Deep brain stimulation in clinical trials and animal models of depression, Eur. J. Neurosci. 32 (2010) 1109–1117.
[107] C. Hamani, et al., Antidepressant-like effects of medial prefrontal cortex deep brain stimulation in rats, Biol. Psychiatry 67 (2010) 117–124.
[108] R. Gersner, et al., Site-specific antidepressant effects of repeated subconvulsive electrical stimulation: potential role of brain-derived neurotrophic factor, Biol. Psychiatry 67 (2010) 125–132.
[109] H. Moshe, et al., Prelimbic stimulation ameliorates depressive-like behaviors and increases regional BDNF expression in a novel drug-resistant animal model of depression, Brain Stimul. 9 (2016) 243–250.
[110] S. Thiele, et al., The effects of bilateral, continuous, and chronic Deep Brain Stimulation of the medial forebrain bundle in a rodent model of depression, Exp. Neurol. 303 (2018) 153–161.
[111] J. Rummel, et al., Testing different paradigms to optimize antidepressant deep brain stimulation in different rat models of depression, J. Psychiatr. Res. 81 (2016) 36–45.
[112] B.H. Kopell, et al., Deep brain stimulation for psychiatric disorders, J. Clin. Neurophysiol. 21 (2004) 51–67.
[113] M. Kukleta, et al., The level of frontal-temporal beta-2 band EEG synchronization distinguishes anterior cingulate cortex from other frontal regions, Conscious Cogn. 19 (2010) 879–886.
[114] M.S. George, et al., Prefrontal cortex dysfunction in clinical depression, Depression 2 (1994) 59–72.
[115] M.S. George, et al., What functional imaging studies have revealed about the brain basis of mood and emotion, in: J. Panksepp (Ed.), Advances in Biological Psychiatry, JAI Press, Greenwich, Conn, 1996, pp. 63–113.
[116] M.S. George, et al., The expanding evidence base for rTMS treatment of depression, Curr. Opin. Psychiatry 26 (2013) 13–18.
[117] M.S. Reddy, M.S. Vijay, Repetitive transcranial magnetic stimulation for depression: state of the art, Indian J. Psychol. Med. 39 (2017) 1–3.
[118] A.P. Hermida, et al., Electroconvulsive therapy in depression: current practice and future direction, Psychiatr. Clin. North Am. 41 (2018) 341–353.
[119] T. Paus, et al., Transcranial magnetic stimulation during positron emission tomography: a new method for studying connectivity of the human cerebral cortex, J. Neurosci. 17 (1997) 3178–3184.
[120] M.S. George, et al., Prefrontal repetitive transcranial magnetic stimulation (rTMS) changes relative perfusion locally and remotely, Hum. Psychopharmacol. 14 (1999) 161–170.
[121] D.E. Bohning, et al., Mapping transcranial magnetic stimulation (TMS) fields in vivo with MRI, Neuroreport 8 (1997) 2535–2538.
[122] F. Bouckaert, et al., ECT: its brain enabling effects: a review of electroconvulsive therapy-induced structural brain plasticity, J. ECT 30 (2014) 143–151.
[123] K.M. Ryan, D.M. McLoughlin, From molecules to mind: mechanisms of action of electroconvulsive therapy, Acta Psychiatr. Scand. 138 (2018) 177–179.
[124] T.D. Perera, et al., Necessity of hippocampal neurogenesis for the therapeutic action of antidepressants in adult Nonhuman primates, PLoS One 6 (2011) e17600.
[125] L. Santarelli, et al., Requirement of hippocampal neurogenesis for the behavioral effects of antidepressants, Science. 301 (2003) 805–809.
[126] C.C. Conway, et al., Chronic environmental stress and the temporal course of depression and panic disorder: a trait-state-occasion modeling approach, J. Abnorm. Psychol. 125 (2016) 53–63.
[127] S.A. Swanson, et al., The contribution of stress to the comorbidity of migraine and major depression: results from a prospective cohort study, BMJ Open 3 (2013) e002057.
[128] A.H. van Stegeren, Imaging stress effects on memory: a review of neuroimaging studies, Can. J. Psychiatry 54 (2009) 16–27.
[129] A. Coito, et al., Altered directed functional connectivity in temporal lobe epilepsy in the absence of interictal spikes: a high density EEG study, Epilepsia 57 (2016) 402–411.
[130] P. Blomstedt, et al., Deep brain stimulation in the treatment of depression, Acta Psychiatr. Scand. 123 (2011) 4–11.
[131] T. Morishita, et al., Deep brain stimulation for treatment-resistant depression: systematic review of clinical outcomes, Neurotherapeutics 11 (2014) 475–484.
[132] C. Zhou, et al., A systematic review and meta-analysis of deep brain stimulation in treatment-resistant depression, Prog. Neuropsychopharmacol. Biol. Psychiatry 82 (2018) 224–232.
[133] C.M. Michel, T. Koenig, EEG microstates as a tool for studying the temporal dynamics of whole-brain neuronal networks: a review, Neuroimage 180 (2018) 577–593.
[134] W.K. Strik, et al., Larger topographical variance and decreased duration of brain electric microstates in depression, J. Neural Transmission 99 (1995) 213–222.
[135] R. Ihl, J. Brinkmeyer, Differential diagnosis of aging, dementia of the Alzheimer type and depression with EEG-segmentation, Dement. Geriatr. Cogn. Dis. Extra 10 (1999) 64–69.

7. Conclusion

Intracranial and scalp electroencephalographic (EEG) signals recorded during cognitive tasks and at rest are used to understand the material substrate of the human mind. When searching for associations between EEG features and mental processes, researchers assume that mental operations depend on transmembrane neuronal currents that produce neuronal spike firing patterns. Neuronal spike firing is reflected in local field potentials that can directly be recorded intracranially or captured on the head surface as building blocks of scalp EEG signals.

High-density scalp EEG allows for the reconstruction of a scalp potential map representing the global brain activity. Dynamics in topographic changes of scalp potential maps provide information about dynamics in large-scale brain networks. Moreover, source reconstructed scalp EEG signal allows for a spatially systematic study of brain activity. The intracranial EEG is spatially limited compared to the scalp EEG. It is, however, only minimally affected by artefacts and has a high signal-to-noise ratio, thus providing a focal but magnified view of the brain. Identical basic analytical approaches are used for both intracranial and scalp EEGs. Time-domain analysis of EEG signals provides information on event-related potential components with their amplitude, latency, and spatial characteristics. Frequency-domain analysis reveals EEG rhythms with their topography, frequency ranges, and hierarchical organization. In studies included in this habilitation thesis, all the above-mentioned methods and analytical approaches were used to disclose electrophysiological correlates of both resting-state mental activity and higher brain functions in human.

The almost centenary history of EEG has shown that this method can provide a useful window into different functional brain states associated with relevant mental processes. In this respect, our electrophysiological observations during cognitive tasks and at rest contributed to a better understanding of the neuronal substrate of higher brain functions and resting-state mental activity in human. Additionally, the electrophysiological patterns discovered by our team that are associated with depression or related to bipolar disorder might help improve diagnostics and therapy of affective disorders in the future.

References

Abramovici, S., Antony, A., Baldwin, M. E., Urban, A., Ghearing, G., Pan, J., . . . Bagic, A. (2018). Features of simultaneous scalp and intracranial EEG that predict localization of ictal onset zone. Clinical EEG and Neuroscience, 49(3), 206-212. doi:10.1177/1550059417738688

Amzica F. & Da Silva F. H. L. (2018). Cellular substrates of brain rhythms. In: Schomer D. L. & Da Silva F. H. L., eds. Niedermeyer's electroencephalography: Basic principles, clinical applications, and related fields. 7th ed. Oxford University Press, New York. 20-62.

Andrade, L., Caraveo-Anduaga, J. J., Berglund, P., Bijl, R. V., De Graaf, R., Vollebergh, W., . . . Wittchen, H. (2003). The epidemiology of major depressive episodes: Results from the international consortium of psychiatric epidemiology (ICPE) surveys. International Journal of Methods in Psychiatric Research, 12(1), 3-21. doi:10.1002/mpr.138

Antony, A. R., Abramovici, S., Krafty, R. T., Pan, J., Richardson, M., Bagic, A., & Haneef, Z. (2019). Simultaneous scalp EEG improves seizure lateralization during unilateral intracranial EEG evaluation in temporal lobe epilepsy. Seizure, 64, 8-15. doi:10.1016/j.seizure.2018.11.015

Atluri, S., Wong, W., Moreno, S., Blumberger, D. M., Daskalakis, Z. J., & Farzan, F. (2018). Selective modulation of brain network dynamics by seizure therapy in treatment-resistant depression. NeuroImage: Clinical, 20, 1176-1190. doi:10.1016/j.nicl.2018.10.015

Baccala, L. & Sameshima, K. (2001). Partial Directed Coherence: A new conception in neural structure determination. Biol Cybern, 84(6), 463-74.

Barborica, A., Mindruta, I., Sheybani, L., Spinelli, L., Oane, I., Pistol, C., . . . Bénar, C. G. (2021). Extracting seizure onset from surface EEG with independent component analysis: Insights from simultaneous scalp and intracerebral EEG. NeuroImage: Clinical, 32 doi:10.1016/j.nicl.2021.102838

Bland, B. H. & Oddie, S. D. (2001). Theta band oscillation and synchrony in the hippocampal formation and associated structures: The case for its role in sensorimotor integration. Behavioural Brain Research, 127(1-2), 119-136. doi:10.1016/S0166-4328(01)00358-8

Bender, S., Oelkers-Ax, R., Resch, F., & Weisbrod, M. (2006). Frontal lobe involvement in the processing of meaningful auditory stimuli develops during childhood and adolescence. NeuroImage, 33(2), 759-773. doi:10.1016/j.neuroimage.2006.07.003

Berchio, C., Piguet, C., Michel, C. M., Cordera, P., Rihs, T. A., Dayer, A. G., & Aubry, J. M. (2017). Dysfunctional gaze processing in bipolar disorder. NeuroImage: Clinical, 16, 545-556. doi:10.1016/j.nicl.2017.09.006

Berger H. (1929). Über das Elektroenkephalogramm des Menschen. Arch Psychiatr und Nervenkr, 87, 527-570.

Bielau, H., Trübner, K., Krell, D., Agelink, M. W., Bernstein, H. -., Stauch, R., . . . & Baumann, B. (2005). Volume deficits of subcortical nuclei in mood disorders: A postmortem study. European Archives of Psychiatry and Clinical Neuroscience, 255(6), 401-412. doi:10.1007/s00406-005-0581-y

Bočková, M., & Rektor I. (2019). Impairment of brain functions in Parkinson's disease refected by alterations in neural connectivity in EEG studies: a viewpoint. Clin Neurophysiol 130, 239–247. https://doi.org/10.1016/j.clinph.2018.11.013

Bonnefond, M., Kastner, S., & Jensen, O. (2017). Communication between brain areas based on nested oscillations. eNeuro. https ://doi.org/10.1523/ENEUR O.0153-16.2017

Bora, E., Harrison, B., Davey, C., Yücel, M., & Pantelis, C. (2012). Meta-analysis of volumetric abnormalities in cortico-striatal-pallidal-thalamic circuits in major depressive disorder. Psychological Medicine, 42(4), 671-681. doi:10.1017/S0033291711001668

Brázdil, M., Rektor, I., Dufek, M., Daniel, P., Jurák, P., & Kuba, R. (1999). The role of frontal and temporal lobes in visual discrimination task - depth ERP studies. Neurophysiol Clin, 29, 339- 350.

Brázdil, M., Rektor, I., Daniel, P., Dufek, M., & Jurák, P. (2001). Intracerebral event-related potentials to subthreshold target stimuli. Clin Neurophysiol, 112(4), 650-661. doi:10.1016/S1388-2457(01)00463-1

Brázdil, M., Roman, R., Falkenstein, M., Daniel, P., Jurák, P., & Rektor, I. (2002). Error processing—evidence from intracerebral ERP recordings. Exp Brain Res, 146:460–6

Brázdil, M., Roman, R., Daniel, P., & Rektor, I. (2003). Intracerebral somatosensory event-related potentials: effect of response type (button pressing versus mental counting) on P3-like potentials within the human brain. Clin Neurophysiol, 114, 1489-1496.

Brazdil, M., Roman, R., Daniel, P., & Rektor, I. (2005). Intracerebral error-related negativity in a simple Go/NoGo task. Journal of Psychophysiology, 19, 244-255.

Bréchet, L., Brunet, D., Birot, G., Gruetter, R., Michel, C. M., & Jorge, J. (2019). Capturing the spatiotemporal dynamics of self-generated, task-initiated thoughts with EEG and fMRI. NeuroImage, 194, 82-92. doi:10.1016/j.neuroimage.2019.03.029

Bressler, S. L., & Menon, V. (2010). Large-scale brain networks in cognition: Emerging methods and principles. Trends in Cognitive Sciences, 14(6), 277-290. doi:10.1016/j.tics.2010.04.004

Brown, P., & Williams, D. (2005). Basal ganglia local field potential activity: character and functional significance in the human. Clin Neurophysiol 116, 2510–2519. https://doi.org/10.1016/j.clinph.2005.05.009

Canolty, R. T., Edwards, E., Dalal, S. S., Soltani, M., Nagarajan, S. S., Kirsch, H. E., Berger, M. S., Barbaro, N. M., & Knight, R. et al (2006). High gamma power is phase-locked to theta oscillations in human neocortex. Science 313, 1626–1628. doi:10.1126/science.1128115

Carpenter, A. F., Georgopoulos, A. P., & Pellizzer, G. (1999). Motor cortical encoding of serial order in a context-recall task. Science, 283(5408), 1752-1757. doi:10.1126/science.283.5408.1752

Chang, C., & Glover, G. H. (2010). Time-frequency dynamics of resting-state brain connectivity measured with fMRI. NeuroImage, 50(1), 81-98. doi:10.1016/j.neuroimage.2009.12.011

Crowley, K. E., & Colrain, I. M. (2004). A review of the evidence for P2 being an independent component process: Age, sleep and modality. Clinical Neurophysiology, 115(4), 732-744.

Custo, A., Van De Ville, D., Wells, W. M., Tomescu, M. I., Brunet, D., & Michel, C. M. (2017). Electroencephalographic resting-state networks: Source localization of microstates. Brain Connectivity, 7(10), 671-682. doi:10.1089/brain.2016.0476

Damborská, A. (2012). Event-related potentials registered intracerebrally during visual oddball task in human [Kognitivní evokované potenciály snímané intracerebrálně u lidí během vizuálního oddball úkolu]. PhD thesis in Physiology and Pathological Physiology, Faculty of Medicine, Masaryk University, Brno.

Damborská, A. (2015a). Vzpomínka na významného brněnského neurofyziologa profesora Miloslava Kukletu. Česká a Slovenská Psychiatrie, 111(4), 203.

Damborská, A. (2015b). Prof. MUDr. Miloslav Kukleta, CSc. Activitas Nervosa Superior Rediviva, 57(3), 83.

Damborská, A. (2019a). Zpráva z výzkumného pobytu ve Švýcarsku. Česká a Slovenská Psychiatrie, 115(4), 193-195.

Damborská, A., Brázdil, M., Dufek, M., Jurák, P., & Kukleta, M. (2000). Electrophysiological changes preceding voluntary movement in epileptic patients recorded with depth electrodes. Homeostasis in Health and Disease, 40(3-4), 99-101.

Damborská, A., Brázdil, M., Jurák, P., Roman, R., & Kukleta, M. (2001). Steep U-shaped EEG potentials preceding the movement in oddball paradigm: Their role in movement triggering. Homeostasis in Health and Disease, 41(1-2), 60-63.

Damborská, A., Brázdil, M., Rektor, I., Janoušová, E., Chládek, J., & Kukleta, M. (2012). Late divergence of target and nontarget ERPs in a visual oddball task. Physiological Research, 61(3), 307-318.

Damborská, A., Brázdil, M., Rektor, I., & Kukleta, M. (2003). Temporal characteristics of U-shaped P-3 waves registered with intracerebral electrodes in humans. Homeostasis in Health and Disease, 42(5), 213-215.

Damborská, A., Brázdil, M., Rektor, I., & Kukleta, M. (2004). Variability of peak amplitude latencies of the visual P3 wave obtained in averaging the sweeps with equal stimulus-response intervals. Homeostasis in Health and Disease, 43(2), 63-65.

Damborská, A., Brázdil, M., Rektor, I., Roman, R., & Kukleta, M. (2006). Correlation between stimulus-response intervals and peak amplitude latencies of visual P3 waves. Homeostasis in Health and Disease, 44(4), 165-168. Retrieved from www.scopus.com

Damborská, A., Honzírková, E., Barteček, R., Hořínková, J., Fedorová, S., Ondruš, Š., . . . Rubega, M. (2020). Altered directed functional connectivity of the right amygdala in depression: High-density EEG study. Scientific Reports, 10(1) doi:10.1038/s41598-020-61264-z

Damborská, A., Lamoš, M., Brunet, D., Vulliemoz, S., Bočková, M., Deutschová, B., Baláž, M., Rektor, I. (2021). Resting-state phase-amplitude coupling between the human subthalamic nucleus and cortical activity: A simultaneous intracranial and scalp EEG study. Brain Topography, 34(3), 272-282. doi:10.1007/s10548-021-00822-8

Damborská, A., Piguet, C., Aubry, J-M., Dayer, A. G., Michel, C. M., & Berchio, C. (2019c). Altered electroencephalographic resting-state large-scale brain network dynamics in euthymic bipolar disorder patients. Frontiers in Psychiatry, 10 doi:10.3389/fpsyt.2019.00826

Damborská, A., Roman, R., Brázdil, M., Rektor, I., & Kukleta, M. (2016). Post-movement processing in visual oddball task - evidence from intracerebral recording. Clinical Neurophysiology, 127(2), 1297-1306. doi:10.1016/j.clinph.2015.08.014

Damborská, A., Tomescu, M. I., Honzírková, E., Barteček, R., Hořínková, J., Fedorová, S., Ondruš, Š., & Michel, C. M. (2019b). EEG resting-state large-scale brain network dynamics are related to depressive symptoms. Frontiers in Psychiatry, 10 doi:10.3389/fpsyt.2019.00548

Da Silva, F. H. L., Gorter, J. A., & Wadman, W. J. (2012). Epilepsy as a dynamic disease of neuronal networks doi:10.1016/B978-0-444-52898-8.00003-3

De Pasquale, F., Corbetta, M., Betti, V., & Della Penna, S. (2018). Cortical cores in network dynamics. NeuroImage, 180, 370-382. doi:10.1016/j.neuroimage.2017.09.063

De Stefano, P., Carboni, M., Marquis, R., Spinelli, L., Seeck, M., & Vulliemoz, S. (2022). Increased delta power as a scalp marker of epileptic activity: A simultaneous scalp and intracranial electroencephalography study. European Journal of Neurology, 29(1), 26-35. doi:10.1111/ene.15106

Disner, S. G., Beevers, C. G., Haigh, E. A. P., & Beck, A. T. (2011). Neural mechanisms of the cognitive model of depression. Nature Reviews Neuroscience, 12(8), 467-477. doi:10.1038/nrn3027

Donchin E, Ritter W, McCallum WC. (1978) Cognitive psychophysiology: the endogenous components of the ERP. In: Callaway E, Tueting P, Koslow SH, editors. Event-related brain potentials in man. New York: Academic Press; p. 349–411.

Drobisz, D., & Damborská, A. (2019). Deep brain stimulation targets for treating depression. Behavioural Brain Research, 359, 266-273. doi:10.1016/j.bbr.2018.11.004

Ekstrom, A. D., Caplan, J. B., Ho, E., Shattuck, K., Fried, I., & Kahana, M. J. (2005). Human hippocampal theta activity during virtual navigation. Hippocampus, 15(7), 881-889. doi:10.1002/hipo.20109

Engel, A. K., & Fries, P. (2010). Beta-band oscillations-signalling the status quo? Curr Opin Neurobiol 20:156–165. https://doi.org/10.1016/j.conb.2010.02.015

Ferdek, M. A., van Rijn, C. M. & Wyczesany, M. (2016). Depressive rumination and the emotional control circuit: An EEG localization and effective connectivity study. Cogn. Afect. Behav. Neurosci. 16, 1099–1113

Fox, M. D., Snyder, A. Z., Vincent, J. L., Corbetta, M., Van Essen, D. C., & Raichle, M. E. (2005). The human brain is intrinsically organized into dynamic, anticorrelated functional networks. Proceedings of the National Academy of Sciences of the United States of America, 102(27), 9673-9678. doi:10.1073/pnas.0504136102

Foxe, J. J., & Simpson, G. V. (2002). Flow of activation from V1 to frontal cortex in humans: A framework for defining "early" visual processing. Experimental Brain Research, 142(1), 139-150.

Frauscher, B., Von Ellenrieder, N., Zelmann, R., Doležalová, I., Minotti, L., Olivier, A., . . ., & Gotman, J. (2018). Atlas of the normal intracranial electroencephalogram: Neurophysiological awake activity in different cortical areas. Brain, 141(4), 1130-1144. doi:10.1093/brain/awy035

Georgopoulos, A. P., Lurito, J. T., Petrides, M., Schwartz, A. B., & Massey, J. T. (1989). Mental rotation of the neuronal population vector. Science, 243(4888), 234-236. doi:10.1126/science.2911737

Gomes, J., & Damborská, A. (2017). Event-related potentials as biomarkers of mild traumatic brain injury. Activitas Nervosa Superior, 59(3-4), 87-90. doi:10.1007/s41470-017-0011-2

Gong, Q., & He, Y. (2015). Depression, neuroimaging and connectomics: A selective overview. Biological Psychiatry, 77(3),223-235. doi:10.1016/j.biopsych.2014.08.009

Granger, C. W. J. (1969). Investigating Causal Relations by Econometric Models and Cross-spectral Methods. Econometrica 37, 424–438.

Halgren, E., Baudena, P., Clarke, J. M., Heit, G., Liégeois, C., Chauvel, P., & Musolino, A. (1995a). Intracerebral potentials to rare target and distractor auditory and visual stimuli. I. Superior temporal plane and parietal lobe. Electroenceph Clin Neurophysiol, 94, 191-220.

Halgren, E., Baudena, P., Clarke, J. M., Heit, G., Marinkovic, K., Deveaux, B., Vignal, J., & Biraben, A. (1995b). Intracerebral potentials to rare target and distractor auditory and visual stimuli. II. Medial, lateral and posterior temporal lobe. Electroenceph Clin Neurophysiol, 94, 229-250.

Halgren, E., Marinkovic, K., & Chauvel, P. (1998). Generators of the late cognitive potentials in auditory and visual oddball tasks. Electroenceph Clin Neurophysiol, 106(2), 156-164. doi:10.1016/S0013-4694(97)00119-3

Halgren, E., Squires, N. K., Wilson, C. L., Rohrbaugh, J. W., Babb, T. L., & Crandall, P. H. (1980). Endogenous potentials generated in the human hippocampal formation and amygdala by infrequent events. Science, 210(4471), 803-805. doi:10.1126/science.7434000

Hamilton, J. P., Etkin, A., Furman, D. J., Lemus, M. G., Johnson, R. F., & Gotlib, I. H. (2012). Functional neuroimaging of major depressive disorder: A meta-analysis and new integration of baseline activation and neural response data. American Journal of Psychiatry, 169(7), 693-703. doi:10.1176/appi.ajp.2012.11071105

Harmsen, I. E., Wolff Fernandes, F., Krauss, J. K., & Lozano, A. M. (2022). Where are we with deep brain stimulation? A review of scientific publications and ongoing research. Stereotactic and Functional Neurosurgery, doi:10.1159/000521372

He, Y., Yu, Q., Yang, T., Zhang, Y., Zhang, K., Jin, X., . . . & Luo, X. (2021). Abnormalities in electroencephalographic microstates among adolescents with first episode major depressive disorder. Frontiers in Psychiatry, 12 doi:10.3389/fpsyt.2021.775156

Helmholtz, H. L. P. (1853) Ueber einige gesetze der vertheilung elektrishcher ströme in körperlichen leitern mit anwendung auf die thierisch-elektrischen versuche. Ann Physik und Chemie. 9:211-233.

Hillyard SA, Picton TW, Regan D. (1978). Sensation, perception and attention: analysis using ERPs. In: Callaway E, Tueting P, Koslow SH, editors. Event-related brain potentials in man. New York: Academic Press; p. 223–321.

Holtzheimer, P. E., & Mayberg, H. S. (2011). Stuck in a rut: Rethinking depression and its treatment. Trends in Neurosciences, 34(1), 1-9. doi:10.1016/j.tins.2010.10.004

Honey, C. J., Kötter, R., Breakspear, M., Sporns, O. (2007). Network structure of cerebral cortex shapes functional connectivity on multiple time scales. Proc Natl Acad Sci 104:10240–45. doi: 10.1073/pnas.0701519104

Hutchison, R. M., Womelsdorf, T., Allen, E. A., Bandettini, P. A., Calhoun, V. D., Corbetta, M., . . . & Chang, C. (2013). Dynamic functional connectivity: Promise, issues, and interpretations. NeuroImage, 80, 360-378. doi:10.1016/j.neuroimage.2013.05.079

Iachim, E., Vespa, S., Baroumand, A. G., Danthine, V., Vrielynck, P., de Tourtchaninoff, M., . . . El Tahry, R. (2021). Automated electrical source imaging with scalp EEG to define the insular irritative zone: Comparison with simultaneous intracranial EEG. Clinical Neurophysiology, 132(12), 2965-2978. doi:10.1016/j.clinph.2021.09.004

Ihl, R., & Brinkmeyer, J. (1999). Differential diagnosis of aging, dementia of the alzheimer type and depression with EEG-segmentation. Dementia and Geriatric Cognitive Disorders, 10(2), 64-69. doi:10.1159/000017103

Iwabuchi, S. J., Krishnadas, R., Li, C., Auer, D. P., Radua, J., & Palaniyappan, L. (2015). Localized connectivity in depression: A meta-analysis of resting state functional imaging studies. Neuroscience and Biobehavioral Reviews, 51, 77-86. doi:10.1016/j.neubiorev.2015.01.006

Jeannerod, M., (2009). Le cerveau volontaire. Éditions Odile Jacob, Paris.

Jensen, O., & Mazaheri, A. (2010). Shaping functional architecture by oscillatory alpha activity: gating by inhibition. Front Hum Neurosci. https ://doi.org/10.3389/fnhum .2010.00186

Kaiser, R. H., Andrews-Hanna, J. R., Wager, T. D., & Pizzagalli, D. A. (2015). Large-scale network dysfunction in major depressive disorder: A meta-analysis of resting-state functional connectivity. JAMA Psychiatry, 72(6), 603-611. doi:10.1001/jamapsychiatry.2015.0071

Kim, M. J., Hamilton, J. P., & Gotlib, I. H. (2008). Reduced caudate gray matter volume in women with major depressive disorder. Psychiatry Research - Neuroimaging, 164(2), 114-122. doi:10.1016/j.pscychresns.2007.12.020

Knyazev, G. G., Savostyanov, A. N., Bocharov, A. V., Brak, I. V., Osipov, E. A., Filimonova, E. A., . . . & Aftanas, L. I. (2018). Task-positive and task-negative networks in major depressive disorder: A combined fMRI and EEG study. Journal of Affective Disorders, 235, 211-219. doi:10.1016/j.jad.2018.04.003

Krishnan, V., Chang, B., & Schomer, D. (2018). Normal EEG in wakefulness and sleep: Adults and elderly. In: Schomer D. L. & Da Silva F. H. L., eds. Niedermeyer's electroencephalography: Basic principles, clinical applications, and related fields. 7th ed. Oxford University Press, New York. 202-228.

Kühn, S., & Gallinat, J. (2013). Resting-state brain activity in schizophrenia and major depression: A quantitative meta-analysis. Schizophrenia Bulletin, 39(2), 358-365. doi:10.1093/schbul/sbr151

Kukleta, M., Damborská, A., Roman, R., Rektor, I., & Brázdil, M. (2016). The primary motor cortex is involved in the control of a non-motor cognitive action. Clinical Neurophysiology, 127(2), 1547-1550. doi:10.1016/j.clinph.2015.11.049

Kukleta, M., Damborská, A., Turak, B., & Louvel, J. (2017). Evoked potentials in final epoch of self-initiated hand movement: A study in patients with depth electrodes. International Journal of Psychophysiology, 117, 119-125. doi:10.1016/j.ijpsycho.2017.05.004

Kukleta, M., Brázdil, M., Roman, R., & Jurák, P. (2003). Identical event-related potentials to target and frequent stimuli of visual oddball task recorded by

intracerebral electrodes. Clinical Neurophysiology, 114(7), 1292-1297. doi:10.1016/S1388-2457(03)00108-1

Kukleta, M., Brazdil, M., Roman, R., Bob, P., & Rektor, I. (2009). Cognitive network interactions and beta 2 coherence in processing non-target stimuli in visual oddball task. Physiol Res, 58:139-148.

Kutý, J., Damborská, A., Linhartová, P., Lamoš, M., Jeřábková, B., Rudišinová, D., Bareš, M., & Kašpárek, T. (2021) Electrophysiological correlates of proactive and reactive inhibition in a modified visual Go/NoGo task. bioRxiv 2021.07.12.451610; doi: https://doi.org/10.1101/2021.07.12.451610

Lalo, E., Thobois, S., Sharott, A., Polo, G., Mertens, P., Pogosyan, A., & Brown, P. (2008) Patterns of bidirectional communication between cortex and basal ganglia during movement in patients with Parkinson disease. J Neurosci 28:3008–3016. https://doi.org/10.1523/JNEUROSCI.5295-07.2008

Lavenex, P., & Amaral, D. G. (2000). Hippocampal-neocortical interaction: A hierarchy of associativity. Hippocampus, 10(4), 420-430. doi:10.1002/1098-1063(2000)10:4<420::AID-HIPO8>3.0.CO;2-5

Lehmann D. (1987). Principles of spatial analysis. In: Gevins, A. S., Remont, A., eds. Methods of analysis of brain electrical and magnetic signals. Elsevier p. 309–54.

Lehmann, D., Ozaki, H., Pal, I. (1987). EEG alpha map series: brain micro-states by space-oriented adaptive segmentation. Electroencephalogr Clin Neurophysiol 67:271–88. doi: 10.1016/0013-4694(87)90025-3

Lehmann, D. & Skrandies W. (1984) Spatial analysis of evoked potentials in man – a review. Prog Neurobiol 23:227-250.

Lei, L., Liu, Z., Zhang, Y., Guo, M., Liu, P., Hu, X., . . . & Zhang, K. (2022). EEG microstates as markers of major depressive disorder and predictors of response to SSRIs therapy. Progress in Neuro-Psychopharmacology and Biological Psychiatry, 116 doi:10.1016/j.pnpbp.2022.110514

Li, Z., Fields, M., Panov, F., Ghatan, S., Yener, B., & Marcuse, L. (2021). Deep learning of simultaneous intracranial and scalp EEG for prediction, detection, and lateralization of mesial temporal lobe seizures. Frontiers in Neurology, 12 doi:10.3389/fneur.2021.705119

Litvak, V., Jha, A., Eusebio, A., Oostenveld, R., Foltynie, T., Limousin, P., . . . & Brown, P. (2011) Resting oscillatory cortico-subthalamic connectivity in patients with Parkinson's disease. Brain 134:359–374. https://doi.org/10.1093/brain/awq332

Lorenzetti, V., Allen, N. B., Fornito, A., & Yücel, M. (2009). Structural brain abnormalities in major depressive disorder: A selective review of recent MRI studies. Journal of Affective Disorders, 117(1-2), 1-17. doi:10.1016/j.jad.2008.11.021

Lotze, M., Montoya, P., Erb, M., Hülsmann, E., Flor, H., Klose, U., . . . & Grodd, W. (1999). Activation of cortical and cerebellar motor areas during executed and imagined hand movements: An fMRI study. Journal of Cognitive Neuroscience, 11(5), 491-501. doi:10.1162/089892999563553

Lozano, A. M., & Eltahawy, H. (2004). Chapter 78 How does DBS work? Suppl Clin Neurophysiol 57, 733-736. doi:10.1016/S1567-424X(09)70414-3

Lu, Y., Liang, H., Han, D., Mo, Y., Li, Z., Cheng, Y., . . . & Sun, X. (2016). The volumetric and shape changes of the putamen and thalamus in first episode, untreated major

depressive disorder. NeuroImage: Clinical, 11, 658-666. doi:10.1016/j.nicl.2016.04.008
Ludovico, I., & Damborská, A. (2017). Deep brain stimulation in Parkinson's disease: Overview and complications. Activitas Nervosa Superior, 59(1), 4-11. doi:10.1007/s41470-017-0003-2
Maksymenko, K. Novel algorithmic approaches for the forward and inverse M/EEG problems. (2019) PhD. Thesis, Nice, France. Available from: https://www.researchgate.net/publication/338526603_Novel_algorithmic_approaches_for_the_forward_and_inverse_MEEG_problems [accessed Mar 29 2022]
Meyers, H. R. & Hayne, R. (1948) Electrical potentials of the corpus striatum and cortex in Parkinsonism and hemiballism. Trans Am Neurol Assoc;73,10-14.
Michel, C. M., & He, B. (2018) EEG mapping and source imaging. In: Schomer D. L. & Da Silva F. H. L., eds. Niedermeyer's electroencephalography: Basic principles, clinical applications, and related fields. 7th ed. Oxford University Press, New York. 1135-1156.
Michel, C. M. & Koenig, T. (2018). EEG microstates as a tool for studying the temporal dynamics of whole-brain neuronal networks: A review. NeuroImage, 180, 577-593. doi:10.1016/j.neuroimage.2017.11.062
Michel, C. M., & Murray, M. M. (2012). Towards the utilization of EEG as a brain imaging tool. Neuroimage 61:371–85. doi: 10.1016/j.neuroimage.2011.12.039
Michel, C. M, Murray M. M., Lantz, G., Gonzalez, S., Spinelli, L., & Grave de Peralta, R. (2004) EEG source imaging. Clin Neurophysiol 115:2195-2222-
Murphy, M., Whitton, A. E., Deccy, S., Ironside, M. L., Rutherford, A., Beltzer, M., . . . & Pizzagalli, D. A. (2020). Abnormalities in electroencephalographic microstates are state and trait markers of major depressive disorder. Neuropsychopharmacology, 45(12), 2030-2037. doi:10.1038/s41386-020-0749-1
Näätänen, R., & Picton, T. (1987). The N1 wave of the human electric and magnetic response to sound: A review and an analysis of the component structure. Psychophysiology, 24(4), 375-425.
Niedermeyer E. & Da Silva F. H. L. (eds) (2004) Electroencephalography: Basic Principles, Clinical Applications, and Related Fields. Fifth Edition. Lippincott Williams and Wilkins
Nugent, A. C., Robinson, S. E., Coppola, R., Furey, M. L., & Zarate, C. A. (2015). Group differences in MEG-ICA derived resting state networks: Application to major depressive disorder. NeuroImage,118, 1-12.doi:10.1016/j.neuroimage.2015.05.051
Oswal, A., Brown, P., & Litvak, V. (2013). Movement related dynamics of subthalmo-cortical alpha connectivity in Parkinson's disease. Neuroimage 70:132–142. https://doi.org/10.1016/j.neuroimage.2012.12.041
Paller, K. A., Kutas, M., Mayes, A. R. (1987). Neural correlates of encoding in an incidental learning paradigm. Electroenceph Clin Neurophysiol, 67:360–71.
Paller, K. A. & McCarthy, G. (2002). Field potentials in the human hippocampus during the encoding and recognition of visual stimuli. Hippocampus, 12(3), 415-420. doi:10.1002/hipo.10053
Piguet, C., Dayer, A., & Aubry, J. M. (2016). Biomarkers and vulnerability to bipolar disorders. Swiss Archives of Neurology, Psychiatry and Psychotherapy, 167(2), 57-67. doi:10.4414/sanp.2016.00387

Polich, J. (2007). Updating P300: an integrative theory of P3a and P3b. Clin Neurophysiol 118, 2128-2148

Purves D., Augustine, G. J., Fitzpatrick, D., Hall, W. C., LaMantia A-S., Mooney, R. D., Platt, M. L., White L. E., eds. (2018). Cognitive functions and the organization of the cerebral cortex, In: Neuroscience, Sinaurer Associates, International 6th ed. Oxford University Press, New York. 593-607

Rasmussen, T. & Jasper, H. H. (1958) Temporal lobe epilepsy: Indication for operation and surgical technique. In Bailey P, Baldwin M (eds.). Temporal Lobe Epilepsy. Springfield, IL: Charles C Thomas. pp. 440-460.

Ray, A., Tao, J. X., Hawes-Ebersole, S. M., & Ebersole, J. S. (2007). Localizing value of scalp EEG spikes: A simultaneous scalp and intracranial study. Clinical Neurophysiology, 118(1), 69-79. doi:10.1016/j.clinph.2006.09.010

Rektor I. Cortical activation in self-paced versus externally cued movements: a hypothesis. (2000). Parkinsonism Relat D, 6,181–4.

Rektor, I., Louvel, J., & Lamarche, M. (1998) Intracerebral recording of potentials accompanying simple limb movements: a SEEG study in epileptic patients. Electroenceph Clin Neurophysiol, 107, 277-286.

Rektor, I., Brázdil, M., Nestrašil, I., Bareš, M., & Daniel, P. (2007). Modifications of cognitive and motor tasks affect the occurrence of event-related potentials in the human cortex. Eur J Neurosci, 26, 1371-1380.

Roger, C., Bénar, C. G., Vidal, F., Hasbroucq, T., & Burle, B. (2010). Rostral cingulate zone and correct response monitoring: ICA and source localization evidences for the unicity of correct- and error-negativities. NeuroImage, 51, 391–403.

Roman R. (2004). Electrophysiological response in oddball paradigm studied by intracerebral recordings. [Elektrofyziologická odpověď v oddball paradigmatu studovaná intracerebrálními metodami] PhD thesis in Physiology and Pathological Physiology, Faculty of Medicine, Masaryk University, Brno, 2004.

Roman, R., Brázdil, M., Chládek, J., Rektor, I., Jurák, P., Světlák, M., . . . Kukleta, M. (2013). Hippocampal negative event-related potential recorded in humans during a simple sensorimotor task occurs independently of motor execution. Hippocampus, 23(12), 1337-1344. doi:10.1002/hipo.22173

Roman, R., Brázdil, M., Jurák, P., Damborská, A., & Kukleta, M. (2001). P3 waveform in oddball paradigm can be time locked to target stimulus or the motor response. Homeostasis in Health and Disease, 41(3-4), 115-117.

Roman, R., Brázdil, M., Jurak, P., Rektor, I., & Kukleta, M. (2005) Intracerebral P3-like waveforms and the length of the stimulus-response interval in a visual oddball paradigm. Clinical Neurophysiology, 116(1), 160-171.

Schomer D. L. & Da Silva F. H. L., eds. (2018). Niedermeyer's electroencephalography: Basic principles, clinical applications, and related fields. 7th ed. Oxford University Press, New York.

Shadmehr, R., Smith, M. A., & Krakauer, J. W. (2010). Error correction, sensory prediction, and adaptation in motor control. Rev Neurosci, 33, 89–108.

Sharott A, Gulberti A, Zittel S, Tudor-Jones AA, Fickel U, Münchau A, . . . & Moll, C. K. E. (2014). Activity parameters of subthalamic nucleus neurons selectively predict motor symptom severity in Parkinson's disease. J Neurosci 34:6273–6285. https://doi.org/10.1523/JNEUROSCI.1803-13.2014

Sheline, Y. I., Barch, D. M., Donnelly, J. M., Ollinger, J. M., Snyder, A. Z., & Mintun, M. A. (2001). Increased amygdala response to masked emotional faces in depressed subjects resolves with antidepressant treatment: An fMRI study. Biological Psychiatry, 50(9), 651-658. doi:10.1016/S0006-3223(01)01263-X

Sheline, Y. I., Price, J. L., Yan, Z., & Mintun, M. A. (2010). Resting-state functional MRI in depression unmasks increased connectivity between networks via the dorsal nexus. Proceedings of the National Academy of Sciences of the United States of America, 107(24), 11020-11025. doi:10.1073/pnas.1000446107

Siegle, G. J., Thompson, W., Carter, C. S., Steinhauer, S. R., & Thase, M. E. (2007). Increased amygdala and decreased dorsolateral prefrontal BOLD responses in unipolar depression: Related and independent features. Biological Psychiatry, 61(2), 198-209. doi:10.1016/j.biopsych.2006.05.048

Squires, N. K., Squires, K. C., & Hillyard, S. A. (1975). Two varieties of long-latency positive waves evoked by unpredictable auditory stimuli in man. Electroencephalogr Clin Neurophysiol, 38, 387-401.

Strik, W. K., Dierks, T., Becker, T., & Lehmann, D. (1995). Larger topographical variance and decreased duration of brain electric microstates in depression. Journal of Neural Transmission, 99(1-3), 213-222. doi:10.1007/BF01271480

Sun, Y., Li, Y., Zhu, Y., Chen, X., & Tong, S. (2008). Electroencephalographic differences between depressed and control subjects: An aspect of interdependence analysis. Brain Research Bulletin, 76(6), 559-564. doi:10.1016/j.brainresbull.2008.05.001

Surguladze, S., Brammer, M. J., Keedwell, P., Giampietro, V., Young, A. W., Travis, M. J., . . . Phillips, M. L. (2005). A differential pattern of neural response toward sad versus happy facial expressions in major depressive disorder. Biological Psychiatry, 57(3), 201-209. doi:10.1016/j.biopsych.2004.10.028

Sutton, S., Barren, M., Zubin, J., & John, E. R. (1965). Evoked potentials correlates of stimulus uncertainty. Science, 150, 1187–8.

Talairach, J. & Bancaud, J. (1973). Stereotactic approach to epilepsy. Prog Neurol Surg, 5:297-354.

Tang, Y., Li, Y., Wang, N., Li, H., Li, H., & Wang, J. (2011). The altered cortical connectivity during spatial search for facial expressions in major depressive disorder. Progress in Neuro-Psychopharmacology and Biological Psychiatry, 35(8), 1891-1900. doi:10.1016/j.pnpbp.2011.08.006

Ullsperger, M., Danielmeier, C., & Jocham, G. (2014). Neurophysiology of performance monitoring and adaptive behavior. Physiological Reviews, 94(1), 35-79. doi:10.1152/physrev.00041.2012

Van De Ville, D., Britz, J., & Michel, C. M. (2010). EEG microstate sequences in healthy humans at rest reveal scale-free dynamics. Proceedings of the National Academy of Sciences of the United States of America, 107(42), 18179-18184. doi:10.1073/pnas.1007841107

Veer, I. M., Beckmann, C. F., van Tol, M., Ferrarini, L., Milles, J., Veltman, D. J., . . . & Rombouts, S. A. R. B. (2010). Whole brain resting-state analysis reveals decreased functional connectivity in major depression. Frontiers in Systems Neuroscience, 4 doi:10.3389/fnsys.2010.00041

Wang, C., Sun, C., Zhang, X., Wang, Y., Qi, H., He, F., . . . Ming, D. (2015). The brain network research of poststroke depression based on partial directed coherence

(PDC). Chinese Journal of Biomedical Engineering, 34(4), 385-391. doi:10.3969/j.issn.0258-8021.2015.04.001

Williams, D. (2002), Dopamine-dependent changes in the functional connectivity between basal ganglia and cerebral cortex in humans. Brain 125, 1558–1569. https://doi.org/10.1093/brain/awf156

Wyler, A. R., Ojemann, G. A., Lettich, E., Ward, A. A. (1984) Subdural strip electrodes for localizing epileptogenic foci. J Neurosurg., 60, 1195-1200.

Yan, D., Liu, J., Liao, M., Liu, B., Wu, S., Li, X., . . . & Li, L. (2021). Prediction of clinical outcomes with EEG microstate in patients with major depressive disorder. Frontiers in Psychiatry, 12 doi:10.3389/fpsyt.2021.695272

Yang, J., Yin, Y., Svob, C., Long, J., He, X., Zhang, Y., . . . & Yuan, Y. (2017). Amygdala atrophy and its functional disconnection with the cortico-striatal-pallidal-thalamic circuit in major depressive disorder in females. PLoS ONE, 12(1) doi:10.1371/journal.pone.0168239

Yordanova, J., Falkenstein, M., Hohnsbein, J., & Kolev, V. (2004). Parallel systems of error processing in the brain. NeuroImage, 22, 590–602.

Zhang, J., Riehle, A., Requin, J., & Kornblum, S. (1997). Dynamics of single neuron activity in monkey primary motor cortex related to sensorimotor transformation. Journal of Neuroscience, 17(6), 2227-2246. doi:10.1523/jneurosci.17-06-02227.1997

Zhang, B., Lin, P., Shi, H., Öngür, D., Auerbach, R. P., Wang, X., . . . & Wang, X. (2016). Mapping anhedonia-specific dysfunction in a transdiagnostic approach: An ALE meta-analysis. Brain Imaging and Behavior, 10(3), 920-939. doi:10.1007/s11682-015-9457-6

List of peer-reviewed articles of the candidate

Original articles in journals with impact factor listed in WOS

1. Bartečků, E., Hořínková, J., Křenek, P., **Damborská, A.**, Tomandl, J., Tomandlová, M., Kučera, J., Fialová Kučerová, J., Bienertová-Vašků, J. (2022). Osteocalcin decreases during the treatment of depressive episode *Frontiers in Psychiatry*, in press
   IF(2021) = 5.435, rank Q2

2. **Damborská, A.**, Lamoš, M., Baláž, M., Deutschová, B., Brunet, D., Vulliemoz, S., Bočková, M., & Rektor, I. (2021) Resting-State Phase-Amplitude Coupling Between the Human Subthalamic Nucleus and Cortical Activity: A Simultaneous Intracranial and Scalp EEG Study, *Brain Topography*, 34(3), 272-282.
   IF(2021) = 4.275, rank Q2
3. **Damborská, A.**, Honzírková, E., Barteček R., Hořínková J., Fedorová, S., Ondruš, Š., Michel, C. M., & Rubega, M. (2020). Altered directed functional connectivity of the right amygdala in depression: high-density EEG study. *Scientific Reports*, 4398 (10)
   IF(2020) = 4.380, rank Q1
4. **Damborská, A.**, Tomescu, M.I., Honzírková, E., Barteček, R., Hořínková, J., Fedorová, S., Ondruš Š., & Michel C.M. (2019). EEG resting-state large-scale brain network dynamics are related to depressive symptoms. *Frontiers in Psychiatry*, 548 (10)
   IF(2019) = 2.849, rank Q2

5. **Damborská, A.**, Piguet, C., Aubry, J-M., Dayer, A. G., Michel C. M., & Berchio, C. (2019). Altered EEG resting-state large-scale brain network dynamics in euthymic bipolar disorder patients. *Frontiers in Psychiatry*, 826 (10)
   IF(2019) = 2.849, rank Q2
6. **Damborská, A.**, Roman, R., Brázdil, M., Rektor, I., & Kukleta, M. (2016). Post-movement processing in visual oddball task - evidence from intracerebral recording. *Clinical Neurophysiology,* 127 (2), 1297 – 1306. IF(2016) = 3.866, rank Q1

7. **Damborská, A.**, Brázdil, M., Rektor, I., & Kukleta, M. (2012). Late divergence of target and nontarget ERPs in a visual oddball task. *Physiological research, 61*(3), 307-318. IF(2012) = 1.531, rank Q3

8. Kukleta, M., **Damborská, A.**, Turak, B., & Louvel, J. (2017). Evoked potentials in final epoch of self-initiated hand movement: A study in patients with depth electrodes. *International Journal of Psychophysiology*, 117, 119-125.
   IF(2017) = 2.868, rank Q2
9. Kukleta, M., **Damborská, A.**, Roman, R., Rektor, I., & Brázdil, M. (2016). The primary motor cortex is involved in the control of a non-motor cognitive action. *Clinical Neurophysiology*, 127 (2), 1547 – 1550. IF(2016) = 3.866, rank Q1

10. Roman, R., Brázdil, M., Chládek, J., Rektor, I., Jurák, P., Světlák, M., **Damborská, A.**, Shaw, D. J., & Kukleta, M. (2013). Hippocampal negative event-related potential recorded in humans during a simple sensorimotor task occurs independently of motor execution. *Hippocampu*s, 23 (12), 1337-1344. IF(2013) = 4.302, rank Q1

11. Světlák, M., Bob, P., Roman, R., Ježek, S., **Damborská, A.**, Chládek, J., Shaw, D. J., & Kukleta M. (2013). Stress-Induced Alterations of Left-Right Electrodermal Activity Coupling Indexed by Pointwise Transinformation. *Physiological Research*, 62(6), 711-719. IF(2013) = 1.487, rank Q4

Original articles in journals without impact factor listed in Scopus

1. **Damborská, A.**, Brázdil, M., Dufek, M., Jurák, P., & Kukleta, M. (2000). Electrophysiological changes preceding voluntary movement in epileptic patients recorded with depth electrodes. *Homeostasis in Health and Disease,* 40(3-4), 99-101.
2. **Damborská, A.**, Brázdil, M., Jurák, P., Roman, R., & Kukleta, M. (2001). Steep U-shaped EEG potentials preceding the movement in oddball paradigm: Their role in movement triggering. *Homeostasis in Health and Disease,* 41(1-2), 60-63.
3. **Damborská, A.**, Brázdil, M., Rektor, I., & Kukleta, M. (2003). Temporal characteristics of U-shaped P-3 waves registered with intracerebral electrodes in humans. *Homeostasis in Health and Disease,* 42(5), 213-215.
4. **Damborská, A.**, Brázdil, M., Rektor, I., & Kukleta, M. (2004). Variability of peak amplitude latencies of the visual P3 wave obtained in averaging the sweeps with equal stimulus-response intervals. *Homeostasis in Health and Disease,* 43(2), 63-65.
5. **Damborská, A.**, Brázdil, M., Rektor, I., Roman, R., & Kukleta, M. (2006). Correlation between stimulus-response intervals and peak amplitude latencies of visual P3 waves. *Homeostasis in Health and Disease,* 44(4), 165-168.
6. Roman, R., Brázdil, M., Jurák, P., **Damborská, A.**, & Kukleta, M. (2001). P3 waveform in oddball paradigm can be time locked to target stimulus or the motor response. *Homeostasis in Health and Disease,* 41(3-4), 115-117.
7. Světlák, M., Hodoval, R., **Damborská, A.**, Pilát, M., Roman, R., Černík, M., Obereignerů, R., & Bob, P. (2013). The emotional impact of the text of cigarette package health warning on older school age and adolescent children. *Česko-Slovenská Pediatrie,* 68(2), 78-91.

Review article in journal with impact factor listed in WOS

1. Drobisz D. & **Damborská A.** (2019). Deep brain stimulation targets for treating depression, *Behavioural Brain Research*, 359 (1), 266-273.

IF(2019) = 2.977, rank Q2

Review articles in journals without impact factor listed in Scopus

1. Gomes, J. & **Damborská, A.** (2017). Event-related potentials as biomarkers of mild traumatic brain injury. *Activitas Nervosa Superior*, 59 (3-4), 87-90.
2. Ludovico, I. C. & **Damborská, A.** (2017). Deep brain stimulation in Parkinson's disease: Overview and complications. *Activitas Nervosa Superior*, 59(1), 4-11.
3. Roman, R., Světlák, M., **Damborská, A.**, & Kukleta, M. (2014). Neurophysiology of defence behaviour. *Česká a Slovenská Psychiatrie*, 110(2), 96-104.

Review articles in journals without impact factor

1. Da Silva, A. M. & **Damborská, A.** (2001). Novas fronteiras de interacção sono – epilepsia. *Vigilia Sueño*, 13(1), 64 -66.
2. Světlák, M., Roman, R., Obereignerů, R., & **Damborská, A.** (2014). Jak se cítíte „teď a tady"? Neuronální pozadí emočního uvědomění. *Psychoterapie*, 8(2), 132-141.